GEOLOGIC STUDIES IN SAN DIEGO

Edited By:
PATRICK L. ABBOTT
Department of Geological Sciences
San Diego State University
San Diego, CA 92182

Prepared for
San Diego Association of Geologists
Field Trips

APRIL 1982

Library of Congress Catalog Card Number:

Printed by:

Diego & Son Printing, San Diego, CA

ACKNOWLEDGEMENTS

The authors deserve our thanks for their time and energy spent in preparing the manuscripts.

The cover is an original design by Julie Pearson. She may be contacted for creation of other work by writing c/o 770 Topa Topa Court, Ventura, CA 93003.

Most of the typing and much of the layout was completed via the talents of Kathy Jessup and Pia Parrish of the SDSU Department of Geological Sciences.

Many of the illustrations were drafted by Scott Fenby of the SDSU Department of Geological Sciences.

Preparation of this volume was aided by a grant from Sun Production Company.

It is by logic that we prove, but by intuition that we discover.

Henri Poincare'

CONTENTS

CONTENTS

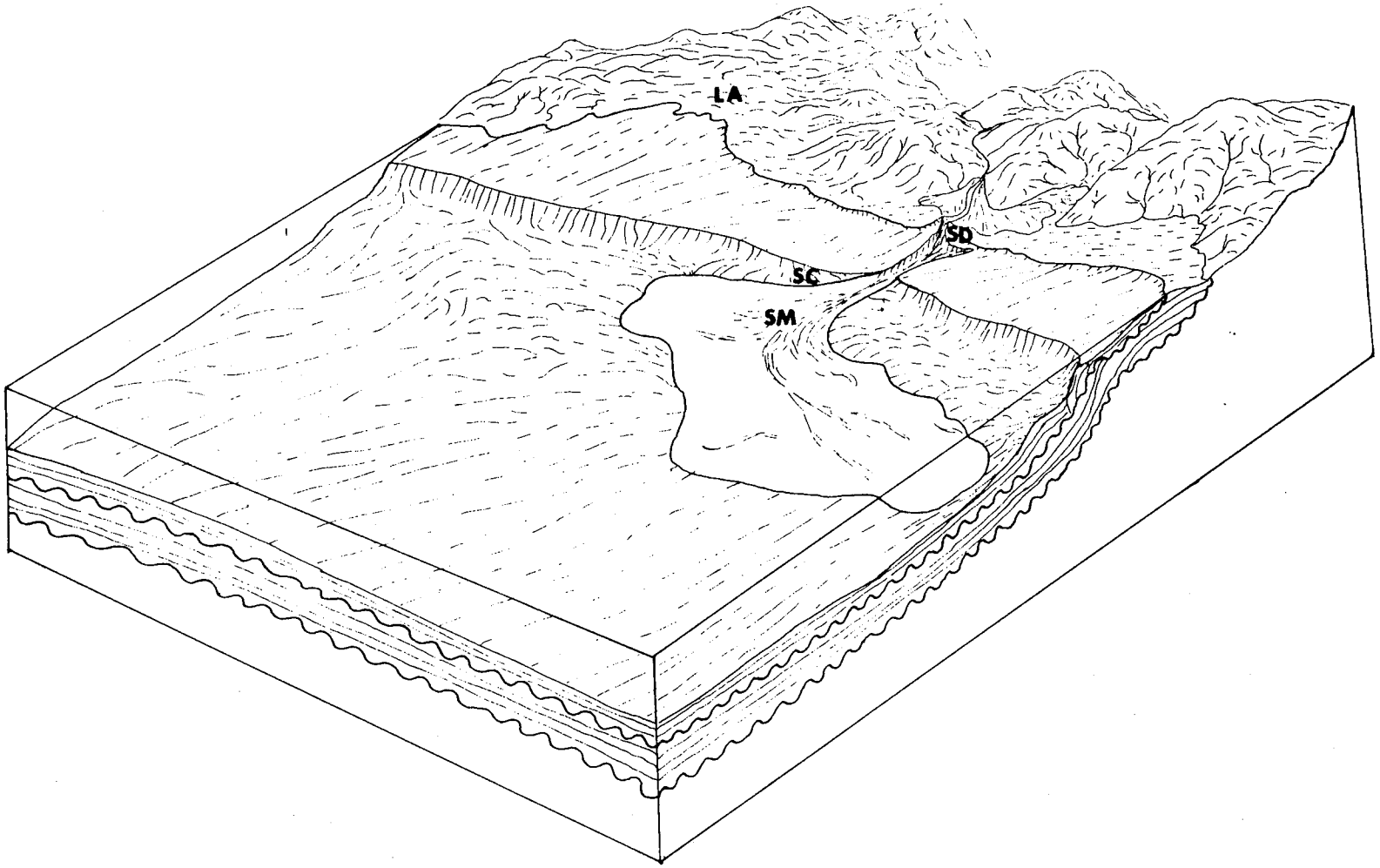

The above sketch outlines the inferred paleogeography of the southern California Borderland during the latter half of the Early Eocene. Prograding alluvial fan deposits by-passed the shelf and this clast material was funneled into submarine feeder canyons: SD=present day San Diego; at the terminous of the primary submarine canyon(s) a bathyl fan was present: SM=pre-rift position of present-day San Miguel Island; SC=Santa Cruz Island; LA=Los Angeles.

PALEOGEOGRAPHY OF THE MT. SOLEDAD FORMATION WEST OF THE ROSE CANYON FAULT

by

Ronald P. Kies
Department of Geological Sciences
San Diego State University
San Diego, California 92182

ABSTRACT

Within the San Diego region are outcrops of the Mt. Soledad Formation which represent six sedimentary environments: 1) paralic/upper estuarine, 2) deltaic, 3) alluvial fan and braided stream, 4) submarine canyon head, 5) inner fan channel and 6) slope. The depositional environments have been combined with analyses of gravel constituents, paleontology and regional stratigraphic correlations throughout the Southern California Borderland for the purpose of defining the range of ages in the Mt. Soledad Fm. and reconstructing the Early Eocene paleogeography. This detailed sedimentologic investigation reveals the following about the strata assigned to the Mt. Soledad Formation: 1) the lowermost estuarine facies are Late Paleocene in age, 2) deltaic conglomerates with a well developed kaolinitic paleosol at the mouth of Indian Trail Canyon near Black's Beach were deposited during the Late Paleocene-Early Eocene, 3) submarine canyon and channel facies are middle to late Early Eocene in age and the overlying slope facies are equivalent in age to the lower part of the Ardath shale, 4) outcrops of submarine canyon facies in the area of Morena Blvd. in Rose Canyon are not offset. Although, to the west and on the opposite side of the Mt. Soledad and Country Club faults, correlative submarine canyon/channel facies are 4 km further to the north which suggests 4 km of right slip within the Rose Canyon Fault Zone.

INTRODUCTION

Lower Eocene sedimentary rocks of the Mt. Soledad Fm. (Kennedy, 1975) are exposed at localities in Rose Canyon, on Mt. Soledad, at La Cañada Ave. and along Tourmaline Beach (Figure 1). Exposed in the east and west walls of Rose Canyon (Figure 1, localities 1 and 2) are strata representing upper estuarine, alluvial fan, braided stream and submarine canyon head facies. These strata exhibit either complex sedimentologic relationships or are separated by disconformity. They are overlain by passive slope, lower Middle Eocene mudstones of the Ardath Shale.

In the large roadcut on the east side of Morena Blvd. (locality 1) all of the paleoenvironmental facies of the Mt. Soledad Fm. west of the Rose Canyon Fault are evident.

MORENA BOULEVARD - LOCALITY 1

The bedding complexity exhibited by the strata in this outcrop as well as structural complication caused by a small fault, are sketched in Figure 2. A fascinating vertically stacked series of seven different lithofacies is recognized here.

LITHOFACIES 1 - UPPER ESTUARINE FACIES

These deposits are composed of very pale green, angular gritty mudstone, muddy coarse sandstone and sparse framework-supported, rounded, pebble and cobble conglomerate. Near the base of the outcrop is an oxidized red-bed of sandy mudstone which exhibits a horizon of sandy mudstone-filled root casts. Sparse framework-supported, round cobble conglomerate is present as lag deposits in broad channels. Poway-type rhyolite clasts are not present. Kaolinitized clasts and kaolinitic debris are ubiquitous constituents in both conglomerate and enclosing finer-grained clastic material.

Depositional sequences are characterized by upward decreasing grain sizes from conglomerate to laminated sandy mudstone to mudstones with root casts or rhizomes. This succession records channel scouring by vigorous fluvial outwash into a mud-rich environment and a later in-filling episode. These deposits are capped by a Poway clast-bearing conglomerate (lithofacies 2) which exhibits a basal erosional surface with up to 1 m of local relief. The sedimentologic characteristics suggest an upper estuarine environment adjacent to a small southwest-flowing stream. Shifting depositional base levels are recorded by the red-bed and root-cast soil profiles which appear at different stratigraphic levels and as intraclasts in many of the conglomerates. The presence of kaolinitized clasts, kaolinitic debris, shallow marine/paralic sedimentary structures and absence of Poway clasts, suggest a Late Paleocene age for these deposits. This age assignment is based on: 1) comparison to the Late Paleocene Silverado Fm. (Yerkes et al, 1965) in the Santa Ana Mountains, which is a conglomerate rich in kaolinitized clasts (Kies, 1982), 2) the fact that Poway-type clasts were present in the Southern California Borderland only as early as the Late Paleocene-Earliest Eocene (Kies, 1982), and 3) the extreme weathering event which produced the kaolinitic weathering profile from which the kaolinitized material was derived is Paleocene to Early Eocene in age (Peterson and Abbott, 1979). Kaolinite clastic material is unknown in the Cretaceous deposits in San Diego (Gray, 1979). Based on these data and the disconformable contact with the overlying Poway clast-bearing conglomerate, the previous Cretaceous age assignment (Kennedy, 1975) may be in error.

LITHOFACIES 2 - ALLUVIAL FAN FACIES

Resting disconformably on lithofacies 1 is an interval of framework-supported, angular pebble, cobble and boulder conglomerate. The interstices between the highly fractured and angular clasts are filled with muddy fine to medium sandstone, muddy siltstone and angular to very angular granules and pebbles. This disorganized conglomerate has at its base at least 2.5 m of framework-supported, rounded, pebble, cobble and rare boulder conglomerate. The lower, more organized and rounded conglomerate which rests on lithofacies 1 exhibits normal grading, good sorting, long axis parallel to current imbrication and very dense packing. These deposits are considered to be the product of either a channelized fluvial environment or a wave-reworked conglomeratic shoreface. The overlying disorganized conglomerate is more difficult to interpret. The conglomerate clasts are not rounded but are found as sharp, very angular fragments of granule to cobble size with abundant muddy siltstone and sandstone matrix. Many of the broken clasts are ultradurable Poway rhyolites and quartzite and it is unlikely that simple abrasion is responsible for the fracturing. Rather, it is suggested that these deposits are the product of debris flows of in-situ salt-weathered

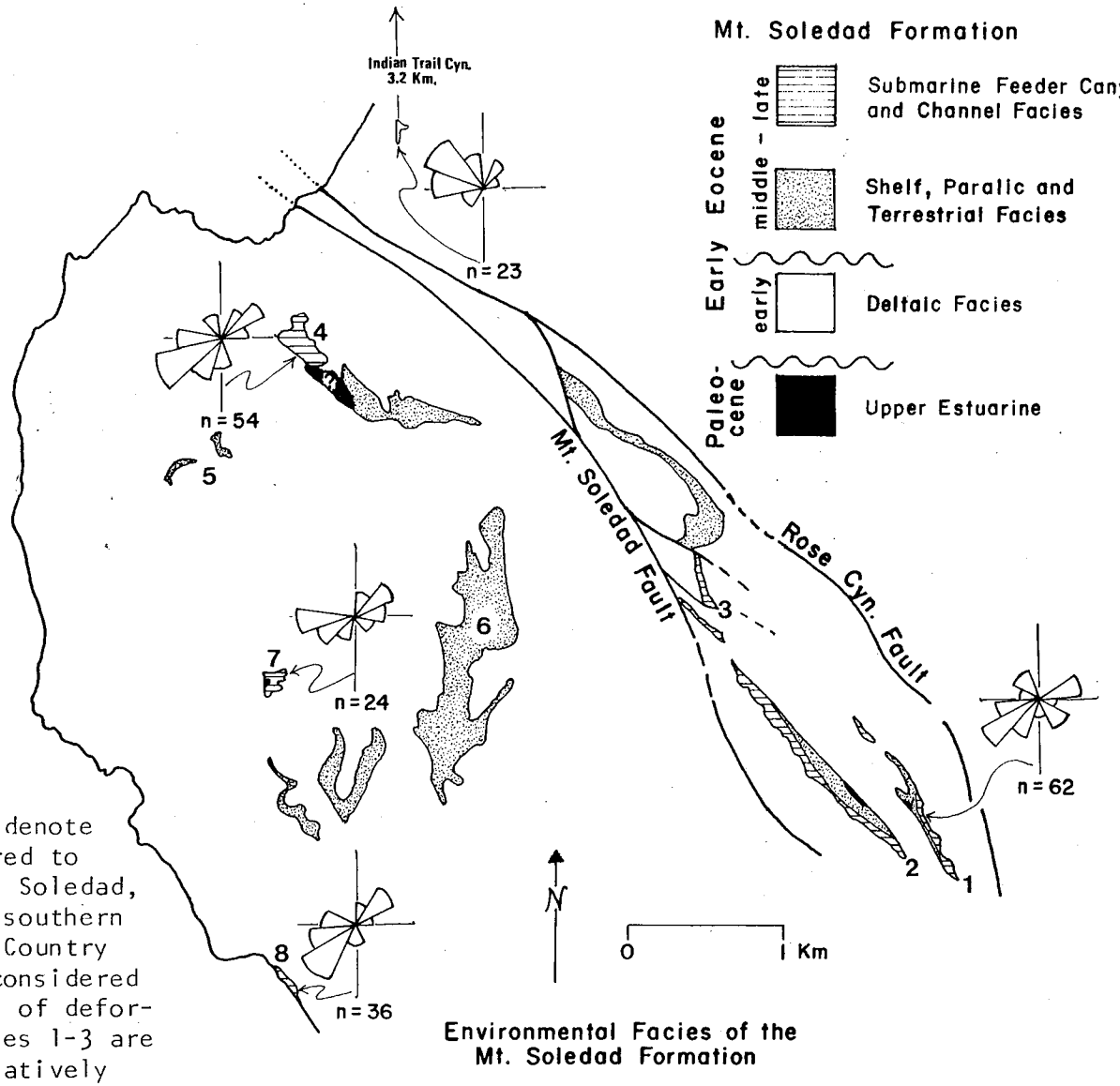

Figure 1. Numbers denote localities referred to in text. The Mt. Soledad, Rose Canyon, and southern extension of the Country Club faults are considered the primary zones of deformation. Localities 1-3 are situated in a relatively undeformed, fault-bounded block.

1) Morena Blvd. roadcut, east of the industrial park, 2) outcrops on the west side of I-5, 3) roadcut west of I-5, approx. 2.5 km north of the Balboa exit, 4) Romero Street, just east of Country Club Lane on Mt. Soledad, 5) small canyon 100 m south of the La Jolla Country Club, 6) large canyon just east of Rutgers Rd. 7) east end of La Canada Ave., 8) Tourmaline Beach

conglomerate. The resedimentation event occurred after the originally rounded clasts were fractured in-place by salt weathering during temporary alluvial storage on a small coastal alluvial fan. The resultant clast texture, fabric and proportion of relict clasts to matrix material is compatible with the expected products of salt weathering as described by Peterson (1979). The deposits assigned to lithofacies 2 are disconformably overlain by the conglomerates of lithofacies 3.

LITHOFACIES 3 - BRAIDED STREAM FACIES

The more organized clast fabric and channel shaped beds which characterize this facies are in sharp contrast to the deposits of lithofacies 2. Axial trends of many of the larger channels and clast imbrication define a N20W to N30W direction of flow. The channel-fill conglomerates are framework supported, amalgamated, and consist of rounded pebble to boulder size clasts. Clast imbrication is steep with long axis perpendicular to flow. Conglomeratic bar deposits are distinguished by their flat base and dominance of long axis perpendicular to flow, shallow clast imbrication. Alternating with these more organized, coarse clastic deposits are thin (0.5 to 1 m) lentils of angular to subangular cobble conglomerate similar to lithofacies 2. Also interbedded are flat-based lentils of coarse sandstone which exhibit parallel lamination and crossbedding (N70W paleocurrent trends) and are interpreted as finer-grained bars between braided stream channels.

Lithofacies 3 grades upward to a dominance of long axis perpendicular imbrication, less matrix and a denser clast packing. This facies is arbitrarily terminated at a crossbedded, pebbly coarse sandstone. In reality the unit is in gradational contact with lithofacies 4. Upsection the conglomerates of lithofacies 3 were deposited in less concave downward channels, clast imbrication becomes shallower and clast packing becomes tighter. This attests to an increasing dominance of grain flow, or avalanching, sediment transport processes.

LITHOFACIES 4 - TRANSITIONAL FACIES

The clasts in this conglomerate are characterized by their shallow (<5°) imbrication, long axis perpendicular to flow, and deposition in low relief, flat-based channels. Also common in these conglomerates is an absence or near absence of matrix material, tight clast packing and the presence of inverse to normal grading in the upper part. All these features suggest a transitional environment between braided stream and submarine channel, possibly in an area where clastic material temporarily accumulated and was funneled by grain flow and slumping (avalanching) into the head of a submarine feeder canyon.

LITHOFACIES 5 - FEEDER CANYON CONGLOMERATE

This interval is composed entirely of inverse to normally graded, amalgamated, framework-supported, rounded, pebble, cobble, and rare boulder conglomerate. Channels are present and have even, flat bases. Clast imbrication is long axis perpendicular but shows a lot of scatter in the indicated paleocurrent trend.

The upper portion of this unit exhibits a flat-based channel filled with well-sorted, disorganized, rounded, pebble and pebble-cobble

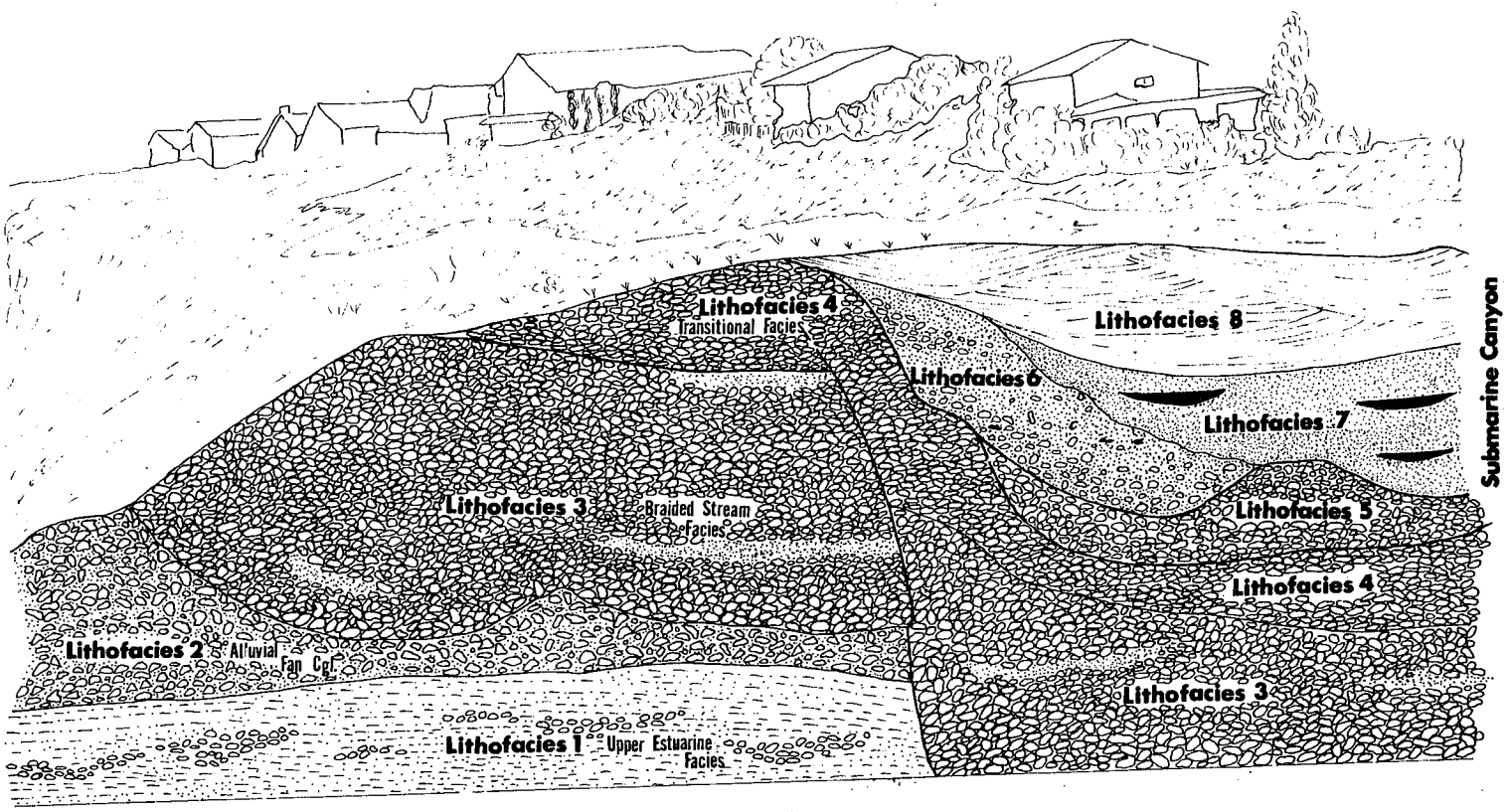

Figure 2. Depositional relationships of lithofacies 1-8 in the large roadcut on Morena Blvd. (locality 1, Figure 1). The top of the outcrop is approximately 50 m above street level.

conglomerate. Above this channel fill the entire unit is capped by a convex-upward surface which is mantled with a silty mudstone drape. Sedimentary structures and clast fabrics which can only be attributed to traction-induced processes are absent. Conversely, features associated with subaqueous debris and grain flows are common.

Upsection within the lithofacies the presence of subaqueously produced sedimentary features persists. This suggests that the erosional surface at the base of lithofacies 5 records the upward change to entirely marine deposits of a feeder canyon.

LITHOFACIES 6 - SUBAQUEOUS DEBRIS FLOWS

These deposits are composed entirely of chaotically bedded, pebbly and shale intraclastic, fine sandstone. This material rests on a silty mudstone drape which mantles the base of a fine sediment-filled, broad channel. Lithofacies 6 attests to a period of channel wall semi-stability which followed depositional abandonment. During this time sand and conglomerate slumps and grain flows were initiated from the channel walls and cascaded toward the channel axis. The deposition of lithofacies 7 and 8 was coeval with that of lithofacies 6.

LITHOFACIES 7 - ABANDONED CHANNELS (INNER-FEEDER CANYON)

This facies rests on the slump deposits and is characterized by massive, fine and very fine sandstones enclosing small (1 to 4 m wide, 0.2-0.75 m thick) shale-filled channels. The sandstones are the product of grain flows and display amalgamation which records funneling of fine material primarily by long-shore drift into the increasingly clastic starved canyon. Periods of scouring between fill events alternated with depositional bypassing in producing the small shale-filled channels.

LITHOFACIES 8 - SHALE-FILLED BROAD CHANNELS

These deposits consist of gently concave upward channels which are filled with laminated siltstone drapes; they form the uppermost exposed lithofacies of the abandoned, feeder canyon-fill sequence. The wide and shallow channels filled with laminated siltstone drapes record deposition during intermittent periods of small-scale channel erosion. The inner-canyon currents formed a braided system of small channels that rapidly shifted position and filled with fine material.

In summary, the deposits of the Mount Soledad Formation at the Morena Blvd. localities in Rose Canyon record a generally regressive then transgressive sedimentation series. The oldest deposits do not contain Poway rhyolite clasts and are probably of Late Paleocene age. These rocks are separated from overlying conglomerates which contain Poway clasts by an erosional surface which may represent a significant amount of time.

The Late Paleocene estuarine facies (Lithofacies 1) lay landward of a submarine feeder canyon and adjacent to a small coastal alluvial fan. Progradation of the alluvial fan into the estuary may have been accentuated by a sea-level lowstand. Following this event, a rising sea level caused landward advance of submarine feeder canyon environments. Continued drowning of the coastline cut off incursion of coarse-clastic material into the submarine channel. The resultant depositional bypassing and canyon

abandonment appears as the fine-grained canyon fill sequence (lithofacies 6, 7, and 8). Walker (1978) also noted that feeder canyons will fill with fine-grained material when sea level rises and coarse sediment becomes trapped at the new shoreline. The Mississippi (Sabate, 1968), Meganos (Dikas and Payne, 1967) and Yoakum (Hoyt, 1959) channels are characterized by this type of eustatic-induced fill.

Passive slope deposits of the Ardath Shale cap the canyon deposits behind the Price Club on Morena Blvd. Samples collected at the base of the Ardath beds yielded lower Middle Eocene coccoliths Discoaster sublodoensis (Bukry and Kennedy, 1969). These data require that the entire succession of depositional environments represented by lithofacies 1-8 must be older than early Middle Eocene.

BIOSTRATIGRAPHIC AGES OF ENVIRONMENTAL FACIES

Figure 3 outlines the biostratigraphic relationships of the Mt. Soledad Formation facies. The age of the middle to upper slope deposits at Tourmaline Beach was revealed by a mudstone sample which yielded early Middle Eocene foraminifera. Specifically, Cibicidoides coalingenesis, Eponides c.f. E. Mexicana and Lenticulina sp. suggesting the late Early to early Middle Ulatisian (Al Almgren, pers. comm., 1981). This fauna is very similar to the fauna obtained from the lower slope facies of the Ardath Shale north of Scripps Pier (Almgren, pers. comm., 1981).

There are lithofacies correlative and petrographically compatible strata to many of the environmental facies of the Mt. Soledad Fm. on Santa Cruz and San Miguel Islands which are fossiliferous and reveal: 1) the deltaic facies of the Mt. Soledad Fm. was deposited sometime between the coccolith zones Discoaster multiradiatus and Discoaster diastyphus (Mark Filewicz, pers. comm., 1981) based on the age of correlative strata on Santa Cruz Island and 2) the submarine facies was deposited during the middle to late Early Eocene based on the age of correlative strata on San Miguel Island (Kies, 1982) which yielded coccoliths associated with the faunal zone Discoaster lodensis (Dave Bukry, pers. comm., 1981).

EARLY EOCENE PALEOGEOGRAPHY AND PALINSPASTIC RECONSTRUCTION

The Lower Eocene feeder canyon head and submarine channel facies crop out throughout the Rose Canyon area. Figure 1 maps the limits of these facies and shows two important features.

The channel is a southwest-trending linear feature roughly perpendicular to the major through-going faults in the region. The area surrounding Morena Blvd. in Rose Canyon represents a relatively undeformed, coherent, fault-encircled block which exposes the submarine canyon and underlying estuarine and terrestrial facies. This is demonstrated simply by looking west from the Morena Boulevard outcrop, across Rose Canyon to the outcrops along Interstate Highway 5. Figure 4 is a line drawing of these outcrops. The estuarine facies is clearly evident as is the contact with the overlying alluvial fan and braided stream facies. The feeder channel canyon head facies is present but obscured by vegetation and recent alluvium. Referring to Figure 3, given the southwest trend of the channel at Morena Blvd. (Figure 2) and the orientation of the contacts between channel, terrestrial and estuarine facies as exposed in the outcrops along I-5, it is clear that there is little or no offset of the channel trend across Rose Canyon.

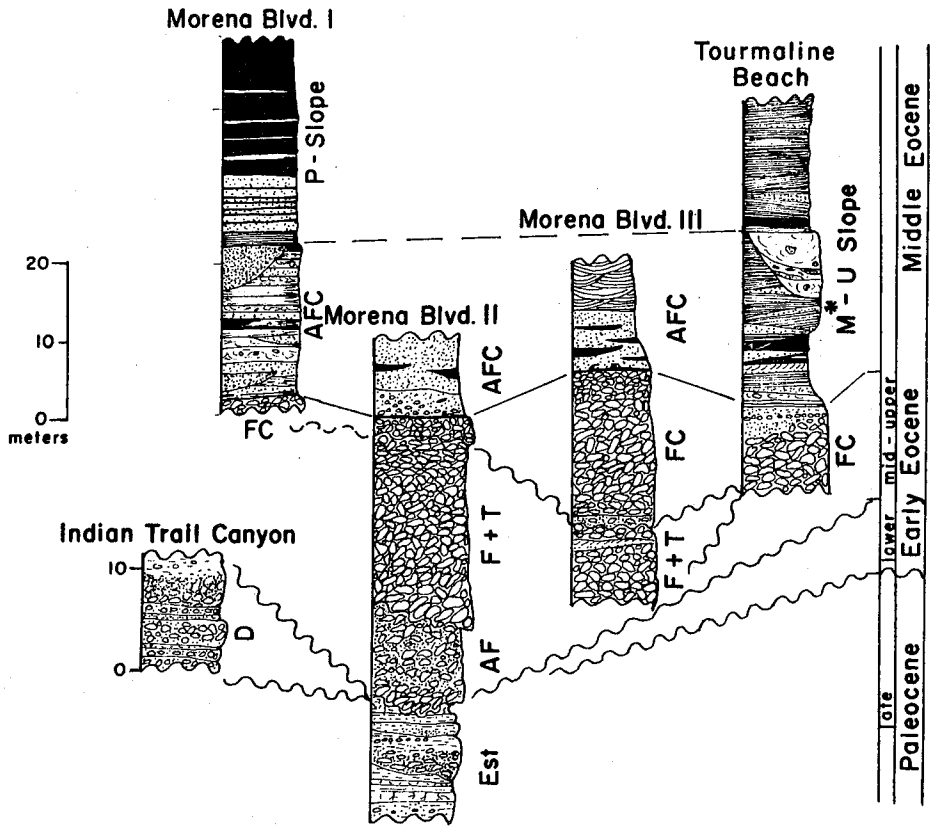

Figure 3. Lithostratigraphic and biostratigraphic relationships of environmental facies of the Mt. Soledad Formation. *denotes position in section at Tourmaline Beach of sample which yielded early Middle Eocene foraminifera.

Environmental Facies:
- Est = Estuarine
- AF = Alluvial fan
- F&T = Braided stream & transitional
- FC = Submarine feeder channel/feeder canyon head
- AF = Abandoned, depositionally by-passed submarine feeder canyon head/ feeder channel
- P-slope = Passive slope
- M-U slope = Middle to upper slope

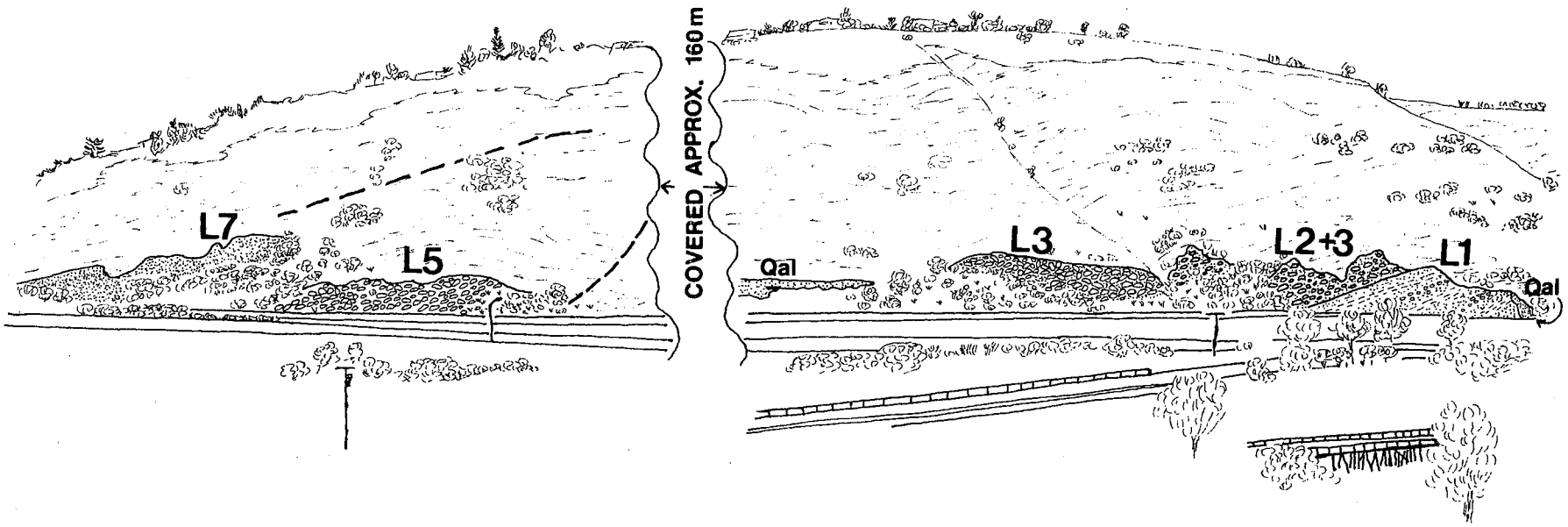

Figure 4. Outcrops of Mt. Soledad Formation along the west side of Interstate 5 just north of the Balboa Ave. exit. The bold dotted line delineates the approximate dimension of the submarine feeder canyon. Beds dip approximately 15° to the south-southwest. This view is taken from midway up on the Morena Blvd. outcrop which is shown in Figure 2.

L1 = Estuarine facies: lithofacies 1
L2+3 = Braided stream/alluvial fan: lithofacies 2 and 3
L5 = Feeder canyon conglomerate: lithofacies 5
L7 = Abandoned feeder canyon fill: lithofacies 7
Qal = Quaternary alluvium

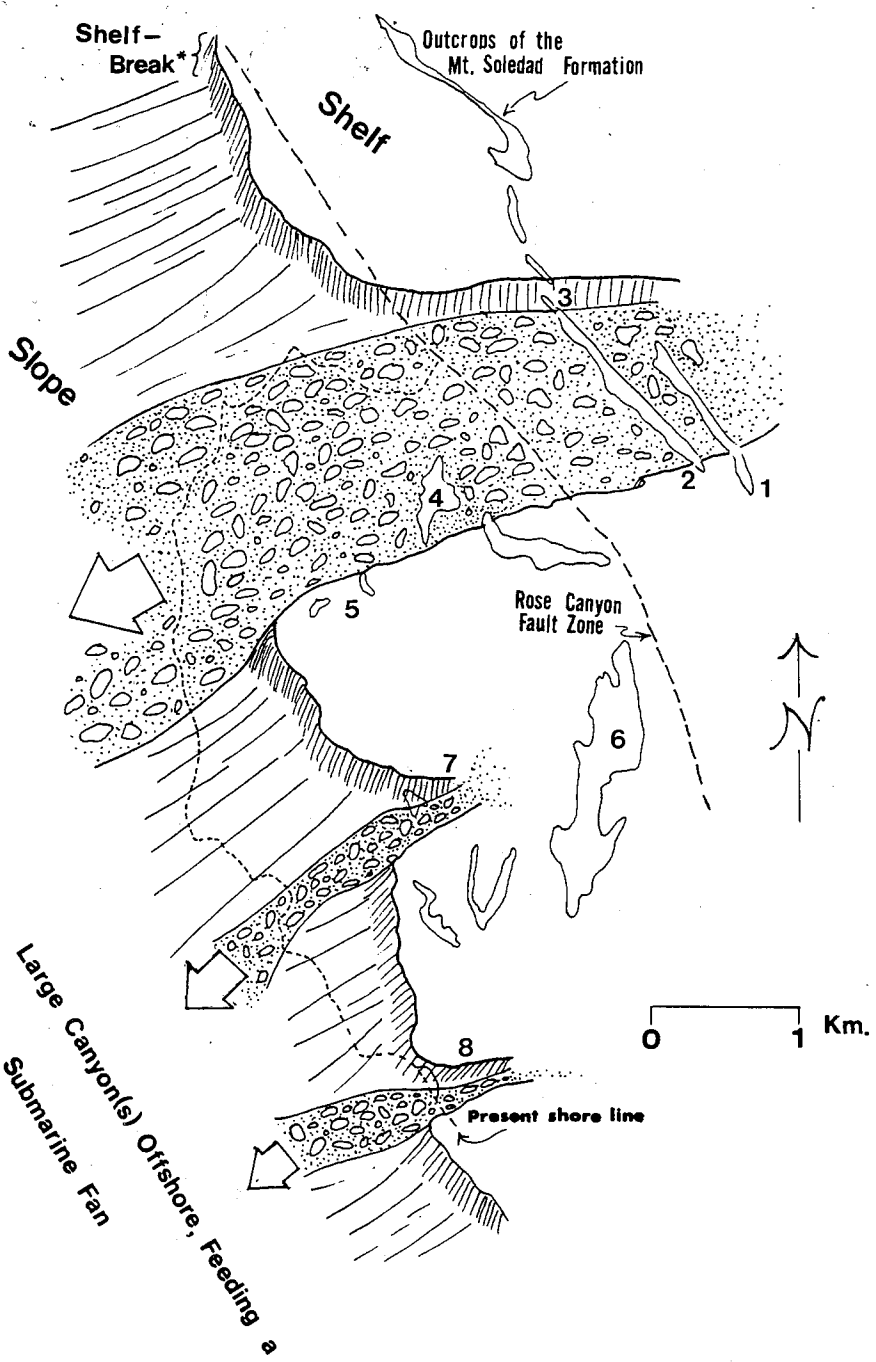

Figure 5. Paleogeographic and palinspastic map of the Lower Eocene Mt. Soledad Formation. The diagram represents the average paleogeography during the latter half of the Early Eocene. The locality numbers correspond to the text and their present-day positions noted on Figure 1. The Romero St. outcrops (4) are aligned with those of Morena Blvd. (1-3) suggesting 4 km (± 1 km) of right-lateral slip within the Rose Canyon Fault Zone. The dotted line denotes where offset occurred. Location of this early fault is difficult as continued deformation and post-faulting sedimentation has obscured much of the original trace. The Mt. Soledad Fault and southern half of the Country Club fault probably record subsequent deformation on this older structure.

Northwest of Morena Blvd. the pinchout of the submarine feeder channel margin is found (locality 3, Fig. 1). At this locality two meters of Mt. Soledad conglomerate represent the feather-edge of the feeder channel and separate the estuarine facies from overlying passive slope/canyon fill deposits assigned to the Ardath Shale by Kennedy (1975). North of locality 3 in Rose Canyon, the remainder of the Mt. Soledad Formation records terrestrial and paralic depositional environments. Conglomerate which appears to be related to the feeder channel/canyon environment is encountered just west of Mt. Soledad (locality 4, Figure 1). The feeder canyon conglomerates at this locality are juxtaposed against paralic conglomeratic facies to the east by the Mt. Soledad Fault. To the south of locality 4 and laterally equivalent to the channel conglomerates are shelf sandstones which rest directly on an Early Eocene shelf-break underlain by Cretaceous conglomerate (locality 5 , Figure 1). These shelf sandstones are also laterally equivalent to paralic facies conglomerates to the east (locality 6, Figure 1). The outlined stratal and paleoenvironmental relationships allow palinspastic restoration of the Early Eocene depositional setting west of the Rose Canyon fault. The canyon facies at localities 1 and 4 (Figure 5) are aligned which suggests 4 km of right lateral slip within the Rose Canyon Fault Zone. To the north and south, the feeder canyon is bounded by shallower water facies (localities 5 and 6, Figure 5). To the southwest and slightly basinward are small feeder channel canyon environments (localities 7 and 8, Figures 1 and 5) which are seen today at La Cañada Ave. (locality 7) and Tourmaline Beach (locality 8).

REFERENCES

Dikas, A. B. and Payne, J. L., 1967, Upper Paleocene buried channel in Sacramento Valley, California: Amer. Assoc. Petroleum Geologists Bull., v. 5, p. 873-882.

Gray, L. D., 1979, Clay mineralogy of the Point Loma and Cabrillo Formations, in Abbott, P. L. (ed), Geological Excursions in the Southern California Area: Geol. Soc. America Guidebook, p. 180-181.

Hoyt, W. V., 1959, Erosional channel in the Middle Wilcox near Yoakum, La Vaca County, Texas: Gulf Coast Assoc. Geological Soc. Trans., v. 9, p. 41-50.

Kennedy, M. P., 1975, Geology of the San Diego Metropolitan Area, California: California Div. Mines and Geology Bull. 200, 56 p.

Kies, R. P., 1982, Paleogene Sedimentology, Lithostratigraphic Correlations and Paleogeography: San Miguel Island, Santa Cruz Island and San Diego, California (M.S. Thesis): San Diego State University, 510 p.

Peterson, G. L., 1979, Salt weathering textures in Eocene conglomerates, southwestern California, in Abbott, P. L. (ed.), Eocene Depositional Systems, San Diego, California: Soc. Econ. Paleontologists and Mineralogists Field-trip Guidebook, p. 115-117.

Peterson, G. L. and Abbott, P. L., 1979, Mid-Eocene climatic change, southwestern California and northwestern Baja California: Paleogeography, Paleoclimatology, Paleoecology, v. 26, p. 73-87.

Sabate, R. W., 1968, Pleistocene oil and gas in coastal Louisiana: Gulf Coast Assoc. Geological Soc. Trans., v. 18, p. 373-386.

Walker, R. G., 1978, Deep-water sandstone facies and ancient submarine fans: models for exploration for stratigraphic traps: Amer. Assoc. Petroleum Geol. Bull., v. 62, p. 932-966.

THE ROSE CANYON FAULT ZONE
DOWNTOWN SAN DIEGO AND CORONADO

by

Daryl Streiff, Woodward-Clyde Consultants
San Diego, California 92110
Dorian Elder-Mills, San Diego State University
San Diego, California 92182
Ernest R. Artim, Leighton and Associates
Diamond Bar, California 91789

INTRODUCTION

The Rose Canyon fault zone is mapped onshore from Point La Jolla southeastward along Mission Bay into the Old Town area of San Diego (Kennedy, 1975). To the south, the fault zone is inferred to trend, in part, through the downtown area of San Diego, across San Diego Bay, and Coronado.

The purpose of this program was to obtain geological data in order to further evaluate the location, style, and characteristic of faulting in the downtown area of San Diego and on Coronado. The extent of the study included:

- Examination and interpretation through the logging of the exposures in two trenches across previously mapped inferred or concealed locations of faults.
- Dating of soil samples by radiocarbon and amino acid racemization techniques, the degree of soil formation and faunal associations.
- Evaluation of the data as compared to the previously known information concerning Quaternary faulting in the San Diego area.

DESCRIPTION OF SAN DIEGO TRENCH

A 1,645-meter (5,400-foot) trench that varied in depth from 1.9 to 6.7 meters (6 to 22 feet) was excavated between February 12 and October 10, 1980 by a private contractor for the City of San Diego as part of a sewer line improvement project. The trench traversed the downtown area starting at the intersection of Kettner Boulevard and "E" Street and continued east to 12th Avenue (Figure 1). The trench was excavated nearly prependicular to several projected fault traces of the Rose Canyon fault zone (Kennedy, 1975). The trench was logged on a scale of 1" = 5' and detailed logging of sedimentary features was recorded in accordance to the time allowed within the trench. Time constraints were imposed by the contractor and the stability of the trench walls. Soil and shell samples were collected for dating.

STRATIGRAPHY OF SAN DIEGO TRENCH

The following eleven marine and terrigenous stratigraphic units were observed in the trench. Descriptions are provided for future references and are in part related to selected logs of the trench. Where possible, absolute ages of the materials are given.

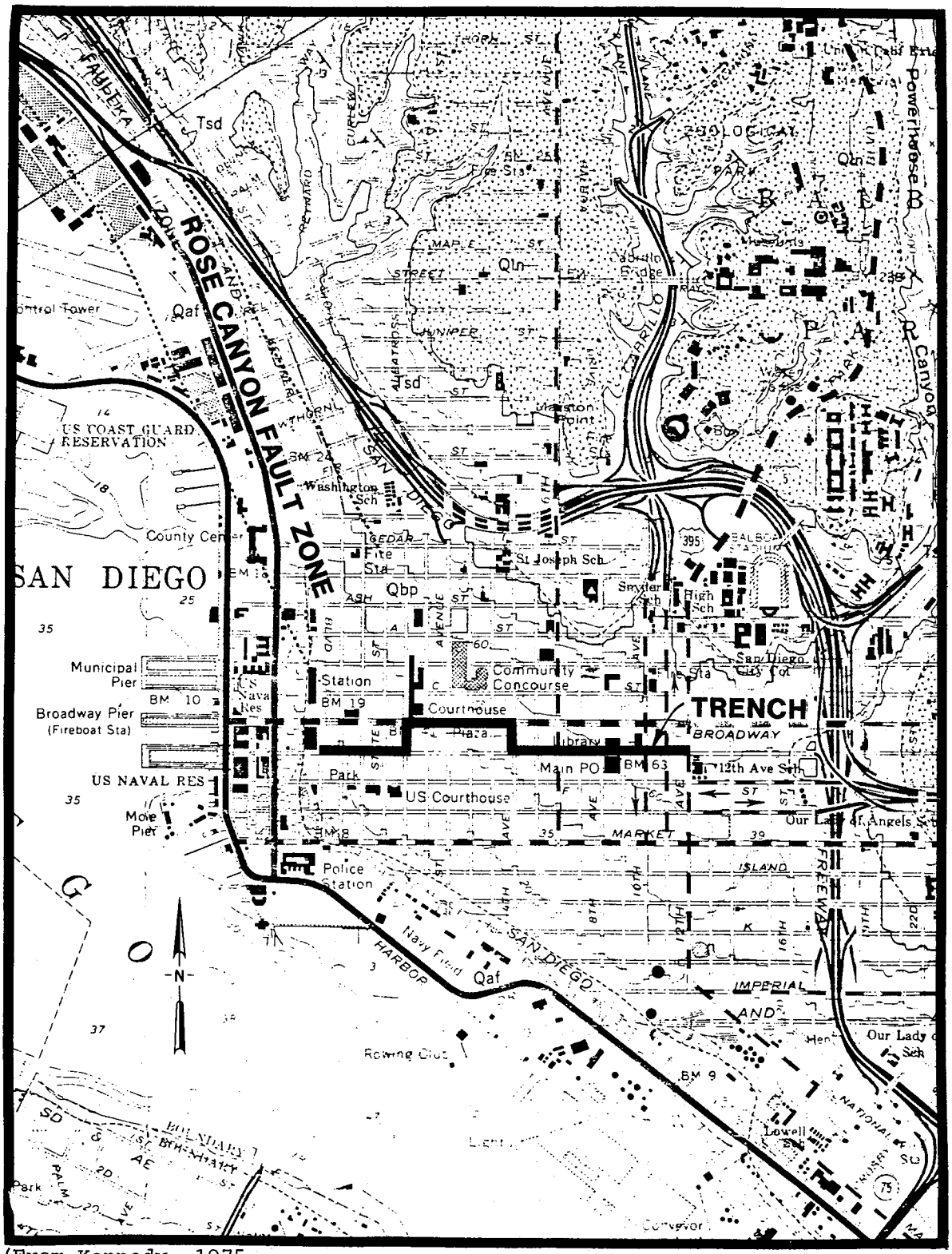

(From Kennedy, 1975, Point Loma Quadrangle)

FIGURE 1. DOWNTOWN SAN DIEGO TRENCH LOCATION

Holocene Aeolian and Alluvial Deposits (a). This unit represents the youngest material observed in the trench. The deposits consist of friable, porous, reddish-brown, clayey to silty, fine-to-medium grained sand. A discontinuous stone and pebble line occurs at the base of this unit. Worm and small animal burrows are common, as are decayed roots. These sands vary in thickness from 20 cm (8 inches) to 1 meter (39 inches) and are poorly bedded. A weakly developed soil profile 10 cm (4 inches) thick, occurs on the unit and consists of a thin "A" horizon that grades into a poorly developed "C" horizon. No development of a "B" (clay) horizon was observed. Similar soils within the San Diego area indicate approximate radiocarbon dates of 2,000 to 3,000 years (Artim and Streiff, 1981, p. 21). There is no evidence of displacement due to faulting within this unit.

Holocene Embayment Deposit (Q_1). This unit was exposed in the first 20 meters (65 feet) of the trench below elevation 8 feet (MSL Datum). The deposit consists of grayish-brown, fine grained clayey sand. The sand has a decaying organic odor similar to the bay muds currently being deposited. Lenses of silty, gray, fine-grained sand are common in this unit. No evidence of faulting was observed in these materials.

Paleosol (S_1). This buried soil horizon consists of reddish-brown to dark-brown, fine-grained sandy clay. The unit varies from 0.6 meters to 0.9 meters (2 to 3 feet) in thickness. The soils are moderately well developed and include an argillic "B" horizon that has developed angular to subangular blocky structure. Calcium carbonate and manganese-oxide stainings are dispersed throughout the soil horizon as a result of the weathering of the sand grains. Concentrations of these salts has resulted in localized cemented zones. The S_1 paleosol was exposed along the majority of the trench, having developed on both older paleosols and formational units. Based on a comparison of the degree of soil profile development elsewhere in San Diego, the paleosol is at least 10,000 years old and may be even as old as oxygen isotope stage 5 or 75,000 to 128,000 years old (Shackleton and Opdyke, 1973). No displacement was observed within this paleosol.

Pleistocene Channel Fill and Estuary Deposits (Q_{3a}, Q_{3b}, Q_{3c}, Q_{3d}). This non-marine unit consists of interbedded sands, gravels and clays. The unit consists of brown to dark brown, gravelly fine to coarse-grained sand, and grayish-brown to dark brown, sandy to silty clay. The sand and gravel units appear to be of an alluvial origin, whereas the silt and clay appear to be of an estuarine to lagoonal origin containing up to 15 percent organic materials. The sand and gravel usually occur as partially oxidized, weakly cemented and localized channel-fill deposits. Sedimentary structures within these deposits include cross-bedding, stratification, sand lenses and graded bedding.

The estuarine nature of the silt and clay is characterized by their organic content and gray to black color which indicates a reducing environment. The irregular and unconformable contact between these materials and adjacent materials indicates that the estuarine materials were deposited in an erosional channel. Unit Q_{3a} has been dated using radiocarbon analysis to be 19,000 ± 2,100 years old.

Figures 2 and 3, located at the intersection of "E" and State Streets, demonstrates a contact between the younger Q_{3a} unit and the older Qt unit.

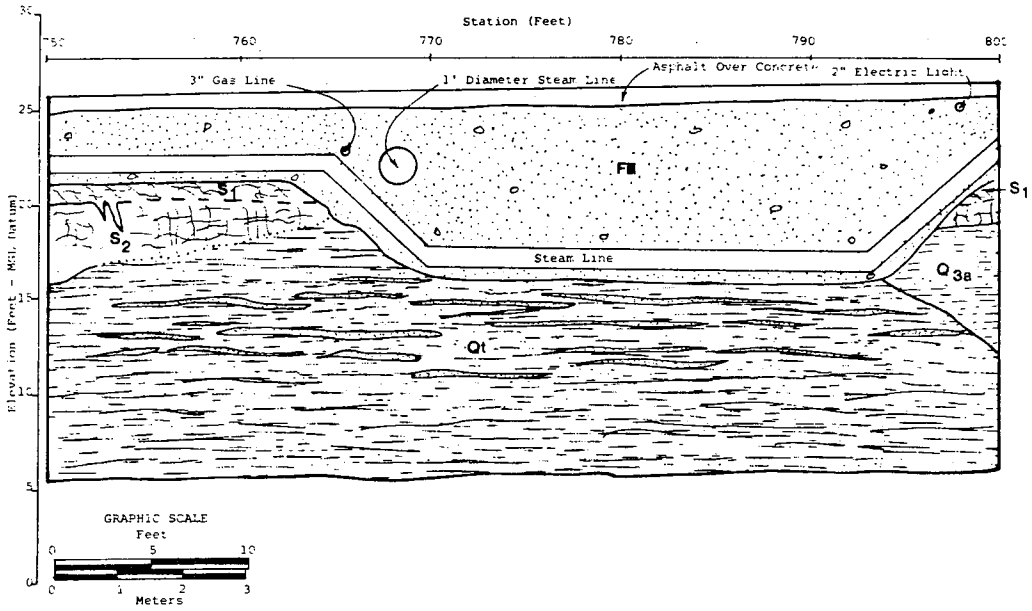

FIGURE 2. TRENCH LOG (NORTH WALL)
STATION 750 TO 800

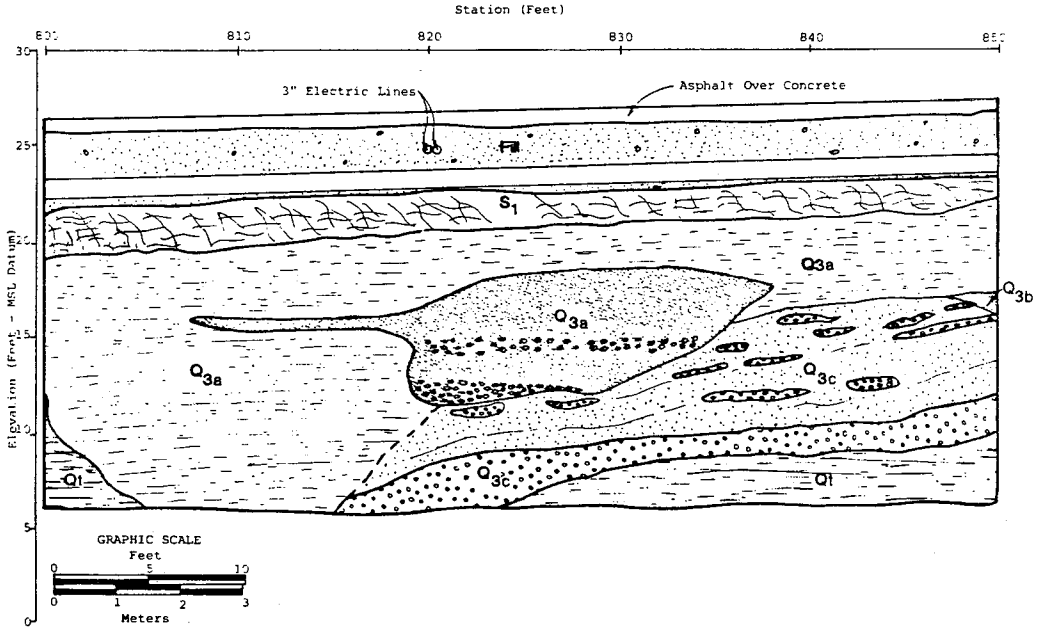

FIGURE 3. TRENCH LOG (NORTH WALL)
STATION 800 TO 850

The western contact is an erosional feature where a channel had been scoured into the Qt and the Q_{3a} unit was then deposited. The eastern contact appears to be an erosional feature, however it could be interpreted as being a fault contact due to its very linear nature and the termination of the Q_{3b} unit. Qt occurs on both sides of the channel fill, however the lithologies above the Qt are different. The deposits east of the Q_{3a} channel, above Qt, are different than those west of the channel, indicating either faulting, a larger channel fill, or possibly a facies change. A sand channel fill, the upper Q_{3a} materials, and the S_1 soil is continuous over all these units, indicating that it is not broken by a fault, if one is present at this location.

Alluvial Deposit (S_{1a}). This deposit consists mainly of dark brown to dark yellowish-brown, clayey to silty, fine-to-medium-grained sand. The deposit is porous and massively to poorly bedded. Animal burrows that have been subsequently backfilled by overlying material are common. Reddish-brown staining occurs sporadically as a result of concentrations of hematite and poorly formed manganese nodules. This deposit pre-dates the S_1 paleosol that has been found, in part, developed upon the S_{1a} alluvial deposit.

Older Paleosol (S_2). This paleosol consists of a hard, dark-brown, fine-to-medium-grained sandy clay. The paleosol has a well-developed, coarse blocky to prismatic structure within the argillic "B" horizon. The lower portion of the paleosol grades into a hard, sandy clay; being a moderately well-developed soil with angular to blocky structure in the "B" horizon.

The paleosol has generally formed on a friable, tan, silty fine-grained sand. Based on the degree of soil development, the paleosol is estimated to be at least 100,000 years old and displays no evidence of being faulted.

Pleistocene Alluvial Deposit (Q_2). These non-marine alluvial sands are fine-to-coarse-grained, light reddish-brown and are interbedded with sand and gravel lenses. These lenses are nearly horizontally bedded and are slightly oxidized, resulting in thin, red-brown laminae that create a cementation within the unit.

The paleosol (S_2) has developed upon these alluvial deposits, creating a gradational contact between the paleosol and the underlying alluvial materials. No evidence of faulting has been observed in the Q_2 unit.

Paleosol (S_3). This paleosol consists of a hard, red-brown to grayish-brown, fine-grained sandy clay. The upper 30 to 45 centimeters (12 to 18 inches) have a blocky to prismatic structure with thick, continuous clay skins and an overall well developed argillic "B" horizon. Abundant manganese oxide stains and nodules occur in the "B" horizon. This is the youngest unit that has been faulted (Figure 4) and has a minimum stratigraphic separation of 60 centimeters (24 inches). This well developed paleosol may be as old as several hundred thousand years, based on its soil development (Dr. Frank Swan, 1980, personal communication).

Middle to Late Pleistocene Marine Deposits (Qt_a, Qt, Qt_b). The youngest unit within this group of deposits, Qt_a, consists of brown to red-brown

clayey and silty sand. The unit varies from 1 to 5 meters (3 to 15 feet) in thickness, depending on the amount of erosion that has taken place since its deposition. The Qt unit consists of gray to light brown, fine-to-medium-grained silty and clayey sand. Bedding thickness varies from a few millimeters to several centimeters. The sand is micaceous and locally contains fossiliferous lenses. The basal portion of this deposit, Qt_b, consists of well rounded cobbles and boulders surrounded by a cemented medium-grained clayey sand matrix. The basal conglomerate varies from 0.6 meter to 1 meter (2 to 3 feet) thick and appears to dip 2°-3° to the west. This deposit unconformably rests upon the San Diego Formation (Figure 5).

This marine and non-marine unit underlies most of the downtown San Diego area. These sediments have been mapped in the past as the Bay Point Formation and have been dated at approximately 120,000 ± 10,000 years old (Kern, 1973). The sediments dated by Kern on Point Loma as the Nestor Terrace have been mapped as being synchronous with those in the downtown area by Kennedy (1975). K.R. Lojoie of the U.S. Geological Survey (personal communication) is of the opinion that the marine sediments in downtown San Diego may be significantly older than 120,000 years.

In order to evaluate ages of the Qt unit exposed in the trench, fossils were collected where exposed in two areas during trenching operations. Fossils were collected on "E" Street between Columbia and State Streets and were dated by Dr. Jeff Bada using amino acid racemization analyses and Dr. T. L. Ku using uranium-thorium analyses to be 200,000 to 300,000 years old. At Broadway and Second Avenue, fossils dated by Dr. Bada and Dr. John Wehmiller using the amino acid racemization analyses determined these to be 560,000 ± 75,000 years. Tom Demere of the San Diego Museum of Natural History has curated the fossils and agrees with the absolute age dates assigned to the fossils.

The range in age of this Qt deposit indicates a transgressing-regressing sea. This deposit onlaps the San Diego Formation and suggests a nearshore, protected environment. The "E" Street faunal assemblages indicate a protected marine environment within the Pleistocene San Diego Embayment. The Broadway fauna can be correlated to other deposits in the San Diego area that have been dated as greater than 500,000 years old, including the Chollas Valley unit (Artim and Streiff, 1981).

The Qt unit has been faulted (Figure 4) with an apparent stratigraphic separation of 2 to 3 meters (6 to 10 feet). Subsequent work indicates 9 to 10 meters (30 to 33 feet) of apparent normal separation within the Qt unit.

Pleistocene Deposit (Qtt). This unit ranges from a light to dark reddish-brown, sandy to clayey cobble conglomerate to a clean, pebbly, medium to coarse grained sand. The beds are iron stained and are locally cemented by iron oxide. The sediments are stratigraphically equivalent to Qt and occur, in general, above elevation 65 feet (Figure 6). The deposit appears to represent a terrestrial depositional environment that occurred during deposition of the main Qt unit.

Pliocene San Diego Formation (Tsd). The San Diego Formation underlies the downtown San Diego area at depth. It first appears in the trench at elevation 25 feet (MSL Datum) near Broadway and Second Avenue. The San Diego Formation is a fine grained, silty sand, micaceous, and locally cemented. The San Diego Formation appears to be a Middle to Late Pliocene

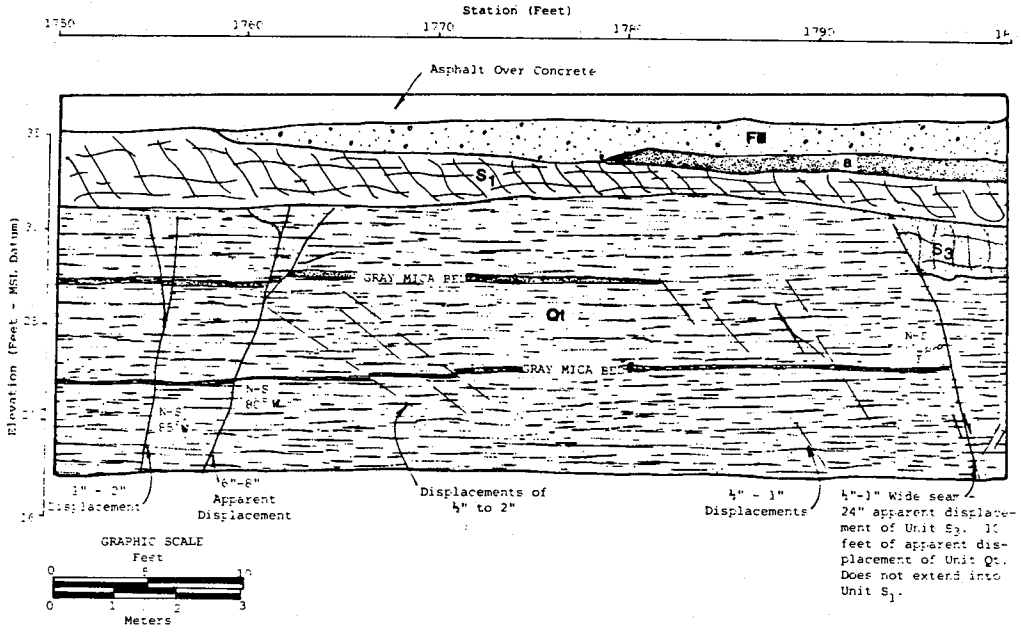

FIGURE 4. TRENCH LOG (NORTH WALL) STATION 1750 TO 1800

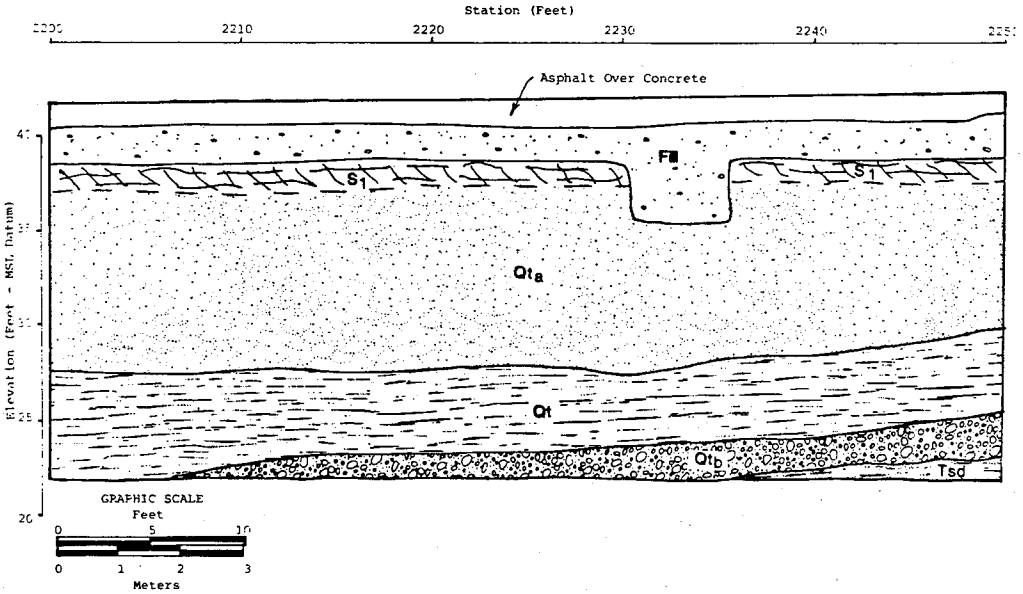

FIGURE 5. TRENCH LOG (NORTH WALL) STATION 2200 TO 2250

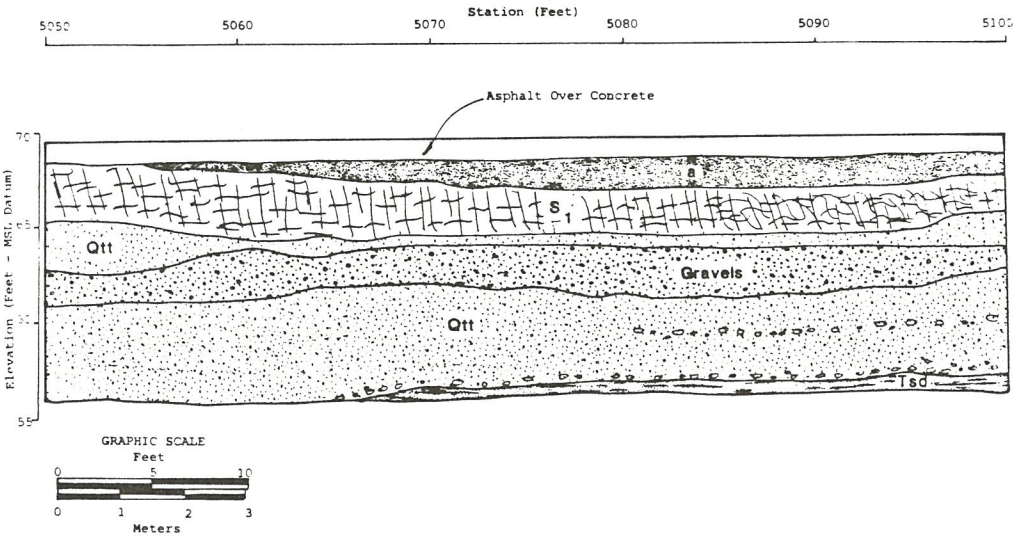

FIGURE 6. TRENCH LOG (NORTH WALL)
STATION 5050 TO 5100

aged unit that may extend into the Early Pleistocene. The approximate age ranges from 1.5 to 4 million years old.

SUMMARY OF FINDINGS - SAN DIEGO TRENCH

One distinct area of faulting was observed during the trench logging. The general vicinity of faulting was Broadway between Front and First Streets. The faulting is contained within a 48-meter (60-foot) wide zone. As shown on Figure 5, apparent movement on the primary shear of the fault is normal with the downthrown block to the east. The primary shear is 0.6 to 1.3 cm (¼ to 1 inch) wide and several paper thin shears were observed to the west and east of the primary shear. Weathered zones extend down into the shears and some alteration to clay has occurred. Neither clay gouge nor slickensided surfaces were observed along the shears.

The amount of displacement on the geologic units exposed in the trench appears to increase in older units as does the rate of displacement. The upper paleosol (S_1) is estimated to be at least 20,000 years old and did not show evidence of stratigraphic separation. An older paleosol (S_3) estimated to be at least 75,000 to 128,000 years old is displaced a minimum of 60 cm (23 inches), which is a rate of displacement of 0.005 to 0.008 mm per year. Results from a trench study of this fault for an adjacent project by Woodward-Clyde Consultants indicates that the upper Qt unit has an apparent vertical displacement of 2 to 3 meters (6 to 10 feet). Subsequent excavation of the city block to the south for a commercial building revealed that the lower part of the Qt unit could be correlated with materials exposed to the east in the sewer trench excavation. Projection of the units based upon observed dips indicated that the lower unit has an apparent vertical stratigraphic separation of 9 to 10 meters (30 to 33 feet). Assuming the upper materials to be closer to the 360,000 upper age of this unit, the displacement rate is 0.008 to 0.01 mm per year. Correlating the lower part of the unit to 560,000 years old indicates a displacement rate of 0.02 mm per year. As a relative index of fault activity, these rates are compared to rates of other San Diego faults (Figure 7).

Based on its lack of surface expression, low rates of displacement, sense of displacement, and lack of direct tie-in to more pronounced fault features in the San Diego area, we consider this fault to be an antithetic or subsidiary feature. Such features should not be considered unusual in the extensional stress environment that is present in the southern San Diego area. Similar faults with very short horizontal extent and limited vertical displacement have been identified in the southern part of San Diego and may also be located elsewhere in downtown San Diego.

We found no other significant evidence of faulting in the trench exposures, thus leading us to conclude that major north-south faulting does not extend through Middle to Late Pleistocene deposits exposed along the trench in the downtown San Diego area.

DESCRIPTION OF CORONADO TRENCH

A trench 61 meters (200 feet) long and 3 meters (10 feet) deep was excavated across the concealed Coronado fault of the Rose Canyon fault zone (Kennedy and Welday, 1980) in the City of Coronado. The fault was identified by Kennedy and Welday (1980) as a topograhpic expression with a west

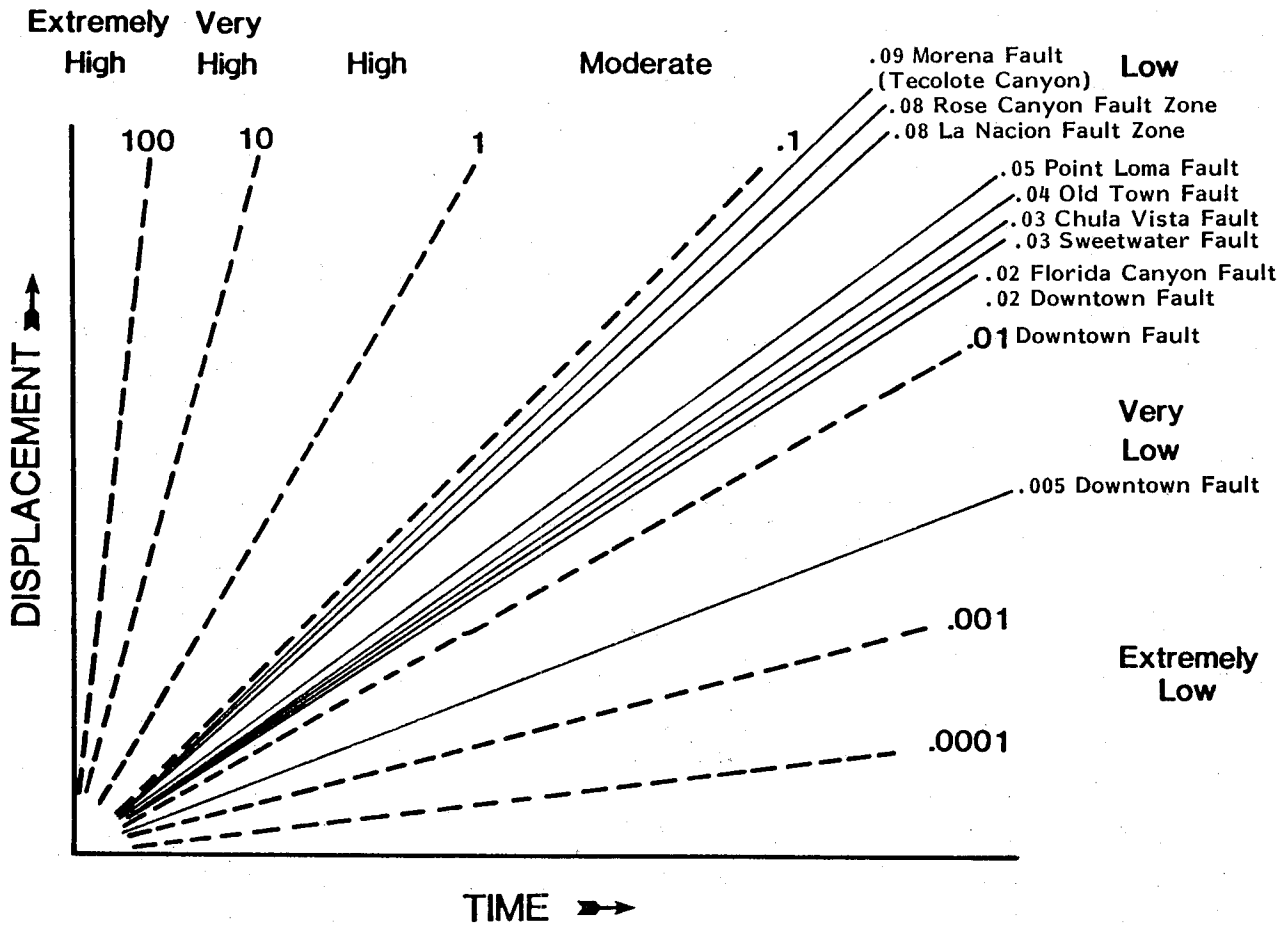

DEGREE OF ACTIVITY SLIP RATE IN MM/YEAR

FIGURE 7

side up change in elevation. The trench was excavated across this topographic expression (Figure 8) between November 17 and December 12, 1980. The trench was perpendicular to a gentle break in slope and extended from the high elevation on the west to the lower eastern elevation. Shell samples were collected and dated using amino acid racemization techniques.

STRATIGRAPHY OF CORONADO TRENCH

Four significant stratigraphic units were exposed in the trench. These units are described below in order of increasing age. The unit name is followed by a symbol used to identify that unit on the trench logs which are included as Figure 9. Where materials for absolute dating were lacking, other methods, such as degree of weathering (soil formation), and stratigraphic or paleontologic correlations, were used to estimate the ages of materials.

Holocene Aeolian Deposit (a_1). This unit consists of very porous, friable, pale brown, silty, very fine grained sand, deposited unconformably on an erosional scarp.

The deposit appears to overlie and to be younger than an alluvial deposit (a_2). The age of the aeolian unit may vary from a few hundred to a few thousand years old.

Holocene Alluvial Deposit (a_2). This unit consists of silty fine sand that is porous, friable, and light reddish-brown. A poorly formed soil profile has begun to develop in the upper 5 cm and consists of grayish-brown, slightly clayey, silty sand exhibiting local manganese oxide staining. The profile grades from an "A" horizon to a "C" horizon with no distinct "B" horizon present.

Based on the degree of weathering and soil profile development, this unit is estimated to be less than 5,000 to 10,000 years old.

Paleosol (S). This paleosol consists of dard reddish-brown, clayey sand. The soil has a poorly to moderately well developed, medium angular to crumbly structure, and thin clay skins. Manganese oxide staining is concentrated along the base of this paleosol.

Based on the degree of weathering, this paleosol is estimated to be at least 10,000 years old.

Middle to Late Pleistocene Marine Deposit (Qt). This unit consists of sand that is light gray to light reddish-brown, silty fine to coarse grained and contains thin, scattered pebble layers. The beds are friable and tend to be lenticular. The light reddish brown color appears to be secondary and confined to within 3 meters of the ground surface. Bedding thickness varies from a few millimeters to several centimeters. Some small shell fragments were present in the trench, and a test boring excavated into this unit at the west end of the trench recovered fossil shells from elevation +5 to elevation -8 feet (MSL Datum). A faunal assemblage in similar materials was recovered from an excavation at 10th Street and "B" Avenue in the City of Coronado. Fossil shells were also recovered from lithologically similar deposits at Ynez Place and Pomona Avenue.

The results of several amino acid age dates performed on shells from this unit indicated ages of approximately 220,000 ± 30,000 years. These

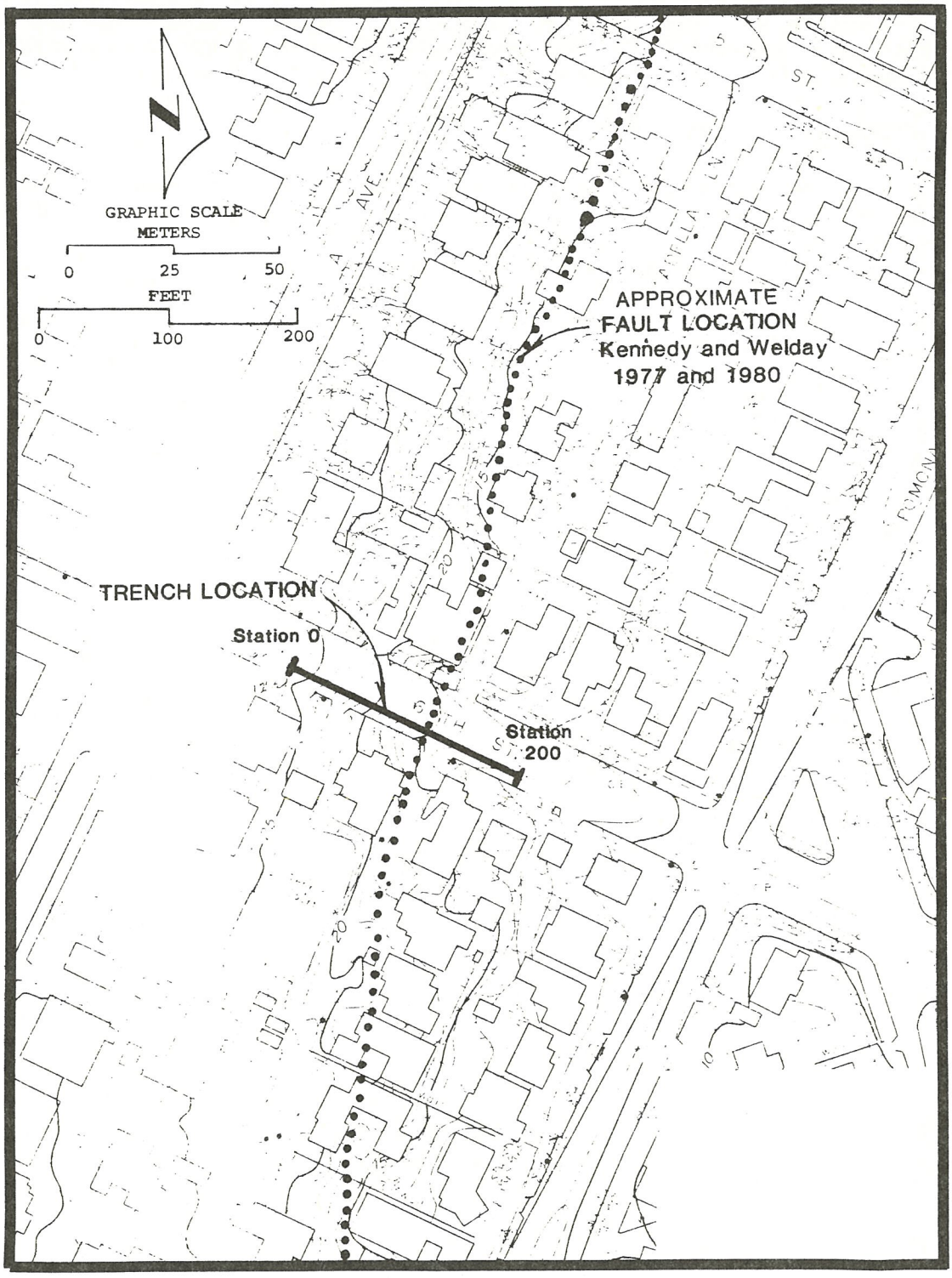

FIGURE 8. CORONADO TRENCH LOCATION

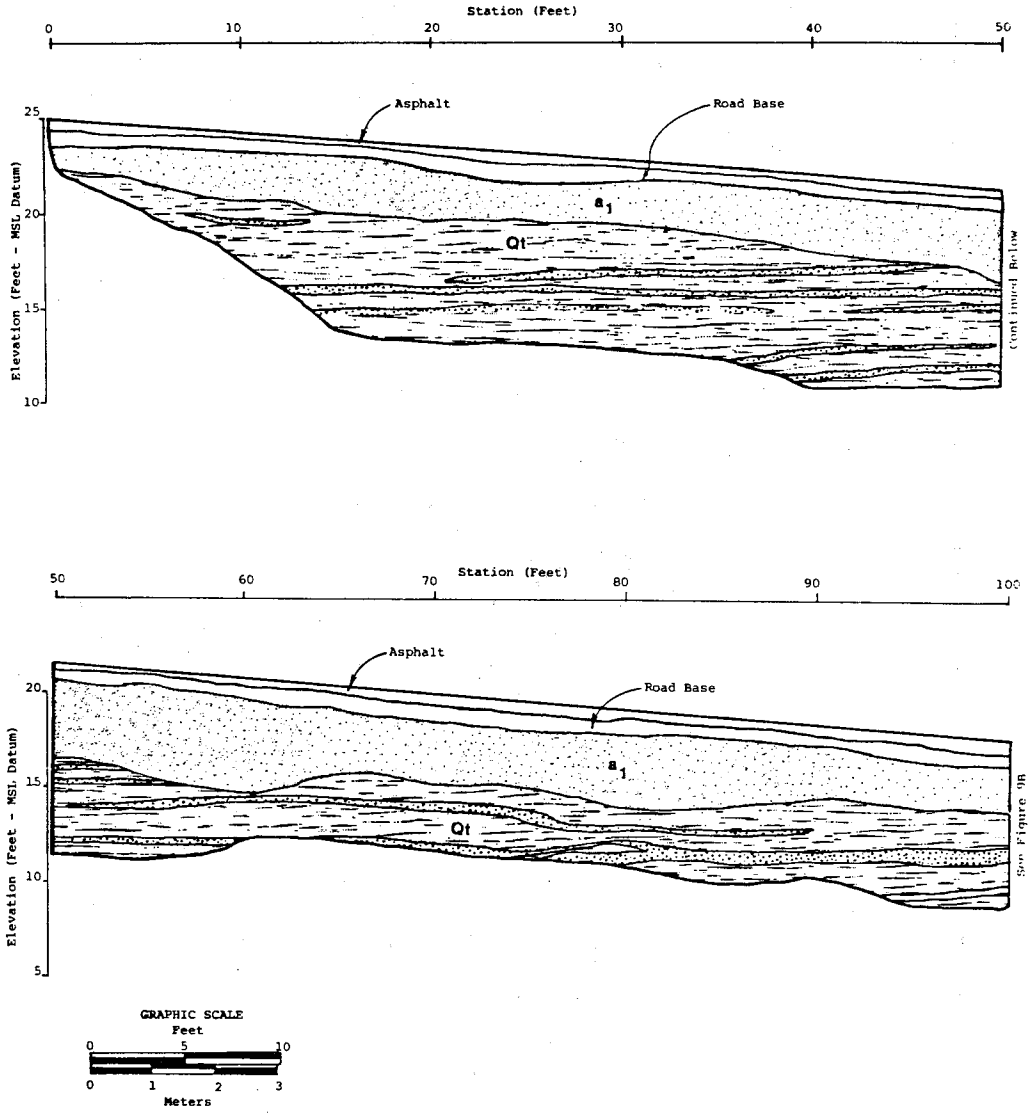

FIGURE 9A. TRENCH LOG (NORTH WALL) STATION 0 TO 100

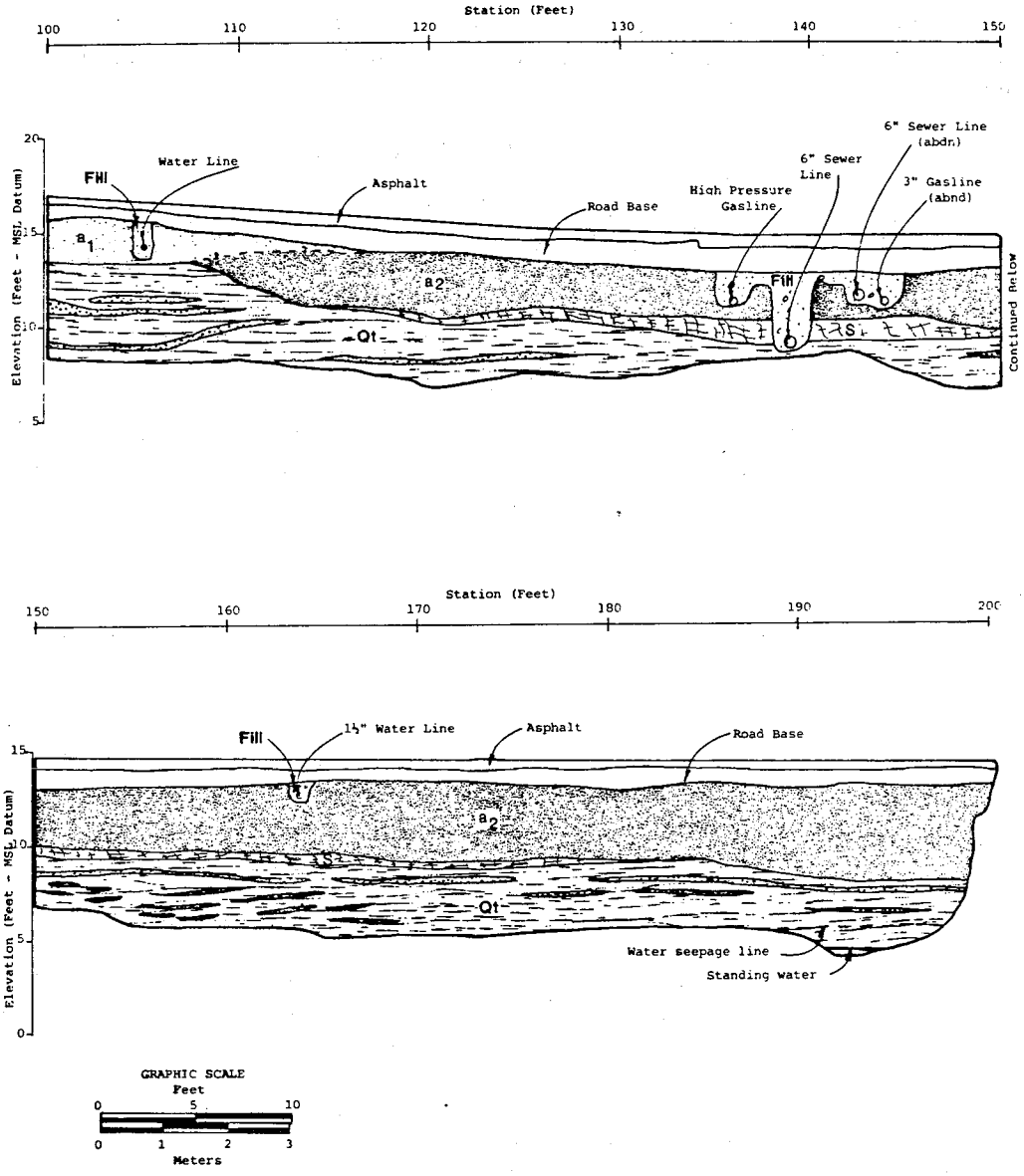

FIGURE 9B. TRENCH LOG (NORTH WALL) STATION 100 TO 150

results are comparable to unpublished amino acid dates obtained in the general area of the City of Coronado (Artim and Streiff, 1981).

SUMMARY OF FINDINGS - CORONADO TRENCH

No evidence was found to support previous hypotheses that the scarp through the City of Coronado is a fault, or is a fault-related feature. However, evidence was found to suggest that the scarp is an erosional feature not unlike numerous other low bluffs in the existing San Diego shoreline area.

ACKNOWLEDGMENTS

This work was supported by the U.S. Geological Survey's National Earthquake Hazards Reduction Program (Contract No. 14-08-0001-19118). A more extensive report which contains a complete set of logs for the San Diego trench is available as U.S.G.S. Open-file Report No. 81-878.

REFERENCES

Artim, E.R. and Streiff, D., 1981, Trenching the Rose Canyon Fault zone, San Diego, California, U.S. Geological Survey, Open-file Report No. 81-878, and Final Technical Report, U.S.G.S. Contract No. 14-08-0001-19824.

Kennedy, M.P., 1975, Geology of the San Diego Metropolitan Area, California: California Division of Mines and Geology, Bulletin 200, Section A, pp. 1-39.

Kennedy, M.P. and Peterson, G.S., 1975, Geology of the San Diego Metropolitan Area, California: California Division of Mines and Geology, Bulletin 200, Section B, pp. 45-56.

Kennedy, M.P., Clark, S.G., Greene, H.G., and Legg, M.R., 1980, Recency and character of faulting offshore metropolitan San Diego, California: California Division of Mines and Geology, Map Sheet 42.

Kennedy, M.P., Greene, H.G., Clarke, S.H. and Bailey, K.A., 1980, Recency and character of faulting offshore metropolitan San Diego, California: California Division of Mines and Geology, Map Sheet 41.

Kennedy, M.P. and Welday, E.G., 1980, Recency and character of faulting offshore metropolitan San Diego, California, California Division of Mines and Geology, Map Sheet 40.

Kern, J.P., 1973, Late Quaternary deformation of the Nestor terrace on the east side of Point Loma, San Diego, California, in Ross, A. and Dowlen, R.J., eds., Studies on the geology and geologic hazards of greater San Diego area, California: San Diego Association of Geologists Guidebook, p. 43.

Kern, J.P., 1977, Origin and history of upper Pleistocene marine terraces, San Diego, California: Geol. Soc. America Bull., Vol. 88, pp. 1553-1566.

Kies, R., 1979, The Rose Canyon fault zone from Point La Jolla to Balboa Avenue, San Diego: San Diego State University Geology Department, Undergraduate Research Report.

Moore, G.W., 1972, Offshore extension of the Rose Canyon fault, San Diego, California: U.S. Geological Survey Professional Paper 800-C, pp. C113-C116.

Moore, G.W. and Kennedy, M.P., 1975, Quaternary faults at San Diego Bay, California: U.S. Geological Survey, Journal of Research, Vol. 3, No. 5, pp. 589-595.

Peterson, G.D., 1970, Quaternary deformation of the San Diego area, southwestern California: American Association of Petroleum Geologists (Pacific Section), Fall Guidebook, pp. 120-126.

Pinckney, C.J., Streiff, D. and Artim, E.R., 1979, The influence of bedding-plane faults in sedimentary formations on landslide occurrence, western San Diego County, California, Bulletin of the Association of Enginering Geologists, Vol. XVI, No. 2, pp. 289-300.

Schmalfuss, B.R., 1979, Late Quaternary slip on the Rose Canyon fault: San Diego State University Geology Department, Undergraduate Research Report, 21 pp.

Shackleton, N.J. and Opdyke, N.D., 1973, Oxygen isotope and paleomagnetic stratigraphy of equatorial Pacific Core J-28-238, Oxygen isotope temperature and ice volumes on a 10^5 year and 10^6 year scale: Quaternary Research, Vol. 3, p. 39.

Ziony, J.I., 1973, Recency of faulting in the greater San Diego area, California, in Ross, A. and Dowlen, R.J., eds., studies on the geology and geologic hazrads of greater San Diego area, California: San Diego Association of Geologists Guidebook, p. 68.

THE ROSE CANYON FAULT AT SPINDRIFT DRIVE, LA JOLLA, CALIFORNIA

by

Daryl Streiff, Woodward-Clyde Consultants
San Diego, California 92110
Mark Schmoll, Woodward-Clyde Consultants
San Diego, California 92110
Ernest R. Artim, Leighton and Associates
Diamond Bar, California 91789

INTRODUCTION

The Rose Canyon Fault zone comprises a number of closely spaced subparallel faults that displace Cretaceous and Tertiary strata near Mount Soledad. The fault zone, as mapped, continues offshore to the north, and it has been suggested that the fault continues to the south under San Diego Bay and offshore of Coronado. The Rose Canyon Fault zone has been shown on land to extend for approximately 15 km south of the La Jolla Cove and La Jolla Shores area (Kern, 1973; Ziony, 1973; Kennedy, 1975).

The Rose Canyon Fault is dominated by slightly northwest trending, en echelon faults and folds. Onshore, adjacent to La Jolla, the fault has been interpreted as having evidence of right-lateral displacement (Kennedy, 1975; Moore and Kennedy, 1975; Kern, 1977; Schmalfuss, 1979). The strike-slip style of deformation has been suggested on the basis of postulated displaced stratigraphic units (Kennedy, 1975), displaced geomorphic features (Kern, 1977; Keis, 1980), and reported horizontal slickensides (Kennedy, 1975).

Approximately 140 meters of vertical separation of the base of the Lindavista Formation has been recognized near Mount Soledad (Peterson, 1970). Evidence for vertical displacement has been documented at several locations (Kennedy, 1975; Kern, 1977); however, the sense of displacement (normal and reverse) varies throughout the zone. Kennedy (1975) reported that the rocks on the west side of the zone have moved relatively up in some areas and down in other areas. Kennedy (1975) indicates that continental-type igneous and metamorphic rocks form the basement on both sides of the fault zone.

Previous investigators have suggested evidence of tectonic displacement of the Rose Canyon Fault zone in Late Pleistocene and younger sediments (Kennedy, 1975; Moore and Kennedy, 1975; Kern, 1977; Kennedy and others, 1978; Schmalfuss, 1979). Published evidence includes scattered earthquake activity in the general San Diego area (Simons, 1979), and suggested displacement of postulated Holocene age sediments on the sea floor (Moore, 1972; Moore and Kennedy, 1975; Kennedy and Welday, 1980; Kennedy and others, 1980a and 1980b).

In order to define more clearly the style and recency of faulting within the zone, a trench was excavated across the mapped projection of the Rose Canyon Fault along Spindrift Drive in the La Jolla Shores area of San Diego, California (Figure 1). This paper is a synthesis of the work by Artim and Streiff (1981).

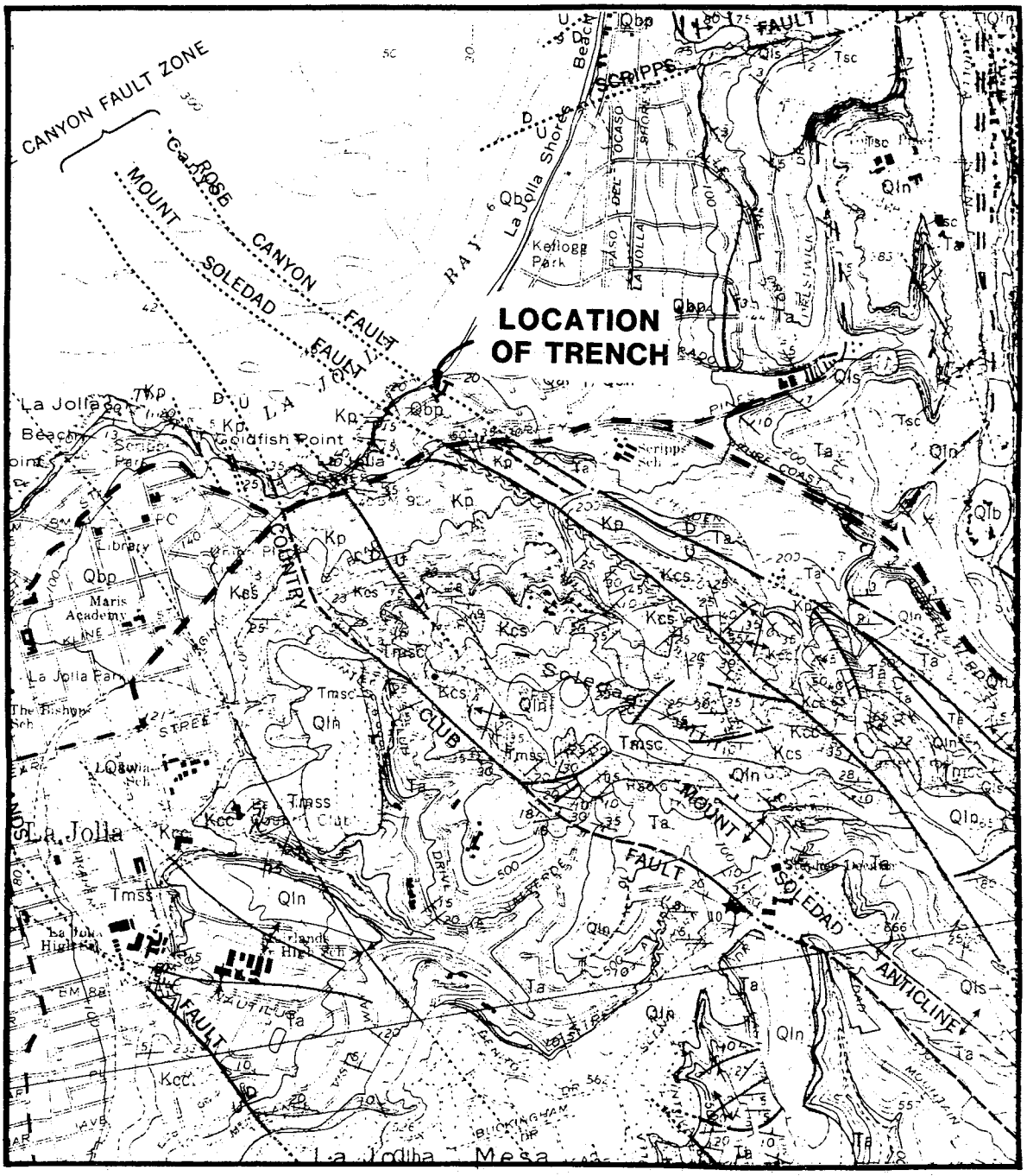

FIGURE 1. SITE LOCATION MAP NORTHWEST PORTION OF LA JOLLA 7.5-MINUTE QUADRANGLE (FROM KENNEDY, 1975)

FIELD INVESTIGATION

The field work was performed between August 10 and August 28, 1981. It was necessary to minimize the length of the trench due to the presence of many subsurface utility lines along Spindrift Drive. Consequently, the approximate location of faulting was delineated by carefully examining and mapping the adjacent sea cliffs. The next step consisted of drilling thirteen 6-inch-diameter test borings at 75-foot intervals along Spindrift Drive. This provided a subsurface profile of the Quaternary deposits and indicated the approximately extent of the Eocene Ardath Shale and Late Cretaceous Point Loma Formation. Based upon anomalous conditions between Borings 3 and 6, a trench location was selected between Roseland Drive to the northeast and St. Louis Terrace to the southwest (Figure 2).

A trench 228 feet long was excavated in approximately 50-foot sections. Depending on the stability of trench walls and water conditions, some sections remained open for several days while other sections (primarily areas of fill and water seeps) were open for only a few hours before being backfilled. The geologic conditions exposed in the trench were logged and evaluated and samples were collected for radiocarbon dating.

GEOLOGIC CONDITIONS IN THE TRENCH

STRATIGRAPHY

Four distinct geologic units were exposed within the vicinity of the zone of faulting in the trench and are shown on Figure 3. Recent fill soils placed during utility line and road construction are shown on the log but their description is not discussed.

Residual Soil and Slopewash (Ql). The youngest unit exposed along most of the trench consists of residual soil and slopewash. Two fire pits 2 to 3 feet below the road surface within this unit were partially excavated along with shell and bone fragments, quartzite rock chips, and a broken piece of ceramic. Based on information from Charles S. Bull (oral communication, 1982) of Regional Environmental Consultants, San Diego, the two firepits could be tentatively classified as Late Prehistoric Stage occupied by the Diegueno or Kumeyaay culture. The results of two radiocarbon dates performed on shells from the base of the soil unit, one in the vicinity of the fire pits and the other at the fault zone location, indicate ages of approximately 660 ± 75 and 1,140 ± 80 years, respectively.

Pleisocene Terrace Deposit (Qbp). Underlying Ql and occurring above the approximate elevation of 28 to 33 feet are sands mapped by Kennedy (1975), as belonging to the Late Pleistocene Bay Point Formation. No datable materials were found within this unit. The Bay Point Formation has been dated at approximately 120,000 ± 10,000 years old (Kern, 1973), and recent results of several amino acid age dates performed on shells from similar marine deposits in the San Diego area resulted in ages ranging from approximately 200,000 to 560,000 ± 75,000 years old (Artim and Streiff, 1981).

Eocene Ardath Shale (Ta). The Ardath Shale exposed within the trench consists of highly weathered, thinly laminated siltstone and claystone with thin interbeds of silty sandstone. The unit has a steep northeasterly dip and several clay-filled fractures and bedding plane faults (Pinckney et al., 1979) are exposed rougly subparallel to bedding.

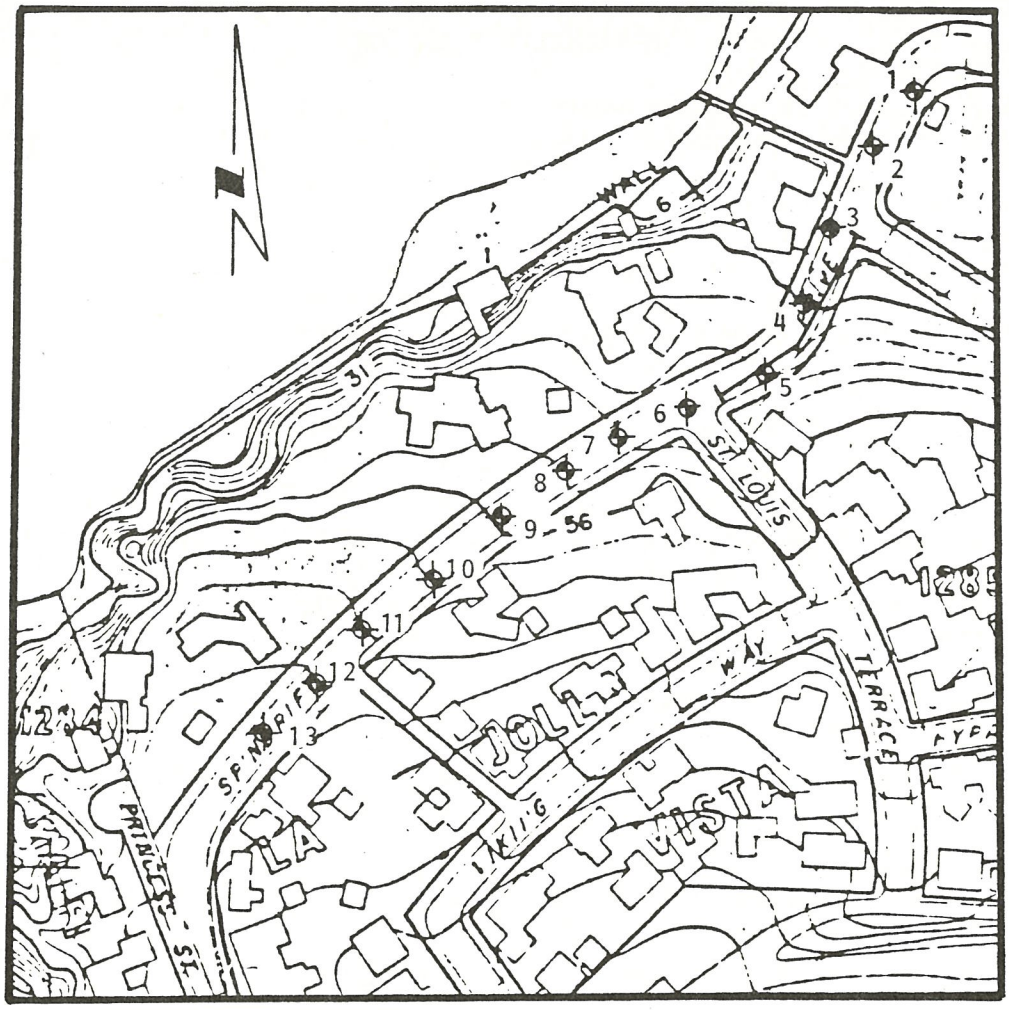

LEGEND:

INDICATES APPROXIMATE LOCATION OF TEST BORING.

INDICATES APPROXIMATE LOCATION OF TRENCH.

GRAPHIC SCALE (Feet)

0 100 200

FIGURE 2. TRENCH AND BORING LOCATIONS ON SPINDRIFT DRIVE

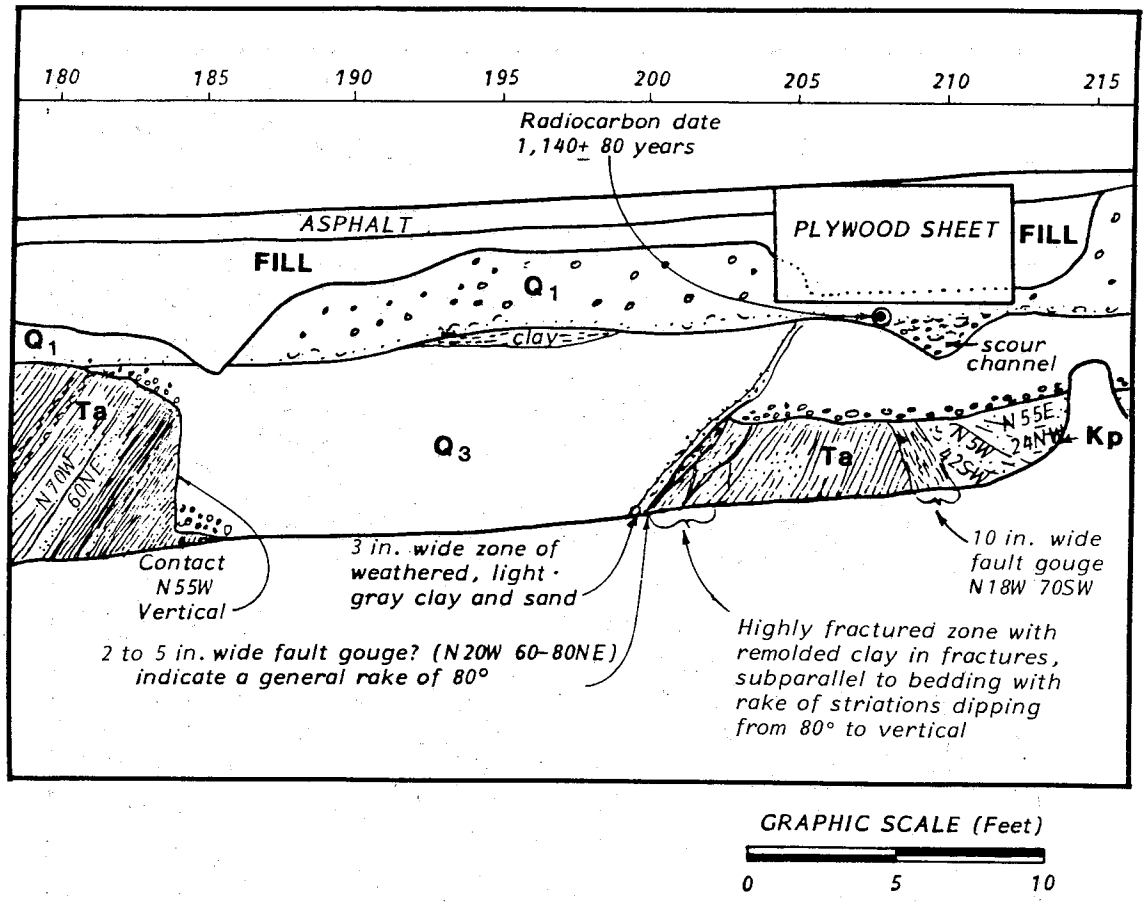

LEGEND:

Q_1 RESIDUAL SOIL AND SLOPEWASH DEPOSIT

DARK BROWN TO GRAYISH-BROWN, CLAYEY SILTY FINE-TO-MEDIUM- GRAINED SAND WITH FINE PIECES OF CHARCOAL, BONES, ASH, GRAVEL CHIPS, SHELL AND SHELL FRAGMENTS, AS WELL AS REMNANTS OF TWO FIRE PITS.

Q_3 PLEISTOCENE TERRACE DEPOSIT (BAY POINT FORMATION?)

LIGHT TO DARK REDDISH BROWN SILTY FINE-TO-COARSE GRAINED SANDSTONE. THE UNIT IS IRON-OXIDE STAINED AND IS LOCALLY CEMENTED BY CLAY AND IRON OXIDE. SOME OF THE SANDSTONE BEDS ARE MOTTLED LIGHT RED IN A GENERALLY DARK REDDISH BROWN SEQUENCE. THE BASE OF THIS UNIT IS MARKED BY A LAYER OF PEBBLE TO COBBLE CLASTS. THE CLASTS ARE GENERALLY WELL-ROUNDED AND RANGE FROM ABOUT 1 CM TO MORE THAN 15 CM.

Ta EOCENE ARDATH SHALE

WEAKLY FISSILE, OLIVE GRAY, THINLY LAMINATED SILTSTONE AND CLAYSTONE WITH THIN INTERBEDS OF SILTY SANDSTONE.

Kp CRETACEOUS POINT LOMA FORMATION

OLIVE-GRAY TO LIGHT YELLOWISH-BROWN, FINE-GRAINED SANDSTONE WITH A FEW THIN BEDS OF OLIVE GRAY SHALE.

FIGURE 3. PORTION OF EAST WALL OF TRENCH LOG
(FROM ARTIM AND STREIFF, 1981)

Late Cretaceous Point Loma Formation. This unit, which is in fault contact with the Ardath Shale, consists of fine grained sandstone with occasional thin interbeds of siltstone and claystone. The unit is exposed along the sea cliffs adjacent to Spindrift Drive and in the southern end of the trench.

FAULTING

Two distinct shears were observed in the trench at Stations 203 and 208 (Figure 3). The primary fault located at Station 208 separates the Ardath Shale and the Point Loma Formation. This fault trace strikes N18°W and dips 70° southwest and contains a fault gouge zone approximately 10 inches wide. The gouge zone contains numerous short omnidirectional striations and several longer striations with the rake ranging from 40° to 80°. Unfaulted Bay Point Formation overlies this fault.

A secondary shear at Station 203 displaces the Bay Point Formation adjacent to the Ardath Shale in an apparent normal fault which strikes N20°W and dips 60° to 80° northeast. This shear has an apparent vertical displacement of approximately 7 to 9 feet based upon the projection of the base of the unit which is marked by a gravel layer. An irregular gouge zone approximately 2 to 5 inches in width is developed between the Ardath Shale and Bay Point Formation with several striations with the rake of 80° or greater. No gouge zone was observed in the shear which extends into the Bay Point Formation. This shear is overlain by unfaulted residual soil and slopewash deposits (Ql).

CONCLUSIONS

The primary fault exposed in the trench, previously identified at this approximate location as the main branch of the Rose Canyon Fault, is an oblique reverse fault overlain by unfaulted Bay Point Formation of Middle to Late Pleistocene age. The secondary shear has displaced the Bay Point Formation approximately 7 to 9 feet and is overlain by an unfaulted residual soil and slopewash deposits radiocarbon dated to be approximately 1,140 ± 80 years old. An alternative hypothesis that could explain the secondary shear by other than tectonic origin is landsliding or block gliding along previously developed bedding plane faults or fractures within the Ardath Shale. Features such as these are common within the Ardath Shale in the Mount Soledad area.

ACKNOWLEDGMENTS

Work for this study was supported in part by the U.S. Geological Survey's National Earthquake Hazards Reduction Program (Contract No. 14-08-0001-19824).

REFERENCES

Artim, E.R. and Streiff, D., 1981, Trenching the Rose Canyon Fault zone, San Diego, California, U.S. Geological Survey, Open-file Report No. 81-878, and Final Technical Report, U.S.G.S. Contract No. 14-08-0001-19824.

Kennedy, M.P., 1975, Geology of the San Diego Metropolitan Area, California: California Division of Mines and Geology, Bulletin 200, Section A, pp. 1-39.

Kennedy, M.P. and Peterson, G.S., 1975, Geology of the San Diego Metropolitan Area, California: California Division of Mines and Geology, Bulletin 200, Section B, pp. 45-56.

Kennedy, M.P., Clark, S.G., Greene, H.G., and Legg, M.R., 1980, Recency and character of faulting offshore metropolitan San Diego, California: California Division of Mines and Geology, Map Sheet 42.

Kennedy, M.P., Greene, H.G., Clarke, S.H. and Bailey, K.A., 1980, Recency and character of faulting offshore metropolitan San Diego, California: California Division of Mines and Geology, Map Sheet 41.

Kennedy, M.P. and Welday, E.G., 1980, Recency and character of faulting offshore metropolitan San Diego, California, California Division of Mines and Geology, Map Sheet 40.

Kern, J.P., 1973, Late Quaternary deformation of the Nestor terrace on the east side of Point Loma, San Diego, California, in Ross, A. and Dowlen, R.J., eds., Studies on the geology and geologic hazards of greater San Diego area, California: San Diego Association of Geologists Guidebook, p. 43.

Kern, J.P., 1977, Origin and history of upper Pleistocene marine terraces, San Diego, California: Geol. Soc. America Bull., Vol. 88, pp. 1553-1566.

Kies, R., 1979, The Rose Canyon fault zone from Point La Jolla to Balboa Avenue, San Diego: San Diego State University Geology Department, Undergraduate Research Report.

Moore, G.W., 1972, Offshore extension of the Rose Canyon fault, San Diego, California: U.S. Geological Survey Professional Paper 800-C, pp. C113-C116.

Moore, G.W. and Kennedy, M.P., 1975, Quaternary faults at San Diego Bay, California: U.S. Geological Survey, Journal of Research, Vol. 3, No. 5, pp. 589-595.

Peterson, G.D., 1970, Quaternary deformation of the San Diego area, southwestern California: American Association of Petroleum Geologists (Pacific Section), Fall Guidebook, pp. 120-126.

Pinckney, C.J., Streiff, D. and Artim, E.R., 1979, The influence of bedding-plane faults in sedimentary formations on landslide occurrence, western San Diego County, California, Bulletin of the Association of Enginering Geologists, Vol. XVI, No. 2, pp. 289-300.

Schmalfuss, B.R., 1979, Late Quaternary slip on the Rose Canyon fault: San Diego State University Geology Department, Undergraduate Research Report, 21 pp.

Ziony, J.I., 1973, Recency of faulting in the greater San Diego area, California, in Ross, A. and Dowlen, R.J., eds., studies on the geology and geologic hazrads of greater San Diego area, California: San Diego Association of Geologists Guidebook, p. 68.

THE ROSE CANYON FAULT: A REVIEW

by

Ernest R. Artim and Dorian Elder-Mills
Leighton and Associates, Inc.
Walnut, California
San Diego, California

INTRODUCTION

The Rose Canyon Fault has been identified on early geologic maps of the San Diego area by Ellis and Lee, 1919; Hanna, 1926; Hertlein and Grant, 1944 and 1954. Structural implications were not addressed as the fault was considered to be a minor structural feature as suggested by Gastil (1961). However, in the early 1970's the Rose Canyon Fault was suggested to be a major structural feature primarily by Moore and Kennedy (1970); Kennedy and Moore (1971); Moore (1972) and was suggested to be capable of producing a magnitude event of 6.5 every 200 to 300 years.

In this paper we will present a comprehensive background and data base of the Rose Canyon Fault and re-evaluate the fault based on previous and ongoing work.

BACKGROUND AND DISCUSSION

Three primary sets of faults; the La Nacion Fault zone, the Rose Canyon Fault zone, and the San Diego and offshore faults form the boundaries of the roughly defined San Diego Bay graben. This is a structurally depressed block bounded on the east by the La Nacion Fault zone, on the west by the San Diego Bay and offshore faults, and on the north by the Rose Canyon Fault (Figure 1). Since all of these faults may belong to the same tectonic environment they are discussed in more detail below.

LA NACION FAULT ZONE

The La Nacion fault zone extends north from near the U.S.-Mexico border to at least the south side of Mission Valley (Artim and Pinckney, 1973a, 1973b; Marshall; 1980). This fault zone is composed of a number of closely to widely spaced, parallel to subparallel faults (including the Sweetwater fault and the Chula Vista fault) that displace Tertiary and Quaternary deposits. The main branch of the fault system displaces the Early Pleistocene Lindavista Formation with stratigraphic separation as much as 70m (Artim and Pinckney, 1973a, 1973b; Foster, 1973; Ziony, 1973). In addition, Late Pleistocene units show evidence of several feet of displacement (Artim and Elder, 1979). Several traces as long as 1.2 km, exposed between San Diego Bay and the main branch of the fault system, displace Pleistocene deposits with stratigraphic separation of as much as 30m (Artim and Elder, 1979).

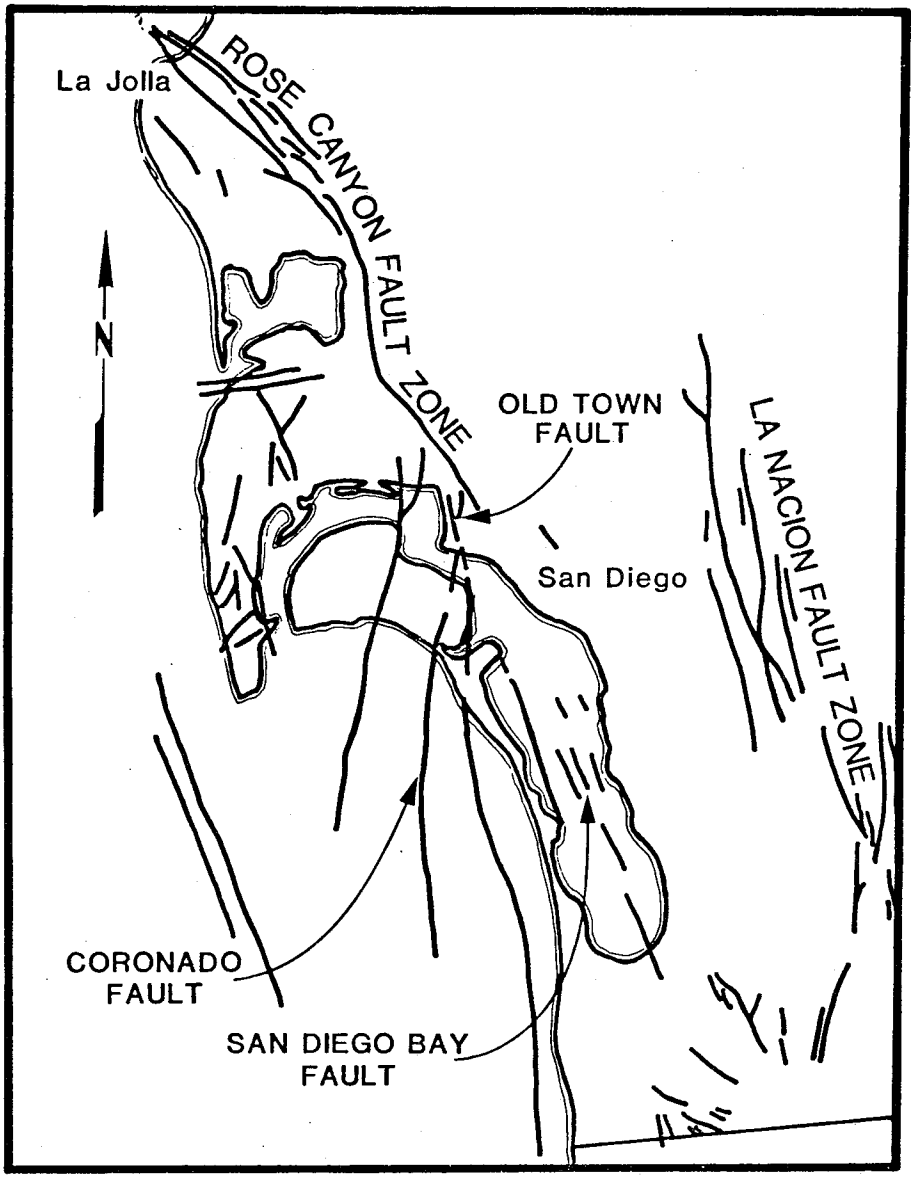

FAULT LOCATION AND AREA MAP, SAN DIEGO, CALIFORNIA

Modified from Kennedy, Clark, and Greene and Legg, 1980.

FIGURE 1

ROSE CANYON AND SAN DIEGO BAY FAULTS

The Rose Canyon fault zone has been shown to extend for approximately 15km south on land from the La Jolla Cove Shores area (Kern, 1973a; Ziony, 1973; Kennedy, 1975) (Figure 1). The fault zone comprises a number of closely spaced, subparallel faults that displace Cretaceous and Tertiary strata near Mount Soledad. The fault zone, as mapped, continues offshore to the north. Analysis of subbottom acoustical profiles (Moore, 1972) suggests the Rose Canyon fault zone projects as far north as Camp Pendleton. Moore further states, "Projection of the zone farther north suggests that the Rose Canyon fault may be related to the Newport-Inglewood fault system; to the south, it may join the San Miguel fault in Baja, California." It should be noted that these are merely postulated continuations of the Rose Canyon fault. Significant earthquakes have been recorded or noted along the San Miguel and Agua Blanca Faults in Baja California, and along the Newport-Inglewood Fault Zone; however, no such events have been recorded on the Rose Canyon Fault Zone.

It has been suggested that the fault continues to the south under San Diego Bay (Wiegand, 1970) and/or offshore of Coronado (Kennedy, et al, 1980). South of Mission Bay, the limits of the Rose Canyon fault zone are diffuse and unclear. Studies of the fault zone (Kennedy, 1975) have included the Morena fault and the Old Town fault, which are the most easterly faults associated with the zone. Recently, Kennedy (1979, oral communication) projected the Rose Canyon fault 1.2 to 1.8km west of downtown San Diego to connect with offshore faults identified near Coronado Island. The Old Town fault is now not considered by Kennedy (1979, personal communication) to be a part of the Rose Canyon fault zone.

Kennedy and Welday (1980) have since concluded that the major zone of faulting can be projected across Coronado to connect with offshore faulted features.

RECENCY OF MOVEMENT

The Rose Canyon fault is dominated by slightly northwest trending, en-echelon faults and folds. Onshore adjacent to La Jolla the fault has been interpreted as having evidence of right-lateral displacement (Kennedy, 1975; Moore and Kennedy, 1975; Kern, 1977; Schmalfuss, 1979). About 1 kilometer of right lateral movement was postulated along the Rose Canyon fault over the past 1-million years (Moore and Kennedy, 1975), which would result in an average slip of about 1 meter per 1,000 years or 1 millimeter per year. The strike-slip style of deformation has been suggested on the basis of postulated displaced stratigraphic units (Kennedy, 1975), displaced geomorphic features (Kern, 1977; Kies, 1980), and reported horizontal slickensides (Kennedy, 1975). In our opinion, however, actual measurements of laterally displaced features are neither well documented nor confirmed by supportive evidence and actual locations have not been cited for "horizontal slickensides".

Approximately 140 meters of vertical separation of the base of the Lindavista Formation has been recognized near Mount Soledad (Peterson, 1970). Evidence for vertical displacement has been documented at several locations (Kennedy, 1975; Kern, 1977); however, the sense of displacement (normal and reverse) as well as fault location varies throughout the zone. Kennedy (1975) reported that the rocks on the west side of the zone have moved relatively up in some areas and down in other areas. Kennedy (1975) indicates that continental type igneous and metamorphic rocks form the basement on both sides of the fault zone.

Investigators have suggested evidence of tectonic displacement of the Rose Canyon Fault zone in Late Pleistocene and younger sediments (Kennedy, 1975; Moore and Kennedy, 1975; Kern, 1977; Kennedy and others, 1978; Schmalfuss, 1979). Published evidence includes scattered earthquake activity in the general San Diego area (Simons, 1979), and suggested displacement of postulated Holocene age sediments on the sea floor (Moore, 1972; Moore and Kennedy, 1975; Kennedy and Welday, 1980; Kennedy and others, 1980a and 1980b).

Kennedy (1975) states, "The possibility of Holocene fault activity in the area is not ruled out, though no direct field evidence supports this fact." Kennedy and Peterson (1975) conclude, "Holocene seismic activity along several faults that lie within 10km of the area is supported by the historic seismicity believed to be associated with the Rose Canyon Fault zone in the San Diego Bay area..."

An examination of a 300 foot east-west sewer trench excavation in 1970 at the mouth of Rose Canyon just north of Balboa Avenue, indicated no significant north-south faulting across the mapped main trace of the Rose Canyon fault (Kennedy, 1975). This excavation extended through Holocene materials. If the Rose Canyon fault is present in this area it has to be located east of the railroad tracks (Pinckney, 1970, personal communication).

A set of inferred faults, including the Coronado Fault and the Spanish Bight fault, have been suggested to displace Quaternary sediments in San Diego Bay and just offshore of San Diego (Kennedy and Welday, 1977; Kennedy and Welday, 1980). These faults have recently been described as the southern extension of the Rose Canyon fault zone (Kennedy and Welday, 1980). The faulting is largely based on interpretations of subbottom geophysical profiling investigations (Moore and Kennedy, 1975; Kennedy and Welday, 1977; Kennedy and others, 1978; Kennedy and others, 1979; Kennedy and Welday, 1980). The trends of these faults vary from slightly northwest to slightly northeast. Kennedy and Welday (1980) suggest that the faults displace an estimated 7m of near-surface sediments; however, the inferred faulted material has not been dated, therefore there is some uncertainty as to the age of faulting. The authors suggested that the most recent slip along the Rose Canyon fault was in Late Pleistocene or early Holocene, and suggested that the eastern break in topography on Coronado was a fresh fault scarp. A trench recently excavated across the fault scarp (Artim and Streiff, 1981) indicates this to be an erosional feature and not related to tectonic displacement.

Geologically young materials in San Diego have been displaced by faults. Faulted sediments in the southeast Mission Bay area have been radiocarbon dated at 28,000 (+1,500) years (Liem, 1977). Unpublished information from Mr. William Elliott (1980, personal communication) indicates that a fault in Chula Vista has displaced sediments radiocarbon dated as approximately 25,000 years old. Sediments in the downtown San Diego area dated by amino acid methods as approximately 200,000 to 300,000 years old possibly have up to 3 meters of displacement (Artim and Streiff, 1981). Recent work on this fault fermed the San Diego fault, (Elder-Mills, 1982) revealed up to 10 meters of displacement in geologically older materials, establishing an average slip rate with time. A deposit on Point Loma dated at approximately 120,000 years old (Kern, 1973a) has up to 4.6 meters of displacement.

Sediments mapped as the Bay Point Formation (with ages that range from approximately 10,000 to 560,000 years old) have been identified as being faulted in many areas of San Diego, including La Jolla, Point Loma, Chula Vista, and National City (Peterson, 1970a, 1970b; Kern, 1973a, 1973b; Moore and Kennedy, 1975; Kennedy, 1975; Kennedy and Welday, 1977). There is

geologic evidence of no displacement of a soil radiocarbon dated as approximately 1,000 years old (Charles J. Pinckney, personal communication). There is geological evidence of no displacement in alluvial deposits radiocarbon dated as approximately 7,000 years old (Farrand, et al, 1981). An oblique reverse exposure of the Mount Soledad fault shows no displacement of soil radiocarbon dated as about 8,000 years old (Berggreen and Streiff, 1979). The rake of striations of two exposures of the Rose Canyon fault near Ardath Road range between 44^{o} and 85^{o} with an average of about 56^{o}, indicating an oblique component of displacement (Artim and Streiff, 1982). Artim and Streiff (1982) describe the dip of the rake of striations on the Rose Canyon fault at Spindrift Drive in La Jolla to be between 40^{o} to 80^{o}, but primarily steeper. Exposures of the Rose Canyon fault in Rose Canyon reveal striations with the dips of the rake at about 80^{o} (Hart, 1981).

The main branch of the Rose Canyon fault in La Jolla is overlain by unfaulted Middle to Late Pleistocene deposits, (Artim and Streiff, 1982). A secondary shear was described to apparently displace a Middle to Late Pleistocene deposit about 3 meters. A residual soil and colluvial deposit, radiocarbon dated to be as young as 1,140±75 years old, showed geological evidence for no displacement or stratigraphic separation.

Perry Ehlig (unpublished report, 1981) presents an excellent data base to suggest that the Rose Canyon fault is an old tectonic feature which may have been displaced by sympathetic movement during the Pleistocene from movement on other more active tectonic features. Threat (1979) presented a list of data suggesting alternate interpretations for the Rose Canyon fault.

CONCLUSIONS

To date, no direct evidence for Holocene faulting has been established in the San Diego area. No direct evidence has been reported for tectonic displacement of material younger than Pleistocene on the Rose Canyon fault. Topographic features such as sag ponds, offset stream courses, or sharply defined scarps, commonly associated with Holocene faulting elsewhere in California, are not generally observed in conjunction with local faulting, which suggests that these faults, if they are active, have a very low rate of activity. Based upon investigations along the Rose Canyon Fault, we conclude that the Rose Canyon Fault onshore is primarily an en-echelon series of oblique reverse and normal faults.

The geologic structure of the San Diego area includes en-echelon, north-northwest-striking faults that characteristically dip steeply and have normal, reverse, and normal and reverse oblique displacement. These faults lie subparallel to the regional tectonic grain and are believed to result from rotational and extensional stress environments. The component of extensional stress in southwestern San Diego is aligned generally east-west; the resulting strain is expressed by normal faults that strike generally north-south.

Most of the Quaternary faults in the coastal San Diego area are generally considered within the guidelines of the California Division of Mines and Geology to be classified as "potentially active" because of the lack of definitive evidence for the presence or absence of Holocene activity.

Average confirmed slip rates for the Rose Canyon fault are much less than those suggested by authors in the early 1970's. Confirmed slip rates are about .1mm per year or less (Woodward-Clyde Consultants, unpublished data, 1980 and 1981). Based upon the work by Cluff (1979), such a slip rate suggests that

the actual degree of fault activity of the Rose Canyon fault is low, and although the fault map be considered by some geologists to be geologically capable of producing a Richter Magnitude earthquake greater than 6.0, the recurrence interval is more likely on the order of once every 5,000 or more years. Based upon the confirmed geological data the recurrence interval is more likely even greater possibly as long as 10,000 or 20,000 years. Based upon work from a recent report (Yeats and others, 1981), we also suggest that the Rose Canyon fault may belong to a group of faults which possess a potential for displacement by groundsurface rupture, but may not be capable of producing an earthquake or seismic shaking hazard. This is not to say that the fault is the same as those described in Yeats, however the Rose Canyon fault may have similar aseismic characteristics. We are proceeding to complete the re-evaluation study of the Rose Canyon fault utilizing not only previous published and unpublished literature, but also supplemented with field work at selected localities.

ACKNOWLEDGEMENTS

This paper is based upon a personal geologic work history in the San Diego area dating from 1968 to 1981, with Woodward-Clyde Consultants and stimulated by work performed for two U.S. Geological Survey Research contracts (14-08-0001-19118 and 14-08-0001-19824) both awarded to Woodward-Clyde Consultants San Diego office. We gratefully acknowledge those opportunities and support grants.

REFERENCES

Artim, E.R., Bemis, C.G., Pinckney, C.J., and Smillie, B.R., 1971, Western San Diego County fault system: Geological Society of America Abstracts with Programs, v. 3, no. 2, p. 75.

Artim, E.R., and Pinckney, C.J., 1973a, La Nacion Fault system, San Diego, California: Geological Society of America Bulletin, v. 84, p. 1075.

Artim, E.R., and Pinckney, C.J., 1973b, La Nacion Fault system, San Diego, California, in Ross, A., and Dowlen, R.J. (eds.), Studies on the Geologic Hazards of the Greater San Diego Area, California: San Diego Association of Geologists Guidebook, p. 77.

Artim, E.R. and Pinckney, C.J., 1978, Anatomy and History of Two test Trenches, La Nacion Fault, San Diego, California; presented to San Diego Association of Geologists, March 1978 meeting.

Artim, E.R., and Elder, D.L., 1979, Late Quaternary deformation along the La Nacion Fault system, San Diego, California: Geological Society of America Abstracts with Programs, v. 11, no. 7, p. 381.

Artim, E.R. and Streiff, D., 1981, Trenching the Rose Canyon Fault Zone, San Diego, California; U.S. Geological Survey, Open-file Report No. 81-878; USGS Contract No. 14-08-0001-19118.

Artim, E.R. and Streiff, D., 1982, Trenching the Rose Canyon Fault Zone, San Diego; U.S. Geological Survey, Final Technical Report; USGS Contract No. 14-08-0001-19824.

Berggreen, R.G., and Streiff, D., 1979, Recency of faulting on the Mount Soledad branch of the Rose Canyon Fault zone in northwestern metropolitan San Diego, California (abs.): Geological Society of American Abstracts with Programs, v. 11, no. 7, p. 387.

Cluff, L., 1979, Geologic considerations for seismic microzonation: Woodward-Clyde Consultants Geotechnical Environmental Bulletin, v. XII, no. 1, p. 4-13.

Dorn, D., 1980, Geophysical Investigations in North Park, San Diego, California: Unpublished Senior report, San Diego State University, Department of Geological Sciences, San Diego, California.

Dowlen, R., Hart, M., and Elliott, W., 1975, New evidence concerning age of movement of the La Nacion Fault, southwestern San Diego County, California (abs.): 1975, Association of Engineering Geologists, Annual Meeting, p. 20.

Ehlig, P., 1981, A critical examination of Rose Canyon fault, unpublished report.

Elder-Mills, D., 1982, Recognition and Age of the San Diego Fault, San Diego, California; GSA Cordilleran Section Meeting, v. 14, no. 4, p. 161.

Elliott, W. J., and Hart, M. W., 1977, New evidence concerning age of movement of the La Nacion Fault, southwestern San Diego County, California, in Farrand, G.T., (ed.), Geology of southwestern San Diego County, California and northwestern Baja California: San Diego Association of Geologists, p. 53.

Ellis, A.J., and Lee C., 1979, Geology and ground waters of the western part of San Diego County, California: U.S. Geological Survey Water-Supply Paper 446, p. 321.

Farrand, G.T., Bemis, C.G. and Jansen, L.T., 1981, Radiocarbon dates of alluvium, Rose Canyon Fault zone, San Diego, California, Geological Society of America, Cordilleran Section, Abstracts with Programs, p. 55.

Foster, J.H., 1973, Faulting near San Ysidro, southern San Diego County, California; in Ross, A., and Dowlen, R. J. (eds.), Studies on the geology and geologic hazards of the greater San Diego area, California: San Diego Association of Geologists Guidebook, p. 83.

Gastil, R.G., 1961, The elevated erosion surfaces, in Thomas, B.E., ed., Field trip guidebook: Geological Society of America, 57th Annual Meeting (Cordilleran Section), p. 1-3.

Gastil, R.G., Kies, R., and Melius, D.J., 1979, Active and potentially active faults, San Diego County and north-westernmost Baja California: in Abbott, P.L., and Elliott, W.J. (eds.), Earthquakes and other perils: San Diego region, San Diego Association of Geologists, p. 47-60.

Gastil, G., and Higley, R., 1979, Guide to San Diego Area Stratigraphy: San Diego State University, Department of Geological Sciences, San Diego, California.

Goldstein, G.F., 1956, Geology of the Sweitzer Formation at San Diego, California: M.A. thesis, Univeristy of California, Los Angeles, California, 86 p.

Green, H.G., Bailey, K.A., Clarke, S.H., Ziony, J.I., and Kennedy, M.P., 1979, Implications of fault patterns of the inner California continental borderland between San Pedro and San Diego: in Abbott, P.L., and Elliott, W.J. (eds.), Earthquakes and Other Perils, San Diego Region, San Diego Association of Geologists, p. 21-29.

Hanna, M.A., 1926, Geology of the La Jolla Quadrangle, California: California University Publications in Geological Sciences, v. 16, p. 187-246.

Harrington, J.M., 1980, A gravity survey of metropolitan San Diego, California: Unpublished Senior report, San Diego State University, Department of Geological Sciences, San Diego, California, 30 p.

Hart, M., 1974, Radiocarbon ages of alluvium overlying La Nacion Fault, San Diego, California: Geological Society of American Bulletin, v. 85, p. 1329-1332.

Hart, M. W. and Farrand, G.T., 1981, The Rose Canyon Fault Zone in San Diego, California: new evidence concerning strike-slipe and seismic risk implications, Association of Engineering Geologists, Meeting Program with Abstracts, p. 38.

Hertlein, L.G., and Grant, U.S., IV, 1944, The geology and paleontology of the marine pliocene of San Diego, California: San Diego Society Nat. History Mem., v. 2 p. 72.

Hertlein, L.G., and Grant, U.S., 1954, Geology of the Oceanside-San Diego coastal area, Southern California: California Division of Mines and Geology, Bulletin 170, p. 53-63.

Jennings, C.W., 1977, Geologic map of California: California Geologic Data Map Series, California Division of Mines and Geology, scale 1:750,000.

Kennedy, M.P., and Moore, G.W., 1971, Stratigraphy and structure of the area between Oceanside and San Diego, California, geologic road log, field trip no. 8: in Field Trip Guidebook for Cordilleran Section, Geological Society of America, p. 149-166.

Kennedy, M.P., 1976, Geology of the San Diego Metropolitan Area, California: California Division of Mines and Geology, Bulletin 200, Section A, pp. 1-39.

Kennedy, M.P. and Peterson G.L., 1975, Geology of the San Diego Metropolitan Area, California: California Division of Mines and Geology, Bulletin 200, Section B, pp. 45-56.

Kennedy, M.P., Tan, S.S., Chapman, R.H., and Chase, C.W., 1975, Character and recency of faulting, San Diego Metropolitan Area, California: California Division of Mines and Geology Special Report 123, 33 p.

Kennedy, M.P. and Tan, S.S., 1977, Geology of National City, Imperial Beach, and Otay Mesa Quadrangle, Southern San Diego, Metropolitan Area, California: California Division of Mines and Geology Map Sheet 29, 1:24,000.

Kennedy, M.P., and Welday, E.E., 1977, Character and recency of faulting offshore metropolitan San Diego, California: California Division of Mines and Geology, Map Sheet 40, 1:50,000

Kennedy, M.P., Greene, H.G., Clarke, S.H. and Bailery, K.A., 1980, Recency and character of faulting offshore metropolitan San Diego, California: California Division of Mines and Geology, Map Sheet 41.

Kennedy, M.P., Clark, S.G., Greene, H.G. and Legg, M.R., 1980, Recency and character of faulting offshore metropolitan San Diego, California: California Division of Mines and Geology, Map Sheet 42.

Kern, J.P., 1973a, Late Quaternary deformation of the Nestor terrace on the east side of Point Loma, San Diego, California, in Ross, A., and Dowlen, R.J. (eds.), Studies on the Geology and Geologic Hazards of the Greater San Diego Area, California: San Diego Association of Geologists and the Association of Engineering Geologists Guidebook, p. 43.

Kern, J.P., 1973b, Origin and history of two upper Pleistocene marine terraces at San Diego, California: Geological Society of America Bulletin, v. 88 p. 1553.

Kies, R., 1979, The Rose Canyon fault zone from Point La Jolla to Balboa Avenue, San Diego: San Diego State University Geology Department, Undergraduate Research Report.

Legg, M.R., and Kennedy, M.P., 1979, Faulting offshore San Diego and northern Baja California: in Abbott, P.L., and Elliott, W.J. (eds.), Earthquakes and Other Perils, San Diego Region: San Diego Association of Geologists, p. 29-46.

Leighton and Associates, 1978, Preliminary review of fault locations and activity, proposed marina redevelopment project: Unpublished report submitted to City of San Diego, California, by Leighton and Associates, San Diego, California.

Liem, T.J., 1977, Late Pleistocene maximum age of faulting, southeast Mission Bay area, San Diego, California, in Farrand, G.T. (ed.), Geology of southwestern San Diego County, California and northwestern Baja California: San Diego Association of Geologists Guidebook, p. 61.

Lough, C., 1973, Faults and epicenters, County of San Diego: San Diego County Planning Department map.

Marshall, M., 1979, Geophysical survey of the La Nacion Fault zone San Diego, California, in Abbott, P.L., and Elliott, W.J., (eds.) Earthquakes and Other Perils San Diego Region: San Diego Association of Geologists, p. 73-93.

Marshall, M., 1980, Unpublished geophysical data, Department of Geology, San Diego State University.

McEuen, R.B., and Pinckney, C.J., 1972, Seismic risk in San Diego: San Diego Society of Natural History Transactions, v. 17, p. 33.

Milow, E.D., and Ennis, D.B., 1961, Guide to geologic field trip of southwestern San Diego County, in Thomas, B.E. (ed.), Guidebook for Field Trips, Geological Society of America 57th Annual Meeting, Cordilleran Section, p. 23.

Moore, G.W., 1972, Offshore extension of the Rose Canyon fault, San Diego, California: U.S. Geological Survey Professional Paper 800-C, pp. C113-C116.

Moore, G.W., and Kennedy, M.P., 1970, Coastal geology of the California border area, in Pacific slope geology of northern Baja California and adjacent Alta California: American Association of Petroleum Geologists (Pacific Section) Fall Field Trip Guidebook, p. 4.

Moore, G.W., and Kennedy, M.P., 1975, Quaternary faults at San Diego Bay, California U.S. Geological Survey Journal Research, v. 3, no. 5, p. 589-595.

Peterson, G.L., 1970a, Quaternary deformation of the San Diego area, southwestern California, in Pacific Slope Geology of Northern Baja California and Adjacent Alta California: American Association of Petroleum Geologists (Pacific Section) Fall Field Trip Guidebook, p. 120.

Peterson, G.L., 1970b, Pleistocene deformation of the Lindavista terrace near San Diego, California: Geological Society of America Abstracts with Programs, v. 2, no. 2, p. 131.

Pinckney, C.J., Streiff, D. and Artim, E.R., 1979, The influence of bedding-plane faults in sedimentary formations on landslide occurrence, western San Diego County, California, Bulletin of the Association of Engineering Geologists, Vol. XVI, No. 2, pp. 289-300.

San Filipo, J., 1978, A magnetic survey of the Rose Canyon Fault Zone: San Diego State University, Department of Geological Sciences, San Diego, California, 32 p.

Schmalfuss, B.R., 1979, Late Quaternary slip on the Rose Canyon Fault: Unpublished Senior research paper, San Diego State Univeristy, Department of Geological Sciences, San Diego, California, 19 p.

Sprain, J. C., 1980, A gravity survey of two small faults in east San Diego; Unpublished Senior report, Department of Geology, San Diego State University.

Threet, R.L., 1973, Birth and death of a fault in Mission Valley, San Diego, California, in Ross, A., and Dowlen, R.J. (eds.), Studies on the Geology and Geologic Hazards of the Greater San Diego Area, California: San Diego Association of Geologists and the Association of Engineering Geologists Guidebook, p. 105.

Threet, R.L., 1977, Texas Street Fault, San Diego, California in Farrand, G.T. (ed.), Geology of Southwestern San Diego County, California and Northwestern Baja California: San Diego Association of Geologists, p. 43.

Threet, R.L., 1979, Rose Canyon Fault: An alternative interpretation, in Abbott, P.L., and Elliott, W.J., (eds.), Earthquakes and Other Perils, San Diego, California: San Diego Association of Geologists, p. 61-71

Wiegand, J.W., 1970, Evidence of a San Diego-Tijuana Fault: Association of Engineering Geologists Bulletin, v. 7, no. 2, p. 107.

Yeats, R.S., Clark, M.N., Keller, E.A., and Rockwell, T.K., 1981, Active fault hazard in Southern California: Grand Rupture versus seismic shaking, Geological Society of America Bulletin, v. 92, no. 4, p. 189-196.

Ziony, J.I., 1973, Recency of faulting in the greater San Diego area, California in Rosee, A., and Dowlen, R.J. (eds.), Studies on the geology and geologic hazards of the greater San Diego area, California: San Diego Association of Geologists Guidebook, p/ 68.

Ziony, J.I., and Buchanan, J.M., 1972, Preliminary report on recency of faulting in the greater San Diego area, California: U.S. Geological Survey, Open File Report, 16 p.

Ziony, J.I., Wentworth, C.M., Buchanan-Banks, J.M., and Wagner, H.C., 1974, Preliminary map showing recency of faulting in coastal southern Califorina: U.S. Geological Survey Map MF-585, 3 plates, 8 p, 1:25,000.

BLACK'S BEACH LANDSLIDE, JANUARY, 1982

by

W. Lee Vanderhurst, Richard J. McCarthy, Dennis L. Hannan
Leighton and Associates, Inc.
7290 Engineer Road, Suite H
San Diego, California 92111

INTRODUCTION

On January 29, 1982, at approximately 9:00 a.m., a large-scale, deep-seated landslide occurred in the coastal bluff south of the glider port above "Black's Beach", La Jolla (Figure 1). Geotechnical mapping conducted for the City of San Diego Recreation Department in late 1979 identified the area as being susceptible to an "imminent failure" based on field evidence and aerial photograph analysis. Reconnaissance mapping of the site after landsliding showed that the pre-slide mapping had accurately predicted the areal limits and the mode of failure. Because of the location and topography, standard stabilization methods are not considered economically or environmentally feasible. Recommendations for protection of the general public include; fencing, warning signs,and possible removal of unstable blocks and/or slabs.

PHYSIOGRAPHY AND GEOLOGIC SETTING

The Torrey Pines Bluffs form a 3km long, 88m- to 118m- high, westerly facing coastal bluff extending from Scripps Institution of Oceanography, north to the Soledad Valley. The bluff is broken in several locations by the mouths of canyons draining west to the Pacific Ocean. The bluff face is typically inclined between 40 and 70 degrees, although locally, there are vertical sections and narrow "benches" with slopes of less than 20 degrees. The bluffs are capped with the relatively flat, Lindavista Marine Terrace.

The recent landslide occurred on a prominent "finger ridge" that is separated from the remaining mesa to the east by Box Canyon. The canyon has a northeasterly trend and terminates on Black's Beach, roughly 15m south of the landslide. Prior to the recent landslide, the bluff face topography could be characterized by two 30m- high, 40 degrees slopes separated by a 30m- high vertical slope.

The physiography of the bluff is controlled in large part by the lithology and geologic structure of the bedrock underlying the area. The bluffs are underlain by a thick section of gently southwest dipping, jointed Eocene marine sedimentary rocks consisting of interbedded mudstone, sandstone and conglomerate. The steeper portions of the bluff are formed by the more resistant cemented sandstone and conglomerate, whereas the flatter slopes are underlain by mudstone and erodible sandstone. The north-south general trend of the bluffs may be controlled by a prominent north-south striking, steeply dipping joint system.

The combination of steeply sloping bluff, lithology and geologic structure has created an environment extremely susceptible to erosion through mass wasting. In general, three types of mass wasting are evident along the bluffs; deep-seated landslide, block or slab topples and slaking (Figure 2). The numerous narrow benches located on the middle and upper portions of the bluff are a result of

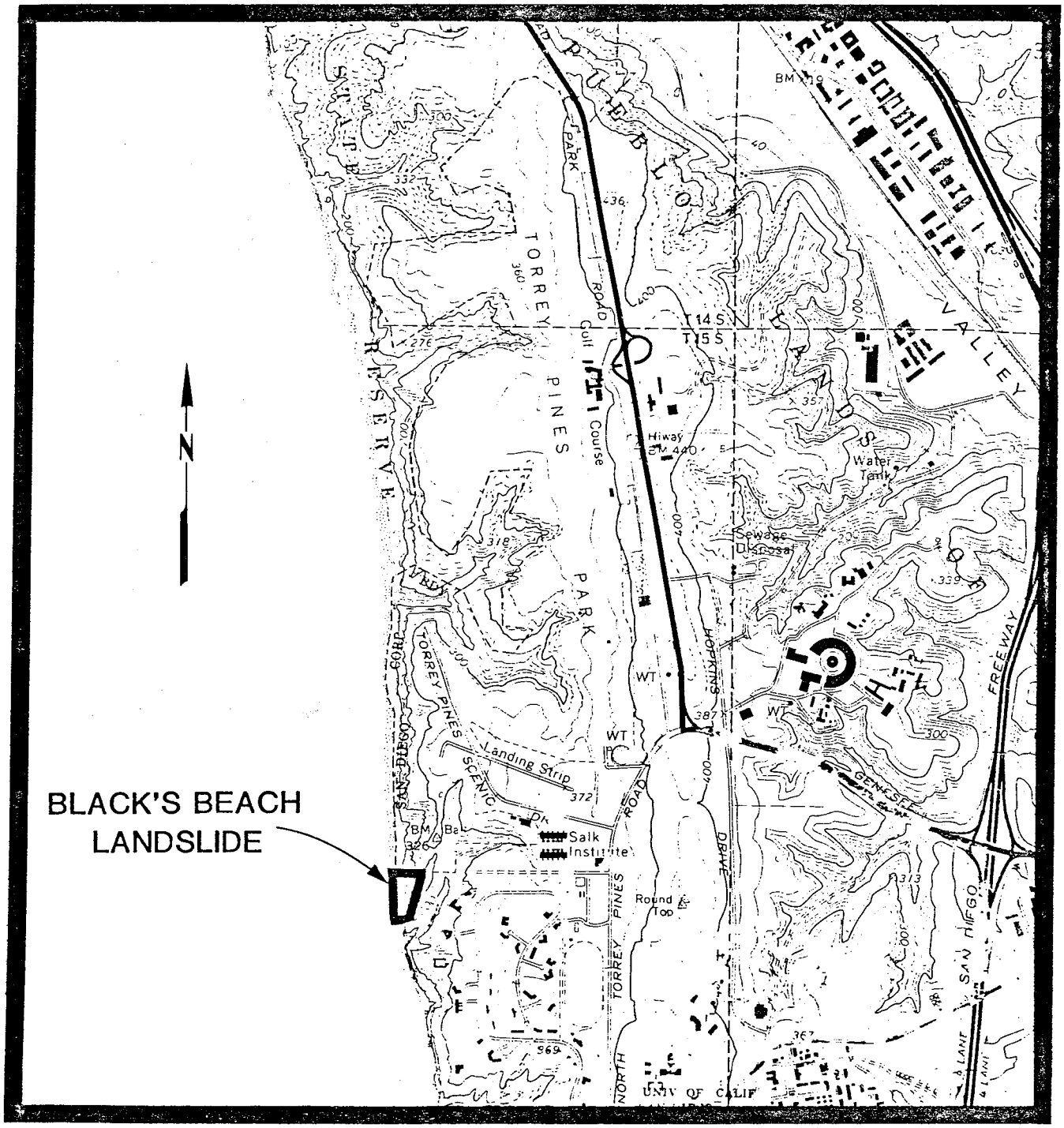

Figure 1 Location of the recent Black's Beach landslide, Torrey Pines City Park.

Base:

Del Mar Quadrangle

(U.S.G.S. 7.5 minute series)

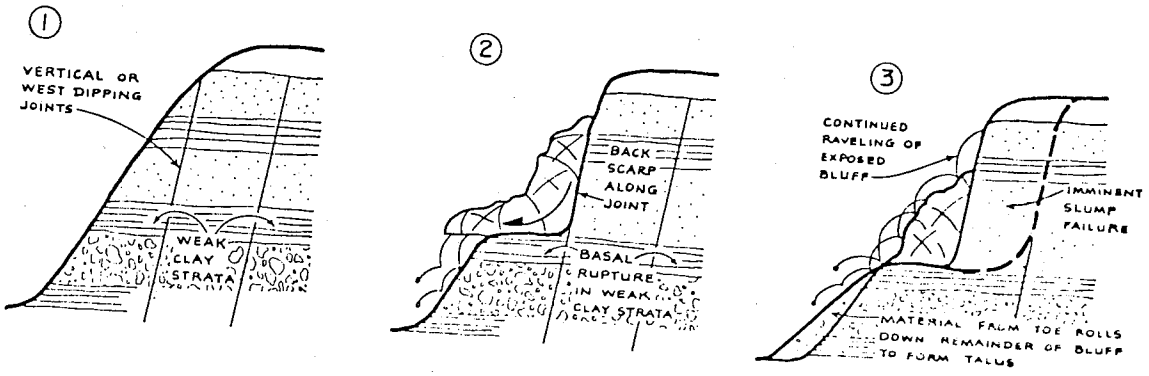

A

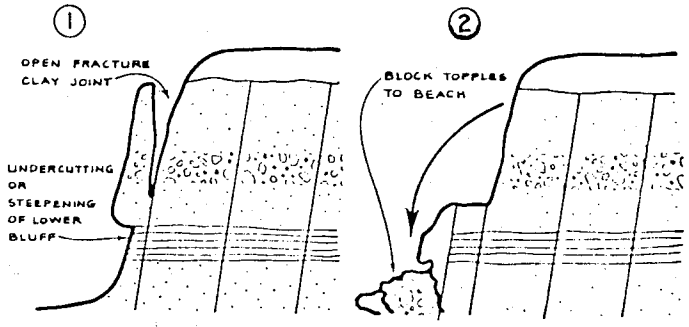

B

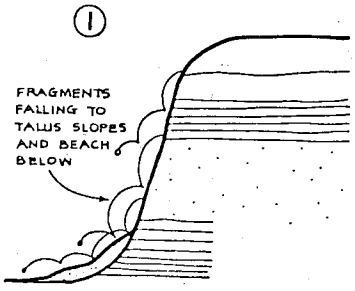

C

Figure 2 Typical modes of mass wastage along Torrey Pines Bluffs: A-translational block slide, B-slab failure, C-slaking.

translational block glide landslides (Figure 2A). The slides apparently separate from the remaining bluff along steeply dipping joints and slide on or within mudstone beds. These slides are often perched high on the bluff as the basal rupture is controlled by the elevation of the weak mudstone layer.

Block or slab topples usually occur in the cemented sandstone and conglomerate and are controlled by jointing (Figure 2B). As the block separates from the bluff face, debris falls into the open fracture and acts as a wedge, forcing further separation. When the slab or block has been wedged far enough from the bluff face, it topples to the beach.

Slaking (Figure 2C) is an ongoing process where physical weathering and animal activity loosen the face of the bluff. The loose material falls or rolls to the beach where it accumulates in talus aprons at the toe of the bluff. The debris ranges in size from sand grains to cobble sized fragments.

SITE SPECIFIC GEOLOGY

A detailed study of the bluffs between Indian Canyon and Box Canyon was initiated by the San Diego City Recreation Department as part of a general planning study for Torrey Pines City Park. The study included analysis of oblique and vertical stereo pair photographs, and a detailed field mapping program. The purpose of the study was to map and describe the general geologic conditions and prepare a map showing areas of potential danger to the public.

The area of the recent landslide is underlain by a thick section of Eocene sedimentary rocks comprised of lower middle Eocene Ardath Shale and middle Eocene Scripps Formation (Kennedy, 1975). The bedrock is overlain by several ancient, dormant and active landslides and talus slopes (Leighton and Associates, 1981).

ARDATH SHALE

The Ardath Shale is composed of gray, fissile siltstone and silty claystone and is exposed in the lower portion of the bluff (Figure 3). The exposed Ardath thickens northward from 10m, near the terminus of Box Canyon,to 40m at the northern edge of the recent landslide.

SCRIPPS FORMATION

The Scripps Formation consists of 50m of pale, yellow-brown to reddish brown, fine-grained sandstone. The sandstone is generally thinly bedded and exhibits broad, large-scale cross stratification. The Scripps Formation has a unique, "cavernous" weathering characteristic that consists of shallow pits, ledges and rills. The Scripps Formation is located in the uppermost 50m of bluff and is separated from the underlying Ardath Shale by a 35m thick section of well-undurated sandstone and cobble conglomerate (Figure 3).

LANDSLIDES

Figure 3 depicts the distribution of three landslides noted during the study in the area of the recent slide. The slides are designated as active (als) or old (ols). Several factors were used to determine the activity of the slides including; open tensional cracks, fresh looking scarps, and recent debris falls at the toes of the slides. The landslides have failed on a thin claystone

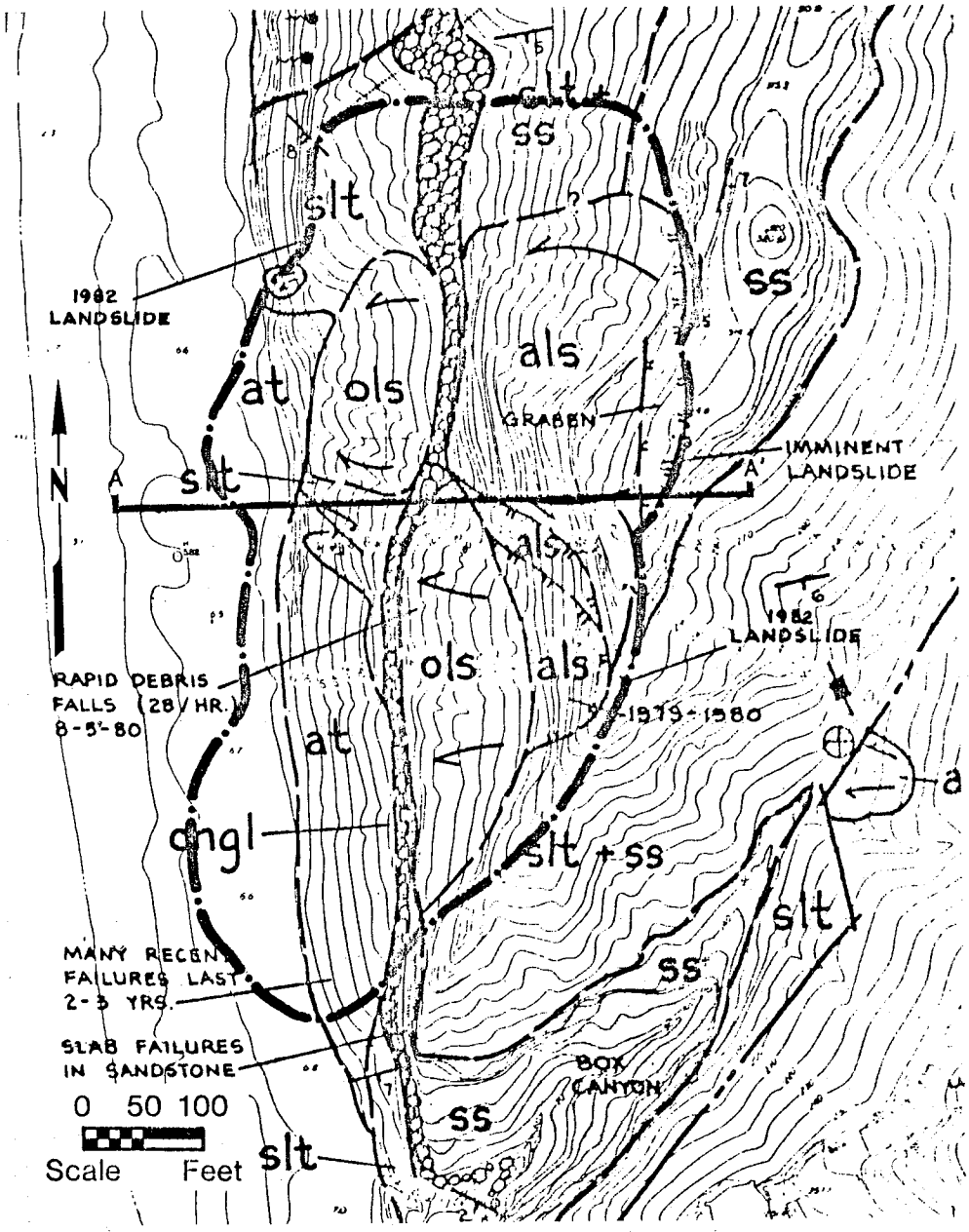

Figure 3 General geologic map of south Torrey Pines City Park. Dot-dash line depicts the approximate limits of the recent Black's Beach landslide. Other slides are designated; als (active landslide), ols (older landslide), at (active talus slope). Bedrock is mapped as slt (siltstone), ss (sandstone). Hatchured lines represent scarps. Original mapping conducted in 1979-81.

strata at the contact between the Scripps Formation sandstone and the resistant sandstone and conglomerate section located at elevation 130 feet. The slides are generally translational block slides as evident by the lack of internal fracturing within the translated blocks.

TALUS

A twenty meter high talus apron is located at the toe of the bluff. The talus consists of debris derived from landslide movement (slabs up to 1m in diameter) and slaking.

STRUCTURE

The formational materials generally strike northwest to east-west and dip between 3 and 10 degrees to the west and southwest. The prominent joint pattern strikes north-south and dips steeply to the west.

HAZARD MAP

A planning map was prepared following the geologic mapping. Based on open fractures and rapid debris falls at the toe of the landslides, the area above and below the landslides was designated as a potential hazard to the public (Figure 4). The anticipated scarp was judged a hazard from materials giving way and falling down slope and the toe was a hazard from debris falling from above. Recommendations included warning signs, closure of trails crossing the slide (Broadway Trail) and control of pedestrians (fences).

RECENT LANDSLIDES

The first evidence of landslide instability in the area of the recent landslide was noted six years ago (Woodward-Clyde Consultants, 1976) when open joints were reported in the area of the present landslide scarp. In 1980, these open joints were recognized as the tensional features related to deep-seated landslide movement (Leighton and Associates, 1981). Interviews with City lifeguards determined that over the last 3 years, numerous debris falls, slab topples, and talus slope failures had occurred in the area of the toe of the recent slide. The fresh tensional features at the bluff top and the high rate of small failures at the toe of the bluff indicated that the landslides were actively creeping and that the area could be subjected to large scale failure in the near future (Figure 3).

On January 29, 1982, at approximately 9:00 a.m., roughly 1.4 million cubic meters of previously mapped landslide debris and undisturbed materials failed. Although, not observed by lifeguards, the failure probably occurred over a period of several minutes.

DESCRIPTION

Figure 5 depicts the recent landslide morphology. The predominately vertical head wall scarp is as much as 22m-high and extends along the ridge top for 177 meters. Most of the scarp is located on the seaward side of the ridge, however portions of the scarp are located up to 5m east of the ridgetop. Immediately west of the scarp is a 44m-wide graben area composed of highly fractured older landslide debris. The graben formed as the main blocks of debris moved up to 15m laterally to the west. Two pinnacles represent the main

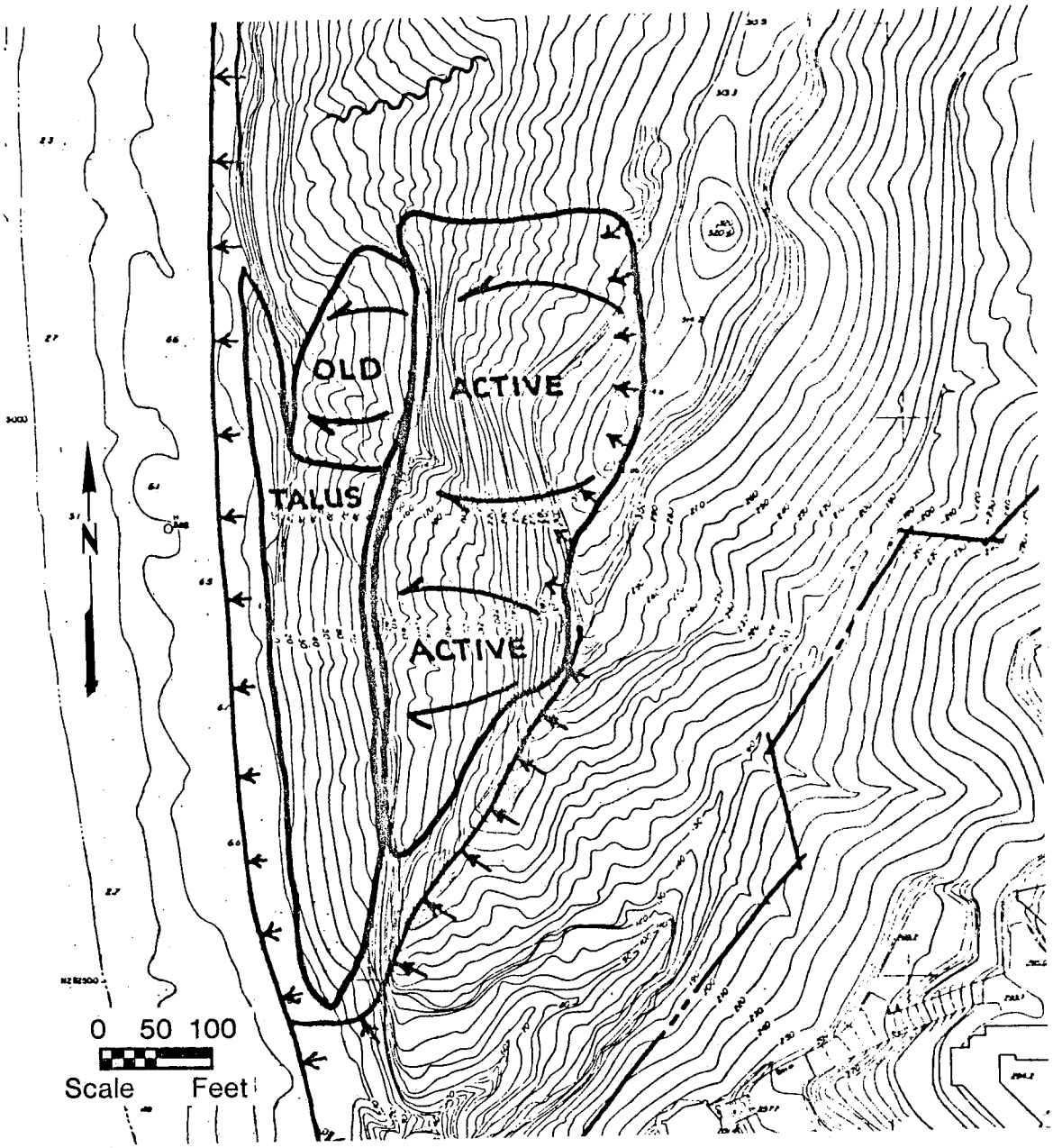

Figure 4 Southern portion of Geotechnical Planning map for Torrey Pines State Park completed in 1981. Line with arrows pointing away designates the area as a hazard to pedestrians from debris giving way. Line with arrows pointing toward the line indicates area of danger due to falling debris from above.

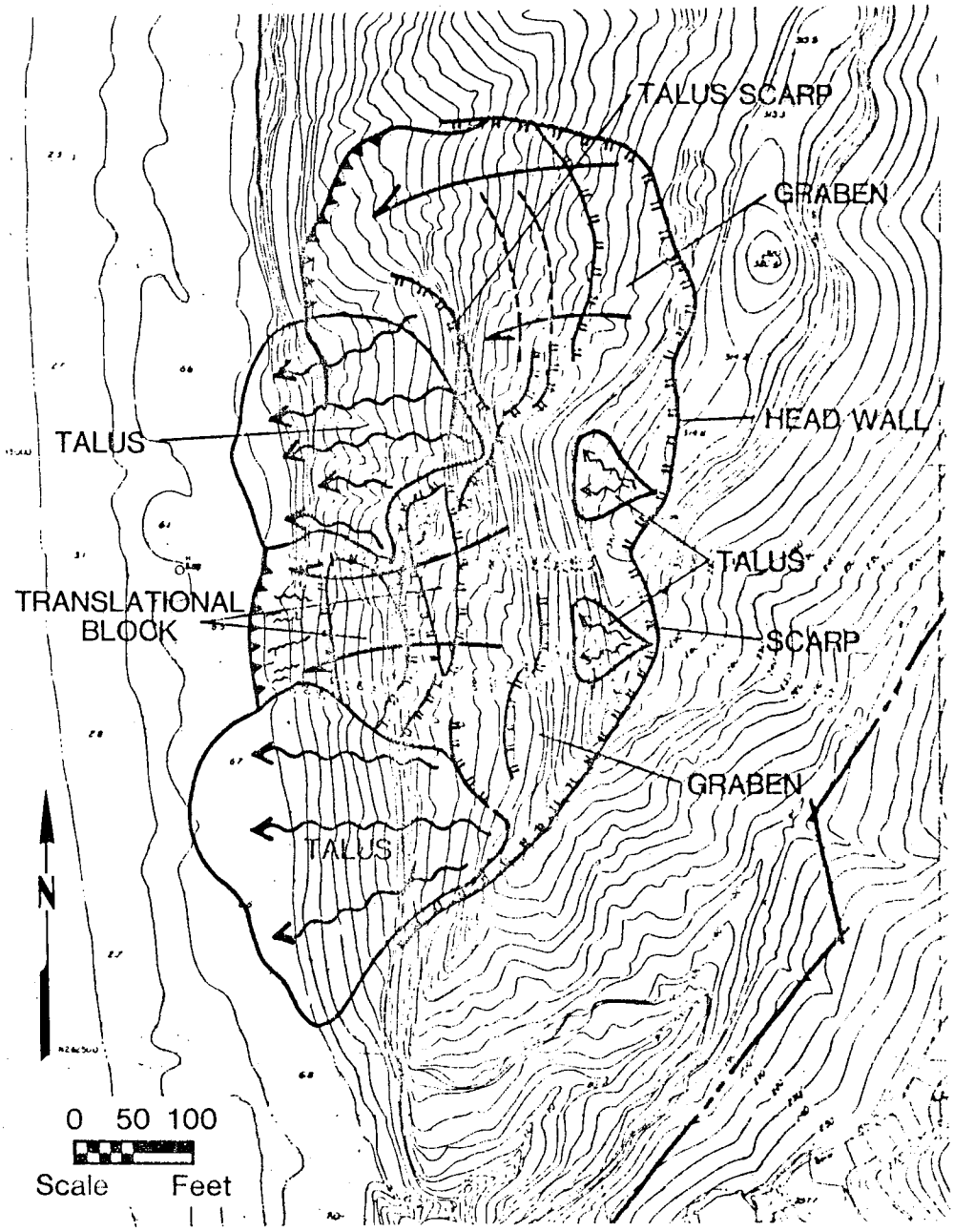

Figure 5 Reconnaissance map of the approximate limits of recent Black's Beach landslide. Hatchured lines represent scarps mapped in February, 1982. Barbed lines represent toe of block slides. Arrows show direction of rolling debris in talus lobes.

body of the landslide debris. The blocks consists of relatively coherent, fractured monoliths of older slide debris and the well indurated sandstone and conglomerate situated between the Ardath Shale and the overlying Scripps Formation. Two distinct talus lobes were formed near the northern and southern flanks of the slide and are composed of large blocks (up to 3m in diameter) of debris derived from the head scarp, graben and translational block portions of the slide.

The basal rupture, although concealed by the overriding debris over much of its length, is believed to have occurred on or within the upper meter of Ardath Shale exposed at the toe of the bluff. The rupture dips gently south and east with the southern portion located at elevation 40 feet and the northern portion exposed at a elevation 140 feet. The recent rupture is roughly 29 meters below the rupture surface of the older slides (Figure 6).

POSSIBLE CAUSES

It is believed that landslide creep has been occurring in the area of the recent landslide since sometime before 1976, although it is not certain whether the creep was occurring in the older, shallower landslides or within the deeper, recent landslide. Extensive groundwater seeps have been noted at the contact between the Ardath Shale and the well-indurated sandstone and conglomerate. Groundwater with its associated pore pressure and "lubricating" affects was most likely, the largest single contributing factor for the pre-slide creep and ultimate failure of the bluff.

Additional contributing factors may include:

1. A gradual redistribution of driving forces as a result of landslide creep in the older landslide masses.

2. Unloading of the toe area by wave erosion of the talus apron or slumping within the talus.

3. Biologic activity (animal burrows and nests) allowing rain water to enter the slide debris thereby increasing the weight and driving forces.

4. More remote factors may include earthquake shaking, sonic booms and earth tides (James Birkland, personal communication).

There were apparently no significant factors that may have triggered the slide. Rainfall over the past two years has been normal. There was no heavy rainfall prior to the recent landslide and there were no felt earthquakes in the area within the time frame of the recent failure. It is believed that a combination of causitive factors, acting over a long period of time, allowed the landslide driving forces to finally overcome the resisting forces resulting in the massive failure of January 29, 1982.

RECOMMENDATIONS

The recent Black's Beach landslide presents a unique dilemma to the City of San Diego. Although the slide occurred in an undeveloped area as a result of natural causes, does not threaten structures and property, and cannot (for economic and aesthetic reasons) be corrected however, the following areas do present a hazard to the public:

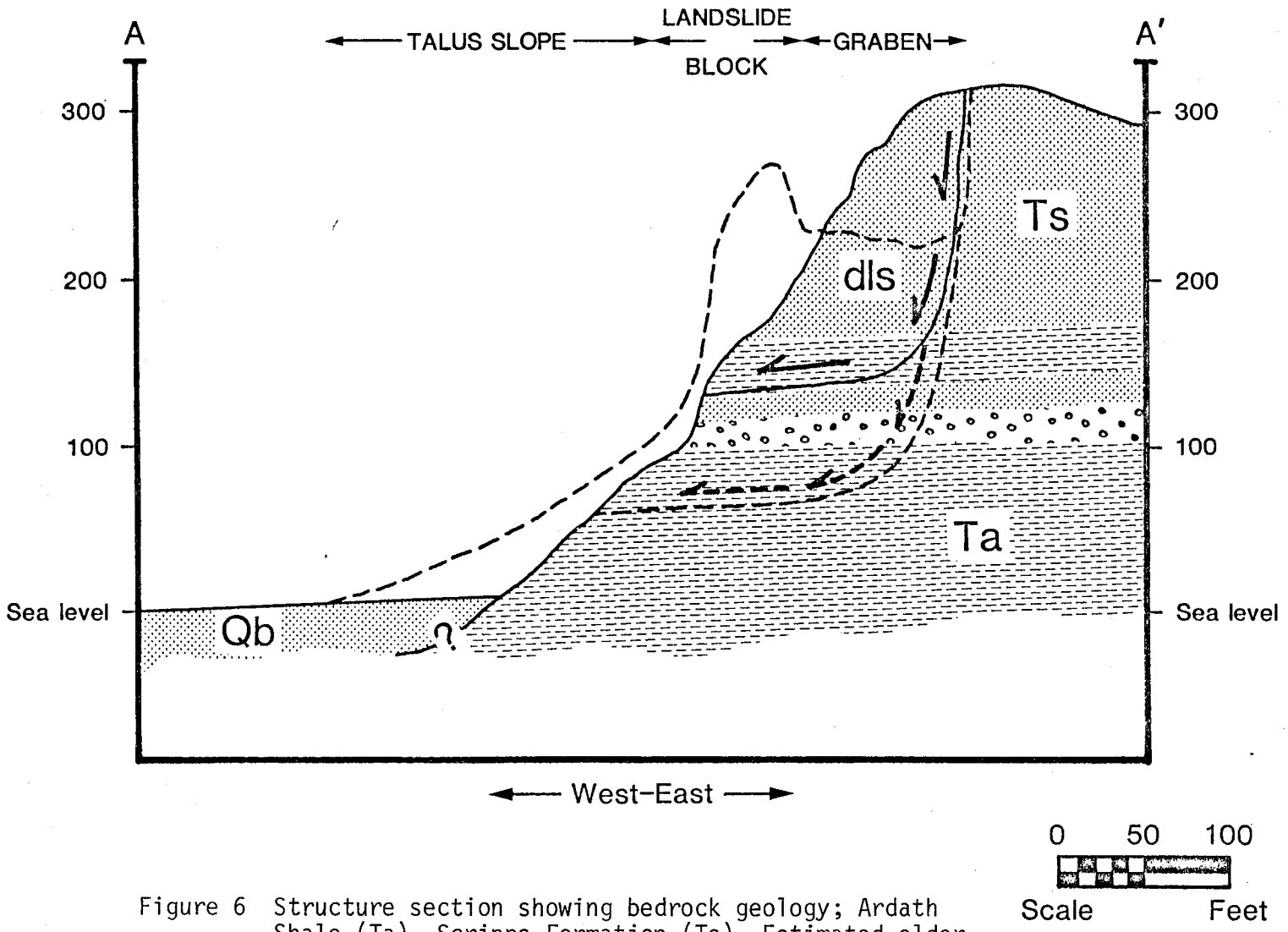

Figure 6 Structure section showing bedrock geology; Ardath Shale (Ta), Scripps Formation (Ts). Estimated older landslide configuration in solid lines, recent landslide configuration in dashes. Note that the recent landslide occurred well below older basal rupture.

1. Retreat of the headwall wherein large slabs peal from the scarp and present a danger to people standing at the top of the ridge or where falling debris may hit pedestrians in the garben area, or potentially on the beach.

2. Failure of slabs on the translational block spires and on the bluff face south of the landslide which fall without warning endangering beach users.

3. Beach goers using the talus lobes for sunbathing could be in danger of being crushed by periodic failures of the main landslide body due to rolling debris.

Since a grading correction of the slide is not feasible, aid in public protection will be through other means. The most feasible protection will be construction of numerous fences and warning signs at appropriate locations. An additional hazard reduction program might include the removal of highly unstable slabs and blocks. Blasting would only be considered as a final resort as there would be a potential for creating additional hazards. Another possible method would be to wrap a cable loop around the block and pull it down with a bulldozer located on the bench. Placement of the cable would probably require rappelling off the bluff or use of a helicopter.

SUMMARY

Geologic mapping of the Torrey Pines Park property for use in park planning, identified a number of hazardous conditions related to landslide potential. Plans for the park had excluded the recent slide area from public use, but the master plan has not been finally approved or implemented. Other areas of the park where landslide hazards are apparent have been considered in the park's master plan and future landslide events are not anticipated that would endanger park improvements.

Like all coastal benches backed by a bluff or sea cliff, beach users must be conscious of the hazard from falling debris. No coastal bluff is immune to mass wastage events and economic solutions to stabilize against continued failures of the bluffs are not feasible. Engineering geologists can best serve the public by recognizing the history of coastal bluff degredation and by applying their knowledge of geomorphic processes to planning and increased public awareness.

REFERENCES

Leighton and Associates, Inc., 1981, Final geotechnical planning report, Torrey Pines City Park, San Diego, California; prepared for the City of San Diego, 16 p.

Leighton and Associates, Inc., 1982, Preliminary investigation, Torrey Pines Park Beach (Black's Beach) La Jolla, California; prepared for the City of San Diego, 6 p.

Kennedy, M.P., 1975, Geology of the San Diego Metropolitan area, California: California Division of Mines and Geology Bulletin 200 (Section A), 39 p.

Woodward-Clyde Consultants 1976, Reconnaissance study, Black's Beach and Sunset Cliffs areas, San Diego, California; prepared for the City of San Diego, 36 p.

140 million years
'Tithonian' (late Jurassic)

Lambert equal-area
$N = 33$ Alpha-95 = 5·4

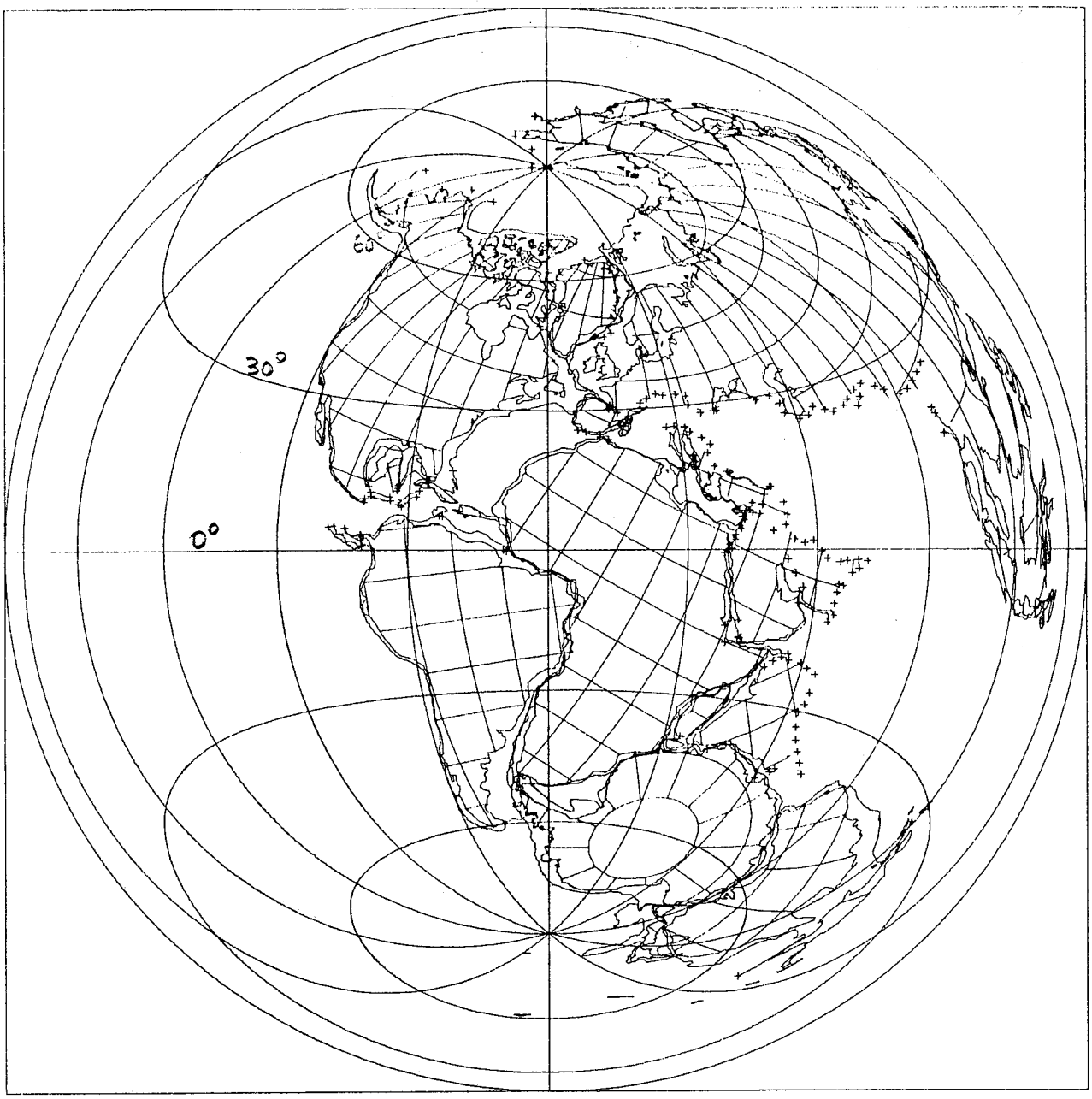

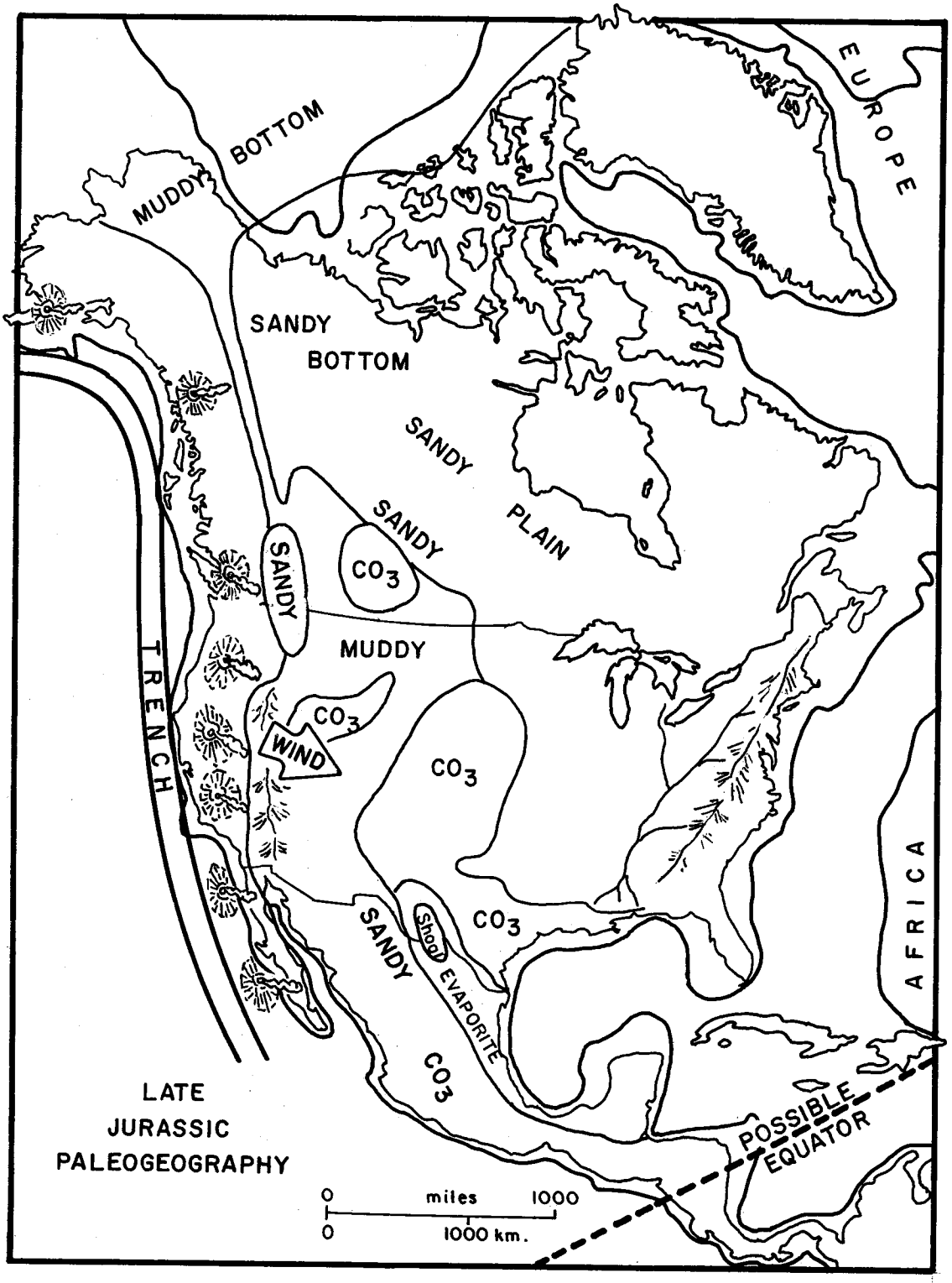
EUROPE
MUDDY
BOTTOM
SANDY
BOTTOM
SANDY
PLAIN
SANDY
SANDY
CO3
MUDDY
TRENCH
CO3
WIND
CO3
SANDY
Shoal
EVAPORITE
CO3
CO3
AFRICA
POSSIBLE
EQUATOR
LATE
JURASSIC
PALEOGEOGRAPHY
0
miles
1000
0
1000 km.

THE DEPOSITIONAL ENVIRONMENT OF THE SANTIAGO PEAK VOLCANICLASTIC ROCKS, WESTERN SAN DIEGO COUNTY, CALIFORNIA

by

Duane C. Balch
Sun Production Co.
Valencia, CA 91355

Sarah M. Hosken
Hrubetz Oil
Walnut Creek, CA 94598

Patrick L. Abbott
Department of Geological Sciences
San Diego State University
San Diego, CA 92182

INTRODUCTION

Mildly metamorphosed, volcanically derived, bedded sedimentary rocks associated with the pre-batholithic Upper Jurassic Santiago Peak Volcanics are in five isolated stream canyons in western San Diego County. Detailed sedimentological and facies analyses were made for those exposures found, from south to north, in Los Peñasquitos Canyon, La Zanja Canyon, Circo Diegueño Canyon, Lusardi Canyon, and within the San Dieguito River canyon at the base of the Lake Hodges Dam (Figure 1).

The sedimentary strata, hereafter referred to as the Santiago Peak volcaniclastic rocks, are generally located due west of the main body of the meta-volcanic flows, breccias, agglomerates and tuffs which make up the bulk of the Santiago Peak Volcanics (Hanna, 1926; Larsen, 1948). Exposures of the Santiago Peak Volcanics physiographically trend north-northwest along the western edge of the Peninsular Ranges batholith from the San Ysidro Mountains east of Chula Vista to the type locality in the Santa Ana Mountains of Orange and Riverside Counties.

Measured sections from each of the canyons are presented in Figures 3, 4, 5, and 6. Los Peñasquitos Canyon contains a thick sequence of massive, andesitic-dacitic, granule to boulder breccias interbedded with feldspathic andesitic litharenites and mudstones. La Zanja Canyon is composed almost entirely of siltstones, silty mudstones and mudstones. Circo Diegueño Canyon is made up largely of interbedded siltstones and very fine sandstones with occasional massive sequences of granule- to boulder-bearing, feldspathic andesitic-dacitic litharenites. The Lusardi Canyon exposure predominantly includes interbedded siltstones and mudstones, rarely interrupted by granule- to boulder-bearing sandstone stringers. The Lake Hodges section principally contains mudstones and siltstones with rare muddy sandstone lenses.

The depositional environment of the Santiago Peak volcaniclastic rocks has been previously described as marine due to the presence of marine fossils within the strata (Milow and Ennis, 1961). Subsequent work by Fife et al. (1967) established a Late Jurassic (Portlandian) age based upon identification of the pelecypod Buchia piochii. Fife et al. (1967) believed that the marine sedimentary strata were "demonstrably" interbedded with the volcanic rocks of the Santiago Peak Volcanics, and thereby assigned the Late Jurassic (Portlandian) age to the Santiago Peak Volcanics as well.

Although a marine depositional environment has been generally inferred, no detailed work has been done on the depositional environments of the Santiago Peak volcaniclastic rocks. Recent analyses of the sedimentological features preserved in the canyon exposures of these rocks (Balch, 1981; Hosken, 1981) indicate that they were deposited by a variety of sediment-gravity flow mechanisms (Bouma, 1962; Middleton and Hampton, 1973, 1976) into various submarine fan-type depositional environments (Mutti and Ricci

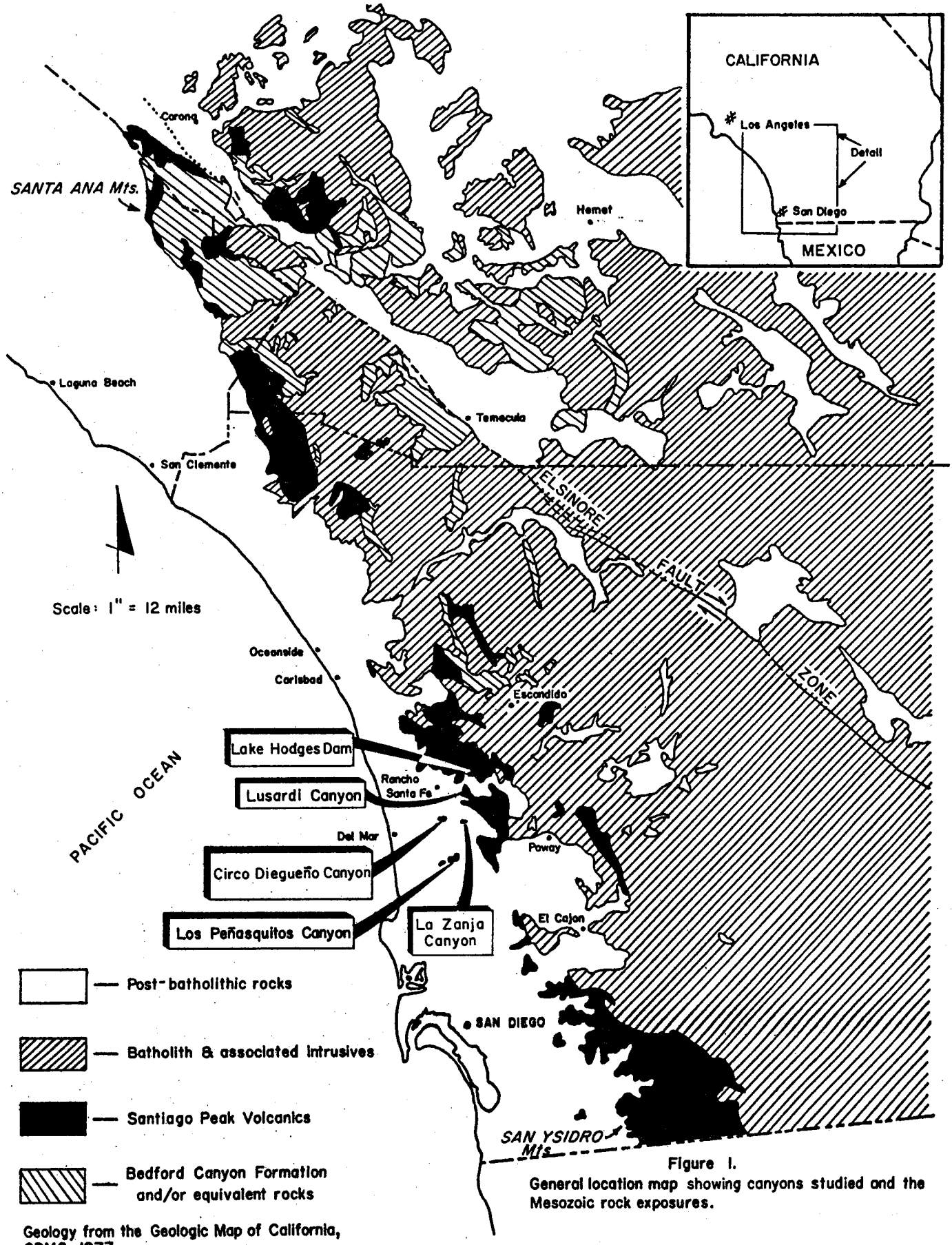

Figure 1.
General location map showing canyons studied and the Mesozoic rock exposures.

Lucchi, 1972, 1975; Walker and Mutti, 1973). Sedimentary facies associations may include inner fan, middle fan channel and depositional lobe, lobe fringe or outer fan, and slope to basin-plain.

DEPOSITIONAL PROCESSES AND FACIES ASSOCIATIONS

Specific depositional processes and sedimentary facies associations can be seen in the various canyon exposures of the Santiago Peak volcaniclastic rocks. Different types of sediment gravity flow mechanisms produced the deposits which make up a large part of the Santiago Peak volcaniclastic rocks. Recognizable are debris-flow, fluidized-flow, and grain-flow deposits, as well as incomplete "Bouma" sequences or turbidites deposited by turbidity current mechanisms.

Models of turbidite facies and turbidite facies associations have been developed in recent years by several workers based upon studies of ancient turbidite sequences (Mutti and Ricci Lucchi, 1972, 1975; Mutti, 1977) and based upon modern submarine fans (Normark, 1970, 1974, 1978). The model used here combines data from modern and ancient submarine fan systems as developed by Walker and Mutti (1973) and later refined by Walker (1978).

Turbidite facies classifications have come to include other types of sediment gravity flow deposits since the turbidite sequence was first outlined by Bouma (1962). The "classical" turbidite consists of five divisions going from base to top: (a) massively bedded sandstone, commonly graded, with basal flute and scour marks, (b) plane parallel laminated sandstone or siltstone, (c) rippled, wavy, or convolute laminated sandstone or siltstone, (d) horizontal laminated siltstone, and (e) a pelitic interval. Incomplete Bouma sequences are common with the (a) or (b) division frequently missing.

As other types of turbidite facies were recognized, it was shown that the Bouma sequence describes but one part of a wide spectrum of depositional processes involving sediment gravity flows. As outlined in Table 1, the whole and partial Bouma sequences make up but three parts of the seven facies types first described by Mutti and Ricci Lucchi (1972) and adapted by Walker and Mutti (1973). Recognition of the various facies and their associations, both laterally and vertically, can be used to determine their depositional environment. Figure 2 illustrates the relationships between certain facies assemblages and their associated depositional environments in a submarine fan system.

Submarine fan systems commonly are complex morphological features along submarine slopes which grow or prograde by the migration of one or several active channels in the middle fan depositional lobe to outer fan, lobe-fringe areas. Facies associations change, both laterally and vertically, as channel migration occurs. Large-scale thinning- and fining-upward sequences are commonly associated with channel-filling and abandonment in the middle fan channeled portions of a system, whereas thickening- and coarsening-upward cycles are indicators of progradation in the middle fan depositional lobe, lobe-fringe and outer fan areas (Walker and Mutti, 1973).

The morphology of the submarine slope and basins may also affect the distribution of facies associations, controlling channel direction and progradation. Slopes may be simple basin-bounding features where fan development is controlled largely by sediment supply, or slopes may be tectonically complex, controlled by active faulting, containing steep canyons and

TABLE I

BASIC CLASSIFICATION OF TURBIDITE AND OTHER RESEDIMENTED FACIES, BASED UPON MUTTI AND RICCI LUCCHI (1972) AND WALKER (1967, 1970 AND UNPUBLISHED).

BOUMA SEQUENCE NOT APPLICABLE	FACIES A -- Coarse grained sandstones and conglomerates A1 Disorganized conglomerates A2 Organized conglomerates A3 Disorganized pebbly sandstones A4 Organized pebbly sandstones. FACIES B -- Medium-fine to coarse sandstones B1 Massive sandstones with "dish" structure B2 Massive sandstones without "dish" structure.
BEDS CAN REASONABLY BE DESCRIBED USING THE BOUMA SEQUENCE	FACIES C -- Medium to fine sandstones -- classical proximal turbidites beginning with Bouma's division A. FACIES D -- Fine and very fine sandstones, siltstones -- classical distal turbidites beginning with Bouma's division B or C. C-D FACIES SPECTRUM -- can be described using the ABC index of Walker (1967). FACIES E -- Similar to D, but higher sand/shale ratios and thinner more irregular beds.
BOUMA SEQUENCE NOT APPLICABLE	FACIES F -- Chaotic deposits formed by downslope mass movements, e.g. slumps. FACIES G -- Pelagic and hemipelagic shales and marls -- deposits of very dilute suspensions.

(after Walker and Mutti, 1973)

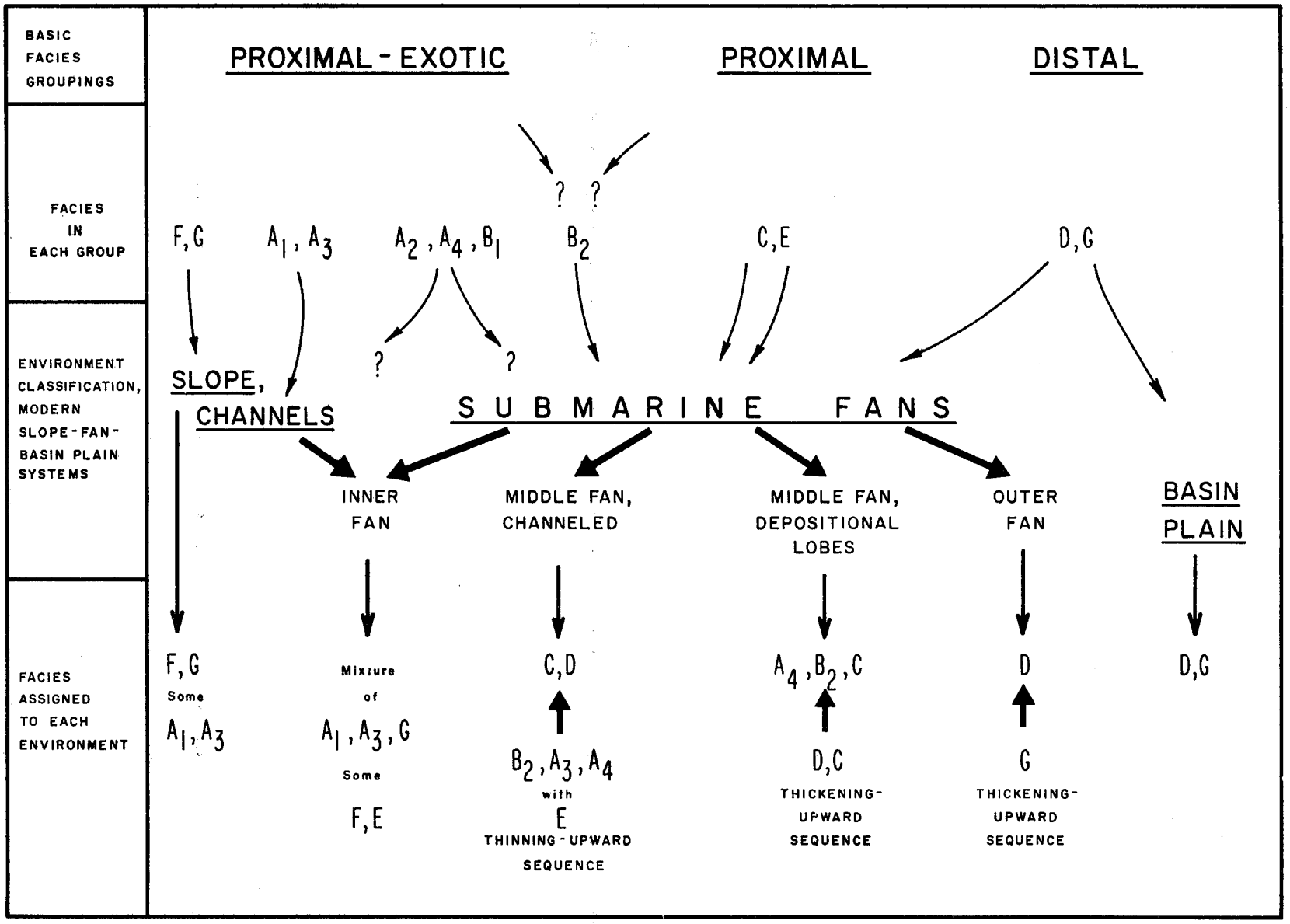

Fig. 2. Diagram showing main relationships between facies (Walker and Mutti, 1973).

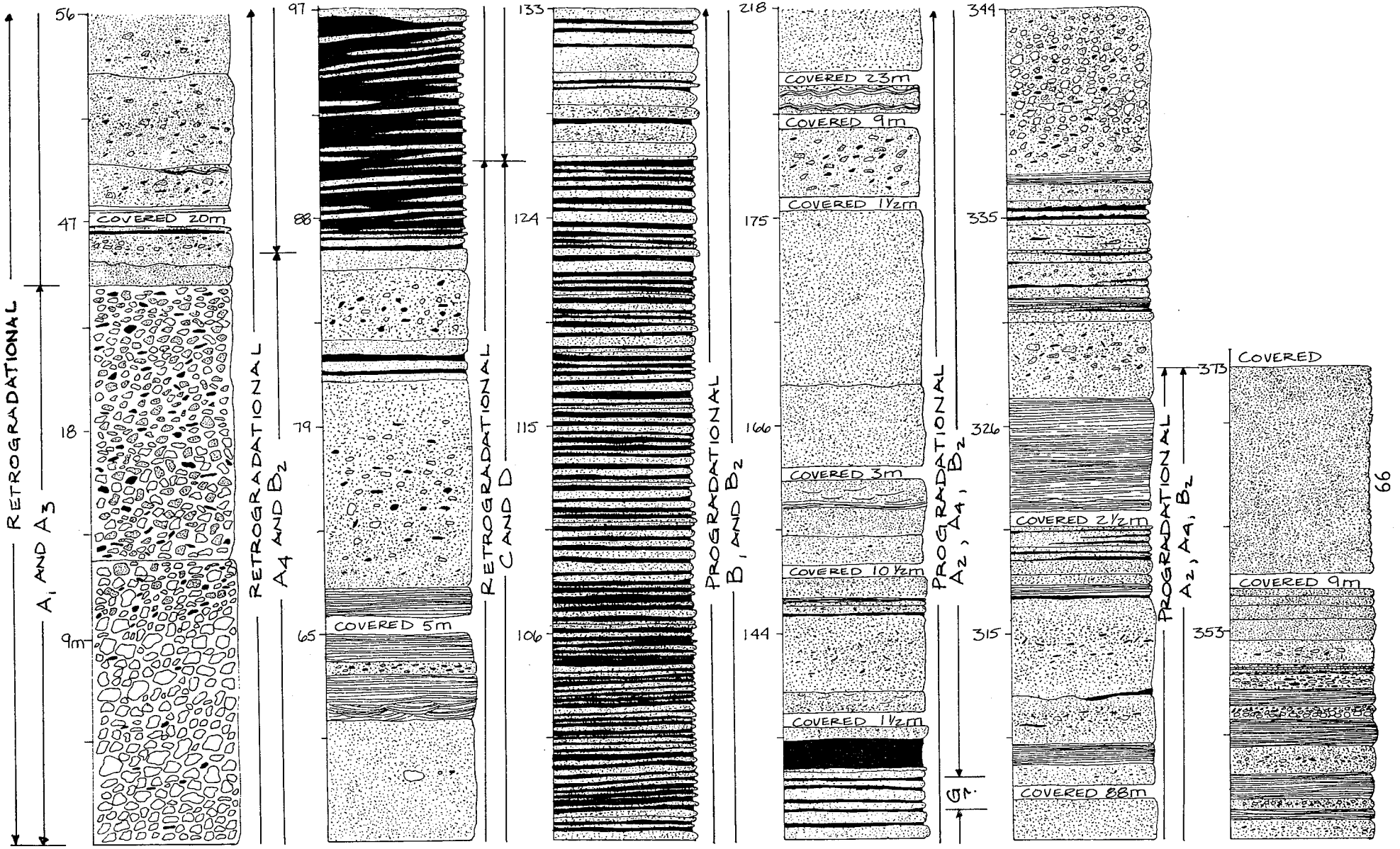

Figure 3. Overview of Los Penasquitos Canyon section. Turbidite facies after Walker and Mutti (1973).

middle fan depositional environments. For the series of breccias, pebbly and massive sandstones, and interbedded sandstones to mudstones previously described, an inner to middle fan channeled environment appears most probable. This initial sequence of strata suggests a migrating channel or retrogradational event.

Continuing up through the section, massive sandstones and pebble- to cobble-bearing sandstones and breccias become dominant again. The massive sandstones are commonly made up of poorly sorted, feldspathic, silty, very fine to very coarse sandstone with mudstone clasts. Load forms are seen where the massive sandstones are interbedded with isolated mudstone stringers. Internal structures are rare, with some weak normal grading and ill-defined "dish" structures. Scoured bases are common. These massive sandstones are facies B_1 and B_2 type deposits laid down by grain flows or fluidized flows.

The massive "sandstone" located between 164 and 175 m (Figure 3) may be a localized deposit of pyroxene andesite (M. J. Walawender, pers. comm., 1981). Compositionally, it is made up of 5% subangular to subrounded, coarse sand- to pebble-sized pyroxene grains mixed with a predominance of subangular, fine to coarse sand-sized plagioclase grains. The pyroxene and plagioclase grains are set in a matrix of randomly oriented, subangular, silt- to very fine sand-sized plagioclase microlaths and tablets. Finely crystalline chlorite and semi-opaque, glassy blebs fill the interstices. Angular grain outlines which may have been softened by diagenetic alteration or by primary igneous reaction rims along with the lack of sedimentary features helps suggest a volcanic origin for the massive "sandstone". Deposition of this massive, tuffaceous pyroxene andesite may have been by volcanic flow, although subaqueous deposition is not clear due to the lack of chilled zones or pillows and both the basal and upper contacts are covered. It is equally possible that this unit is a sandstone deposited as a massive grain flow from a nearby pyroxene andesitic source material.

Slightly farther upsection, a similar appearing "volcanic bed" or "sandstone" grades upwards into a volcaniclastic rock fragment-rich massive sandstone indicating the close affinity between volcanic source rocks and volcaniclastic sedimentary rocks.

The 88 m of covered exposures depicted in Figure 3 may be composed in part of fissile mudstone sequences. The topography of the surrounding area is of relatively low relief and mudstone chips or "float" can be found along strike on the hillsides in this interval. From these observations it is inferred that mudstone is the dominant lithology. This mudstone sequence is interpreted as facies G, with deposition by low density turbidity currents, hemi-pelagic and pelagic processes.

Thinner, massive sandstones, pebble- to cobble-bearing sandstones and breccias with occasional thin interbeds of sandstone, siltstone and mudstone comprise the rest of the measured section. The pebble- to cobble-bearing sandstones and breccias are moderately organized, moderately to poorly sorted, and exhibit normal, reverse, and "coarse tail" grading. They show some stratification in the form of laminations and linear trains of granule to cobble clasts, and in subparallel orientations of the mudstone clasts to the bedding contacts. As facies A_2 and A_4 turbidites, they were deposited as debris flows and grain flows.

The thinner, massive sandstones and interbedded sandstones, siltstones, and mudstones exhibit load forms, flames, and trace fossils with some scour

marks present at bedding interfaces. These sediments are facies B_2, with minor sequences of facies C or D. They were deposited by grain flows and turbidity currents. A small-scale thinning-upward cycle is recognizable in the sandstones at 353 m (Figure 3).

Taken as a group, the massive sandstones, including the volcanic appearing section, the pebble- to cobble-bearing sandstones and breccias, and interbedded sandstones to mudstones are a thickening- and coarsening-upward sequence of facies A_2, A_4, B_1, B_2, and minor facies C or D. This association indicates the prograding channel and depositional lobe portions in the middle of a submarine fan system. The 88 m of largely covered interval within this part of the section are taken to represent facies G deposits. Thus it appears two prograding mid-fan sequences are present that are separated by a slope or basin-plain mid-fan sequence. This alternation of environmental facies suggests the fans were fairly small and that they were being deposited in a tectonically active area where basin configuration was continually changing.

For the sequence of volcaniclastic rocks exposed in Los Peñasquitos Canyon the following scenario is proposed. The massive breccias and sandstones, pebbly sandstones, and interbedded sandstone to mudstone sequences represent deposition from a nearby volcanic source by sediment gravity flows into the inner (?) to middle fan channeled portions of a submarine fan-type system. Large-scale thinning- and fining-upward cycles indicate channel deposition. Subsequent deposition of a thick sequence of massive sandstones with gross thickening-upward cycles suggests establishment of depositional lobe environments. The minor volcanic sequence with stratigraphically adjacent massive volcaniclastic sandstones may have eventually filled or diverted the feeder channel marking the onset of facies G mudstone deposition. A new channel or lateral migration of the earlier channel is seen in the renewed deposition of the breccias and sandstones with thickening-upward cycles suggesting progradation of a mid-fan associated depositional lobe environment.

LA ZANJA CANYON

The La Zanja Canyon exposures of the Santiago Peak volcaniclastic rocks are located approximately 6.5 km north-northeast from the exposure in Los Peñasquitos Canyon. Bedding attitudes have measured dips between 36° to 42° east and strikes from due north to N5°W. Current ripple marks near the top of the measured section indicate that the strata are not overturned.

As depicted in Figure 4, silty mudstones and mudstones make up most of the section. Siltstone interbeds occur and a single, slightly channeled, 60 cm thick sandstone unit was observed. Bedding thicknesses range from one to 30 cm, averaging one to three cm. No sense of grading was detected, and no syndepositional deformation or slumping was seen.

The mudstones in La Zanja Canyon are facies G sequences probably deposited in an outer fan to basin-plain environment. A lack of slumping or syndepositional deformation suggest low energy deposition by pelagic, hemi-pelagic and nepheloid processes away from the slope environments. The sandstone bed may represent a singular input of a facies D turbidite from the lobe-fringe or outer fan environment. The current ripple marks in the mudstone near the top of the section may be the result of basinal contour currents or very low density turbidity currents. While a submarine fan-

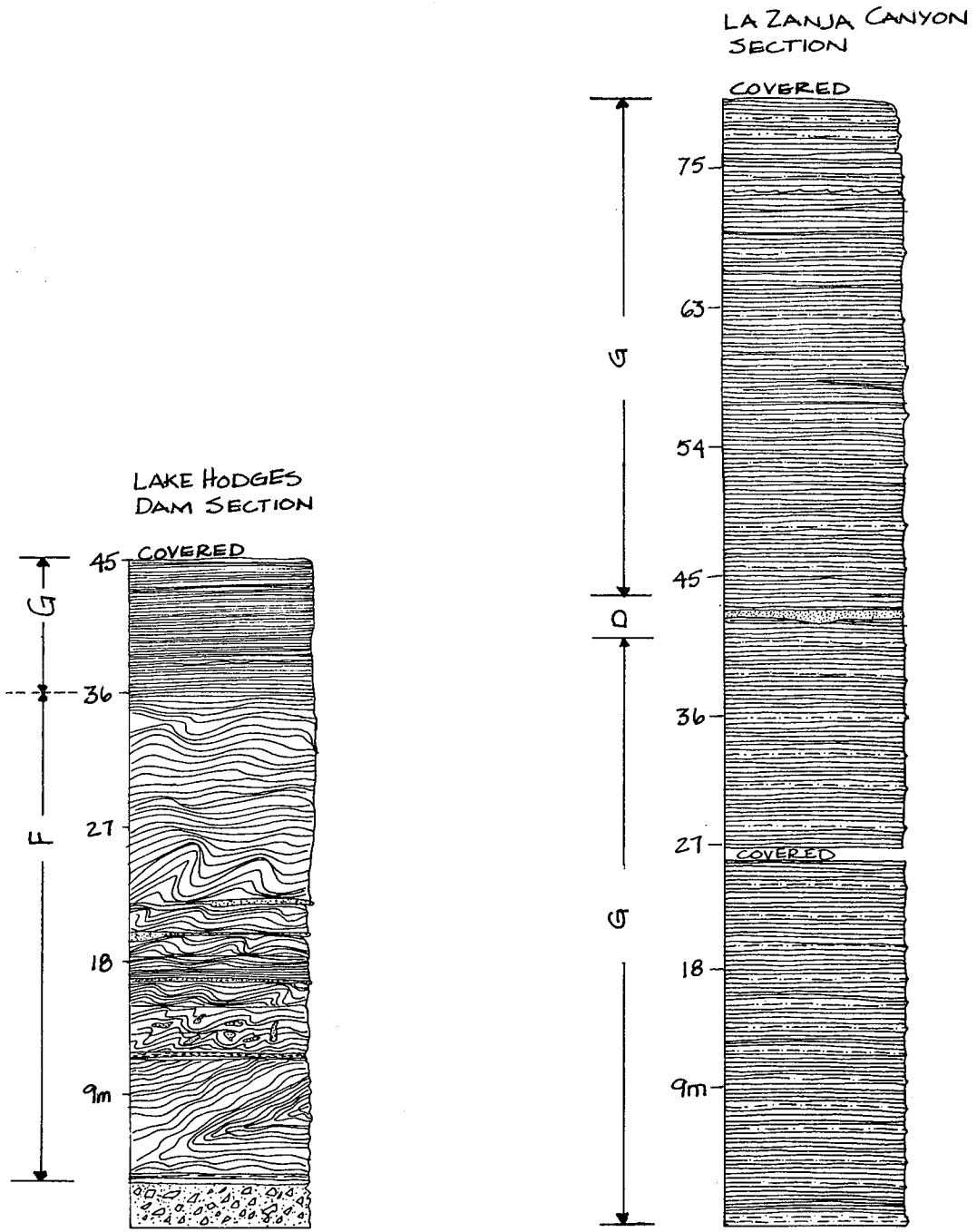

Figure 4. Overview of Lake Hodges Dam section and La Zanja Canyon sections. Turbidite facies after Walker and Mutti (1973).

type environment is inferred, assigning such an overall model based on a single exposure of facies G deposits is tenuous.

CIRCO DIEGUEÑO CANYON

The Santiago Peak volcaniclastic rocks in Circo Diegueño Canyon are located approximately three km west-northwest of the La Zanja Canyon sequence. Based upon a variety of flames, load forms and scour marks, the strata are observed to be slightly overturned and dip an average of 80° E and strike N11°E. Previous workers (Hanna, 1926; Larsen, 1948; Fife et al, 1967; Balch, 1981) referred to this exposure as "the small canyon north of La Zanja Canyon", but it is now referred to as Circo Diegueño Canyon after the access road on the south side of the canyon.

The Circo Diegueño Canyon exposures are principally made up of interbedded siltstones and sandstones (Figure 5). Thinly bedded siltstones and sandy siltstones are the predominant lithologies and consist of facies D and some facies C type turbidites. Bouma sequences are frequently observed and may begin with the (a), (b), or (c) division. The mudstone (e) divisions are generally very thin between individual sequences.

The beds are commonly normally graded in the coarser fraction, exhibit planar to convolute laminations, and quickly grade upward into a thin veneer of mudstone. Trace fossil burrows and trails (Zoophycos and Nereites facies, after Seilacher, 1967) are common along the upper portions of beds. Basal contacts frequently contain load forms and casts, flames, and some scour or flute marks.

The syndepositional deformation of finer grained sediments by overlying events can be seen where mudstone rip-ups and some large laminated siltstone blocks have been ripped up and incorporated into the overlying deposit. Slumped units indicate deposition upon a sloped substratum or base.

Small-scale thinning- and fining-upward cycles, followed by thickening-upward cycles (Hosken, 1981) are repeated across short intervals of the siltstone and sandstone interbeds suggesting variable sediment input and small scale channel migration. These facies D and C turbidites were deposited in the regions transitional to the middle fan depositional lobes and outer fan areas by normal turbidity currents possibly originating as overbank events from laterally adjacent channels.

Within the facies D and C deposits, isolated, thick-bedded sandstone units occur at least three times. They are massively bedded, with vague normal grading, and some inverse grading and are interpreted to be gradational between facies A_4 and facies B_2 turbidites. They contain granule- to boulder-sized rip-up clasts of finely laminated siltstones and mudstones (at 60, 100, and 189 m, Figure 5). A thickening-upward sequence occurs for those massive sandstones located between 85 and 111 m (Figure 5). Sand grain size variations are minimal but clast sizes increase upwards. Within this thickening-upward sequence are found the nearshore, shallow water marine mollusc fossils.

The massive granule- to boulder-bearing sandstones were deposited as debris flows or possibly as grain flows. They carried slope or levee derived mudstone rip-ups, shallow water organisms, and volcanically derived sands down onto a middle fan depositional lobe environment.

The sequence of siltstones and sandstones in Circo Diegueño Canyon represents fairly continuous deposition of facies D and facies C turbidites

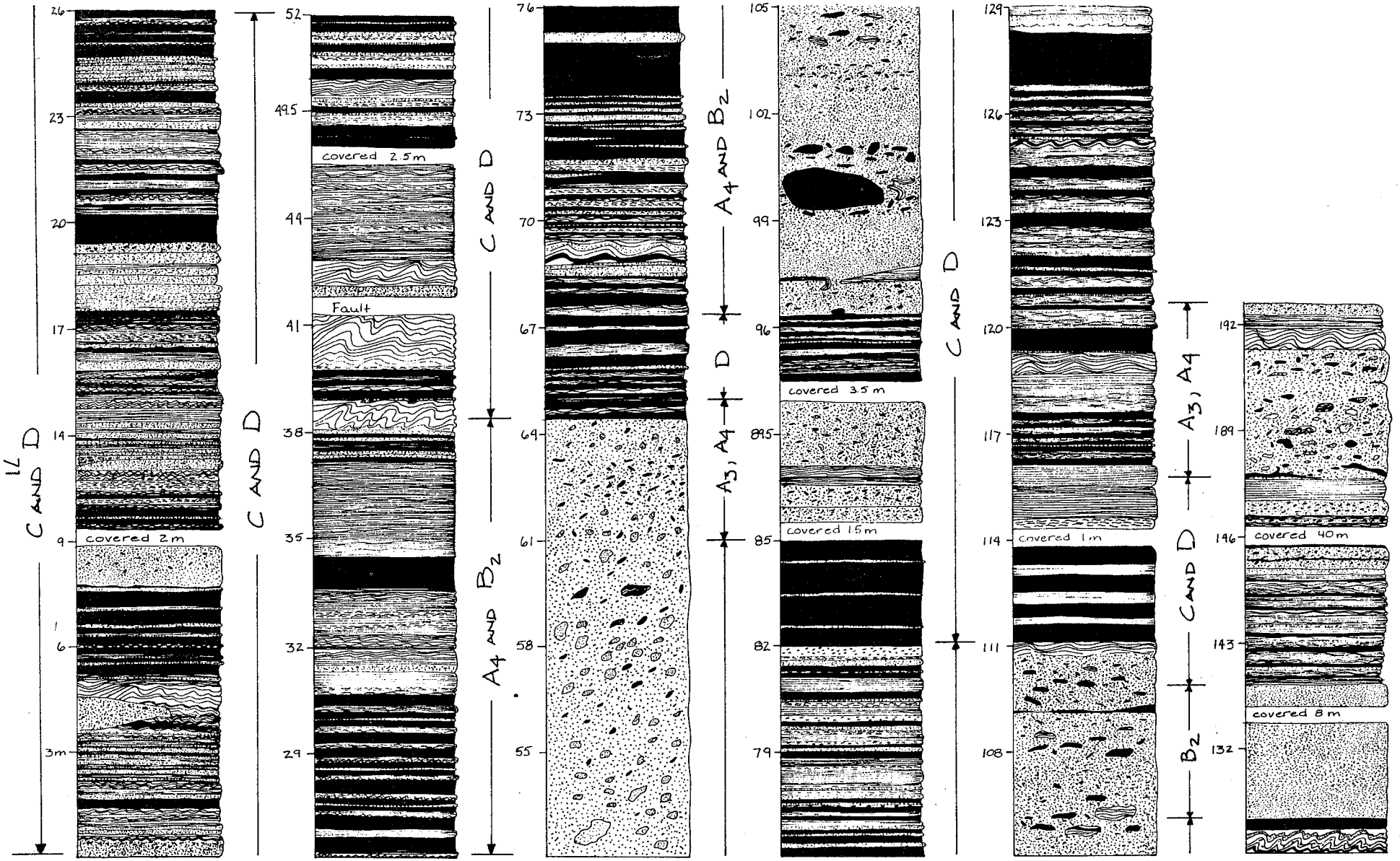

Figure 5. Overview of Circo Diegueno Canyon Section. Turbidite facies after Walker and Mutti (1973).

in a lobe-fringe or outer fan to middle fan depositional lobe environment. Small-scale thinning- and thickening-upward cycles are seen in thin stratigraphic packages but large-scale megasequences are not present. Interjections of facies A_4 to B_2 sandstone turbidites suggest the possible migration or progradation of sandier portions of the middle fan depositional lobes, perhaps as large crevasse splays, into the transition area between middle fan depositional lobes and outer fan environments.

LUSARDI CANYON

Exposures of the Santiago Peak volcaniclastic rocks in Lusardi Canyon are located three km northeast of Circo Diegueño Canyon. Structural attitudes vary between N35°W and N55°W with dips ranging from 22° to 50°NE. The main body of the sedimentary strata is overturned.

East of the measured section are massive pyroxene-bearing andesitic flow rocks. An underlying ash-tuff bed containing flame structures indicates that this sequence is not overturned. A fault trending N15°W and dipping steeply towards the west cuts the ash-tuff and flow rocks. Across this fault, scour of the ash-tuff unit by the overlying flow rocks indicates that the section is overturned, and this marks the beginning of the measured section depicted in Figure 6 (Hosken, 1981).

The volcaniclastic strata begin at 98 m and the contact with the underlying volcanic flow rocks is covered. The sedimentary section is dominated by finely laminated mudstones and laminated, occasionally graded, siltstones. The mudstones and siltstones are considered to be examples of facies G turbidites deposited by low density turbidity currents and by pelagic and hemi-pelagic processes. Laminations are planar tabular to slightly wavy, and very small-scale load forms and wisps or flames may be present. No trace fossil trails or burrows could be found.

A few interbeds of laminated siltstones and silty sandstones contain thin Bouma sequences beginning with the (b) or (c) division. Rare, thicker sandstone units contain granule- to pebble-sized clasts of mudstone and volcaniclastic rock fragments. Portions of the interbedded siltstone sequences exhibit large-scale slumping and are interpreted to be facies F type deposits. The Bouma sequences beginning with (b) or (c) divisions correspond to facies D turbidites. Rare load forms and channeling can be seen in some of the interbedded sandstone, siltstone, and mudstone sequences.

At approximately 235 m (Figure 6) a discontinuous exposure of interbedded sandstone and granule- to boulder-bearing breccia mark the coarsest deposits in Lusardi Canyon. The basal sandstone unit is finely laminated and weakly normal graded. Flame structures and load forms are visible along the contact with the underlying mudstone unit, and mud rip-ups and scours are present at the interface with the overlying breccia deposits. The breccias contain boulder-sized mudstone clasts and granule- to pebble-sized clasts of volcanic rock fragments. The breccias are poorly sorted, with no sense of grading except for coarse-tail grading of the larger clasts. The breccias are discontinuously overlain by another massive sandstone unit containing granule- to pebble-sized mudstone clasts. This sandstone unit is partially covered at 239 m, yet appears to be conformably overlain by a continuation of the dominant mudstone sequence (Balch, 1981).

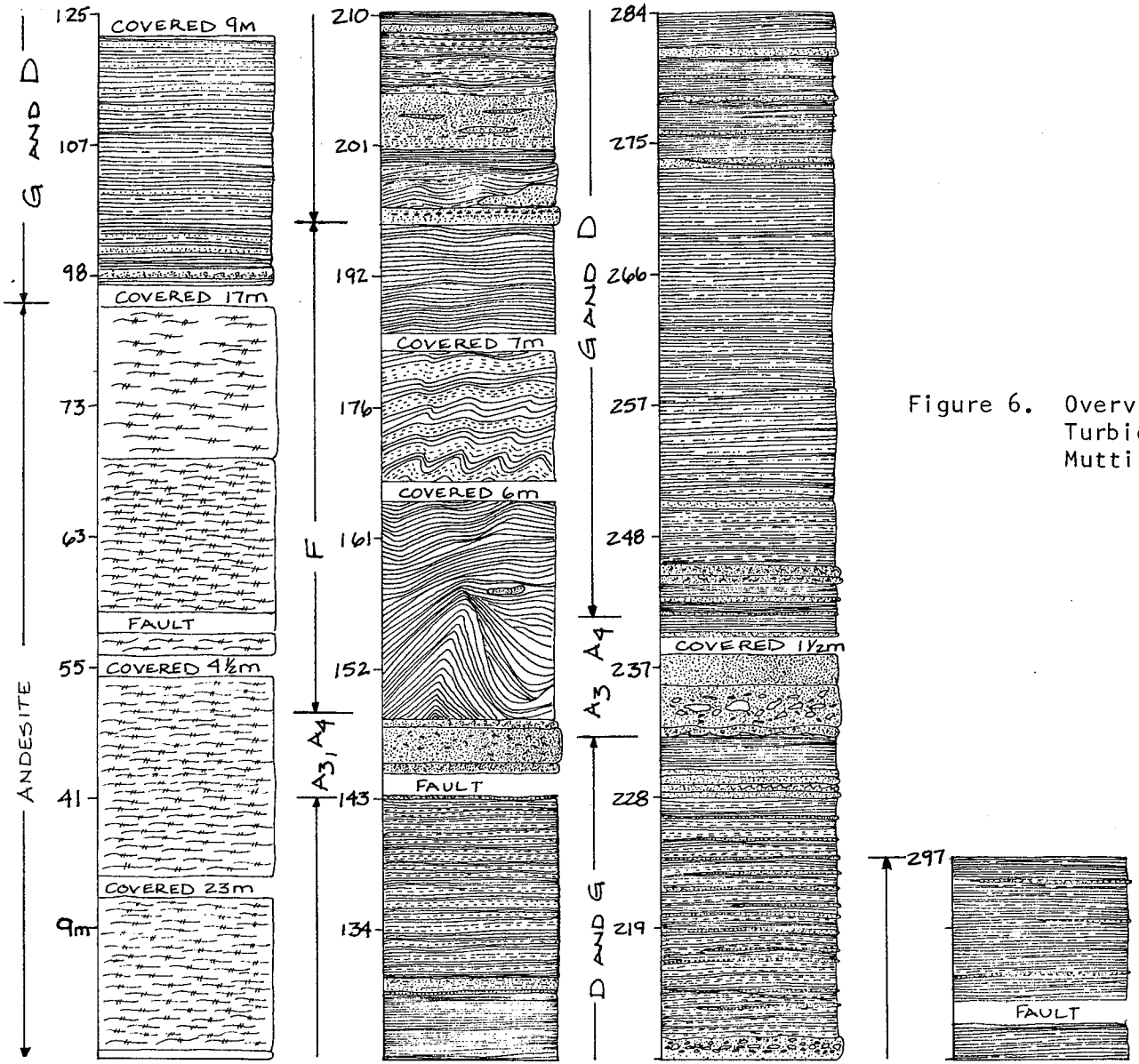

Figure 6. Overview of Lusardi Canyon section. Turbidite facies after Walker and Mutti (1973).

Due to the discontinuous nature of the sandstone-breccia series at 235 m, it is suggested that these facies A_3 to A_4 turbidites were slump-generated, toe-of-slope debris flow deposits.

The Santiago Peak volcaniclastic rocks within Lusardi Canyon are composed mainly of facies G, facies F, and some facies D type sequences. Recognizable are sedimentary sequences deposited by pelagic and hemi-pelagic processes, by slumping, and by turbidity currents. A toe-of slope or slope to basin-plain depositional environment appears to be indicated (Figure 2).

LAKE HODGES DAM SECTION

Approximately one mile downstream from the Lake Hodges Dam, a sedimentary section of the Santiago Peak volcaniclastic rocks is exposed. This section is approximately four km north-northeast of the Lusardi Canyon exposures. The rocks strike due east-west and dip 85°N. Depositional features show that the section is not overturned.

The Lake Hodges Dam section (Figure 4) consists of mostly mudstone and silty mudstone units grading from slightly wavy, occasionally scoured laminations to mildly then chaotically deformed, slumped beds. Rare muddy sandstones are also present as thin interbeds. The entire section appears to conformably overlie dark, plagioclase-bearing volcanic rocks and ash-tuff breccias which in turn overlie a sequence of tuffaceous ash beds.

As with the exposures in Lusardi Canyon, the Lake Hodges Dam section appears to be made up largely of facies F and G type deposits. They were laid down by low energy turbidity currents and hemi-pelagic to pelagic processes. Abundant slumped beds indicate syndepositional deformation probably due to deposition on sloped or inclined surfaces. The underlying volcanic rocks may represent a progradational event where volcanism entered the toe-of-slope or slope to basin plain depositional environment, only to be followed by the continuation of low energy turbidity currents, slumps, and hemi-pelagic to pelagic mudstone deposition.

SUMMARY OF DEPOSITIONAL ENVIRONMENTS

Sediment gravity flow depositional processes are recognizable within each canyon exposure of the Santiago Peak volcaniclastic rocks. A variety of sedimentary facies associations is seen in each canyon. However, large-scale megasequences of fining- or coarsening-upward cycles, typical of mature submarine fan systems, are generally lacking except possibly within Los Peñasquitos Canyon. It is proposed that each canyon exposure of the Santiago Peak volcaniclastic rocks represents submarine deposition in individual, immature fan systems and/or in isolated intraslope basins. Restricted basins affect the development and progradation of depositional lobes, which limits channel migration and thus the development of megasequences.

Of the canyon exposures studied, Los Peñasquitos Canyon contains the best megasequences of fining- or coarsening-upward cycles. Facies A, B, C, and D associations suggest channel migration and abandonment followed by two progradational channel events. A moderately well developed inner fan channel to middle fan channel and depositional lobe environment is surmised.

The Circo Diegueño Canyon section contains numerous crevasse splays and channel deposits with a majority of the interchannel or overbank turbidites displaying facies D and C associations. A nearby, poorly defined, middle fan channel or depositional lobe environment is indicated.

La Zanja Canyon is made up of bedded siltstones and mudstones deposited by hemi-pelagic and pelagic processes. While facies G may be indicated, a submarine fan association is not conclusively shown. A basin-plain environment may be represented.

Lusardi Canyon and the Lake Hodges Dam sections both contain thick mudstone sequences and deformed beds. Facies G and facies F associations are common to both. A toe-of-slope or slope to basin plain environment appears to be the likely depositional environment.

Faunal evidence shows deeper water, trace fossil burrows and trails (Zoophycos and Nereites) to be common in the siltstones and mudstones of Los Peñasquitos and Circo Diegueño Canyons. The lack of these trace fossils in the mudstone-dominated sections of Lusardi, La Zanja, and the Lake Hodges canyons may indicate that the depositional basins contained anoxic waters. Pelecypods and echinoid fragments found in the sandstones and breccias at Circo Diegueño Canyon demonstrate the transport of shallow water organisms into the deep water, submarine fan environments. Free-swimming belemnoid cephalopods were found in the breccias, sandstones, and mudstones in Los Peñasquitos, Circo Diegueño, and Lusardi Canyons.

Paleocurrent data have been collected from a number of sedimentary features in Circo Diegueño and La Zanja Canyons, and in the Lake Hodges Dam section. Bidirectional indicators in La Zanja Canyon and in the Lake Hodges Dam section indicate northeast-southwest transport directions. In Circo Diegueño Canyon a variety of directions are indicated. Small-scale cross-bedding at two locations indicates a northerly direction of transport, and a single, slumped siltstone sequence suggests a northerly-tilted paleoslope. Lateral injection features show sediment movement trending west-northwest and east-southeast. Other flame structures, flute casts, and crescent ripples indicate easterly to southeasterly current directions. Asymmetric current ripples give southwesterly current directions. Thus, a variety of paleocurrent directions appear to be indicated, particularly for the strata in Circo Diegueño Canyon. While each directional indicator may be accurate only for the individual bed in which it is found, a larger-scale sense of paleocurrent direction may be inferred.

If the main transport direction is southwesterly as indicated by the asymmetric ripples, associated lateral injections would be directed southeast and northwest. Crevasse splays from such channels might produce northerly directed slumps and ripple marks as the depositional lobes migrated. With a volcanic source located to the east, these paleocurrent directions generally agree with the present physical distribution of the Santiago Peak Volcanics due east of the volcaniclastic rocks.

Complications arise if the east to southeasterly paleocurrent indicators represent the main transport direction. This configuration puts the volcanic source for the sediments west of the depositional basins. As outlined by Gastil et al. (1978, 1981) segmentation of a volcanic island arc system, associated with oblique subduction along the western coast of peninsular California, could have produced two subducting plates and two parallel arc systems during the Late Triassic and Jurassic. The outer fringe arc could have deposited volcanic detritus into basins to the east between the two arc systems. Collision of the two arc systems occurred during the Early Cretaceous, possibly producing the structural complications and widely varying attitudes presently seen in the different canyon exposures of the volcaniclastic rocks.

Present paleocurrent data, uncorrected for the probably complex structural history, indicate main transport directions to the southwest with the source rocks to the east as well as sediment transport to the east to southeast from source rocks located west of the depositional basins.

CONCLUSIONS

The Upper Jurassic Santiago Peak volcaniclastic rocks were deposited by sediment gravity flow mechanisms into immature submarine fan-type environments. Sedimentary facies associations are partially recognizable, though megasequences of thinning- or coarsening-upward cycles are essentially lacking, except within Los Peñasquitos Canyon. Restricted depositional basins in the intraslope to trench slope portions of the Santiago Peak Volcanics island arc system limited the development and progradation of depositional lobes and channel migrations, thus affecting the development of well defined megasequences.

Sedimentary facies associations include inner (?) to middle fan channeled environments, middle fan depositional lobe to lobe-fringe or outer fan environments, and slope to basin-plain (?) environments. While these various associations can be inferred, a single, mature submarine fan system is not indicated. The canyon exposures represent poorly developed sedimentary facies associations found in an immature fan system and/or restricted depositional basins.

Paleocurrent data may indicate main sediment transport either in a southwesterly direction into the intraslope to trench slope regions west of the volcanic arc system, or eastward representing sediment transport into basins located east of a volcanic arc terrane possibly produced by arc segmentation associated with oblique subduction. Paleocurrent indicators may reflect rotation accompanying faulting along the borderland.

REFERENCES

Balch, D. C., 1981, Sedimentology of the Santiago Peak volcaniclastic rocks, San Diego County, California (M.S. thesis): San Diego State University, 135 p.

Bouma, A. H., 1962, Sedimentology of some Flysch Deposits, a Graphic Approach to Facies Interpretation: Amsterdam, Elsevier, 168 p.

Fife, D. L., Minch, J. A., and Crampton, P. J., 1967, Late Jurassic age of the Santiago Peak Volcanics, California: Geol. Soc. America Bull., v. 78, p. 299-303.

Folk, R. L., 1974, Petrology of Sedimentary Rocks: Austin, Texas, Hemphill Publishing Co., 182 p.

Gastil, R. G., Morgan, G. J., and Krummenacher, D., 1978, Mesozoic history of peninsular California and related areas east of the Gulf of California, in Howell, D. G., and McDougall, K. A., eds., Mesozoic Paleogeography of the Western United States: Pacific Section, Soc. Econ. Paleontologists and Mineralogists, Pacific Coast Paleogeography Symposium No. 2, p. 107-115.

Gastil, R. G., Morgan, G. J., and Krummenacher, D., 1981, The tectonic history of peninsular California and adjacent Mexico, in Ernst, W. G., ed., The Geotectonic Development of California: Englewood Cliffs, New Jersey, Prentice-Hall, p. 284-306.

Hanna, M. A., 1926, Geology of the La Jolla quadrangle, California: Univ. of Calif. Dept. Geological Sci. Bull., v. 16, p. 187-246.

Hosken, S. M., 1981, Sedimentology of Upper Jurassic Santiago Peak volcaniclastic strata of northern San Diego County, California: Senior thesis, San Diego State University, 78 p.

Kennedy, M. P. and Peterson, G. L., 1975, Geology of the San Diego metropolitan area, California: Calif. Div. of Mines and Geology Bull., v. 200, 56 p.

Larsen, E. S., Jr., 1948, Batholith and associated rocks of Corona, Elsinore, and San Luis Rey quadrangles, southern California: Geol. Soc. America Memoir 29, 182 p.

Middleton, G. V., and Hampton, M. A., 1973, Sediment gravity flows: mechanics of flow and deposition, in Middleton, G. V., and Bouma, A. H., eds., Turbidites and Deep-water Sedimentation: Pacific Section, Soc. Econ. Paleontologists and Mineralogists, Short Course Lecture Notes, p. 1-38.

Middleton, G. V., and Hampton, M. A., 1976, Subaqueous sediment transport and deposition by sediment gravity flows, in Stanley, D. J., and Swift, D. J. P., eds., Marine Sediment Transport and Environmental Management: New York, John Wiley and Sons, p. 197-218.

Milow, E. D., and Ennis, D. B., 1961, Guide to geologic field trip of southwestern San Diego County, in Thomas, B. E., ed., Guidebook for field trips, Cordilleran Sec., Geol. Soc. America: San Diego State Coll. Geol. Dept., p. 23-43.

Mutti, E., 1977, Distinctive thin-bedded turbidite facies and related depositional environments in the Eocene Hecho Group (south-central Pyrenees, Spain): Sedimentology, v. 24, p. 107-131.

Mutti, E., and Ricci Lucchi, F., 1972, Le torbiditi dell'Appennino settentionale: introduzione all'analisi di facies: Soc. Geol. Italiana Mem., v. 11, p. 161-199; English translation by T. H. Nilsen, 1978, Internat. Geology Rev., v. 20, p. 125-166; AGI Reprint Ser. 3.

Mutti, E., and Ricci Lucchi, F., 1975, Turbidite facies and facies associations, in Examples of turbidite facies and facies associations from selected formations of the northern Apennines: 9th Internat. Cong. Sedimentology, Nice, France, Field Trip Guidebook, A-11, p. 21-36.

Normark, W. R., 1970, Growth patterns of deep-sea fans: Am. Assoc. Petrol. Geologists Bull., v. 54, p. 2170-2195.

Normark, W. R., 1974, Submarine canyons and fan valleys: Factors affecting growth patterns of deep-sea fans, in Modern and ancient geosynclinal sedimentation: Soc. Econ. Paleontologists and Mineralogists Spec. Pub. 19, p. 56-68.

Normark, W. R., 1978, Fan valleys, channels, and depositional lobes on modern submarine fans: Characters for recognition of sandy turbidite environments: Am. Assoc. Petrol. Geologists Bull., v. 62, p. 912-931.

Seilacher, A., 1967, Bathymetry of trace fossils: Marine Geology, v. 5, p. 413-428.

Walker, R. G., 1978, Deep-water sandstone facies and ancient submarine fans: Models for exploration for stratigraphic traps: Am. Assoc. Petrol. Geologists Bull., v. 62, p. 932-966.

Walker, R. G., and Mutti, E., 1973, Turbidite facies and facies associations, in Middleton, G. V., and Bouma, A. H., eds., Turbidites and deep water sedimentation: Pacific Section, Soc. Econ. Paleontologists and Mineralogists, Short Course Lecture Notes, p. 119-157.

PETROLOGY OF UPPER JURASSIC SANTIAGO PEAK VOLCANICLASTIC ROCKS, WESTERN SAN DIEGO COUNTY, CALIFORNIA

by

Duane C. Balch
Sun Production Company
Valencia, CA 91355

Patrick L. Abbott
Dept. of Geological Sciences
San Diego State University

INTRODUCTION

Detailed petrographic analyses have been completed for selected rock samples of the Santiago Peak volcaniclastic rocks from three of five known stream valley exposures found in western San Diego County. A total of 43 thin sections were studied, including 19 modal analyses from specimens gathered in Circo Diegueño, Lusardi and Los Peñasquitos Canyons (Figure 1 in preceding paper). Point-counting was done on a standard petrographic microscope with a hand-operated mechanical stage with about 300 points counted for each sample. The sandstone classification outlined by Folk (1974) was used for describing the sandstones. The actual percentages of the three major framework grains (Q=quartz, F=feldspar, R=rock fragments) along with the total number of framework grains (F) including pyroxenes, were recalculated along with the points counted as matrix materials (M), as cement (C), and as porosity (P) (Table 1). The short-hand notation of QFR:FMCP can be used to compositionally describe the individual sandstone samples. Grain-size, sorting, skewness, rounding, and sphericity data gathered from the point counts were plotted according to the methods outlined by Folk (1974).

In addition to the petrographic analyses, x-ray diffraction analyses were run on 9 samples in order to identify the major phyllosilicates present in the sandstones and in the mudstones. Two of the point-counted samples, RSP and RSX, were in this group of 9 specimens. Chlorite (ripidolite) was found to be the primary phyllosilicate present in both the sandstones and in the mudstones. Strong illite peaks were also recorded for the mudstones in Lusardi Canyon. Chemical analyses for selected samples are shown in Table II.

PETROGRAPHY

CIRCO DIEGUEÑO CANYON

Thin-sections studied from the Circo Diegueño Canyon exposures represent lithologies from different sandstone depositional styles. Samples RFA, RFB, RFD, RSP, RSQ, are debris-flow sandstone units. The remaining thin-sections are from thin-bedded sandstones in the Bouma (a) or (b) division, found in "classic" turbidites. Fossils, such as oyster fragments and echinoid spines, found in several of the thin-sections suggest that these sandstones were deposited in a marine environment.

For the 15 sandstone samples from Circo Diegueño Canyon, the average composition was calculated to be quartz (Q) 3%, feldspars (F) 52%, and rock fragments (R) 45%. Including the detrital pyroxenes, total framework grains (F) constitute 64% of the total rock volume. Matrix material (M), including protomatrix, orthomatrix, epimatrix, and pseudomatrix of Dickinson (1970), makes up the remaining volume at 36%. The average composition is $Q_3F_{52}R_{45}$: $F_{64}M_{36}C_oP_o$ and is an andesitic lithic arkose.

The matrices of the sandstones and the groundmasses of the andesitic-dacitic volcanic rock fragments were compositionally very similar, if not identical. Depositional disaggregation and diagenetic alteration of many of the unstable volcanic rock fragments made it difficult to determine where the rock fragment grains ended and "matrix" began. As a result, many of the plagioclase grains which may have actually belonged as "phenocrysts" within the volcanic rock fragments were point counted as detrital framework grains. This probably accounts for the high feldspar percentages in several of the samples. A more probable composition would be similar to samples RFA and RSP. Therefore, the average composition of the Circo Diegueño Canyon sandstones could be more accurately described as feldspathic andesitic-dacitic litharenite or andesitic-dacitic litharentie.

The average mean grain size for the framework grains is medium sandstone (1.13Ø or 0.46 mm). Mean grain sizes ranged between 2.38Ø (fine sand) and -0.08Ø (very coarse sand). Average sorting was 1.12Ø or poorly sorted, with individual sorting values indicating moderate to poor sorting of the total framework grains. Other average values for the total framework grains include skewness at -0.13, or coarse skewed; mean angularity at 3.11ρ, or subrounded; roundness sorting at 0.31ρ, or very good roundness sorting (probably due to diagenetic alteration of angular grains); and a mean sphericity of 0.63; or transitional between elongate and subelongate grain shapes. The sandstones of Circo Diegueño Canyon are both compositionally and texturally immature.

As a percentage of the total framework grains, plagioclase feldspar dominates in the sandstones at 47%. Andesine and labradorite are the typical compositions seen, with some oligoclase present. Plagioclase grains are subangular to subrounded, and exhibit good crystal forms as elongate laths and tablets. Albite and carlsbad twinning are common, while crystal zonation is less common. Relict embayments are occasionally present, though some may be the result of post-depositional diagenetic replacement by chlorite.

Plagioclase framework grains range from fine- to very coarse-sand size, are poorly to moderately sorted, and can be found to contain varying degrees of alteration minerals, such as fine to coarsely crystalline chlorite, illite-sericite, and calcite. Plagioclase is also present as silt-sized microlaths within the groundmasses of the volcanic rock fragments, and within the matrices of the sandstones. Average mean size for the plagioclase framework grains is 1.52Ø (0.35 mm or medium sand) with a mean angularity of 3.03ρ, or subrounded.

The plagioclase framework grains and the sand-sized plagioclase phenocrysts within the volcanic rock fragments have similar andesine-labradorite compositions, and similarities between the matrices and groundmasses suggest a common source rock parentage for the framework plagioclase grains and the plagioclase phenocryst-bearing volcanic rock fragments.

Potassium feldspar (K-feldspar) is nearly lacking in the sandstones. The rare grains counted were subangular, very fine to medium sand-sized sanidine. Sample RSC has 4% K-feldspar, of which nearly all is sanidine. The near absence of orthoclase feldspar and the presence of sanidine indicate a volcanic source terrane.

Andesitic to dacitic, medium to very coarse sand-sized volcanic rock fragments (VRF's) represent over 38% of the total framework grains present. Mean grain sizes average 0.63Ø (0.65 mm, coarse sand) and average mean

angularity at 3.24ρ or subrounded. The VRF's are usually more subrounded than the framework plagioclase grains and tend to have irregular to indistinct grain boundaries. Average sorting of the VRF's is 1.01Ø or poorly sorted, with the medium sand-sized fractions in some of the samples showing slightly better sorting than the very coarse sand-sized fractions in other sandstones. Most VRF's within the sandstone samples collected from the massive sandstone units are more poorly sorted (Table 1).

Based upon phenocryst and/or groundmass compositions, four varieties of volcanic rock fragments are recognizable. The first and most common variety includes fine to coarse sand-sized plagioclase phenocrysts, randomly oriented and set in a nearly aphanitic, chloritic and glassy (?) matrix with very fine to medium silt-sized plagioclase microlaths. While the phenocrysts do not generally show a preferred orientation, the microlaths are occasionally found to exhibit a trachytic texture around the phenocrysts. The second type of VRF also includes recognizable quartz crystals in the groundmass and subangular, coarse silt to fine sand-sized quartz phenocrysts.

Volcanic rock fragments similar to the first two varieties, but including subangular to subrounded, very fine to coarse sand-sized pyroxene phenocrysts, make up the third variety of VRF's. The pyroxenes are commonly twinned, occasionally polycrystalline, and partially replaced by chlorite. The fourth type of VRF is made up of the groundmasses of the first two varieties and lacks the phenocrysts. These VRF's could have easily been counted as pseudo-matrix points except that their irregular boundaries could be made out from the surrounding framework grains and other matrix materials. The groundmass of this fourth variety of VRF is nearly aphanitic, appears to be glassy (?), and is replaced by finely crystalline patches of chlorite and calcite.

K-feldspar phenocrysts are very rare and, where suspected, are of questionable identity due to their fine grain sizes. Distinguishing between silt-sized plagioclase microlaths and quartz crystals is also difficult, except that albite twinning and elongated crystal habit readily identified the plagioclase microlaths when they were observed.

Subangular to subrounded phenocryst grain shapes are possibly a result of igneous processes, such as crystal resorption, and/or the result of post-depositional diagenetic alteration. Evidence for the former process has been largely obscured by the latter.

Other minor rock fragments include sparse sedimentary rock fragments (SRF's), usually intraformational siltstones and mudstone clasts, though some appear to be microcrystalline aggregates of chert (?) or quartz. Metamorphic rock fragments (MRF's) are very fine to coarse sand-sized, subrounded aggregates of elongated, silt-sized quartz crystals with interlocking straight to sutured grain contacts. They may represent recrystallized metamorphic quartz of Folk (1974). A high grade schist may be the source of these grains. Plutonic rock fragments (PRF's) are rare and are made up of fine to very coarse sand-sized aggregates of silt-sized quartz and plagioclase crystals. The grain contacts are straight and interlocking. Occasionally fine to medium sand-sized crystals of plagioclase (albite to oligoclase) are also present within these aggregates. A plutonic or possibly gneissic source terrane may be suggested by the PRF's.

TABLE I
PETROGRAPHIC ANALYSES

	Quartz	Feldspar	Rock Fragment	Framework	Matrix	Cement	Porosity	Plagioclase	K-feldspar	Pyroxene	Volc. Rk. Frag.	Sed. Rk. Frag.	Plut Rk. Frag.	Meta. Rk. Frag.	TOTAL FRAMEWORK GRAINS: Mean Size (M_z) ϕ	Sorting (σ_I) ϕ	Skewness (Sk_I)	Mean Angularity ρ	Roundness	Sorting (σ_D)	Mean Sphericity	QUARTZ: Mean size ϕ	Sorting (σ_I) ϕ	Mean Angularity ρ	PLAGIOCLASE: Mean size ϕ	Sorting (σ_I) ϕ	Mean Angularity ρ	K-FELDSPAR: Mean size ϕ	Sorting (σ_I) ϕ	Mean Angularity ρ	PYROXENE: Mean size ϕ	Sorting (σ_I) ϕ	Mean Angularity ρ	VOLC. RK. FRAG: Mean size ϕ	Sorting (σ_I) ϕ	Mean Angularity ρ
CIRCO DIEGUEÑO CANYON																																					
RFA	8	37	55	68	31	1	0	32	TR	13	39	8	TR	0	0.62	1.85	+0.12	3.28	0.54	0.66	3.03	1.95	2.72	1.18	1.36	3.08	—	—	—	1.10	0.90	2.87	-.04	1.04	3.54
RFB	6	9	85	68	31	1	0	8	1	2	79	1	1	2	0.06	1.57	+0.21	3.06	0.43	0.64	3.29	1.19	2.93	2.08	1.19	2.93	2.22	—	2.50	0.18	0.24	3.18	-.31	1.28	3.18
RSC	7	56	37	56	44	0	0	52	4	0	35	0	2	0	2.38	0.85	+0.14	3.03	0.45	0.63	2.82	0.93	2.14	2.64	0.84	3.04	2.50	0.48	2.63	—	—	—	1.84	0.51	3.28
RSP	1	33	66	71	29	0	0	32	TR	2	64	0	0	0	0.49	1.59	-0.15	3.12	0.30	0.61	1.93	—	3.00	1.59	0.95	3.04	—	—	—	1.84	0.65	2.94	-.05	1.48	3.21
RSQ	1	71	28	70	30	0	0	65	0	9	24	0	TR	1	0.85	0.77	+0.27	3.25	0.30	0.65	0.91	0.26	2.91	0.89	0.74	3.14	—	—	—	0.87	0.86	3.17	0.74	0.81	3.50
RSW	0	62	38	73	25	0	2	48	0	22	26	2	TR	1	0.34	1.11	-0.07	3.27	0.28	0.65	—	—	—	0.79	0.87	3.19	—	—	—	0.58	0.78	3.15	-.48	1.14	3.50
RSX	1	61	38	61	39	0	0	59	0	4	30	2	TR	4	1.83	0.94	-0.14	3.21	0.18	0.63	3.25	—	2.75	1.87	0.92	3.16	—	—	—	2.26	0.89	3.12	1.67	1.00	3.30
RFD	2	39	59	35	65	0	0	38	1	2	53	4	0	0	1.96	1.14	-0.34	3.16	0.17	0.59	3.13	—	2.00	2.24	0.95	3.08	2.95	—	3.30	3.05	—	2.85	1.03	1.40	3.21
RFF	3	86	11	73	25	2	0	70	2	16	6	3	0	1	1.49	0.84	+0.10	3.21	0.19	0.63	1.35	0.58	2.68	1.43	0.82	3.19	1.49	0.65	2.94	1.90	0.90	3.23	1.28	0.62	3.27
RFH	2	64	34	60	40	0	0	59	1	6	29	TR	TR	2	1.57	0.87	+0.05	3.19	0.21	0.64	1.19	0.65	2.97	1.79	0.81	3.16	1.10	—	2.90	2.09	0.90	3.44	1.23	0.80	3.27
RFJ	7	85	8	33	67	0	0	75	2	9	7	0	0	0	2.31	1.09	-0.30	3.00	0.19	0.60	3.00	0.27	2.62	2.35	1.01	3.03	2.89	—	2.85	3.04	0.77	3.08	0.94	0.92	3.17
RFM	TR	70	30	70	30	0	0	63	0	10	20	3	TR	3	0.80	1.05	+0.17	3.00	0.18	0.63	—	—	—	0.93	0.93	2.92	—	—	—	1.16	1.32	2.98	0.14	0.86	3.11
RFN	0	78	22	69	31	TR	0	70	0	11	13	1	3	2	1.63	0.86	-0.07	3.07	0.22	0.65	—	—	—	1.67	0.82	3.00	—	—	—	2.02	0.77	3.04	1.14	0.84	3.27
RFQ	0	19	81	67	33	0	0	18	0	6	71	2	3	0	0.68	0.96	-0.02	3.08	0.20	0.64	—	—	—	1.31	0.69	3.03	—	—	—	1.31	0.73	2.97	0.44	0.93	3.07
AQL	0	16	84	83	17	0	0	15	0	4	81	0	0	0	-0.08	1.34	-0.10	2.70	0.80	0.64	—	—	—	0.11	1.18	2.40	—	—	—	0.70	1.27	2.80	-.05	1.48	2.70
LUSARDI CANYON																																					
LCA	4	6	90	80	5	6	9	6	0	0	89	0	0	0	1.24	1.37	-0.15	2.13	1.00	0.57	1.74	0.24	2.10	1.62	1.28	1.50	—	—	—	—	—	—	1.09	1.14	2.20
LCB	1	16	83	48	9	26	17	16	0	0	83	0	0	0	1.80	1.20	+0.50	4.10	1.00	0.57	1.00	—	3.50	1.80	0.82	2.77	—	—	—	—	—	—	1.60	0.83	3.50
LCC	25	24	51	66	32	2	0	20	4	0	26	1	0	23	3.35	1.19	+0.23	3.15	0.87	0.64	3.88	1.39	2.71	3.46	0.98	3.22	3.46	0.98	3.22	—	—	—	3.23	1.10	3.18
LOS PEÑASQUITOS CANYON																																					
ADD	7	42	51	66	22	12	0	42	0	0	32	13	0	0	2.57	1.14	+0.37	3.38	0.86	0.63	2.89	0.98	2.20	2.28	0.78	3.21	—	—	—	—	—	—	1.85	0.73	4.10

Mean Size, Sorting, Skewness, etc., after R.L. Folk, 1974. TR = Trace = 1/2 % or less, usually one or two grain points total.

TABLE II
CHEMICAL ANALYSES

	CIRCO DIEGUEÑO CANYON				LUSARDI CANYON						LOS PEÑASQUITOS CANYON
	AQL	ARV	ARW	ARX	LCA	LCB	LCD	LCE	LCF_1	LCF_2	ADD
SiO_2	58.0	65.4	54.5	64.4	58.8	58.0	59.0	64.5	58.8	59.0	58.5
Al_2O_3	14.7	14.6	15.4	16.5	15.6	16.9	17.2	18.1	15.9	16.0	17.5
Fe_2O_3	8.3	2.6	7.8	4.6	5.3	6.3	6.1	5.1	5.7	5.3	5.9
MgO	6.5	1.7	6.2	2.9	4.9	5.8	5.4	3.2	5.6	4.5	4.6
MnO	0.3	0.1	0.4	0.1	0.2	0.2	0.1	0.1	0.3	0.3	0.2
CaO	9.5	13.0	12.0	4.0	9.0	7.5	5.5	0.5	5.5	5.0	9.0
Na_2O	1.6	0.1	2.7	3.6	1.6	0.1	0.1	0.1	3.2	3.1	2.4
K_2O	0.1	0.1	0.8	0.7	0.9	1.1	1.3	3.0	0.3	0.5	0.3
TiO_2	0.8	0.2	0.7	0.5	0.4	0.6	0.7	0.9	0.6	0.6	0.5
Total Weight %	99.8	97.8	100.5	97.3	96.7	96.5	95.4	95.5	95.9	94.3	98.9
Na_2O / K_2O	8	1	3.4	5.1	1.8	0.09	0.08	0.03	10.7	6.2	16

The average percentage of quartz framework grains amounts to slightly less than 3%. Quartz grains are monocrystalline, clear, subangular (2.67ρ mean), and exhibit very sharp to, occasionally, slightly undulose extinctions. Average mean size is 2.39Ø (0.19 mm or fine sand) and the average sorting value is 0.83Ø, or moderately sorted. Beta crystal forms and embayments typical of volcanic quartz were not widely observed, though it is suggested that these grains are from a volcanic source terrane.

Some of the point-counted quartz grains are clearly not of volcanic origin, for they are cloudy, sometimes with minute inclusions, and show moderately undulose extinctions. They are larger grained (medium to coarse sand sized) than the clear quartz grains, and are subangular to subrounded. A plutonic, or even gneissic source terrane may be the origin for these larger quartz grains.

As discussed with the volcanic rock fragments, silt-sized, subangular quartz crystals are found in the groundmasses of certain VRF's, and as part of the matrices in some of the sandstones.

With the exception of a single brown biotite grain observed in sample RFM, pyroxene grains are the only ferromagnesian minerals found in the sandstones examined. An average of 8% of the framework grains are composed of augite. Sample RSW contains 22% pyroxene framework grains. The same pyroxenes are also present within the volcanic rock fragments, suggesting that both kinds of framework grains were derived from augite-bearing andesites. The pyroxenes may also have been equally derived by the disaggregation of the pyroxene-bearing volcanic rock fragments.

Augite framework grains are very fine to coarse sand-sized, with an average mean size of 1.58Ø (0.33 mm or medium sand). Average grain angularities are 3.06ρ, or subrounded; and they are moderately sorted (0.85Ø average). Augite grains are commonly twinned with many appearing broken and fractured, and nearly all show some degree of replacement by chlorite.

Pyrite crystals are commonly disseminated throughout the siltstones and sandstones, particularly along dark brown, organic-rich laminae and micro-stylolites as seen in thin-section. They range from silt-sized euhedra to very coarse sand-sized aggregates. As an authigenic mineral, the pyrite was formed after the deposition of the sediments under reducing conditions.

The amount of matrix material within the sandstones of Circo Diegueño Canyon averages 36% of the total rock volume. The matrices are typically composed of silt-sized plagioclase microlaths and quartz, which are set in a nearly aphanitic glassy (?) and chloritic groundmass. Crystal edges appear to be subangular, and grain orientations are random. The similarity between the matrices and the volcanic rock fragment groundmasses suggests that most of the matrix materials were derived from the physical disaggregation and compaction, and diagenetic alteration of the volcanic rock fragments. According to Dickinson (1970) these matrices would be called "pseudomatrix" and "epimatrix" respectively. Distinguishing between the two types of matrices in these sandstones is difficult due to the large amount of chlorite alteration.

Chlorite is the dominant phyllosilicate mineral present within the sandstones. Chlorite alteration is most strongly seen on the matrices, followed by partial replacement of the phenocrysts and groundmasses within the VRF's, and finally the plagioclase feldspar and pyroxene framework grains. Chlorite occurs as pale yellow-green to dark green, fibrous sheaths and tiny blebs. When in the form of patchy replacement, it is randomly oriented and appears as tiny, finely crystalline blebs. Where the chlorite completely replaces the matrix, it is long, fibrous, fine to coarsely crystalline, and internally parallel.

In a few of the sandstones, fibrous, coarsely crystalline chlorite appears to be a pore-filling cement between some of the framework grains. These rare occurrences were counted as "cement", though it is believed that they may represent places where chlorite has completely replaced the interstitial epimatrix. Clay coats and rims, as discussed by Galloway (1974), are not commonly seen and the crystal habit of the chlorite does not indicate it grew from the framework grain boundaries into open pore spaces.

Plagioclase grains tend to show the greatest variety of alteration by chlorite. Fairly fresh grains showing mild, patchy chlorite replacement can be found along side completely replaced pseudomorphs. This could indicate that fresh and weathered feldspars were deposited together and were derived from a rugged topography.

Additional minor alteration mineralogies include finely crystalline illite-sericite, which occurs as a patchy replacement of the plagioclase framework grains and the plagioclase phenocrysts within the VRF's, and less commonly, fine to coarsely crystalline patches of calcite, which replace both the framework grains and the matrices.

Cement and porosity are essentially lacking in the sandstones. As discussed above, a few chlorite "cement" points were noted, though it is doubtful that they represent pore-filling precipitates. The sandstones have been diagenetically altered and recrystallized to such an extent that any relict porosity has been obliterated. Original porosities may have been as great as 40%, for such is the porosity of sands deposited in modern volcanic arc-related sedimentary basins (Galloway, 1974).

LUSARDI CANYON

The sedimentary section in Lusardi Canyon is dominated by finely laminated mudstones and siltstones. Rare interbeds of discontinuous sandstones and granule- to boulder-bearing breccias are the source of the studied thin-sections LCA, LCB, and LCC. Table 1 summarizes the petrographic data for each sandstone sample from Lusardi Canyon. Samples LCA and LCB are both andesitic litharenites, while sample LCC is feldspathic andesitic litharenite. The sandstones are texturally immature, poorly sorted (1.25Ø average), and are made up of subangular to rounded, very fine to medium sand-sized framework grains.

The principal framework grains in each sample are volcanic rock fragments, though sample LCC also has subequal amounts of quartz, plagioclase, and metamorphic rock fragments. The VRF's are subangular to subrounded, moderately to poorly sorted, have elongated, irregular grain outlines, and are composed of andesite and minor dacite. Grain sizes

range from very fine to medium sand. Their distribution is random, with the long grain axes subparallel to the bedding laminae.

Compositionally, the VRF's are similar to those described for Circo Diegueño Canyon, except for the absence of any pyroxene phenocrysts, and the presence of spherical vesicles in 25% of the VRF's. Trachytic textures are seen in the groundmasses of the vesicular VRF's. Generally sand-sized phenocrysts are found to be made up of euhedral, very fine to fine grained plagioclase (andesine). Nearly two thirds of the VRF's lack sand-sized phenocrysts.

Whereas the volcanic rock fragments in the Circo Diegueño Canyon samples were primarily altered to chlorite, the VRF's in Lusardi Canyon exhibit a wider range of alteration textures within themselves and along their grain boundaries. Calcite pore-filling cement and clay coats and rims are present along grain outlines, while finely crystalline chlorite and silica, and fine to coarsely crystalline calcite frequently replace the groundmasses and phenocrysts.

The metamorphic rock fragments seen in LCC are made up of subrounded, medium silt- to medium sand-sized aggregates of polygonal, interlocking quartz platelets. Extinctions are straight, and minor replacement (?) by illite-sericite and calcite can be seen along the grain contacts. The MRF's appear to be recrystallized and may have been derived from a gneissic source terrane.

Plagioclase feldspars average 14% of the framework grains. They are moderately to poorly sorted, subrounded to subangular, very fine to medium sand-sized. The plagioclase grains are nearly all replaced by coarsely crystalline calcite, though relict albite and carlsbad twinning can occasionally be seen. Clay rims are frequently seen around plagioclase grain edges. The plagioclase framework grains are typically larger than the plagioclase phenocrysts within the volcanic rock fragments.

Potassium feldspar grains are seen only in sample LCC. They are clear, monocrystalline grains of sanidine. Phyllosilicate rims and coats are common, usually composed of illite-sericite and chlorite. Calcite alteration was less common. A volcanic source is indicated by the sanidine grains.

Quartz framework grain percentages are 4% and 1% in samples LCA and LCB, respectively. Sample LCC has 25% very fine sand-sized quartz that was probably derived from quartz-bearing volcanic rocks and rock fragments. Much of the pseudomatrix and epimatrix in sample LCC are probably from disaggregated and diagenetically altered groundmasses of the VRF's which contained quartz phenocrysts.

The quartz grains have slightly undulose to straight extinctions, and several euhedral grains have partially embayed beta quartz crystal outlines. Clay coats and rims are fairly common, and epitaxial quartz overgrowths are occasionally seen. Quartz framework grains range in size between very fine to medium sand. While a volcanic origin is inferred, sand-sized phenocrysts are not seen in the volcanic rock fragments. This may indicate a mixture of volcanic sources or preferential disaggregation of quartz-bearing rock fragments.

Pyrite crystals occur throughout the sandstones as silt-sized euhedra, and as sand-sized polycrystalline aggregates in association with the dark, organic-rich laminae.

The percentage of matrix found in the sandstones varies with the amount of compaction and diagenetic alteration present in each rock. Samples LCA and LCB have relatively low matrix contents, while LCC has 32% matrix. The matrix in sample LCC is very similar to the VRF groundmasses and is composed predominantly of silt-sized quartz and plagioclase microlaths, set in an isotropic, glassy (?) groundmass. The laths and crystals are subangular to subrounded, randomly oriented and often intermixed with finely crystalline illite-sericite, calcite, chlorite, and chalcedony.

The matrices of LCA and LCB are limited to clay coats and rims made up of illite-sericite and chlorite, precipitated along the framework grain boundaries. Sample LCC exhibits higher degrees of diagenetic alterations, over LCA and LCB, as is evidenced by its higher percentage of epimatrix and pseudomatrix.

Fine to coarsely crystalline calcite replaces framework grains and matrices indiscriminately. Plagioclase framework grains, plagioclase phenocrysts, and then the VRF groundmasses appear to be replaced in that order. Patchy calcite replacement of the matrices and the nearly complete alteration of the framework grains by calcite indicates an advanced stage of burial diagenesis as outlined by Galloway (1974).

Clay coats and rims were formed at the expense of the feldspars and volcanic rock fragments along their grain edges. Later formed chalcedony and vuggy quartz-filled veinlets and interstices are seen to be separated from the framework grains by the finely crystalline sheaths of illite-sericite and chlorite clay coats and rims.

Sample LCB shows the highest percentage of early stage calcite pore-filling cement with 25% of the interstices containing fine to coarsely crystalline cement. The most common cement is fine to coarsely crystalline chlorite, which is separated from the framework grains by the earlier formed clay coats and rims. The previously mentioned chalcedony and vuggy quartz may represent late stage replacement of earlier clay cements and/or matrices.

Relict pore spaces, now filled with phyllosilicate and calcite cements or matrix materials but still recognizable in thin-section, indicate that early stage diagenetic pore-filling precipitates preserved some of the early depositional textures (Sample LCB, Table 1). Samples LCA and LCC have fewer preserved relict textures indicating a slightly different alteration history. All three sandstone samples show the same heavy calcite replacement of framework grains, matrices, and cement, reflecting ultimate deep burial diagenesis (Galloway, 1974, 1979). Original porosities may have been as high as 40%.

LOS PEÑASQUITOS CANYON

The Santiago Peak volcaniclastic rocks exposed in Los Peñasquitos Canyon are composed of massive breccias and sandstones. Thin-section examination of samples from the sandy matrices of the breccias, and from the massive sandstones may be summarized as being composed of poorly sorted, subangular to subrounded, very fine sand- to granule-sized plagioclase and

pyroxene grains, with occasional sand-sized grains of quartz and orthoclase, set in a finely crystalline chloritic paste with randomly oriented laths and crystals of silt-sized plagioclase and quartz.

Detailed examination was made of sample ADD, which was taken from a fine-grained sandstone unit associated with the massive breccia units. ADD is a feldspathic andesitic litharenite. Compositional percentages and framework data are listed in Table I. It is a texturally immature, poorly sorted, subrounded, fine-grained sandstone.

Plagioclase framework grains are composed of andesine, ranging from oligoclase to labradorite. Crystal habits are very elongate, and albite and carlsbad twinning is fairly common. Partial alteration to finely crystalline sericite and chlorite is also common, frequently obscuring original grain fabrics. Zoned plagioclases are relatively rare. Plagioclase crystals are also seen as silt-sized microlaths in the matrix of the sandstone and within the volcanic rock fragments.

Potassium feldspar grains are not seen in sample ADD, though rare, subrounded, coarse sand-sized orthoclase grains were observed in some of the massive sandstones. The orthoclase grains may represent detritus from a minor non-volcanic source, or weathered grains derived from the contemporaneous deep erosion of the magmatic arc.

Volcanic rock fragments are like those described for Circo Diegueño Canyon. However, ADD contains only the first variety previously described and lacks the quartz phenocrysts. Silt-sized plagioclase microlaths and very fine to coarse sand-sized plagioclase phenocrysts are found set in glassy, opaque matrix. The VRF's are partially altered to sericite, with the plagioclase phenocrysts showing less alteration than the plagioclase framework grains. Andesite is the dominant composition for the very fine to coarse sand-sized VRF's.

Sedimentary rock fragments are composed of intraformational clasts of dark brown, rounded grains of silty mudstone with silt-sized inclusions of plagioclase microlaths and pyrite crystals. The SRF's are deformed and exhibit subparallel orientations to the microlaminae within the sandstone. The SRF's are medium sand-sized.

The quartz grains within sample ADD are somewhat elongated, are monocrystalline and clear, and have straight extinctions. Grain sizes range from coarse silt to medium sand. The quartz grains were derived from a volcanic source, as some minor embayments can still be seen.

Pyroxene grains are not present in sample ADD, though pyroxene is commonly greater than 5% in the massive breccias and sandstones. Their occurrence and habit is the same as described for the sandstones in Circo Diegueño Canyon suggesting a similar augite andesitic source terrane for both canyon exposures.

Other minor framework grains include 2% clear to brown, subangular, elongated, glass shards; broken and partially altered to chlorite and calcite. Relict shard shapes are nearly obliterated by depositional disaggregation, devitrification, and diagenetic alteration. Silt-sized crystals of authigenic pyrite are scattered throughout thin-section ADD. Carbonaceous microlaminae parallel to the bedding planes are often congested with pyrite crystals.

The matrix materials found in ADD are essentially the same as found in the groundmasses of the volcanic rock fragments. Finely crystalline sericite and chlorite partially attack the microlaths and phenocrysts making the original VRF grain outlines indistinguishable. Post-depositional compaction and alteration of the unstable VRF's have transformed them into pseudomatrix and epimatrix.

Finely crystalline aggregates and patches of sericite and chlorite, as well as fine to medium crystalline calcite, are found replacing both the framework grains and the matrix. Very fine to medium sand-sized patches of irregularly shaped, fibrous chlorite are observed where they have completely replaced the matrix and unstable framework grains.

Fine to medium crystalline calcite cement was counted in sample ADD; however, the random formation of calcite around and between framework grains, as well as across framework grain-matrix boundaries, makes it difficult to ascertain whether the calcite represents Stage 1 pore-filling cement or more complex later stage replacement and alteration of the framework grains and matrix (Figure 1).

Porosity is not present in sample ADD. Any original pore spaces have since been filled by calcite or destroyed by post-depositional compaction, alteration, and recrystallization of the volcanic rock fragments and unstable framework grains.

DIAGENESIS

In a model developed by Galloway (1974, 1979), "a predictable sequence of diagenetic features" found in volcanogenic sediments of active or recently active arc-related sedimentary basins can be described. Figure 1 illustrates the various stages of physical and chemical diagenetic alterations volcanogenic sediments may undergo with increasing depths of burial (and subsequently increasing temperatures and pressures).

Stage 1 calcite pore-filling cement, indicative of burial depths from 0 to as great as 3,000 m is found only in sample LCB from the isolated, discontinuous sandstone sequence in Lusardi Canyon. The presence of calcite-filled pores may have helped to partially support the sediment preventing further compaction. Later stage diagenetic alterations can be seen since calcite only fills 25% of the pore spaces in sample LCB.

Authigenic clay rims (oriented perpendicular to the grain boundaries) and clay coats (oriented parallel or tangential to the grain boundaries) distinguish stage 2. They are formed by the mobilization of aluminum and silica from the unstable framework grains. A burial depth of 300 to 1300 m may be indicated (depending upon the local geothermal gradient). With increasing burial pressures, compaction of the sediment squeezes the clay coats and rims around the areas of the grain-to-grain contacts creating epimatrix and pseudomatrix. Stage 2 clay coats and rims of chlorite and illite-sericite are found in the Lusardi Canyon sandstones, but are not common in the sandstones of the other two canyon exposures.

Between burial depths of 900 and 3,000 m, stage 3 diagenesis may occur. Further recrystallization and cementation in the remaining pore spaces may begin in the form of authigenic zeolites (laumontite) and/or phyllosilicates

(chlorite or smectite). Relict clay rims are usually preserved as halos around the detrital grains (Galloway, 1974, 1979).

Zeolites were not seen in the thin-sections, nor were zeolite peaks identified during the x-ray analyses. Relict pore spaces are filled by chlorite, and once again, this was only found in the interstices of the sandstones from Lusardi Canyon.

At even greater burial depths, complex replacement and alteration mineral assemblages begin to appear (stage 4 in Galloway's (1979) updated model). Calcite and chlorite replacement of the volcanic rock fragments, plagioclase, and matrix occurs, with quartz and feldspar overgrowths occasionally seen, giving a welded or sutured appearance to compacted grain contacts. Additional replacement mineralogies may include albite, epidote, and muscovite. Different aspects of stage 4 mineralogies and textures are present in all the sandstones from Circo Diegueño, Lusardi, and Los Peñasquitos Canyons.

The Lusardi Canyon sandstones have had their framework grains and matrices extensively replaced by calcite. Quartz veinlets and epitaxial quartz overgrowths are evidence for late stage alterations as well. The diagenetic textures preserved in the Lusardi Canyon exposures range from stage 1 through stage 4. The slow accumulation of the thick sequence of mudstones overlying the Lusardi Canyon sandstones may have prevented the sandstones from being quickly compacted and allowed the early stages of diagenesis to be preserved. Subsequently, the rocks of Lusardi Canyon were deeply buried, possibly to depths greater than 3,000 m, then eventually uplifted and eroded to their current state of exposure.

Stage 4 alteration minerals within the Los Peñasquitos Canyon exposures are primarily the pervasive chlorite and patches of calcite. Earlier stages of alteration were not seen. The matrices of the sandstones are largely derived from the deformed and recrystallized VRF's as pseudomatrix and epimatrix. Some of the sandstones contained epidote and sericite-muscovite replacement mineralogies, perhaps indicating a higher degree of alteration bordering the lowest grade of metamorphism.

The breccias and sandstones of Los Peñasquitos Canyon were also deeply buried, 3,000 m or greater, based upon the stage 4 alterations observed. Rapid deposition and compaction prevented the formation of or preservation of earlier diagenetic alteration stages.

The Circo Diegueño Canyon sandstones exhibit stage 4 mineral assemblages similar to those in Los Peñasquitos Canyon. Large percentages of chlorite replaced pseudomatrix and epimatrix are seen, and chlorite and patchy calcite replace the VRF's, plagioclase, pyroxenes and matrices extensively. As seen in the Los Peñasquitos Canyon exposures, deep burial diagenesis below 3,000 m may be indicated, though shallower depths and a higher geothermal gradient might produce similar assemblages.

The high Na_2O/K_2O ratios (Table II) are a result of the albitization of the Ca-rich andesine-labradorite plagioclase phenocrysts and framework grains. Partial early stage calcite cementation (25%) in sample LCB may account for its low Na_2O/K_2O ratio, for the calcite has effectively isolated some of the plagioclase grains. Albitization could release CaO from the andesines and labradorites which in turn might have been used to crystallize

late stage calcite (Pettijohn et al., 1972). Samples LCD and LCE (Table II) are mudstone and sandy mudstone. Their Na_2O/K_2O ratios are low due to their illitic compositions.

The Santiago Peak Volcanics have undergone mild, regional metamorphism to the greenschist facies of Eskola (Larsen, 1948). Larsen felt that the metamorphism occurred "during the close folding of the rocks and before the intrusion of the batholith". While the mudstones in Lusardi Canyon tend to exhibit "good platy structure parallel to bedding" (Larsen, 1948), the related sandstones clearly show preserved sedimentary textures. Schistosity is not present with the Santiago Peak volcaniclastic rocks, though the pervasive chloritization is common to both the volcanic rocks and the volcaniclastic rocks.

The Santiago Peak volcaniclastic rocks are best described in terms of the degree of diagenetic alteration they have undergone, as outlined in Galloway's (1974, 1979) model of the various stages of burial diagenesis. The ubiquitous chlorite found throughout the volcaniclastic rock is interpreted as being caused by a combination of stage 4 alteration and the added imprint of chloritization associated with the onset of the regional greenschist metamorphism.

The tectonic deformation which buried and altered the Santiago Peak volcaniclastic rock also brought about the regional low-grade greenschist metamorphism reflected in the Santiago Peak Volcanics. As a result, the Santiago Peak volcaniclastic rocks exhibit diagenetic textures bordering the transition between highest-grade burial diagenesis and lowest-grade metamorphism.

PROVENANCE AND CONCLUSIONS

The Santiago Peak volcaniclastic rocks were derived from the volcanic rocks of the Santiago Peak Volcanics. Petrological comparisons show that nearly all of the framework grains and volcanic rock fragments within the sedimentary rocks are mineralogically equivalent to the phenocrysts and volcanic rocks found in the Santiago Peak Volcanics.

The Santiago Peak Volcanics are made up largely of andesites, dacites, and latites (Larsen, 1948). The Santiago Peak volcaniclastics contain andesitic to dacitic rock fragments. Both groups contain andesine plagioclase as a principal feldspar, pyroxene is common to both, and the low volcanic quartz percentages are equally shared by both the volcanic rocks and the volcaniclastic rocks (Larsen, 1948; Adams, 1979).

Cobble- to boulder-sized volcanic rock clasts in the breccias and subangular textures in the unstable plagioclase and pyroxene framework grains indicate moderately short distances of transport and very little reworking of the sediments.

Minor amounts of metamorphic and plutonic rock fragments probably represent fragments brought out by deep erosion into the core of the Santiago Peak magmatic arc.

Both the volcanic rocks and the volcaniclastic rocks show the ubiquitous presence of chlorite. The volcanic rocks exhibit varying degrees of greenschist metamorphism, generally increasing from the west to east (Larsen, 1948),

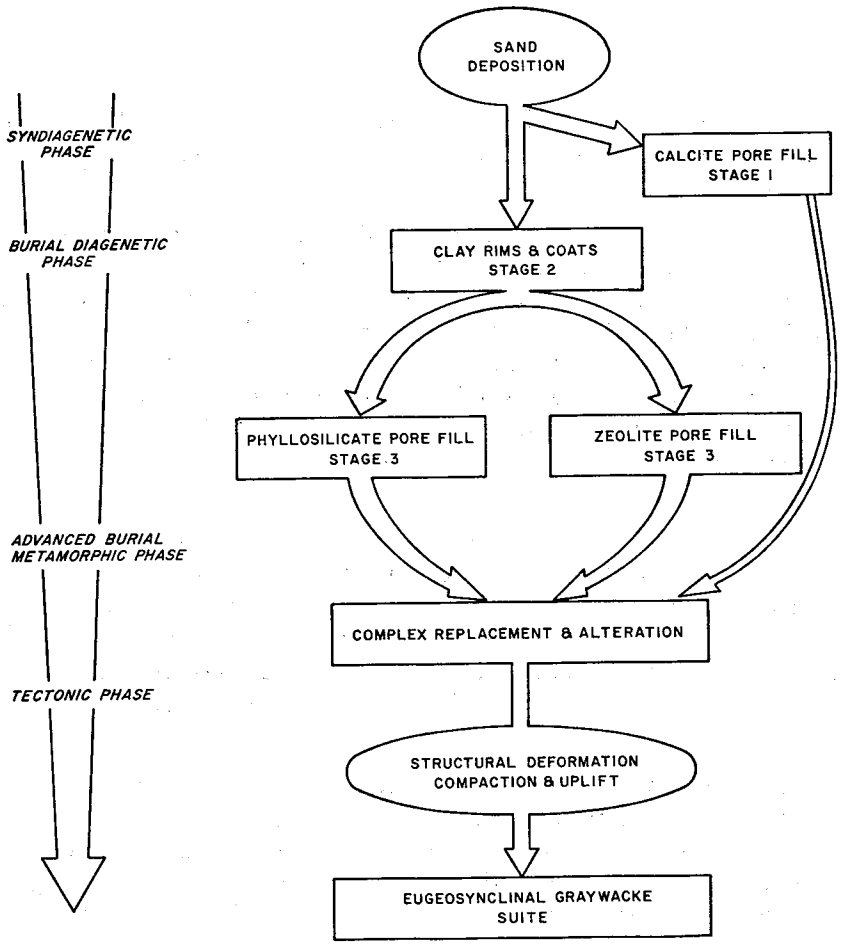

Figure 1
Diagram outlining the sequential stages of physical and chemical diagenetic alterations as they relate to the increasing burial of the sediment (Galloway, 1974).

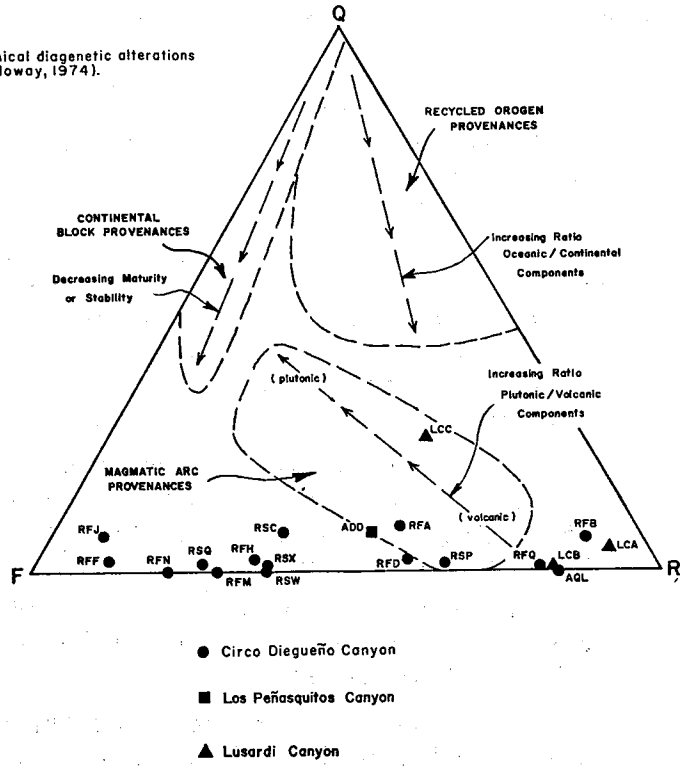

Figure 2
Triangular QFR plot of point counted framework grains for selected samples. Q equals total quartzose grains, F equals total feldspar grains, and R equals total rock fragments. Provenance areas are from Dickinson and Suczek, 1979.

while the volcaniclastic rocks, which are located west of the volcanic rocks, retain their sedimentary textures and do not exhibit any schistosity. The chlorite common to both is a diagenetic alteration mineralogy and a reflection of the chloritization associated with the mild regional metamorphism.

Mineralogically, the volcaniclastic rocks and the volcanic rocks share similar compositions and both reflect the same general degree of mild, regional metamorphism. Therefore, it is concluded that the Santiago Peak volcaniclastic rocks were derived from the volcanic rocks of the Santiago Peak Volcanics.

Figure 2 is a plot of the sandstone compositions (Table 1) on a QFR diagram. Superimposed on this diagram are the various provenance areas as determined by Dickinson and Suczek (1979).

The relatively high concentration of sandstone compositions plotted towards the feldspar (F) apex is a result of counting plagioclase "phenocrysts" as framework grains when the enclosing VRF grains were indistinguishable from the epimatrices and pseudomatrices surrounding them. A subjective "recount" would plot most of the sandstone compositions nearer to samples ADD or RSP.

The sandstone compositions of the Santiago Peak volcaniclastic rocks plot in or around the region identified by Dickinson and Suczek (1979) as a magmatic arc provenance, with volcanic components dominating (Figure 2). According to Dickinson and Suczek (1979) rocks with these compositions were derived from "volcanogenic highlands along active island arcs". They go on to state that "sites of deposition include trenches and fore-arc basins on the frontal side of the arc".

Based upon the petrology of the Santiago Peak volcaniclastic rocks, it is concluded that they were derived from the Santiago Peak Volcanics in just such a volcanic arc system; they were deposited in a marine environment, were rapidly and deeply buried, underwent burial diagenesis and mild metamorphism, then finally were uplifted and exposed.

REFERENCES

Adams, M.A., 1979, Stratigraphy and petrography of the Santiago Peak Volcanics east of Rancho Santa Fe, Calfiornia (M.S. thesis): San Diego State Univ., 123 p.

Balch, D.C., 1981, Sedimentology of the Santiago Peak volcaniclastic rocks, San Diego County, California (M.S. thesis):San Diego State University, 135 p.

Dickinson, W.R., 1970, Interpreting detrital modes of graywacke and arkose: Jour. Sed. Petrology, v. 40, p. 695-707.

Dickinson, W.R., and Suczek, C.A., 1979, Plate tectonics and sandstone compositions: Am. Assoc. Petrol. Geologists Bull., v. 63, p. 2164-2182.

Folk, R.L., 1974, Petrology of Sedimentary Rocks: Austin, Texas, Hemphill Publishing Co., 182 p.

Galloway, W.E., 1974, Deposition and diagenetic alteration of sandstone in northeast Pacific arc-related basins: Implications for graywacke genesis: Geol. Soc. America Bull., v. 84, p. 379-390.

Galloway, W.E., 1979, Diagenetic control of reservoir quality in arc-derived sandstones: Implications for petroleum exploration, in Scholle, P.A., and Schluger, P.R., eds., Aspects of Diagenesis: Soc. Econ. Paleontologists and Mineralogists Special Publication No. 26, p. 243-250.

Larsen, E.S., Jr., 1948, Batholith and associated rocks of Corona, Elsinore, and San Luis Rey quadrangles, southern California: Geol. Soc. America Memoir 29, 182 p.

Pettijohn, F.J., Potter, P.E., and Siever, R., 1972, Sand and Sandstone: New York, Springer-Verlag, 618 p.

JURASSIC FOSSILS FROM THE SANTIAGO PEAK VOLCANICS, SAN DIEGO COUNTY, CALIFORNIA

by

David A. Jones and Richard H. Miller
Allison Center and Department of Geological Sciences
San Diego State University

ABSTRACT

Several sections of volcaniclastic rocks in San Diego County are assigned to the Santiago Peak Volcanics. The rocks consist of well indurated argillites, muddy siltstones, coarse sandstones and volcanic breccias. The sections are distinct from one another and have not been lithologically or structurally related to each other. Fossils are rare and poorly preserved and include the bivalve *Buchia piochii* (Gabb), a belemnite *Cylindroteuthis* sp., oyster and echinoid fragments, sponge spicules, and radiolaria. These taxa indicate a late Late Jurassic (Tithonian) age.

INTRODUCTION

Dark gray, poorly fossiliferous and slightly metamorphosed volcaniclastic sedimentary rocks are exposed in a discontinuous band that extends from the Los Angeles basin southward into Mexico (Kennedy and Peterson, 1975, p. 14). In San Diego County these rocks are exposed in only a few areas and have been previously assigned to the Black Mountain Volcanics (Hanna, 1926), Santiago Peak Volcanics (Larsen, 1948), and Bedford Canyon and Alisitos Formations (Milow and Ennis, 1961; Crampton, 1961). Because of lithologic differences among the three sections we studied in the San Diego area and their isolation from other outcrops in southern California, there has been no satisfactory resolution of this nomenclatural problem. For this paper we use the name Santiago Peak Volcanics following Larsen (1948), Fife et al. (1967), Kennedy and Peterson (1975), and Balch (1981).

Interest has focused on these rocks because they represent the oldest sedimentary strata in the county. Previous age determinations have been based on poorly preserved fossils (Milow and Ennis, 1961; Crampton, 1961; Fife et al., 1967) and on radiometric dates (Bushee et al., 1963), which have indicated an age of Late Jurassic (approximately 135-150 million years BP). However, existing collections of fossils are from scattered stratigraphic localities and consist of few poorly preserved bivalves and cephalopods; these fossils have not received detailed taxonomic study and the age of the rocks is somewhat uncertain. The main objective of this paper is to review the regional distribution and taxonomy of the specimens from San Diego County. Of significance is the first report of radiolarians from these rocks.

For the present study three sections were considered (Figs. 1 and 2): Lusardi Canyon, Circo Diegueño Canyon, and Los Peñasquitos Canyon (Jones, 1982). The lithology and thickness show little continuity from one canyon to another. Structural attitudes of the three canyons are also dissimilar (Fig. 1). Because of the isolation of the exposures from strata in the Santa Ana Mountains, lithologic dissimilarities with the Bedford Canyon

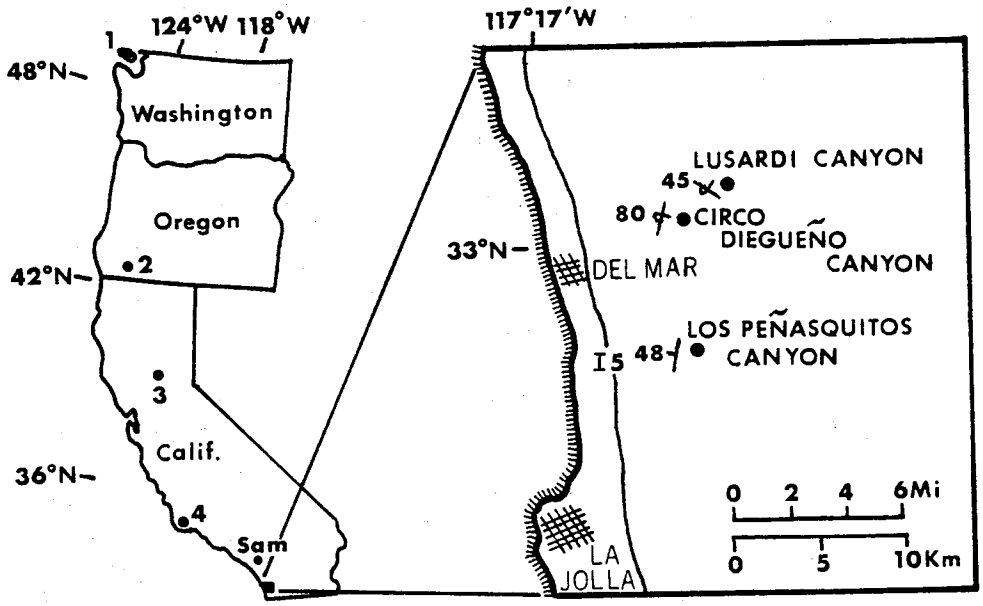

Figure 1. Location map for fossil collections discussed in text. 1. Vancouver Island, British Columbia (Jeletzky, 1965); 2. Southwestern Oregon (Hyatt, 1892; Stanton, 1895; Taliaferro, 1942; Anderson, 1945; Jones et al., 1969); 3. Northern Sacramento Valley, Tehama County, California (Gabb, 1864; Hyatt, 1892; Stanton, 1895; Taliaferro, 1942; Anderson, 1945; Imlay, 1959; Jones et al., 1969); 4. Santa Barbara and San Luis Obispo Counties, California (Kew, 1919; Taliaferro, 1942; Easton and Imlay, 1955). Sam = Santa Ana Mountains, Orange County, California (Holden, 1961; Silberling et al., 1961; Imlay, 1964; Allison, 1970.

Formation and Alisitos Formation, and to maintain consistency in this guidebook, we have retained the name Santiago Peak Volcanics for the rocks described herein.

PALEONTOLOGY

INTRODUCTION

Fossils have been collected from Los Peñasquitos and Circo Diegueño Canyons (Fig. 2) and include the following taxa: Bivalve *Buchia piochii* (Gabb) sensu lato, belemnite *Cylindroteuthis* sp., oyster fragments, echinoid spines and plates, monaxon sponge spicules, and radiolarians (families Actinommidae(?), Hagiastridae(?) and possibly another). The bivalves occur in two distinct lithologies. In Circo Diegueno Canyon they occur in gray to grayish green, poorly sorted, coarse grained sandstone of graywacke type. In Los Peñasquitos Canyon they occur in a dense, dark gray to black, fine grained, well indurated, muddy siltstone. Best preservation is in the sandstones; in the fine grained rocks the bivalves are very compressed. The belemnites occur in boulder breccias as well as fine grained rocks. Oyster and echinoid fragments occur in thin sections of coarse grained sandstones and appear to have been transported and broken. Sponge spicules and radiolarians occur in one thin section of fine grained rock.

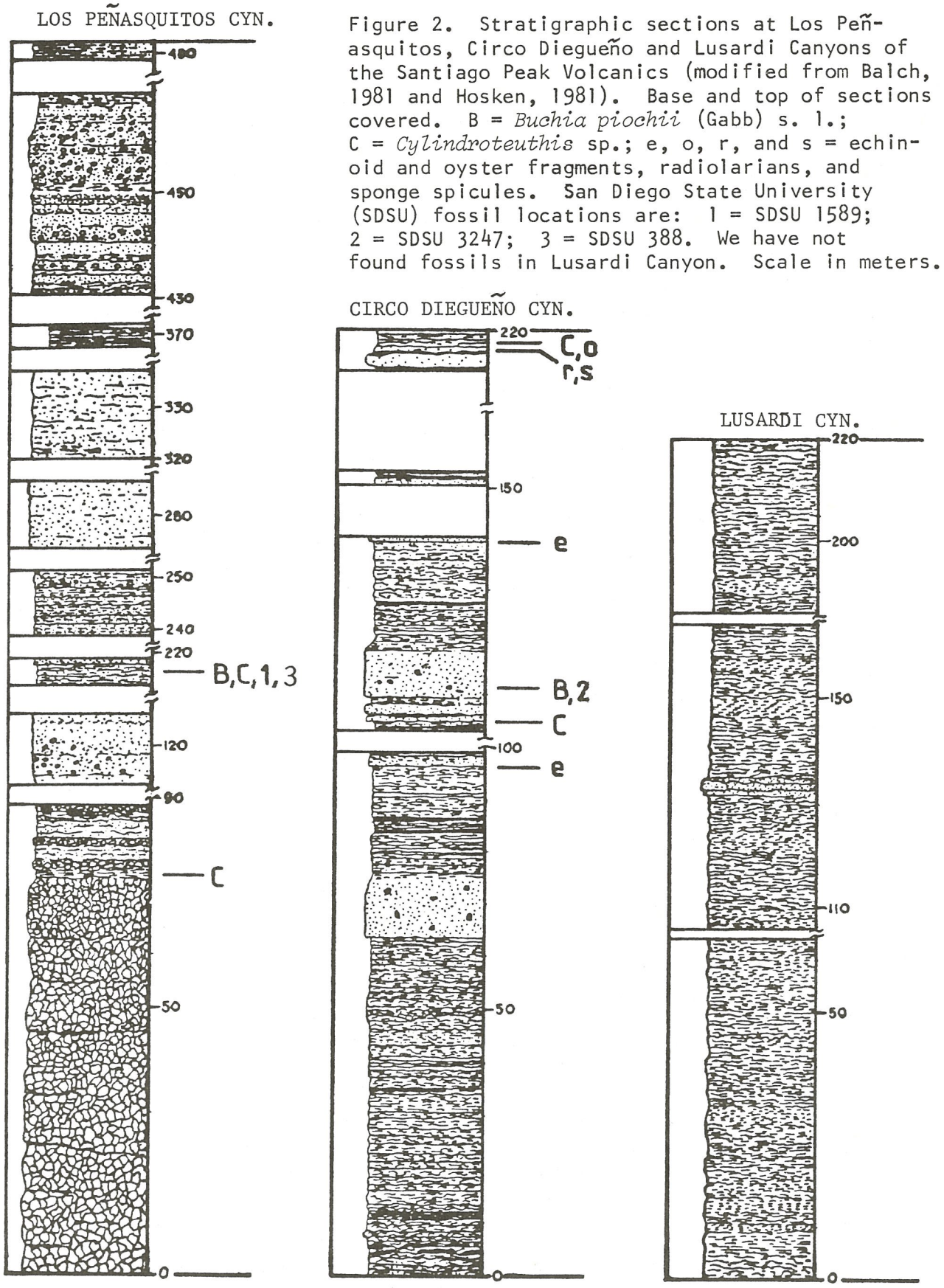

Figure 2. Stratigraphic sections at Los Peñasquitos, Circo Diegueño and Lusardi Canyons of the Santiago Peak Volcanics (modified from Balch, 1981 and Hosken, 1981). Base and top of sections covered. B = *Buchia piochii* (Gabb) s. l.; C = *Cylindroteuthis* sp.; e, o, r, and s = echinoid and oyster fragments, radiolarians, and sponge spicules. San Diego State University (SDSU) fossil locations are: 1 = SDSU 1589; 2 = SDSU 3247; 3 = SDSU 388. We have not found fossils in Lusardi Canyon. Scale in meters.

REGIONAL STUDIES

The bivalve *Inoceramus piochii* was named and described by Gabb (1864, p. 187) from specimens in rocks considered Cretaceous in age in the Sacramento Valley, California. Gabb (1869, p. 194) redesignated *I. piochii* as *Aucella piochii*. Later work in the same area (Hyatt, 1892; Diller and Stanton, 1894; Stanton, 1895) provided abundant specimens. Diller and Stanton (1894) proposed two biozones based on the distribution of *Aucella* species within what were termed the "Knoxville beds". The lower biozone was named from *A. piochii* (Gabb) and the upper biozone was named from *A. crassicollis* (Keyserling). Anderson made numerous investigations of the Sacramento Valley from 1902 to 1945 (Jones et al., 1969). He named many new species within the *Aucella* Biozones and established the *Aucella elderensis* sub-Biozone within the *A. piochii* Biozone (Anderson, 1945, p. 967). Taliaferro (1942) described *Aucella*-bearing strata from the Sacramento Valley, and in the San Luis Obispo area as well as from southwestern Oregon. He recognized Knoxville-equivalent rocks that contained bivalves assigned to *Aucella piochii*. Easton and Imlay (1955) reported *Aucella*-bearing strata in Santa Barbara and San Luis Obispo Counties and identified *A. piochii*, which they assigned to the latest Jurassic.

Imlay (1959) noted that *Aucella* Biozones in various areas of California were placed in different stratigraphic positions within the Franciscan-Knoxville rock assemblage of Late Mesozoic age. He described numerous species of *Aucella*, primarily from the Sacramento Valley, and noted the similar morphologic features of many of the species. He stated (p. 155), "The pelecypod *Aucella* of Jurassic and Cretaceous ages has been sub-divided into greater than 100 species on the basis of minor differences without allowing for biological variation due to crowding that appears to be normal for an attached gregarious pelecypod." He also noted that the genus *Aucella* Keyserling, 1846 had been suppressed in favor of *Buchia* Rouillier, 1845 (opinion 492, ICZN, 1957). We use the designation *Buchia* in this report.

Jones et al. (1969) reviewed work in the Sacramento Valley. Using pre-established *Buchia* Biozones they established correlations on either side of three major faults in the area. They recognized the *B. piochii* Biozone and divided it into a lower *B. elderensis* sub-Biozone and an upper *B. fischeriana* sub-Biozone. Their next higher biozone, *B.* aff. *B. okensis* marked the top of the Jurassic System (Fig. 3).

Jeletzky (1965) recognized well preserved valves of *Buchia* on Vancouver Island, British Columbia. Based on the stratigraphic position of numerous specimens, he developed an evolutionary lineage based on the byssus ear and ligmental plate of the right valves and on a regular change in the direction of curvature of the left beak relative to the long axis of the valve. He established several biozones for this area although some could not be directly correlated with biozones in California and Oregon.

During the pioneering work in the Sacramento Valley, belemnites were recognized in association with the bivalves. Gabb (1864, p. 58) described and named *Belemnites impressus* and considered it to be of Cretaceous age. Most specimens were relatively well preserved and afforded good material for description. Stanton (1895, p. 84) named *B. tehamaensis* and *B.* sp. along with *B. impressus* and associated all three species with *Aucella crassicollis* or *A. piochii* var. *ovata*. Anderson (1945, p. 986-992) revised *Belemnites tehamaensis* to *Cylindroteuthis tehamaensis* and named seven new species of

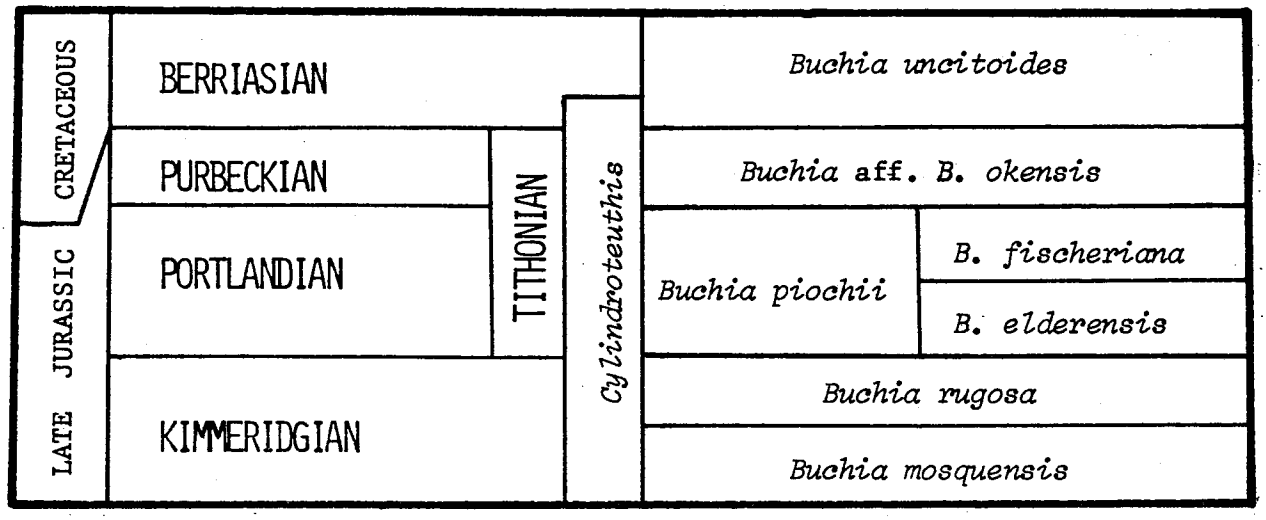

Figure 3. Distribution of Late Jurassic and Early Cretaceous bivalve and belemnite biozones discussed in text. Modified from Imlay (1959) and Jones et al. (1969). These represent biozones established in California and Alaska.

Cylindroteuthis. He also named a new species of *Acroteuthis*, seven new species of *Belemnopsis*, and three new species of *Hibolites*.

Thus within the past 120 years, numerous studies of bivalves and belemnites have provided evidence for construction of well developed biozonal sequences for the Upper Mesozoic rocks that occur from central California northward into Canada and Alaska. In contrast, the rare and poorly preserved specimens in southern California and northernmost Baja California, Mexico have received little study. Considerable variations in taxonomic assignments are evident and this has prevented precise age determinations and correlations with rocks farther north.

LOCAL STUDIES

The rocks of this study were first described by Hanna (1926) as part of his geologic reconnaissance of the La Jolla quadrangle in San Diego County. He named the rocks Black Mountain Volcanics, did not report any fossils, and on the basis of their stratigraphic position considered the rocks Late Triassic or Early Jurassic. Larsen (1948) assigned the rocks to the Santiago Peak Volcanics and considered them to unconformably overlie the Bedford Canyon Formation of the Santa Ana Mountains in Orange County. He reported no fossils and assigned the rocks to the Jurassic System on the basis of their stratigraphic position.

Milow and Ennis (1961, p. 40) were the first to note bivalves and belemnites in the study area. The bivalves were identified as *Buchia* cf. *B. fischeriana* (d'Orbigny) and the belemnites as *Cylindroteuthis*, and they were assigned an age of Medial to Late Jurassic. Crampton (1961, p. 11) identified bivalves as *Buchia* cf. *B. piochii* (Gabb) and through communication with J. A. Jeletzky (Canadian Geological Survey) identified the belemnites as *Cylindroteuthis* sp. indet. Bayle. This belemnite genus has a range of early Medial Jurassic to earliest Early Cretaceous. Fife et al. (1967)

suggested an age of latest Jurassic (Portlandian) based on their identification of *Buchia piochii* (Gabb) from sections in the San Diego area. D. L. Jones (U. S. Geological Survey, pers. Comm. in Balch, 1981) identified bivalves from these rocks as *Buchia elderensis* (Anderson) and considered the rocks Late Jurassic (Tithonian = Portlandian) in age.

The distribution of taxa in sections in the San Diego area can be compared with those in central California (Fig. 3). As developed by Gabb (1864) Hyatt (1892), Diller and Stanton (1894), Stanton (1895), Anderson (1945), Imlay (1959), and Jones et al. (1969) *Buchia piochii* is the characterizing taxon of the *B. piochii* Biozone, which represents latest Late Jurassic (Tithonian) time. The belemnite *Cylindroteuthis* sp. ranges from Medial Jurassic to Early Cretaceous (Callovian to Berriasian). Other taxa recovered from the rocks are not presently useful for age identification, but the discovery of radiolarians suggests further work may provide good radiolarian age dates.

SYSTEMATICS

BIVALVIA

Phylum Mollusca

Class Bivalvia

Order Pterioida

Family Buchiidae

Genus *Buchia* Rouillier, 1845

Type species: *Avicula mosquensis* von Buch, 1844

Buchia piochii (Gabb), 1864 sensu lato

(Plate 1, figs. A-G)

Synonymy.

1864. *Inoceramus piochii* Gabb n. sp., p. 187, Pl. 25, fig. 173.
(not) 1869. *Aucella piochii* (Gabb); Gabb, p. 194, Pl. 32, figs. 92a, b, c.
1895. *Aucella piochii* (Gabb); Stanton, p. 96, Pl. 4, figs. 2-10.
1930. *Buchia piochii* (Gabb); Stewart, p. 108, Pl. 2, fig. 3.
1945. *Aucella piochii* (Gabb); Anderson, p. 1002, Pl. 3, figs. 1-5.
1959. *Aucella piochii* (Gabb); Imlay, p. 157, Pl. 17, figs. 7-10, 12-29.
1969. *Buchia piochii* (Gabb); Jones et al., p. A10, Pl. 2, fig. 16, Pl. 3, figs. 20-29.

Description. Bivalve specimens collected from the sections demonstrate limited morphological variations. Using the terminology of Shrock and Twenhofel (1953), valve heights (measured from hinge line to anterior edge) range from 11 to 18 mm; valve lengths (measured along the long axis beak to ventral edge) range from 18 to 30 mm; thickness of left valves (measured at greatest convexity) ranges from six to 10 mm.

Valve length exceeds height and thickness in each specimen and the convexity varies from mildly to very convex. The hinge lines on complete or nearly complete valves are very straight and nearly parallel the long

axis. All of the beaks are incomplete, appear very stout with a moderate but even taper, are greatly curved inward, and have a slight twist to the left (anterior).

Concentric markings are ribs and possibly constrictions that represent growth stages. These are evident only on one internal mold (Pl. 1, fig. C) and on the latex external cast (Pl. 1, fig. B), which has ribs that range from close, evenly spaced and nearly inconspicuous in surface expression to those that are very bold, wide and irregularly spaced; some probably represent constrictions. The remaining specimens are internal molds and exhibit a low smooth surface that may represent the nacreous inner valve surface of extant species.

Discussion. Previous reports have noted, but not described three different species of *Buchia* from localities in San Diego County. Milow and Ennis (1961) reported *B.* cf. *B. fischeriana*, Crampton (1961) reported *B.* cf. *B. piochii*, Fife et al. (1967) noted *B. piochii*, and Jones (in Balch, 1981) identified *B. elderensis*. All of these specimens have been collected from the same localities and none have been described or illustrated. Examination of these specimens and those from our new collections indicates that all are internal or external molds and many are flattened. None show ligament or hinge line characteristics and on most the beaks are absent or poorly preserved. Overall morphology of the few specimens is poorly preserved and appears intermediate among the three species noted above. We have therefore assigned the specimens to *Buchia piochii* sensu lato.

CEPHALOPODA

Phylum Mollusca

Class Cephalopoda

Subclass Coleoidea

Family Belemnitidae d'Orbigny

Subfamily Cylindroteuthinae Stolley, 1919

Genus *Cylindroteuthis* Bayle, 1878

Type species: *Belemnites puzosianus* d'Orbigny

Cylindroteuthis sp.

(Plate 1, figs. H-L)

Description. The belemnite specimens are poorly preserved. Those examined have a cross-sectional diameter of 11 to 13 mm and 12 to 19 mm, both from the approximate center of the guard. The two most complete guards have lengths of 70 mm and 85 mm, but the specimens are highly fractured and have been cemented together.

Thin sections, oriented transversely, were made of the best belemnite specimens (Pl. 1, fig. L) to expose internal structures that could be compared with photomicrographs of Jeletzky (1966). All of our sections showed considerable recrystallization, which nearly obliterated all internal structures. Very faint growth lines and concentric growth(?) lines are evident on the guard. One specimen has a prominent ventral groove that extends 23 mm from the apical end toward the posterior. None are complete enough to

allow for a description of the transverse section of the alveolar area, and all lack the protoconch or growth stages of the phragmacone.

OTHER TAXA

Oysters. A single fragment in thin section RFQ (Balch, 1981) near the top of Circo Diegueño Canyon has fibrous parallel laminations of calcite and microborings(?). The irregular laminar bunches and thickness of the fragment indicate affinity with oyster shells (Pl. 1, fig. R); this fragment has undergone considerable transportation.

Echinoderms. Small, single-crystal calcite grains containing small central holes are assigned to the phylum Echinodermata. The illustrated specimen (Pl. 1, fig. T) is from thin section RSD (Balch, 1981) near the middle of the section at Circo Diegueño Canyon and represents a transverse cross-section through an echinoid spine. Other specimens consist of single-crystal calcite and represent unidentified echinoderm plates; all appear to have been transported and abraded.

Parazoans (Porifera). A few fragmentary siliceous spicules resemble doubly tapered monaxons (Pl. 1, fig. S) and occur in thin section RFB (Balch, 1981) from near the top of the section at Circo Diegueño Canyon; a few of the spicules appear to have a hollow center, but most are poorly preserved.

Radiolarians. About 12 specimens occur in thin section RFB (Balch, 1981) from near the top of the section at Circo Diegueño Canyon, and they have been assigned to the Radiolaria. Although poorly preserved, some specimens could be assigned to familial rank. Family Actinommidae(?) (Pl. 1, fig. P) is represented by a spherical specimen; Family Hagiastridae(?) is represented by a branched specimen (Pl. 1, fig. Q). The remaining specimens were assigned only to order level; Order Spumellaria(?) (Pl. 1, figs. N, O) and Order Nassellaria (Pl. 1, fig. M).

ACKNOWLEDGMENTS

Tom Demeré provided comments and access to Los Peñasquitos Canyon. Drs. J. A. Jeletzky, D. L. Jones, G. L. Peterson and R. G. Gastil provided specimens and helpful discussions. Duane Balch provided thin sections and information from his masters thesis. Fred Sundberg reviewed the manuscript and made many valuable suggestions. Lou Ella Saul provided important information about some of the specimens.

REFERENCES

Allison, E. C., 1970, Basement rocks of the northern Santa Ana Mountains, in, Headlee, L. A., Warren, A. D. and Wildharber, J. L. (eds.): Pacific Sec. AAPG-SEPM, The southern rim of the Los Angeles Basin, Orange County, California, Field Trip Guidebook.

Anderson, F. M., 1945, Knoxville Series in California Mesozoic, Geol. Soc. America, Bull. 56:909-1014.

Balch, D. C., 1981, Sedimentologic study of the Santiago Peak volcaniclastic rocks: Unpub. Masters Thesis, San Diego State University, 135 p.

Bushee, J., Holden, J. C., Geyer, B. and Gastil, R. G., 1963, Lead-alpha dates for some basement rocks of southwestern California: Geol. Soc. America, Bull., 74:803-806.
Crampton, P. J., 1961, Radiometric dating of pre-bathol thic basement rocks in San Diego County: Unpub. Senior Thesis, San Diego State University.
Diller, J. S. and Stanton, T. W., 1894, The Shasta-Chico Series: Geol. Soc. America, Bull., 5:435-464.
Easton, W. H. and Imlay, R. W., 1955, Upper Jurassic fossil localities in Franciscan and Knoxville Formations in southern California: Amer. Assoc. Petrol. Geol., Bull., 39:2336-2340.
Fife, D. L., Minch, J. A. and Crampton, P. J., 1967, Late Jurassic age of the Santiago Peak Volcanics, California: Geol. Soc. America, Bull., 78:299-304.
Gabb, W. M., 1864, Description of the Cretaceous fossils: Geol. Survey of California, Paleontology 1:55-236.
Gabb, W. M., 1869, Cretaceous and Tertiary fossils: Geol. Survey of California, Paleontology 2, 299 p.
Hanna, M. A., 1926, Geology of the La Jolla quadrangle: Univ. California Pub. in Geol. Sciences 16:187-246.
Holden, J. C., 1961, Radiometric and paleontological age determinations of the Bedford Canyon Formation: Unpub. Senior Thesis, San Diego State University.
Hosken, S. M., 1981, Sedimentology of Upper Jurassic Santiago Peak volcaniclastic strata of northern San Diego County, California: Unpub. Senior Thesis, San Diego State University.
Hyatt, A., 1892, Triassic and Jurassic in the western states: Geol. Soc. America, Bull., 3:395-434.
Imlay, R. W., 1959, Succession and speciation of the Pelecypod *Aucella*: U. S. Geol. Survey, Prof. Paper 314-G, p. 160-169.
Imlay, R. W., 1964. Middle and Upper Jurassic fossils from southern California: Jour. Paleont., 38:505-509.
Jeletzky, J. A., 1965, Late Upper Jurassic and early Lower Cretaceous fossil zones of the Canadian western Cordillera, British Columbia: Canadian Geol. Survey, Bull. 103.
Jeletzky, J. A., 1966, Comparative morphology, phylogeny, and classification of fossil Coleoidea: Univ. Kansas Paleontol. Contrib., Mollusca, Article 7, 162 p.
Jones, D. A., 1982, Fossils from the Santiago Peak volcaniclastic rocks of San Diego County, California: Unpub. Senior Thesis, San Diego State University (in preparation).
Jones, D. L., Bailey, E. H. and Imlay, R. W., 1969, Jurassic (Tithonian) and Cretaceous *Buchia* Zones in northwestern California and southwestern Oregon: U. S. Geol. Survey, Prof. Paper 647-A.
Kew, W. S. W., 1919, Geology of a part of the Santa Ynez River district, Santa Barbara County, California: Univ. California, Department of Geol., Bull., 12:1-21.
Kennedy, M. P. and Peterson, G. L., 1975, Geology of the San Diego metropolitan area, California: Calif. Div. Mines and Geol., Bull., 200, 56 p.
Larsen, E. S., 1948, Batholith and associated rocks of Corona, Elsinore, and San Luis Rey quadrangles, southern California: Geol. Soc. America, Memoir 29, 182 p.
Milow, E. D. and Ennis, D. B., 1961, Guide to geologic field trip of southwestern San Diego County, in, Thomas, B. E. (ed.), Cordilleran section, Geol. Soc. America, Field Trip Guidebook.

Shrock, R. R. and Twenhofel, W. H., 1953, Principles of invertebrate paleontology: McGraw-Hill Pub., New York, 816 p.

Silberling, N. J., Schoellhamer, J. E. Gray, C. H. Jr. and Imlay, R. W., 1961, Upper Jurassic fossils from the Bedford Canyon Formation, southern California: Amer. Assoc. Petrol. Geol., Bull., 45:1746-1765.

Stanton, T. W., 1895, Cretaceous paleontology of the Pacific coast; the fauna of the Knoxville beds. U. S. Geol. Survey, Bull., 103, 132 p.

Stewart, R. B., 1930, Gabb's California Cretaceous and Tertiary type Lamellibranchs: Acad. Natural Sciences, Philadelphia, Spec. Pub. 3, 314 p.

Taliaferro, N. J., 1942, The geological history and correlation of the Jurassic of southwest Oregon and California: Geol. Soc. America, Bull., 53:71-112.

APPENDIX

List of fossil locations discussed in the text; all locations are catalogued in the Allison Center, Department of Geological Sciences, San Diego State University.

SDSU 37. From Crampton (1961). The exact locality cannot be determined from available sources.

SDSU 388. From Milow and Ennis (1961). Los Peñasquitos Canyon, northeast trending canyon bounded on the northeast by the SW 1/4 of section 7, T14S, R2W, and on the southwest by section 32, T14S, R3W of the Del Mar 7.5' quadrangle. Fossils are found in a small northerly trending tributary canyon approximately 460 m due south of Hill 415 at an elevation of about 40 m (130 ft). This corresponds to the 215 m level of the measured section described by Balch (1981).

SDSU 1589. From Fife et al. (1967). This locality is probably the same as that of SDSU 388. Bivalves and belemnites have been collected at this spot by T. Deméré (San Diego Museum of Natural History; see Jones, D. L., 1982).

SDSU 3247. From Jones, D. L. (1982). Circo Diegueño Canyon; east-west trending canyon from NE 1/4 of the NE 1/4 of section 5, T14S, R3W to the N 1/4 of the NE 1/4 of section 4, T14S, R3W of the Del Mar 7.5' quadrangle. Fossils approximately 114 m south of the northeast corner of section 4; corresponds to the 118 m level of the measured section of Balch (1981).

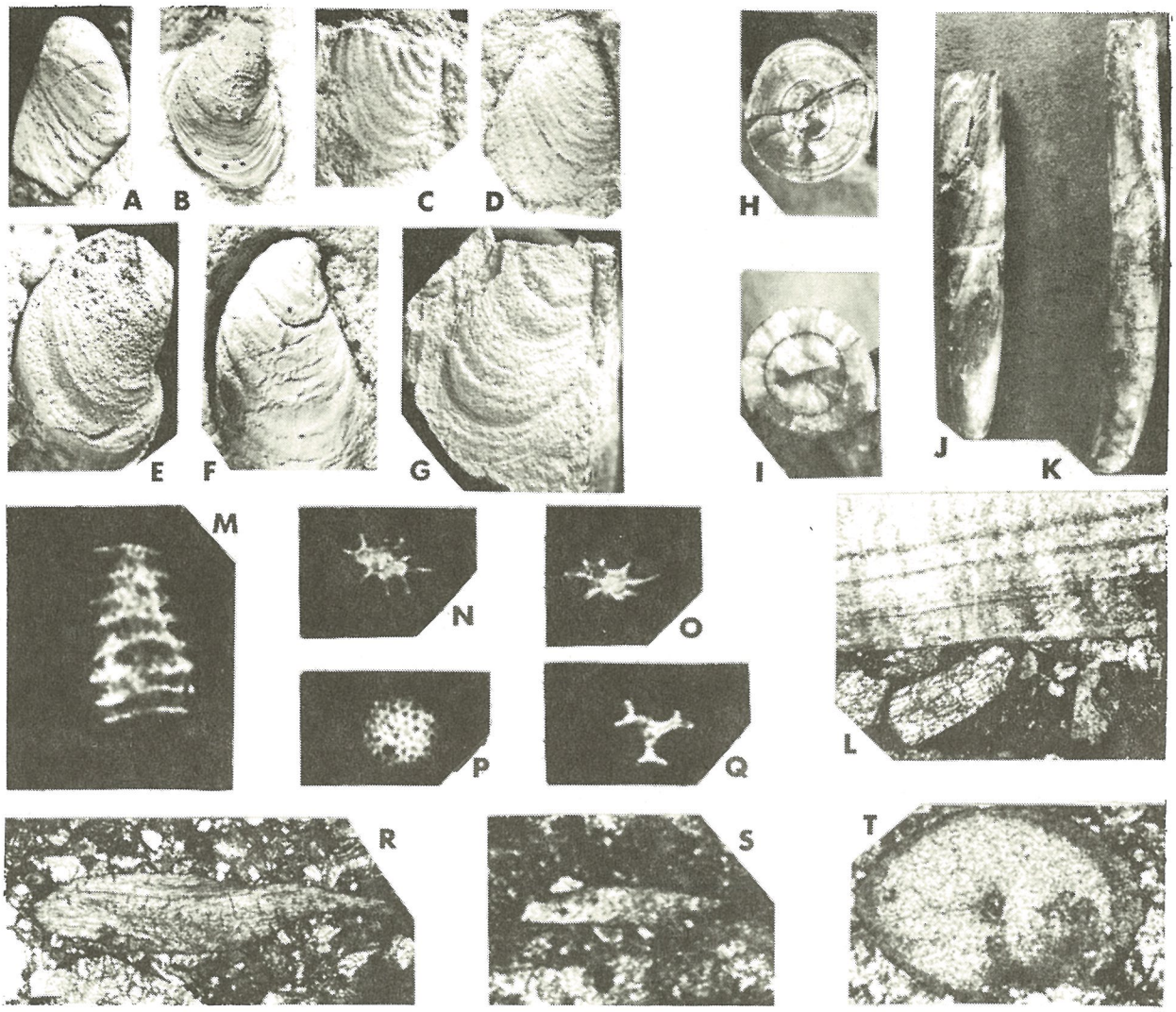

Plate 1.

Figs. A-G. *Buchia piochii* (Gabb) s. l. A, B, E, F from SDSU 3247 (Circo Diegueño Canyon); C, D, G from SDSU 1589 (Los Peñasquitos Canyon). All specimens X1.5 diameters.

H-L. *Cylindroteuthis* sp. H, I from SDSU 1589 (as above), X1.4 J, K from SDSU 37 (Los Peñasquitos Canyon), X 0.75; L, thin section of recrystallized guard in matrix from specimen in float, Circo Diegueño Canyon.

M-Q. Radiolaria. Thin section RFB, 214 m above base, Circo Diegueño Canyon (Balch, 1981). M, Order Nassellaria, X80; N, O, Order Spumellaria(?), X80; P, Order Spumellaria, family Actinommidae(?) X80; R, Order Spumellaria, family Hagiastridae(?), X100.

R. Bivalvia, oyster fragment, thin section RFQ, 8 m above base, Circo Diegueño Canyon (Balch, 1981), X15.

S. Parazoan, siliceous monaxon sponge spicule, thin section RFQ (as above).

T. Echinodermata, class Echinoidea, cross-section of spine from thin section RSD, 140 m above base, Circo Diegueño Canyon (Balch, 1981), X30.

STRUCTURE AND STRATIGRAPHY OF THE SANTIAGO PEAK VOLCANICS EAST OF RANCHO SANTA FE, CALIFORNIA

by

Mark A. Adams and Michael J. Walawender
Department of Geological Sciences
San Diego State University
San Diego, California 92182

INTRODUCTION

Weakly metamorphosed volcanic and volcaniclastic sedimentary rocks of Late Jurassic age, known collectively as the Santiago Peak Volcanics (Larsen, 1948), outcrop in a belt extending from the northern end of the Santa Ana Mountains to near the California-Baja California border (Gastil, et al., 1978). Although the general lithology of these volcanic rocks has been described (Larsen, 1948), little detailed stratigraphic or structural mapping has been attempted within them. This paper is concerned mainly with the sequence of metavolcanic rocks along Black Mountain Road that will be examined on the field trip outlined in this guidebook. Additional areas of exposure (Figure 1) are discussed in detail by Adams (1979). The overall purpose of the study was to define the stratigraphic and lithologic character of the Santiago Peak Volcanics and to evaluate these data in terms of a depositional environment.

In San Diego County, Peterson (1967) and Fife et al. (1967) have worked on the volcanic rocks in areas southeast of Rancho Santa Fe. Fife et al. (1967) showed maps of several small areas where sequences of argillite, graywacke, slate, and metavolcanic rock are overturned to the southwest. Based on broader preliminary mapping, Peterson (1967) concluded that the overturned units were unconformably overlain by an upright upper unit. He postulated thrust faulting as the most plausible explanation for the structural discordance. Adams (1979) concluded that these relationships are also consistent with isoclinal folding along an axial plane with an attitude of N41°W/49°N.

Fife et al. (1967) determined a Late Jurassic (Portlandian) age for the Santiago Peak Volcanics based on the presence of marine fossils found at localities of interbedded argillite, graywacke, and slate. The fossil remains include belemnoids, Buchia piochii, and a few unidentifiable forms. Further evidence for the age of the volcanic rocks was provided by Bushee et al. (1963), who obtained lead-alpha ages of 150 and 155 ± 10% m.y.BP for a metarhyolite and a metadacite, respectively. Later, Krummenacher et al. (1975) derived an age of 121.0 ± 7.5 m.y.BP from K-Ar dating of an andesite porphyry. This Early Cretaceous date reflects an age reset by intrusive rocks of the Peninsular Ranges batholith. Less precise bracketing is provided by the underlying Triassic to Upper Jurassic Bedford Canyon Formation (Imlay, 1964), and the Late Cretaceous granitic rocks of the batholith (Armstrong and Suppe, 1973).

The volcanic rocks typically mantle the western edges of the Peninsular Ranges batholith and separate it from the coastal plain sediments. Gaps in outcrop continuity result from eastward incursions of the sediments or intrusion of younger granitic rocks. Exposed widths are usually less than 10 miles.

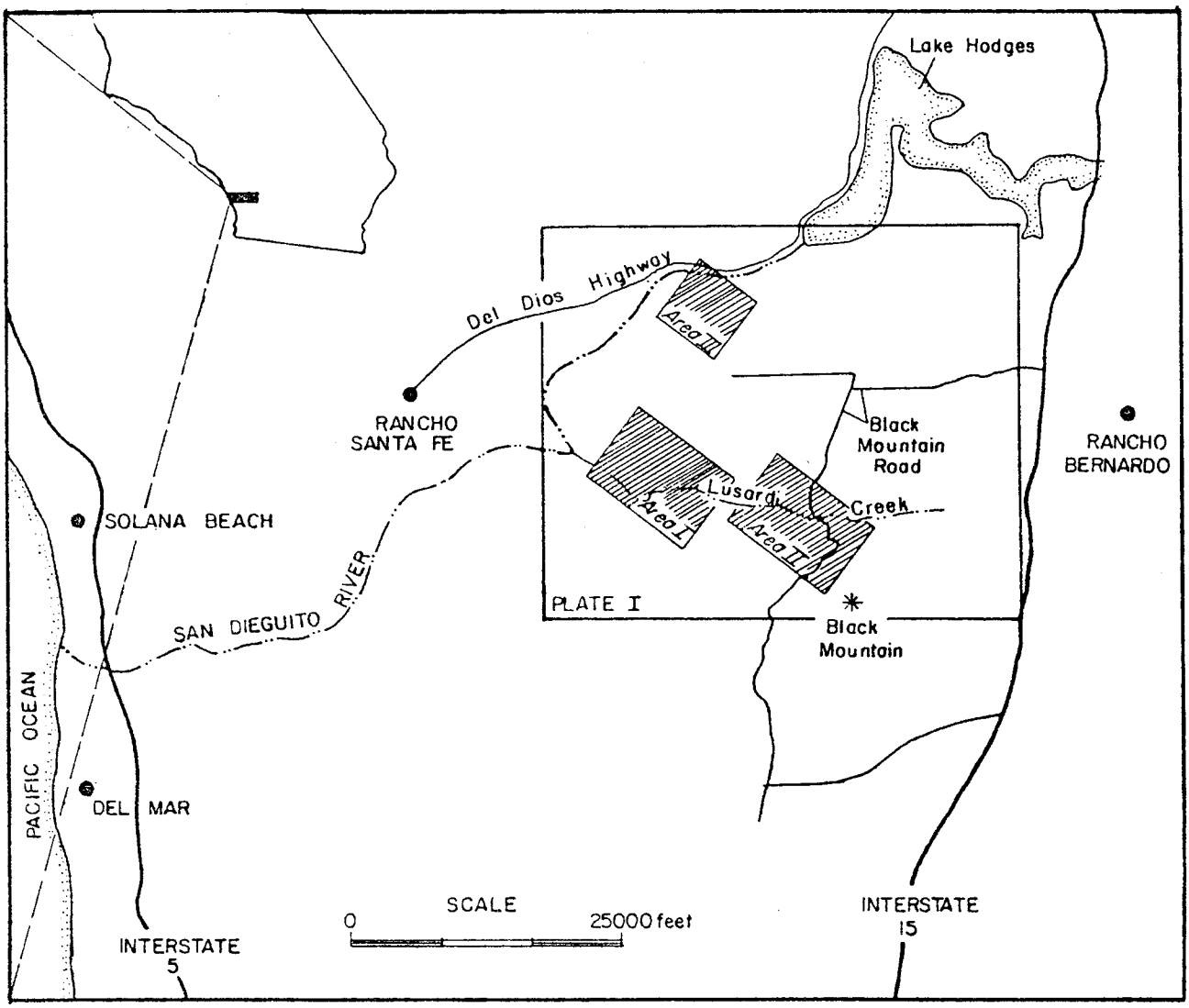

Figure 1. Location Map. Cross-hatched rectangles are areas of detailed mapping.

Volcanic rocks similar in appearance to the Santiago Peak Volcanics continue to outcrop sporadically south of the border. South of the Agua Blanca fault zone, extensive areas of middle Cretaceous marine volcanic strata of the Alisitos Formation are found (Allison, 1964; Gastil et al., 1975). Although lithologically similar to the Santiago Peak Volcanics, they contain a diagnostic Aptian-Albian marine bivalve assemblage (Allison, 1974) and are more distinctly bedded.

The Santiago Peak Volcanics have been altered by a widespread low-grade metamorphism. Larsen (1948) found this development of greenschist facies metamorphism to be mostly independent of intrusive proximity. In only a few cases where xenoliths were incorporated into plutonic bodies or where thin screens separated these bodies were higher-grade amphibolite or hornblende facies attained. In most areas, a uniform low-grade metamorphism prevails, with a general eastward increase in grade. Larsen (1948) interpreted the metamorphism to have been found prior to emplacement of the batholith. His typical greenschist mineral assemblage included chlorite, epidote, serpentine, calcite, epidote, albite, quartz, pyrite, pyrrhotite, and uralite.

TECTONIC RELATIONSHIPS

The Santiago Peak Volcanics resemble island-arc sequences of the circum-Pacific region as described by Matsuda (1964). Lithologically similar rocks also outcrop to the north along the western edge of the Sierra Nevada batholith, and to the south in Baja California (Alisitos Formation) (Clark, 1964; Allison, 1964, 1974). The Sierra Nevada and Peninsular Ranges batholiths form offset, parallel belts to the east of the volcanic belts.

The Santiago Peak Volcanics are separated from the Sierra Nevada segment by the large Transverse Block of Gastil et al. (1972). For the Sierra Nevada segment, Schweickert and Cowan (1975) proposed that the rock units record a Late Jurassic collision between an east-facing island-arc complex and a west-facing marginal-arc. Jones et al. (1976) put forth a similar hypothesis.

Later, Gastil et al. (1978) extended the idea by suggesting that the Alisitos Formation, the Santiago Peak Volcanics, and the Sierra Nevada segment represent a coeval island-arc system which was offset by large-scale transform faulting. The middle or Salinian segment developed no oceanic island-arc and thus today contains no correlative rocks.

Collision of the north and south arcs with the North American continent proceeded to occur at different times--the Sierra Nevadan segment in the Late Jurassic, the Santiago Peak segment in the Early Cretaceous, and, south of the postulated Agua Blanca transform fault, the Alisitos segment in the middle Cretaceous.

Since that time, and continuing today, strike-slip motion in southern California along a proto-San Andreas fault (Suppe, 1970; Gastil et al. 1972) and its modern equivalent (Crowell, 1962; Atwater, 1970) has moved peninsular California northward producing the compressive features typical of the Transverse Ranges, and disrupting the distribution of the volcanic-plutonic belts.

PETROGRAPHY AND STRATIGRAPHY (AREA II)

The volcanic rocks of Area II (Figure 1) begin to outcrop approximately 900 m due east of the last Area I exposure. In between, they are covered by sedimentary rocks of the San Diego embayment and alluvium. Twelve members, comprising a total stratigraphic thickness of approximately 1,400 m, have been delineated in this area which, unlike Area I, contains no slates or argillites, has many less flow units, and has far more breccias. Although the mapped outcrop pattern (Figure 2) and scarce measurable bedding indicates a northwest strike and steep northeast dip similar to that in Area I, no indications of whether the beds are overturned or upright have been found. Of the twelve members, nine are fragmental, ranging from fine tuffs and sandstones to coarse volcanic breccias, and three are flows. All are relatively thick bedded with irregular and undulating contacts between members (Figure 3). Of specific interest are the members that will be traversed on the field trip. For detailed descriptions of the remaining members, the reader is referred to Adams, 1979.

Jsp-b

Jsp-b consists of a series of fine- and coarse-grained epiclastic volcanic breccias. Clast sizes in the finest portions range from 0.5 to 5 mm and in the coarsest from 1 to 55 mm. It is possible that the breccias were not emplaced at the same time nor derived from the same source. Nevertheless, the breccias occupy the southern boundary for three overlying distinct lithologic units, Jsp-cc, Jsp-a, and Jsp-wt, and appear to constitute a coherent unit. The total length of this unit along strike exceeds 6,000 feet including two covered intervals.

In the northern portion, the breccia has a distinctive light green to purple color which changes southeastward to a variegated light green to brown color. No systematic variation in grain size is present. The northern portion is characterized by lithic fragments of scoria, latite, and feldspar lath-bearing types in a murky matrix consisting of chlorite, calcite, hematite, epidote, and microcrystalline material. The scoria, composed of vesicular hematite, provides the distinct purplish color found in this area. As with other breccias, the variety of fragment lithologies indicates a multiple source and deposition of the breccia from a mass-wasting process rather than from a pyroclastic flow.

Jsp-a

Overlying and partially interbedded with Jsp-b are tuffs and slatey-appearing fine tuffs of Jsp-a, similar in appearance to member Jsp-Sh3. The tuffs are black in outcrop and have a well-developed cleavage. A basal coarser-grained portion has fragments which range in size from 0.2 to 25 mm and which are composed of feldspar (as laths), magnetite, and quartz in various proportions. More characteristic, however, are the finer-grained facies. The contact between Jsp-a and Jsp-b, exposed in several places, is drawn at the first occurrence of the typical fine-grained black tuffs. Along Black Mountain Road, two reddish-white pyrophyllitized zones of 3 m and 9 m width are interlayered with the tuffs. From a thin tapered western point (map shape) interbedded with Jsp-b, member Jsp-a swells eastward to a maximum stratigraphic thickness of 150 m before it is truncated by a fault at the Jsp-wt contact.

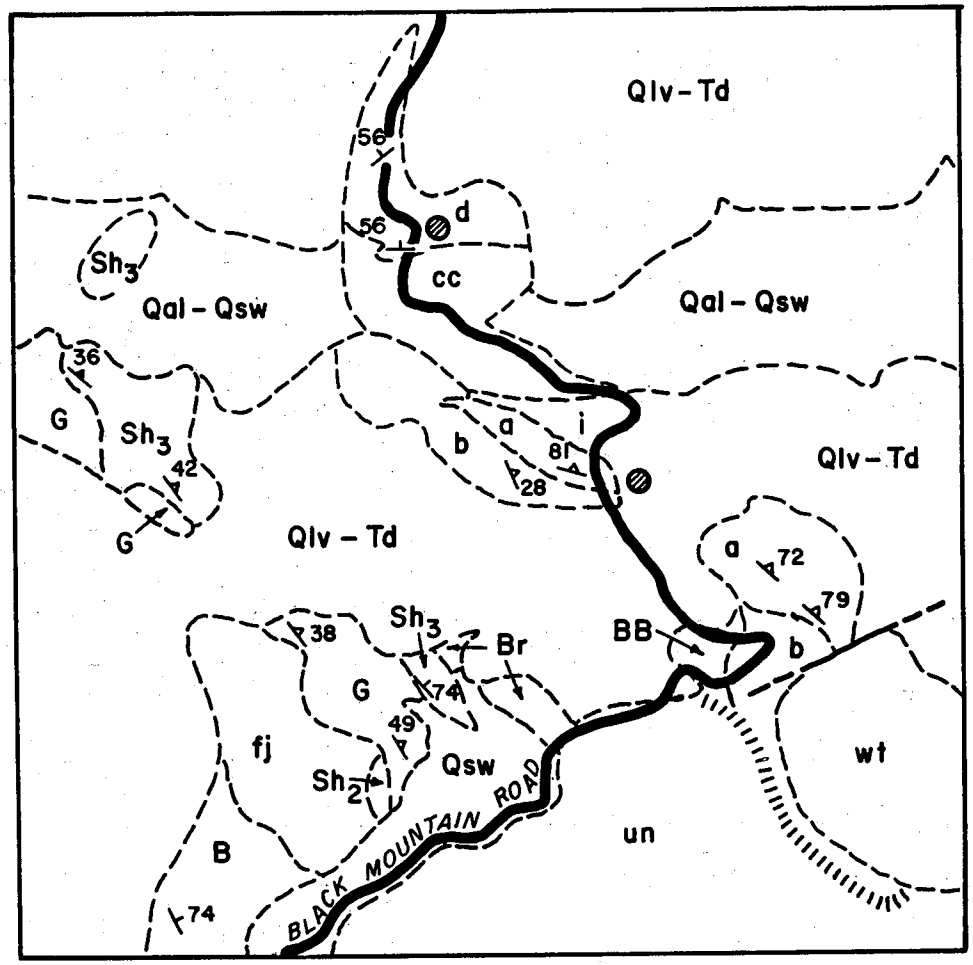

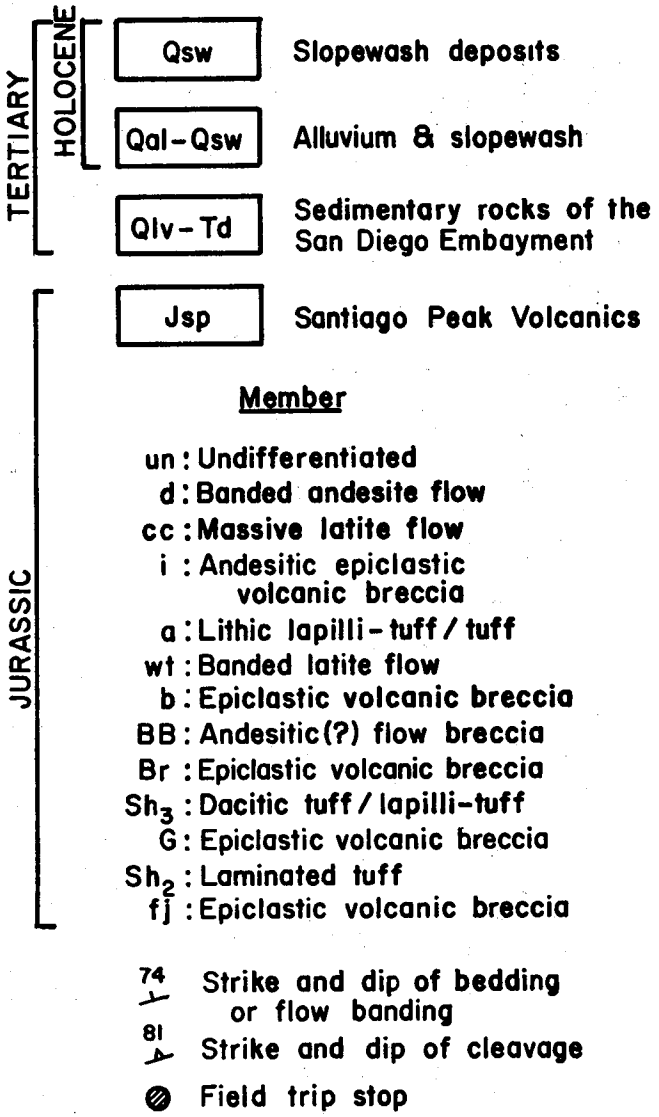

Figure 2 Geologic map of a portion of the La Jolla Valley-Black Mountain area.

COMPOSITE COLUMNAR SECTION: SANTIAGO PEAK VOLCANICS: AREA II

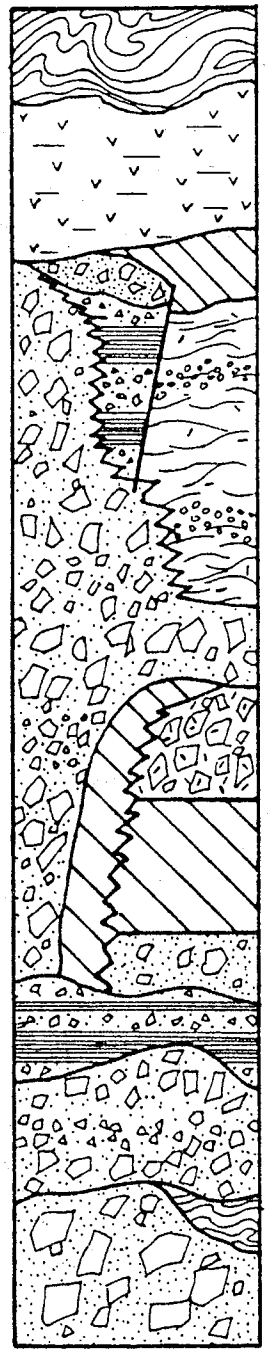

Jsp-d:	Banded andesite flow
Jsp-cc:	Massive latite flow
Jsp-i:	Andesitic epiclastic volcanic breccia
Jsp-a:	Lithic lapilli-tuff and fine tuff
Jsp-wt:	Banded latite flow
Jsp-b:	Epiclastic volcanic breccia
Jsp-BB:	Andesitic(?) flow breccia
Jsp-Br:	Epiclastic volcanic breccia
Jsp-Sh3:	Dacitic fine tuff and lapilli-tuff
Jsp-G:	Epiclastic volcanic breccia
Jsp-Sh2:	Laminated fine tuff
Jsp-fj:	Epiclastic volcanic breccia

Figure 3. Composite Columnar Section of the Santiago Peak Volcanics of Area II. Section may be upright.

: Indicates covered by younger sedimentary rock.

Jsp-wt

Jsp-wt is a massive section of latite flows which, in their central portion, form a minimum thickness of 390 m. Along dip, the flows disappear under younger sedimentary rocks.

Flow banding is well developed with fresh surfaces showing mildly undulating, reddish purple and black lamellae. Scattered throughout are feldspar euhedra averaging 1 mm length and abundant irregular vugs rimmed or filled with quartz. In one area, a unique interlayering of spherulite-rich material occurs. The spherulites--subrounded to nearly spherical, ranging in size from 0.5 to 7 mm, are most often packed densely and are essentially cavities which have variable degrees of quartz filling. These spherulites may have originated as gas bubble concentrations in the flows.

Jsp-l

Jsp-l is exposed in a small area along Black Mountain Road where it conformably overlies Jsp-a. It is a poorly sorted epiclastic andesitic volcanic breccia with fragments ranging in size from 0.07 to 15 mm. Petrographically, the tuff is characterized by a variety of silicified lithic clasts, including andesite, in a dark epidote-rich, silicified matrix containing numerous pyrophyllite flakes and stringers. Although the only exposures of this unit were found in roadcuts along Black Mountain Road, float fragments were found in other areas.

Jsp-cc

The thick section of nonbedded breccias and tuffs just discussed is overlain by a latite flow. Here, the flow (or flows) outcrops as a massive green rock having a medium-grained aspect on weathered surfaces. Broad bands of epidote-rich, aphanitic material are locally abundant as well as spheroidal epidote concentrations unique to this flow. The lower contact with Jsp-l appears conformable, whereas the upper contact with Jsp-d is obscured by a weathering zone 3 m to 15 m wide.

Jsp-d

Jsp-d is one of the more easily defined units in this area. It is a silicified, flow-banded andesite. Fresh surfaces are shades of white and grey, and weathered surfaces are similar but with a slight orangish stain. The flow lamellae, ranging in thickness from less than 1 mm to 10 mm, are a reflection of variations in the size and concentration of quartz, epidote, and pyrite. Although of igneous origin, the lamellae are highly contorted and can appear sedimentary in nature with such textures as pseudo-truncated crossbedding, or plastic flow folding reminiscent of slump structures in unconsolidated sediments.

Petrographically, the andesite(s) consist of euhedral feldspar (plagioclase ± potassium feldspar) phenocrysts almost totally replaced by dark epidote in a highly foliated trachytic matrix of feldspar laths and interstitial and granular quartz. Subparallel anastomosing fractures contain hematite, pyrite, and epidote. The foliation sweeps around the phenocrysts producing vague "pressure shadows."

In summary, approximately 366 m of volcanic flows are exposed in this area (using maximum thicknesses) that essentially cap and/or truncate an underlying 1,075 m of tuffs and breccias. Although a few of the tuffs appear to have a pyroclastic or flow breccia origin, the great majority seem to be chaotic lahar or talus deposits. No evidence for reworking or deposition by water was seen.

STRUCTURE AND MINERALIZATION

The volcanic rocks of the study area are characterized by a variably developed cleavage generally parallel to but not constrained by bedding. The cleavage is discontinuous, ranging in both intensity and distribution, and is localized in northwest-trending zones. This pattern is particularly evident on the northern slopes above Lusardi Creek where well-cleaved rocks are abruptly interlayered with uncleaved or poorly-cleaved rocks which appear to be of identical lithology. The cleavage zones have sharp, or, more typically, gradational boundaries, and along strike are discontinuous, even en echelon, in nature. Where cleavage is most intense, the soil is littered with platy fragments with a micaceous sheen. In areas of lithologic variation, cleavage tends to be concentrated in the finer-grained tuffs rather than in the coarser-grained breccias.

Figures 4 and 5 present contoured stereographic projections of bedding and cleavage measurements. As can be seen, the cleavage maxima occur at N53°W/73°W, as compared to a bedding maxima of N49°W/37°N. This difference in attitude is born out by field observation (of the few outcrops showing bedding) that cleavage generally cuts bedding at a low angle.

Although not always the case, pyrophyllitization of the host rocks has typically occurred in the zones of best developed cleavage. The distribution of the most intense pyrophyllite mineralization (Adams, 1979, Figure 17) clearly shows the localization of pyrophyllite in irregular northwest-trending zones. Figure 6 is a contoured stereographic projection of the poles to the foliation in zones of pyrophyllite mineralization. Despite the lower number of points (as compared to figures 5 and 6), three maxima are apparent. One (N61°W/72°N) closely corresponds to the major cleavage (N53°W/73°N), a second (N29°W/35°N) to the main bedding direction (N49°W/37°N), and the third (N29°W/60°N) to the secondary bedding maxima (N11°W/60°N). Although these "fits" are marginal in terms of the average strike, the low number of points utilized in Figure 6 combined with the overall variability in attitudes indicates that they are not unreasonable. This suggests that the pyrophyllite mineralization postdates the development of all the structural surfaces, i.e., all preexisting surfaces (bedding, cleavage, etc.) were permeable channels for the hydrothermal fluids responsible for the pyrophyllite mineralization. Jahns and Lance (1950) document textural criteria indicating that mineralization did not predate "shearing" (cleavage?).

As has been shown, the cleavage present in the mapped area is nearly parallel to bedding and is, therefore, in descriptive terms, a bedding plane cleavage. Such parallelism may be due to isoclinal folding, in which case the cleavage would be axial-plane cleavage, to mimetic recrystallization, or to flow parallel to bedding (Billings, 1972). No evidence for the latter two has been found. However, some evidence does exist for the former, as follows. First, the existence of isoclinal folding is supported by the observation that overturned beds are in relatively close proximity to upright beds

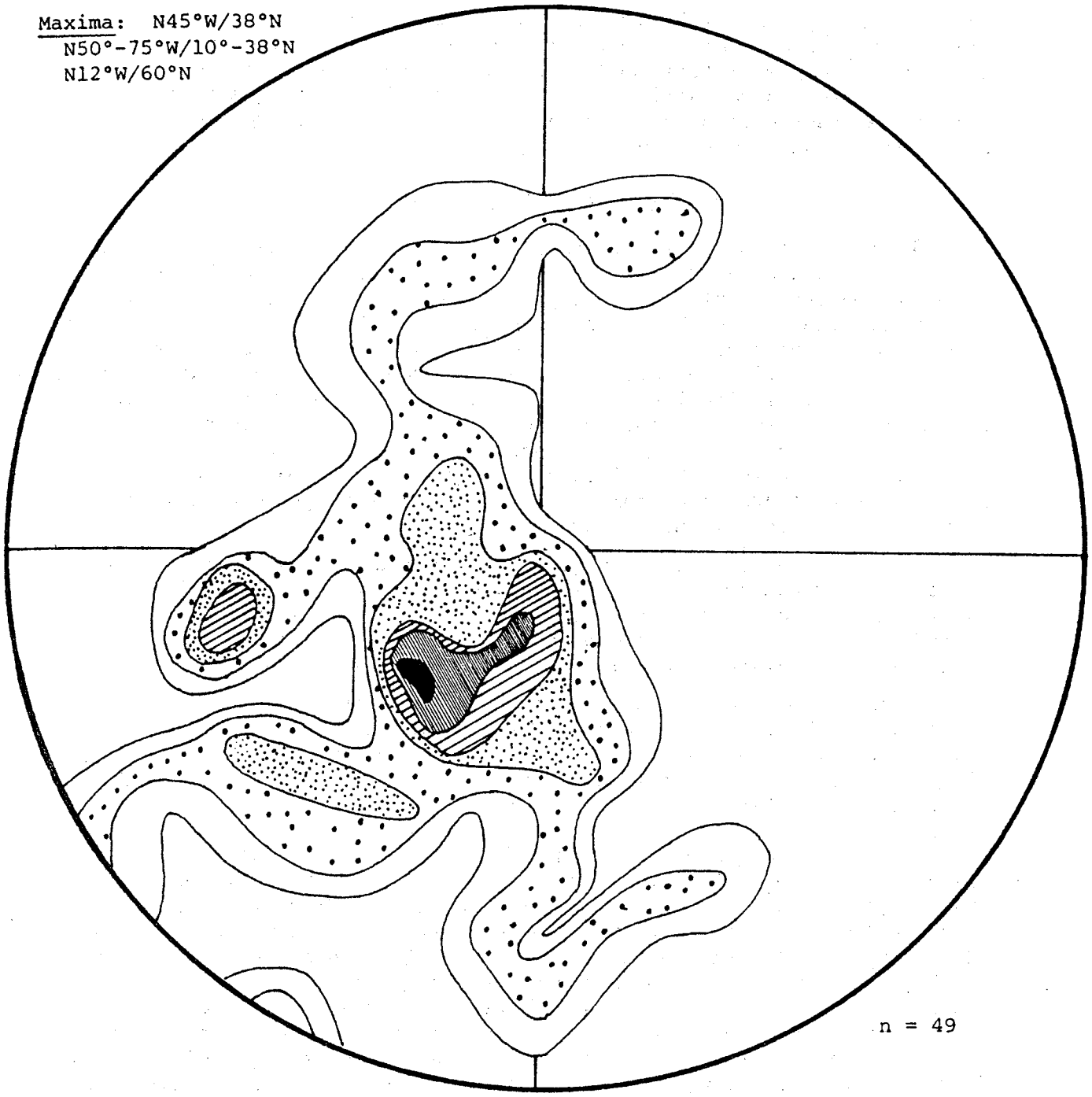

%	0-2	2-4	4-6	6-8	8-10	≥ 10

Figure 4. Contoured Stereographic Projection of Poles to All Bedding and Selected Flow Layering Excluding Member Jsp-ms (plotted on lower hemisphere)

Maxima: N53°W/73°N

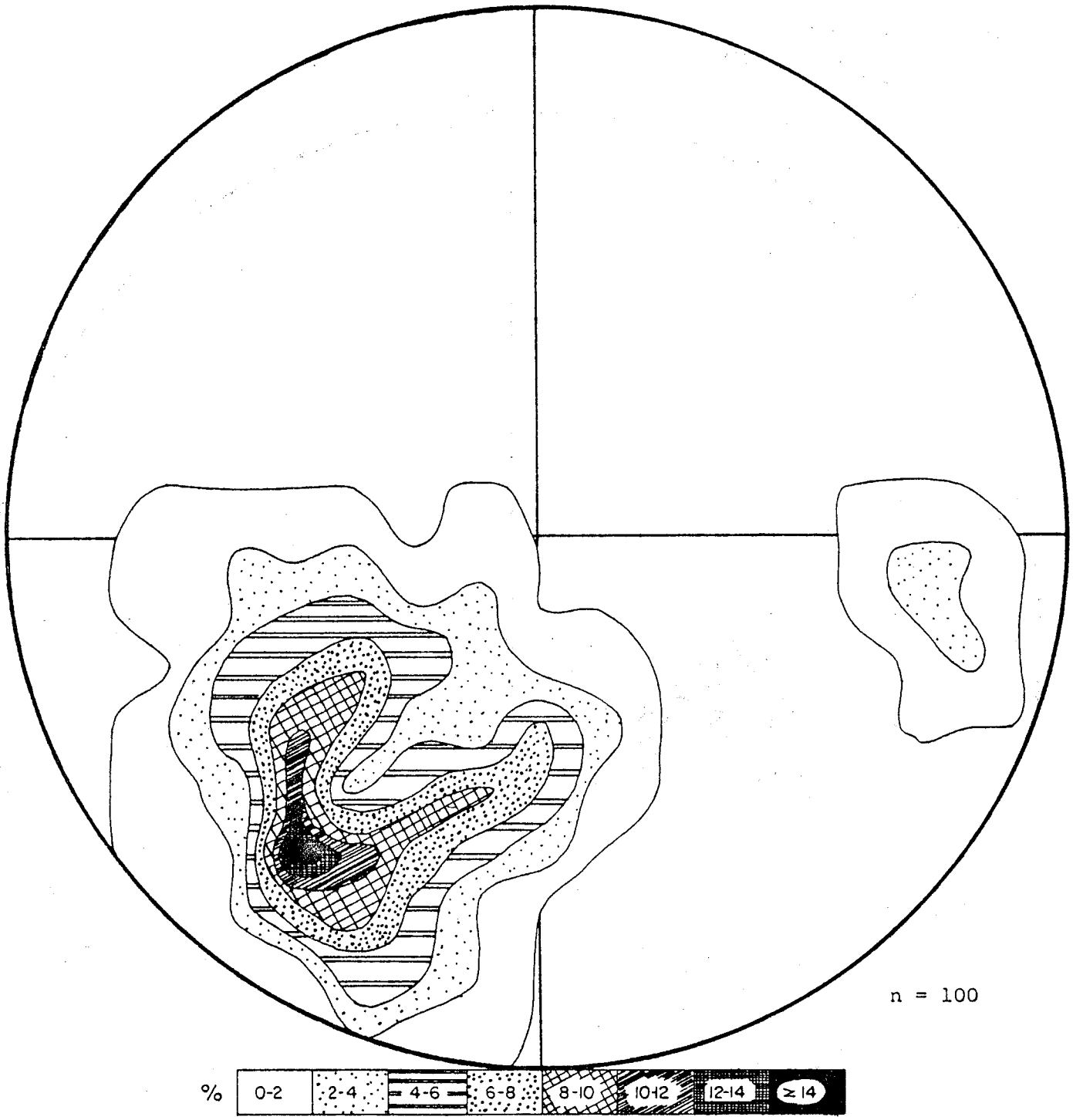

Figure 5. Contoured Stereographic Projection of Poles to All Cleavage (plotted on lower hemisphere)

REFERENCES

Adams, M. A., 1979, Stratigraphy and petrography of the Santiago Peak Volcanics east of Rancho Santa Fe, California: Unpub. M.S. Thesis, S.D.S.U.

Allison, E. C., 1964, Geology of areas bordering the Gulf of California, in Marine Geology of the Gulf of California: Amer. Assoc. of Petroleum Geologists, Mem. 3, p. 3-29.

Allison, E. C., 1974, The type Alisitos Formation (Cretaceous, Aptian-Albian) of Baja California and its bivalve fauna, in Geology of Peninsular California: Pacific Section Amer. Assoc. Petroleum Geologists, AAPG, Soc. Econ. Petrol. and Mineralogy, and Soc. Explor. Geophys. Guidebook, p. 29-59.

Armstrong, R. L., and Suppe, J., 1973, Potassium-argon geochronometry of Mesozoic igneous rocks in Nevada, Utah, and southern California: Geol. Soc. of America Bull., v. 84, p. 1375-1392.

Atwater, T., 1970, Implications of plate tectonics for the Cenozoic tectonic evolution of western North America: Geol. Soc. of America Bull., v. 81, p. 3513-3536.

Beane, R. E., and Titley, S. R., 1981, Porphyry copper deposits: Part I. Hydrothermal alteration and mineralization; Econ. Gol., 75th Anniv. Vol., p. 235-269.

Billings, M. P., 1972, Structural geology, 3rd ed.: Englewood Cliffs, New Jersey, Prentice-Hall, Inc., 606 p.

Bischoff, J. L., and Seyfreid, W. E., 1978, Hydrothermal chemistry of seawater from 25°C to 350°C; Amer. Jour. Sci., v. 278, p. 838-860.

Bushee, J., Holden, J., Geyer, B., and Gastil, G., 1963, Lead-alpha dates for some basement rocks of southwestern California: Geol. Soc. of Amer. Bull., v. 74, p. 803-806.

Clark, L. D., 1964, Stratigraphy and structure of part of the western Sierra Nevada metamorphic belt, California: U.S. Geol. Survey Prof. Paper 410, 70 p.

Crowell, J. C., 1962, Displacement along the San Andreas fault, California: Geol. Soc. of Amer. Special Paper 71, 61 p.

Fife, D. L., Minch, J. A., and Crampton, P. J., 1967, Late Jurassic age of the Santiago Peak Volcanics, California: Geol. Soc. of America Bull., v. 78, p. 299-304.

Gastil, G., Morgan, G., and Krummenacher, D., 1978, Mesozoic history of Peninsular California and related areas east of the Gulf of California, in Howell, D. G., ed., Mesozoic Paleography of the Western United States: Pacific Coast Paleography Symposium No. 2, p. 107-115.

Gastil, R. G., Phillips, R. P., and Allison, E. C., 1975, Reconnaissance geology of the State of Baja California: Geol. Soc. of America Mem. 140, 170 p.

Gastil, G., Phillips, R. P., and Rodriguez-Torres, R., 1972, The reconstruction of Mesozoic California: 24th International Geologic Cong., Section 3, p. 217-229.

Imlay, R. W., 1964, Middle and Upper Jurassic fossils from southern California: Jour. of Paleontology, v. 38, p. 505-509.

Jahns, R. H., and Lance, J. F., 1950, Geology of the San Dieguito prophyllite area, San Diego County, California: Calif. Div. of Mines and Geology Special Report 4, 32 p.

Jones, D. L., Blake, M. C., and Rangin, C., 1967, The four Jurassic belts of northern California and their significance to the geology of the southern California borderland, in Aspects of the Geologic History of the California Continental Borderland, p. 343-362.

Krummenacher, D., Gastil, R. G., Bushee, J., and Doupont, J., 1975, K-Ar apparent ages Peninsular Ranges batholith, southern California, and Baja California: Geol. Soc. of Amer. Bull., v. 86, p. 760-768.

Larsen, E. S., Jr., 1948, Batholith and associated rocks of Corona, Elsinore, and San Luis Rey Quadrangles, southern California: Geol. Soc. of America Mem. 29, 182 p.

Peterson, G. L., 1967, Structure of the late Mesozoic prebatholithic rocks north of San Diego, California: Geol. Soc. of America Spec. Paper 115, Abstracts for 1967, p. 347.

Schweickert, R. A., and Cowan, D. S., 1975, Early Mesozoic tectonic evolution of the western Sierra Nevada, California: Geol. Soc. of Amer. Bull., v. 86, p. 1329-1336.

Suppe, J., 1970, Offset of late Mesozoic basement terrains by the San Andreas fault system: Geol. Soc. of Amer. Bull., v. 81, p. 3252-3258.

GENESIS OF VERNAL POOL TOPOGRAPHY IN SAN DIEGO

by

Patrick L. Abbott
Department of Geological Sciences
San Diego State University
San Diego, California 92182

INTRODUCTION

A microtopography of low mounds separated by unconnected depressions occurs at many sites in the United States as well as in Canada, Iraq, Africa, Australia, and elsewhere. The numerous occurrences of this topography have been referred to as Mima mound, prairie mound, pimple plain, mound and depression, hogwallow, vernal pool, gilgai and other names by different workers in varied areas.

In the San Diego area, vernal pool topography mostly occurs on very gently-sloping terraces away from active canyons or gullies and thus away from stream erosion or deposition. The mounds occur in a loose geometric plan, vary from 0.1 to 2 m high and commonly have circular to ovoid outlines with typical diameters of 3 to 20 m (Figure 1). Sizes of the intervening depressions range from one square meter up to several thousand square meters in composite depressions. Rain here falls mainly during the winter months of December through February; vernal pools may contain water into April or May. The vernal pools support unique flora and fauna that are disappearing beneath the onslaught of southern California suburban development. Distinctive plants develop as the pools desiccate using either annual, bulbous perennial or herbaceous perennial growth habits to survive the dry summer and fall (Zedler et al., 1979). Several vernal pool species have very limited distributions and two are on the federally protected, endangered species list (Pogogyne abramsii, the San Diego mesa mint and Orcuttia californica, a grass). The zooplankton fauna consists of at least 11 species of crustaceans and 16 species of rotifers that tolerate wide ranges of ecological conditions and can form cysts or resting eggs to survive dry periods (Zedler et al., 1979).

PREVIOUS INTERPRETATIONS OF VERNAL POOL TOPOGRAPHY

Several interpretations have been offered for the origin of vernal pool topography in San Diego. Barnes (1879) felt the mounds grew by entrapment of wind-borne dust arrested by shrubs which in turn protected hillocks from the rainwash which eroded the inter-shrub areas into depressions. He also felt that already established hillocks received additional deposition through the activities of gophers.

Hertlein and Grant (1944) suggested that the origin of the prairie mounds or hillocks was connected with the accumulation of aeolian sand around bushes, or irregular deflation between them during a widespread condition different from the present. They also noted a correlation between hillock occurrence and maturely developed soils such as the Redding Series which they attributed to the wide spacing of bushes forced to grow on these acidic, hardpan-containing soils.

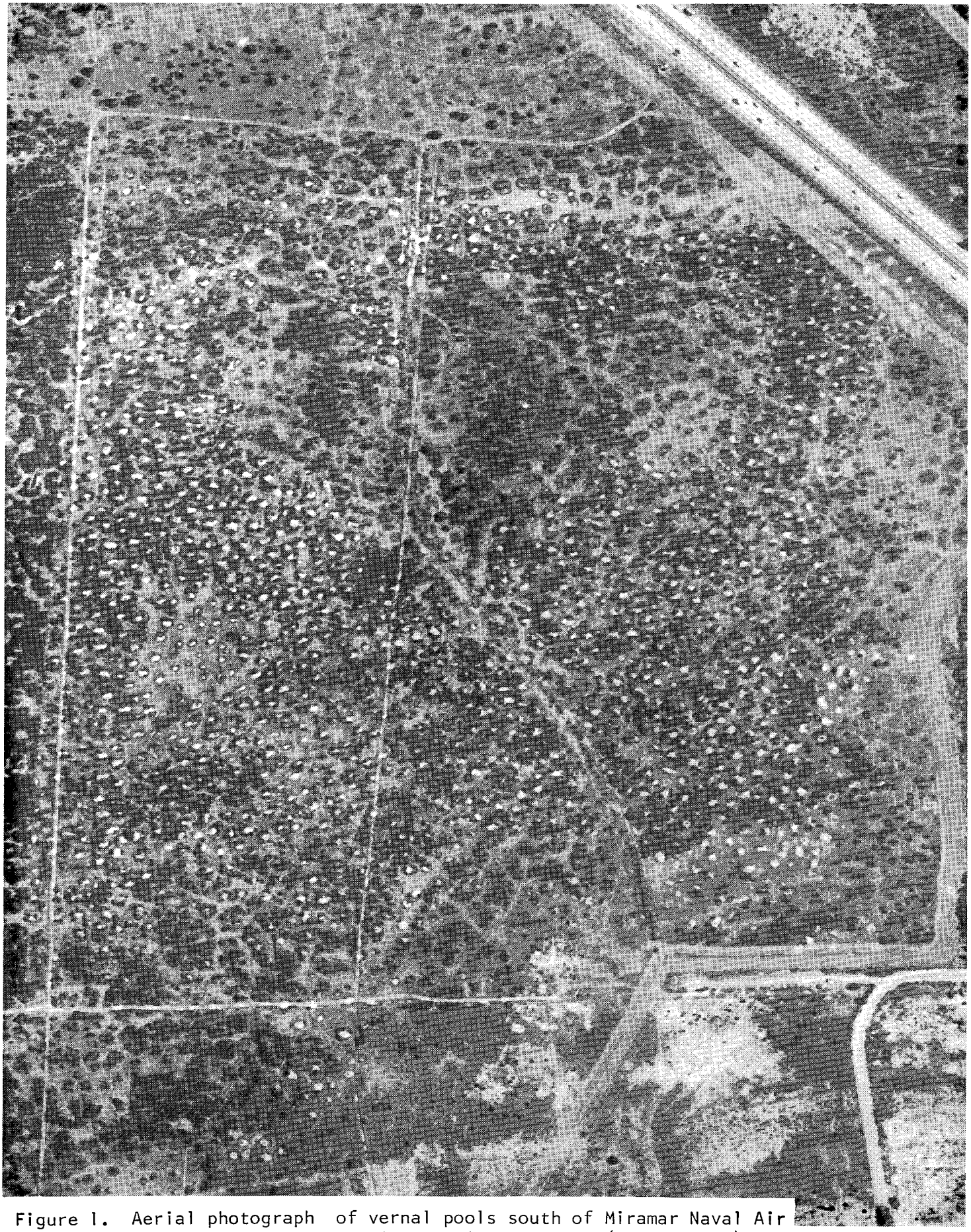

Figure 1. Aerial photograph of vernal pools south of Miramar Naval Air Station on Kearny Mesa in San Diego. Pools (white spots) are mostly a few meters diameter.

Nadolski (1969) suggested that the mounds result from differential ponding of water upon inhomogeneous soils with resultant unequal settling of the ground to form mounds.

Zedler (in Zedler et al., 1979) proposed an origin based on differential settling rates of alluvial material that was initially accelerated by inequitable distribution of water. Mechanical erosion then accentuated the local relief of some areas but did not join the depressions. Shrinking and swelling clays produced some distinctive features but did not greatly affect the size or shape of mounds.

Cox (1980) believes that the mounds were built by the burrowing activities of pocket gophers who have concentrated the shallow soft soils into build-ups to house their burrow system of permanent nest and food storage chambers.

SEDIMENTOLOGIC DATA FROM VERNAL POOLS ON LINDA VISTA TERRACE

Vernal pool topography is largely developed within the B horizons of the ancient soil profile that mantles the Linda Vista Terrace as a relict soil. Information on the Quaternary composite soils (Abbott, 1981) along with data generated by a CALTRANS investigation (Greenwood and Abbott, 1980) have shed new light on the origin of vernal pool topography. If the single most important factor is isolated from the complex genesis of the microtopography, it would have to be the abundance of expandable clays in the surface and near-surface soil and sedimentary rock layers. The expandable clays enlarge their aggregate mass when wetted, contract upon drying with resultant development of desiccation cracks and mud curls, and the whole wetted mass creeps downslope under the pull of gravity. Some of the relevant data that describe these clayey horizons are as follows (Table 1).

PERSPECTIVES FROM A ROADCUT

A fortuitously located roadcut at the intersection of Sundance and Entreken Avenues slices through vernal pool topography and exposes the Redding paleosol horizons in place and little disturbed. The relationships in the roadcut have been sketched in cross section (Figure 2). The roadcut trends east-west and the exposed rock layers/soil horizons dip 1/2 to 5° to the west in this two-dimensional face. Mount dimensions, which must be minimal, are two feet high and 45 feet across. Vernal pools collect in depressions eroded down to the discontinuous paleosol hardpan layer (C_m horizon) which forms an impermeable base. The mounds are composed of pebbly claystone and are masses of the relict soil B_t horizon left high as the adjacent areas were lowered. The intervening pools are floored with gravels suggesting either a lag origin following removal of clays to make the pool depressions or a concentration due to repeated upward lifting of expansive clays.

The early Pleistocene sedimentation units are sandstones and conglomerates of the predominantly marine Lindavista Formation. The western end of the roadcut is dominated by a planar-based shallow marine conglomerate lense up to 2-1/2 feet thick and 70 feet long. Below the conglomerate are friable, immature coarse sandstone beds that contain scattered gravel-filled troughs. Above the conglomerates are pebbly sandstones that received clay minerals while acting as the host for the paleosol B_t horizon. The major planar-based conglomerate lense acted as host for differential development

TABLE 1. SEDIMENT DATA FROM SERIES H POOLS ON LINDA VISTA TERRACE

Sample Number	Mud (% of Total Sample)	Percentage of Total Sample <1 Micron	Clay Mineral Percentages				Plastic Limit	Liquid Limit	Plasticity Index	In-Field Moisture Contents (%) July 1980	In-Field Moisture Contents (%) August 1980	Expansion Tests		
			Expandables	Illite	Chlorite	Kaolinite							Moisture Content	Expansion
1A	63	26	46	40	14	0.2	15	32	17	--	--	Sample 1B	13.5%	12.3%
1B	66	36	76	15	9	0.4	20	51	31	16	--		17.5%	12.1%
													21.7%	9.3%
2A	54	19	53	28	19	0.2				2	3	Sample 3B	13.5%	17.3%
2B	76	47	88	6	6	--				20	19		18.2%	12.7%
													22.2%	6.1%
3A	42	13	10	57	33	--	14	24	10	3	--			
3B	70	45	87	1	12	--	20	56	36	23	--			
9A	50	15	30	47	22	0.6				6	3			
9B	61	30	87	4	9	--				12	10			
10A	64	24	21	59	20	0.4				3	--			
10B	--	48	54	35	10	1.3				19	--			

A = upper loamy layer of soil; includes modern A horizon developed on paleosol B horizons; average thickness = 1.1 feet; average porosity = 37.5%

B = lower clay layer of soil; includes paleosol B_t horizon; average thickness = 2.2 feet; average porosity = 22%

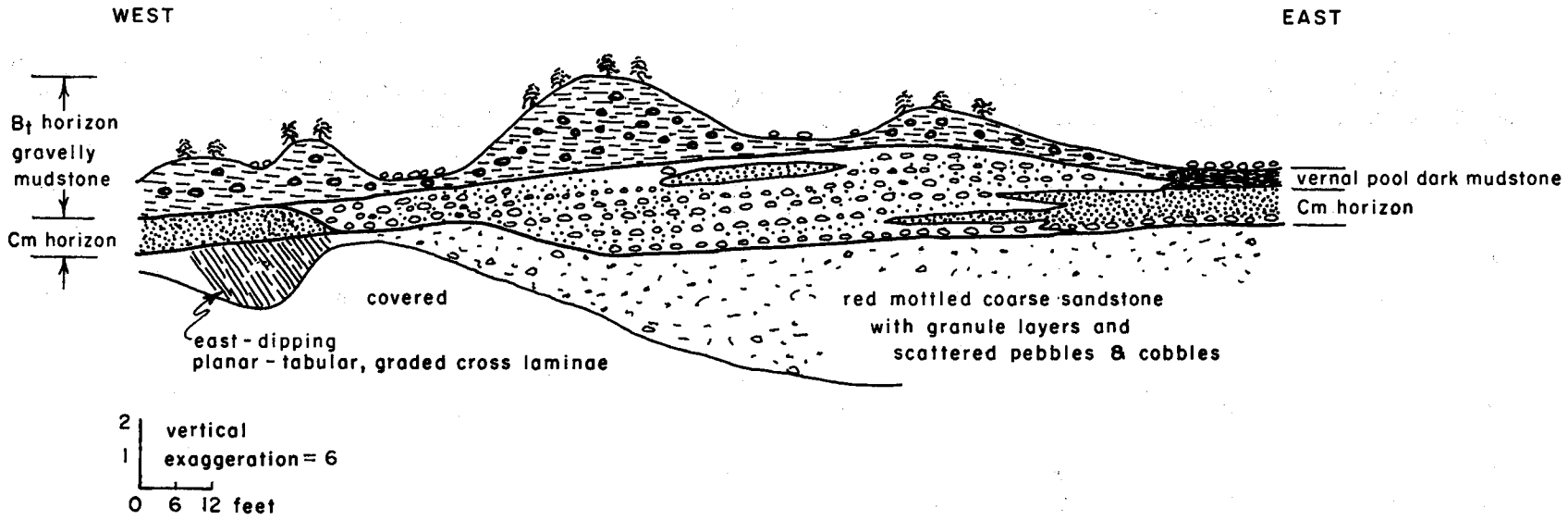

Figure 2. Vernal pool topography exposed in roadcut at Sundance and Entreken Avenues in San Diego. Rocks are all part of the Pleistocene Lindavista Formation. Mounds are composed of gravelly mudstone of the B_t relict soil horizon that rests on cemented sandstone and conglomerate. Mounds appear to be fortuitously located topographic highs between downward eroded depressions mantled by lag gravels.

of the C_m horizon. The C_m layer varies in thickness from 6 inches to 2-1/2 feet but maintains fairly evenly sloping upper surfaces.

ACTIVE PROCESSES

Most of the vernal pool topography is directly controlled by and carved into the expandable clay-rich horizons of relict soil profiles formed on coarse sedimentary rocks that cap gently sloping terraces. Slight irregularities on this Pleistocene surface have been modified by small-scale diapirism, differential subsidence, unequal growth of C_m horizon, baffling of aeolian sediment and organic debris beneath chaparral shrubs, deflation of depressions, and downslope creep or gravity sliding of the entire carpet of expandable clay-rich horizons. These active processes have combined their greater and lesser contributions to create the vernal pool topography.

Evaluation of the relative importance of the active processes is aided by a roadcut exposure through the topography (Figure 2). Evidence of diapirism within the mounds is not seen, mound locations do not always correlate with the unequal thicknesses of the C_m horizon, wind does not have the competence to have deposited the pebbles that are distributed throughout the sediments that compose the mounds, and differential subsidence was not terribly important because the paleosol illuvial layer is thick beneath the mounds and is thin to absent beneath the pools.

The role of water erosion in the development of the topography must have been slight. The isolated locations of pools and mounds (Figure 1) combined with the lack of an integrated drainage pattern rules out a significant role for running water. Even rainwash would be counterproductive, i.e. it would erode from the mounds and deposit in the pools. The only mechanical erosion agent that could have created these unconnected depressions under San Diego's Quaternary climates is the wind.

Downslope creep is promoted by wetting the abundant expandable clays within the illuvial layer. The significance of this process can be seen on the steep slopes of stream valleys next to the mesa edges where the prairie mounds may be observed sliding downslope while remaining intact. This same process, which probably occurs at a greatly reduced rate on the gently sloping terraces, could cause some rumpling of superjacent soil material. However, the overall contribution of this process to creation of the topography seems to be as minimal as the slopes down which the mounds are moving.

A process that seems to be quite important in the topography formation involves desiccation cracks and may best be understood in examining the origin of the small, embryonic or beginner pools. For example, the vernal pool topographic pattern exists in miniature form in the watershed area for the large pools on the mesa north of Penasquitos Canyon, i.e. pools only a meter in diameter with depression depths as shallow as several centimeters abound within the chaparral-covered slopes. Incipient pools appear to be related to large-scale desiccation cracks that form in polygonal patterns when the clayey surface soil undergoes drying. Individual cracks may be one to ten centimeters wide and up to several meters long. Small pools tend to be located at the corners of desiccation polygons where the cracks meet in triple junctions. The combined contractions of three cracks create a little pull-apart depression (Figure 3). Subsequent rains will cause a small pool to form in the pull-apart depression. However, the

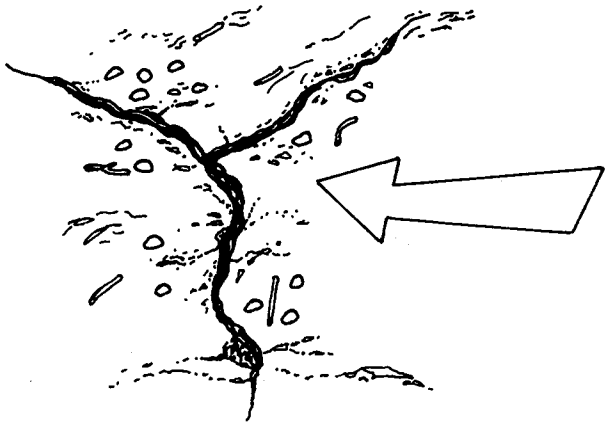

CONTRACTION AND PULLING APART DURING DESICCATION CREATES A TOPOGRAPHIC LOW AT THE INTERSECTION POINT OF CRACKING

Figure 3. Small depression (incipient vernal pool) formed at triple junction of polygonal desiccation cracks.

expansion of sun-dried clays commonly only partly recovers the volume loss that occurred with drying (Grim, 1962). Thus incipient vernal pools would not be totally eliminated by the expansion that occurs with rewetting. As the little pools dry seasonally, the surface mud penetrated with lichen and moss peels back to form flat and curled mud chips. Physical removal of these mud chips from a dried pool is a possible process involved in the deepening and widening of the depression. Because of the lack of integrated drainage, running water has been ruled out as the erosive agent. The wind seems to be the most likely agent to remove mud chips. If the wind is culpable, it also explains the gravel lags that floor the pools.

The small pools formed at desiccation crack junctions tend to coalesce by growth along the large connecting cracks. For example, water accumulates

in a crack that forms one edge of a shrinkage polygon. Removal of desiccation-formed mud chips causes a crack to widen and deepen. When a large crack between two small pools deepens enough the two isolated pools are then connected into a larger pool whose collective growth continues. All the intermediate stages of pool growth are present between a one square meter beginner pool to an advanced pool of a few thousand square meters area. In fact, remnant mounds and local depressions still exist within very large vernal pools to give mute testimony to the former existence of separated local mounds and pools that have coalesced.

PROCESSES THROUGH TIME

The relict soils may be understood best as being the polygenetic products of shifting climates. Abundant rains associated with maximum glacial climates (e.g. 18,000 years before present) were probably most responsible for forming the illuvial clay layer and the acidic pH's after percolating through the litter beneath pine and conifer growths. Aridity and resultant sparse vegetation associated with maximum interglacial climates (e.g. 125,000 years before present) may have allowed the wind to erode unconnected depressions to the best of its ability.

Identifying climates which produced the relict soil is not as important for this investigation as is the recognition that the vernal pool topography has been developed by differential erosion within the illuviated clay layer (B_t horizon) of a paleosol formed under a wetter, maximum glacial climate of the past. Erosion has lowered the surface of the central areas of San Diego's terraces to within or very near the B_t paleosol horizon. During the current climate, intermediate between maximum glacier advances and retreats, vernal pool topographic development is slight. Litter from the dense chaparral covering the mounds makes a minor contribution to mound build-up, and the ground surface has a lichen-moss cover that retards erosion. Vernal pool bottoms have their unique flora which retards wind erosion. Expansion during the wet season and contraction during the dry season keep the topographic development progressing actively, but at a slow rate. However, during drier conditions of maximum interglacials, the vegetative cover was likely to have been sparser, akin to the coastal desert flora of modern Baja California. During those times, wind may have been more effective in moving thin, curled mud chips from dried pools to nearby gullies and also to entrapment beneath the shrubs atop the mounds. The spacing of the pools and mounds is largely attributable to the size of the desiccation polygons but may also be partly due to the wider spacing of xeric shrubs which occupied mounds under a maximum interglacial, coastal desert climate.

Addendum

SDSU Ecology Professor, George Cox, introduced me to a limited occurrence of mound topography in the lowlands of a little creek just east of the intersection of Carmel Mountain Road with Interstate 15. Circular to ovoid mounds nearly three feet tall and 50 feet in diameter have developed without the characteristic, isolated pools that typify the mound topography atop the coastal terraces. The mounds are formed on colluvium from the Friars Formation, a Late Eocene unit composed of greenish clayey sandstone and sandy mudstone deposited in a dry coastal basin. The Friars Formation contains an abundance of the expandable clays smectite and vermiculite (Abbott and Fink,

1975); it is well known in the San Diego area for its classic and costly, Swedish-circle slump and bedding-plane glide landslides. These mounds have a rich brown soil developed upon them but no subsurface exposures were available for study. Also, these mounds have a fairly good system of drainage between them. It appears that these mounds owe their existence to the following conditions: movement of abundant expansive clays within a creeping colluvial blanket that is being dissected by small, fairly well integrated drainageways.

REFERENCES

Abbott, P. L., 1981, Quaternary relict soils, San Diego County, in, Abbott, P. L., and O'Dunn, S. (eds.), Geologic Investigations of the San Diego Coastal Plain: San Diego Assoc. Geologists Guidebook, p. 11-20.

Abbott, P. L. and Fink, K. T., 1975, Clay mineralogy of the Friars Formation, Tierrasanta to Fletcher Hills, San Diego County, California, in, Ross, A. and Dowlen, R. J. (eds.), Studies on the Geology of Camp Pendleton and Western San Diego County, California: San Diego Assoc. Geologists Guidebook, p. 65-70.

Barnes, G. W., 1879, Hillocks or mound-formations of San Diego, California: American Naturalist, v. 13, p. 565-571.

Cox, G. W., 1980, San Diego's mound builders: Environment Southwest, number 490, p. 8-11.

Greenwood, N. and Abbott, P. L., 1980, Investigation of Series H Vernal Pools, Kearny Mesa: Report to Calif. Dept. Transportation.

Grim, R. E., 1962, Applied Clay Mineralogy: McGraw-Hill Co., 422 p.

Hertlein, L. G. and Grant, U. S., IV, 1944, The Geology and Paleontology of the Marine Pliocene of San Diego, California, Part 1, Geology: Memoirs of San Diego Soc. Natural History, v. II, 72 p.

Nadolski, A. F., 1969, An investigation of mima mounds in southwest San Diego County, California: Senior Report (unpub.), San Diego State University, 40 p.

Zedler, P. H., Ebert, T. A. and Balko, M. L., 1979, A survey of vernal pools of Kearny Mesa, San Diego County: Report to Calif. Dept. Transportation, 152 p.

REVIEW OF THE LITHOSTRATIGRAPHY, BIOSTRATIGRAPHY AND AGE OF THE SAN DIEGO FORMATION

by

Thomas A. Demeré

San Diego Natural History Museum

ABSTRACT

The San Diego Formation as exposed along the sea cliffs at Pacific Beach serves as an important reference section for the subdivision of this rock unit into two informal members: a "lower" member characterized by the molluscan fossils, *Patinopecten healeyi*, *Pecten stearnsii*, *Lucinoma annulata* and *Opalia varicostata*, and an "upper" member characterized by *Pecten bellus*, *Nucella lamellosa* and *Dendraster ashleyi*. This preliminary biostratigraphic zonation is useful for the correlation of other isolated marine sections of the San Diego Formation. In addition, this biostratigraphic zonation helps to substantiate a lithostratigraphic subdivision of the San Diego Formation into a primarily fine-grained, sandy "lower" member and a primarily coarse-grained sandy and conglomeratic "upper" member. Much of the "upper" member appears to be nonmarine.

Based on fossil mollusks, echinoids, planktonic foraminifers and calcareous nannoplankton, the San Diego Formation is correlated with the Upper Pliocene of provincial usage but the Upper Pliocene/Lower Pleistocene of DSDP usage.

INTRODUCTION

Although the San Diego Formation was the first formal rock unit to be named in the San Diego area (Dall, 1898; Arnold, 1903) it remains as one of the most poorly defined. The first published reference to these rocks was made by Dall in 1874 when he described an assemblage of molluscan fossils recovered from the "old San Diego well" in Balboa Park. The well penetrated approximately 160 feet of section which was described in the literature simply as "a fine sand, in some cases hardly consolidated at all and in others quite hard" (Dall, 1874, p. 296). Later, Orcutt (1889, p. 84-85) provided a more detailed description of the well section noting that "At the depth of about 90 feet a stratum of indurated sandstone was passed through, in which was found casts of various shells ... from 140 to 160 feet, came a rich variety of well-preserved shells imbedded in a usually rather soft matrix, composed of loosely aggregated grains of sand or fine sandy mud ...". These remain as the only lithologic descriptions of the "old well" section which Hertlein and Grant (1944, p. 49) later designated as the type locality of the San Diego Formation. This designation was based on what these authors perceived as nomenclatural priority (i.e., based on Dall's work) and presents a rather interesting stratigraphic problem. Dall (1898, p. 334) used the name "San Diego beds" to include the fossiliferous rocks penetrated by the well. He also assigned strata along the sea cliffs at Pacific Beach and along the southern flanks of Mount Soledad to these "San Diego beds," and correlated them to rocks at Dead Man's Island and Harbor Hill in the San Pedro area. Dall did not designate any of these localities as containing the type section for his "San Diego beds," and it almost appears as if his

concept of this unit was time-stratigraphic rather than rock-stratigraphic. Later, Arnold (1903, p. 58) used the name "San Diego Formation" for the first time noting that "the best exposure ... is found at Pacific Beach ...". Arnold gave full credit to Dall for naming this unit, although Dall never used the term "formation" in his prior discussions. Arnold (1906, p. 28) specifically referred to the strata exposed at Pacific Beach as the "type section" of the San Diego Formation and included a faunal listing of the contained invertebrate fossils.

In light of the above, I would disagree with Hertlein and Grant (1944, p. 49) when they concluded, from the same evidence, that the "... San Diego well must be considered the type locality of the San Diego Formation." Although Dall was the original worker involved with the formation, his interest was primarily with the fauna and not the rocks. Arnold, on the other hand, devoted more time to the lithostratigraphy and was the first worker to put Dall's and his own San Diego Formation fossils into a biostratigraphic context. As noted by Hertlein and Grant (1944, p. 49) the choice of the San Diego well as the type section is "... unfortunate, since the historic well has long since been filled in ...". The fact that the well was not singled out by Dall to be the type section; that Dall also included the Pacific Beach section in his "San Diego beds"; and that Arnold specifically chose Pacific Beach to be the type section seems to represent sufficient criteria for selecting Pacific Beach as the type section over the "old well" section. This selection is also more reasonable from a utilitarian viewpoint since the well section is no longer accessible while the Pacific Beach section, barring some maniacal, large-scale, gunite project, is and will continue to be a readily accessible reference section.

It is beyond the scope of this paper to formally resurrect and describe the Pacific Beach section as the type for the San Diego Formation. This should be left for publication in a more widely circulated journal. Rather, the observations here offer a progress report on recent work with the San Diego Formation in terms of its lithostratigraphy, biostratigraphy, and geologic age.

LITHOSTRATIGRAPHY

The early work with the San Diego Formation, as discussed above, concentrated on exposures at Pacific Beach and Balboa Park. However, this unit has a much wider area of outcrop extending from the south slopes of Mission Valley throughout the southwestern portion of coastal San Diego County and into Baja California as far south as Rosarito Beach (Minch, 1967). As would be expected, there is considerable lithologic variation in the unit over this area of outcrop. Some workers have attempted to describe this variability and several informal lithologic members have been proposed as a result.

Minch (1967, p. 1170) in mapping Neogene deposits in northwestern Baja California divided the San Diego Formation into a "lower member," up to 200 feet (60 m) in thickness, composed of bluish-gray to yellowish-brown, fine- to medium-grained sandstone with occasional discontinuous layers or lenses of locally indurated conglomerate; and an "upper member," up to 100 feet (30 m) in thickness, composed of interbedded yellowish-brown, medium- to coarse-grained sandstone and sandy cobble conglomerate.

Kennedy and Tan (1977) divided the San Diego Formation in the National City, Chula Vista, and San Ysidro areas into a "lower sandstone part"

composed of marine, yellowish-brown, poorly indurated but locally calcareously cemented fine- to medium-grained sandstone, and an "upper conglomeratic part" composed of pebble, cobble, and boulder conglomerate in a coarse-sandstone matrix. They noted that the conglomeratic part rests generally above and west of the sandstone part, and that in some areas the two interfinger.

Gunther (1964, p. 28-29) divided the San Diego Formation on the south slopes of Mount Soledad into a "lower siltstone member" composed of massive, tan to yellow, micaceous fine-grained sandstone and siltstone with occasional discontinuous beds of pebbly conglomerate and medium-grained sandstone; and an "upper coarse-clastic member" composed of sandy, pebbly conglomerate, massive, brown, coarse-grained sandstone and well-indurated, shelly sandstone (also in Wicander, 1970, p. 106).

In general, these workers recognized a "lower" fine-grained sandstone unit and a "upper" coarser-grained sandstone and conglomerate unit. The "upper" coarse units of Minch (1967) and Kennedy and Tan (1977) appear to be nonmarine, whereas the "upper" coarse unit of Gunther contains marine fossils.

Recent work by Artim (pers. comm.) as well as myself has recognized additional exposures of "upper" San Diego Formation coarse-grained sedimentary rocks in the Florida Canyon area of Balboa Park. They are best exposed at the mouth of Florida Canyon behind the city's maintenance yard. The section here consists of a basal 4.5 m. thick marine sequence of gray to brown, sparsely fossiliferous, massive, coarse-grained sandstones and cross-bedded, fine- to medium-grained sandstones. Some of the cross-bedded layers are well cemented and up to 20 cm. thick. Fossils include *Pecten bellus*, *Ostrea* sp., *Balanus* sp. and *Dendraster ashleyi*. Above this marine sequence begins a 9 m. thick nonmarine sequence of gray to red, massive- to well-bedded, well- to poorly-sorted, very fine- to coarse-grained sandstones. Some of the well-bedded layers are very micaceous and stand out as thin resistant ledges. A few fining-upward horizons with basal gravels stand out in marked contrast to other finely cross-bedded, fine-grained sandstone beds. Overlying this 9 m. sequence is at least one m. of alternating fine sandstone and pebble conglomerate.

The nonmarine, cross-bedded sandstone and pebble conglomerate unit of Florida Canyon is exposed throughout the structural graben bounded by the "Florida Canyon fault" on the west as recognized by Artim (pers. comm.), and the Texas Street fault on the east (Threet, 1977). Within this graben the nonmarine sedimentary rocks of the "upper" San Diego Formation grade imperceptibly upsection into the overlying Lindavista Formation (= Sweitzer Formation of Hertlein, 1929). West of the "Florida Canyon fault," however, the Lindavista Formation rests with marked unconformity on the light gray, fine-grained sandstones of the marine "lower" San Diego Formation. The apparent gradational relationship between the Lindavista Formation and the nonmarine "upper" San Diego Formation within the graben may represent the degradational (erosional) vacuity that elsewhere is represented by an unconformity.

Along the sea cliffs at Pacific Beach, from the west end of Diamond Street to just north of Tourmaline Surfing Park (Tourmaline Street) the San Diego Formation is well exposed in what I have earlier referred to as the "type section" of Arnold (1903; 1906). Both "lower" and "upper" San Diego Formation marine strata occur here. The base of the section is in a one m. thick, basal pebble conglomerate which rests disconformably on

sandstones and shales of the Middle Eocene Mount Soledad Formation (Kennedy and Moore, 1971). Both rock units strike approximately N40°E and display a dip of 10-11°SW. Above the basal conglomerate is a 4 m. thick sequence of gray to yellow, pebbly sandstone, silty sandstone, and conglomerate. The next 15 m. of section are gray to yellow, fossiliferous, very fine- to coarse-grained sandstones containing rare to abundant molluscan fossils and rare marine mammal remains. *Patinopecten healeyi* along with *Lucinoma annulata* and *Opalia varicostata* are the dominant faunal elements. Above this interval, for the next 32 m., is a section of gray to orange, locally cemented, fossiliferous, fine- to coarse-grained sandstones containing locally abundant *Patinopecten healeyi* and *Argopecten invalida*, along with rarer *Lucinoma annulata*, *Pecten stearnsii*, *Opalia varicostata* and *Glottidia albida*. The remaining 21 m. of section overlying these sandstones goes through a sequence of light brown, silty, very fine-grained sandstone; gray, well-cemented, poorly-sorted, fossiliferous sandstone and pebble conglomerate; and gray to brown, fossiliferous, fine- to medium-grained sandstone. Within this upper interval the pecten species of the lower part of the section give way to abundant *Pecten bellus*, which is also joined by *Nucella lamellosa*, *Dendraster ashleyi*, and *Balanus* sp. At Pacific Beach the 72 m. of exposed section is entirely marine and serves as an important reference section to which other isolated "upper" and "lower" marine sections of the San Diego Formation can be correlated.

In terms of overall stratigraphic thickness, the San Diego Formation has been reported by Hertlein and Grant (1944) to attain a total thickness of 1250 feet (375 m.) with the greatest thickness occurring in the Chula Vista and San Ysidro areas. My own fieldwork has been unable to account for more than 75 m. of marine section, with an additional 9 to 10 m. of nonmarine San Diego Formation. Minch (1967) documented only 60 m. of section in his "lower member" of the San Diego Formation with an additional 30 m. of sandstone and conglomerate in his "upper member." These overall thicknesses of 85 to 90 m. are considerably less than the 375 m. of Hertlein and Grant. The recently recognized Miocene Sweetwater and Rosarito Beach Formations (Minch, 1967; Artim and Pinckney, 1973; Scheidemann and Kuper, 1979) were probably included in the San Diego Formation of Hertlein and Grant.

Concerning the lower contact of the San Diego Formation, the base is almost everywhere marked by a basal conglomerate or several conglomeratic layers. However, in places the lower contact is beneath coarse-grained sandstone. Gastil and Higley (1977, p. 37) have suggested that the base of the San Diego Formation is marked in places by conglomerate-filled channels incised into the underlying formations. Good exposures of these basal channel-filling conglomerates can be seen along the east and west sides of the 6th Street extension (Threet, 1977, p. 47).

BIOSTRATIGRAPHY

In addition to lithostratigraphic divisions of the San Diego Formation, there have also been attempts in the past to formulate biostratigraphic divisions of this unit. Arnold (1903, p. 57-58) proposed two faunal horizons within the San Diego Formation based on exposures at Pacific Beach. He recognized a "lower horizon" characterized by *Patinopecten healeyi*, *Pecten stearnsii*, *Opalia anomala*, and *Opalia varicostata* (*P. healeyi* being quite common); and an "upper horizon" characterized by *Pecten bellus* (replacing *P. stearnsii*), *Crepidula princeps*, *Dendraster ashleyi*, and rare *P. healeyi*. Arnold extended this two-fold division to strata on the San Diego Mesa placing the "old well" section into his "lower horizon" and a section near the old Russ School (now San Diego High School) in his "upper horizon."

Woodring *et al.* (1940, p. 113) correlated the beds at San Diego with Pliocene rocks in the southern San Joaquin Valley and attempted to establish three faunal zones in the San Diego Formation. A lower zone from the area around the city of San Diego was characterized by a species of *Trophosycon*, a large form of "*Nassa*" *moraniana* (= *Nassarius grammatus*), and *Dosinia* (probably *Dosinia ponderosa diegoana*). They correlated this zone with the Lower Pliocene Jacalitos Formation. A middle zone was proposed which included the "old well" section and was characterized by *Siphonalia diegoensis*. This zone was tentatively correlated with the middle Pliocene Etchegoin Formation. An upper zone, which they felt was best exposed at Pacific Beach, contained *Dendraster diegoensis*, *Merriamaster pacificus*, *Anadara trilineata* var., *Argopecten* sp., *Lyropecten cerrosensis*, and *Ostrea verspertina*. This zone was correlated with the Upper Pliocene San Joaquin Formation.

Woodring and Bramlette (1951, p. 104-106) somewhat modified their earlier view and, although they still used a three-fold faunal division of the San Diego Formation, placed the majority of the section including the "old well" in their upper zone. The primary reason they retained the lower zones was the occurrence of *Trophosycon*. This genus has its last occurrence within the Lower Pliocene Jacalitos Formation in the San Joaquin Valley. Woodring and Bramlette suggested the possibility that *Trophosycon* may have lived longer at San Diego, possibly not becoming extinct there until the Late Pliocene. If this model was invoked then the San Diego Formation would fall entirely within the Upper Pliocene and be correlative with the San Joaquin Formation.

The crux of the problem discussed above revolves around the fact that no detailed biostratigraphic study has ever been done for the San Diego Formation.

Gunther (1964) examined benthonic foraminiferal assemblages from two measured sections along the southern slopes of Mount Soledad and recognized two distinct faunas that corresponded to his lithologic subdivision of the San Diego Formation. Basically, Gunther detected environmental differences with his "lower siltstone member" containing an outer shelf to shelf edge, cold water fauna, and his "upper coarse-clastic member" containing an inner neritic, cold water fauna.

Ingle (1970) examined both planktonic and benthonic foraminifers from the Pacific Beach section and recognized a warm water (20°C), outer shelf to shelf edge assemblage in the lower part of the section and a cold water (15°C), shallower assemblage in the upper part.

These foraminiferal data may offer some means of biostratigraphically dividing the San Diego Formation. As an example, Mandel (1973) examined planktonic foraminifers from this rock unit as exposed near the border. He recognized a decidely warm water (22-26°C), outer shelf assemblage. Mandel was not aware of the work of Ingle (1970), and had only considered the planktonic data of Wicander (1970) when he suggested that the border section was younger than that at Pacific Beach. However, it appears more likely that the border section is correlative with the warm water facies at Pacific Beach and that the coarse-clastic member of Gunther is younger than both.

Examination of the section at Pacific Beach essentially seconds Arnold's original biostratigraphic division of this section. The mollusks agree with the scenario based on the foraminifers, i.e., that the section reflects shoaling and cooling conditions in the upper part. This relationship is found in many other outcrops of the San Diego Formation and together with the faunal indices appears to represent a useful tool for recognizing a lower and upper portion of this rock unit.

Ingle, J. C., Jr., 1970, Paleoclimatic and paleoceanographic implications of Pliocene Foraminifera from Pacific Beach, California: Preprint November 6, 1970, SEPM Field Trip.

Kennedy, M. P. and G. W. Moore, 1971, Stratigraphic relations of Upper Cretaceous and Eocene formations, San Diego coastal area, California: Am. Assoc. Petrol. Geol. Bull., v. 55, p. 709-722.

Kennedy, M. P. and S. S. Tan, 1977, Geology of National City, Imperial Beach and Otay Mesa quadrangles, southern San Diego metropolitan area, California: Calif. Div. Mines and Geology Map Sheet 29.

Mandel, D. J., Jr., 1973, Latest Pliocene Foraminifera in the upper part of the San Diego Formation, California: in Ross, A., and R. J. Dowlen (eds.), Studies on the Geology and Geologic Hazards of the Greater San Diego area, California: San Diego Association of Geologists, p. 33-36.

Minch, J. A., 1967, Stratigraphy and structure of the Tijuana-Rosarito Beach area, northwestern Baja California, Mexico: Geol. Soc. Amer. Bull., v. 78, p. 1155-1178.

Orcutt, C. R., 1889, Some notes on Tertiary fossils of California, II. The San Diego well: West American Scientist v. 6, p. 84-87.

Scheidemann, R. C., Jr. and H. T. Kuper, 1979, Stratigraphy and lithofacies of the Sweetwater and Rosarito Beach Formation, southwestern San Diego County, California and northwestern Baja California, Mexico: in C. J. Stuart (ed.), Miocene Lithofacies and Depositional Environments, Coastal Southern California and Northwestern Baja California: Soc. Econ. Paleontologists and Mineralogists, Pacific Section, Guidebook, p. 107-118.

Threet, R. L., 1977, Texas Street fault, San Diego, California: in Farrand, G. T. (ed.), Geology of Southwestern San Diego County, California and Northwestern Baja California: San Diego Association of Geologists, p. 45-51.

Wicander, E. R., 1970, Planktonic foraminifera of the San Diego Formation: in Pacific Slope Geology of Northern Baja California and Adjacent Alta California: AAPG Field Trip Guidebook, p. 105-117.

Woodring, W. P., 1952, Pliocene-Pleistocene boundary in California Coast Ranges: Amer. Jour. Sci., v. 250, p. 401-410.

Woodring, W. P. and M. N. Bramlette, 1951, Geology and paleontology of the Santa Maria District, California: U.S. Geol. Survey Prof. Paper 222, 185 p.

Woodring, W. P., R. Stewart and R. W. Richards, 1940, Geology of the Kettleman Hills oil field, California: U.S. Geol. Survey Prof. Paper 195, 170 p.

FRACTURED QUARTZ GRAINS IN THE FRIARS FORMATION: A SCANNING ELECTRON MICROSCOPE STUDY

by

Dennis R. Kerr and Patrick L. Abbott
Department of Geological Sciences
San Diego State University
San Diego, CA 92182

INTRODUCTION

This study came about as the result of conversations on the origin of the conspicuously broken and fractured quartz grains which are common in the Friars Formation. Our initial hypotheses on the genesis of the fracturing included 1) the possibility that grains were fractured during grinding of thin sections, 2) that grains were initially fractured, or at least stressed, by the intense agents of chemical weathering that formed the lateritic paleosol during the Late Paleocene and Early Eocene, or that fracturing was a product of mechanical weathering due to 3) crystallization of salts within microfractures and their differential thermal expansion or the 4) volume expansion upon wetting of the clay minerals in the dry coastal lagoon environment of the Friars Formation. To test these hypotheses, representative samples were taken from the Friars Formation, the lateritic paleosol, and from beneath a modern salt-evaporating pan in southern San Diego Bay. Examination of whole grains beneath a binocular microscope showed they were fractured and thus ruled out a fracturing origin during thin-section grinding. Other samples were examined with a scanning electron microscope (SEM).

SAMPLE MATERIALS

Five samples were studied with the SEM; one from the Paleogene paleosol, one from the bottom of a salt pan, and three from the Friars Formation.

The paleosol sample before disaggregation was composed of about 1/3 quartz grains and 2/3 kaolinite. It was taken from the A horizon of the lateritic Rancho Delicias paleosol developed upon granodiorite (Abbott et al., 1976). A hot and humid paleoclimate dissolved and carried off in solution much of the granodiorite parent rock, converted feldspar to kaolinite, and left original quartz grains but in a corroded state.

The evaporitic pan sample was taken from the Western Salt Company pond 25. It consisted of three buckets of water, gypsum, mud, fetid organic matter, and the quartz grains which were separated for this study.

The nonmarine Friars Formation samples were collected from the west wall of El Cajon valley during grading several hundred feet south of the intersection of Petree St. and Fletcher Parkway (see original definition of Friars Fm. by Kennedy and Moore in 1971 for stratigraphic relations). The Friars is comprised of texturally and mineralogically immature mudstone, sandy mudstone, muddy very fine through coarse sandstone and contains calichified horizons. Sandstones are usually quartz impoverished (35 to 50%) lithic arkose or arkose with common biotite and lesser amphibole and pyroxene. Quartz occurs dominantly as mono- and poly-crystalline grains derived from the Peninsular Ranges batholith. Thin-section study revealed an unexpected fractured nature of the quartz grains including small chips

separated from larger grains that prompted this detailed study. Feldspar crystals, mostly from the batholith, and volcanic rock fragments, mostly from the Santiago Peak Volcanics, show advanced degrees of alteration to clay minerals. The most abundant clays are smectite and vermiculite but illite/sericite and kaolinite also occur which testifies to the variable chemical conditions which produced them.

METHODS

Samples were disaggregated by hand into their constituent parts and then washed through a 0.25 mm screen. The process was repeated until aggregates were eliminated. The salt pond sample required heating in a weak hydrochloric acid solution to just below the boiling point. With regular decantation and replacement of HCl the gypsum was dissolved thus freeing the detrital grains.

The next step was to separate quartz sand grains by passing each sample through a Franz magnetic separator. With several passes, at a low angle and slow feeding speed, a very good partitioning of feldspar and other minerals into the magnetic fraction and quartz into the nonmagnetic was achieved.

The final step before selection of individual quartz grains was to remove adhering clay particles. The quartz-sand separates were washed in hot nitric acid, rinsed in distilled water, then washed in a hot solution of stannous chloride, then rinsed in a calgon solution, and finally rinsed again in distilled water.

Individual quartz sand grains were selected under a binocular microscope. Monocrystalline grains were randomly selected; polycrystalline grains were rejected to avoid the morphologic complexities that occur along crystal boundaries. Approximately ten grains were chosen from each sample and mounted on a SEM stub with double-stick adhesive tape.

The adhered grains were placed in a vacuum evaporator and sputter coated with a 100 angstrom-thick layer of gold. The specimens were then ready for examination in a SEM.

Two scanning electron microscopes were used: an International Scientific Instruments MINI-SEM in the Physiology Lab at Saddleback College, and an International Scientific Instruments M-7 in the Botany Department at San Diego State University. Both SEM's are comparable models with virtually the same capabilities.

Each grain was examined at several magnifications on a rapid-scan CRT. When an interesting feature was observed it was photographed with an attached Polaroid camera.

SCANNING ELECTRON MICROSCOPY

During the past decade, scanning electron microscopy has been employed to interpret modes of transportation, environments of deposition, and diagenesis from surface micro-textures of quartz sand grains (e.g. Margolis, 1971; Krinsley and Doornkamp, 1973; Margolis and Krinsley, 1974). This technique has proved to be useful although no single feature, or the features observed on a single grain, are sufficient to make an environmental interpretation, i.e. a single feature may form under several different conditions. Therefore, a collective approach is necessary that considers

the mechanism that produces a particular micro-feature and then finds a common denominator for all features observed. Of course, all other geologic information must also be considered for a complete environmental interpretation.

SEM RESULTS

Micromorphologic features observed are summarized in Table 1. The micromorphologic features are grouped into five classes: crystal molds, cleavage, conchoidal fracture, blistering, and chemical features.

CRYSTAL MOLDS

The occurrence of crystal molds on detrital quartz grains is rare (Krinsley and Doornkamp, 1973). It is preserved only on a few quartz grains in two of the Friars Fm. samples (Figure 1). Molds in the Friars Fm. grains are typically straight, regularly-spaced (usually 2 microns wide) ridges and depressions with some extreme relief that suggests silica dissolution (Figure 1). In addition, a second set of impressions occurs which are not regularly spaced and are perpendicular to the principal mold features. This mold pattern is probably that of feldspar twinning, either polysynthetic albite, pericline, or Carlsbad.

Crystal molds are inherited from the primary source rocks such as the acid to intermediate plutonic rocks of the Peninsular Ranges batholith. Moreover, their presence suggests that at least some of the quartz detritus liberated from this source had not undergone extensive chemical weathering, or long distance, high-energy tractive transport.

CLEAVAGE

Quartz is typically described in elementary mineralogy textbooks as a mineral without cleavage. However, quartz does have a not commonly observed and generally poorly developed cleavage. Frondel (1962) described quartz cleavage as occurring in seven forms: $r(10\bar{1}1)$, $z(01\bar{1}1)$, $m(10\bar{1}0)$, $c(0001)$, $a(11\bar{2}0)$, $s(11\bar{2}1)$, and $x(51\bar{6}1)$. Of these seven forms, the two rhombohedral cleavages, r and z, are the highest in quality and most easily produced.

Quartz breakage patterns, thought to be of cleavage origin, are present in all samples except the Rancho Delicias paleosol. They consist of four micromorphologic types: (1) flat surface, (2) deep straight fracture, (3) flat plates, and (4) parallel steps (Table 1). A flat surface either comprises an entire grain face, or occupies a large area of a grain surface. It can also occur as a planar surface which can project through and extend out from the middle of a grain (Figure 2). Deep straight fracture extends along grain surfaces for several tens of microns and can be seen to extend over grain edges for a similar distance indicating deep penetration into the grain (Figure 3). Very thin (less than 1 micron), parallel plates constitute the flat plate micromorphologic feature (Figure 4). These plates typically parallel, or comprise a grain surface. Parallel steps are manifested as equally to subequally spaced risers and threads that are traceable for over 100 microns (Figure 5).

Cleaving of quartz grains can occur in a number of settings. Parallel steps are believed to form by crack propagation along cleavage planes during grain-to-grain impact (Margolis and Krinsley, 1974). Flat plates may

TABLE 1. ABUNDANCE OF MICROFEATURES

MICROMORPHOLOGIC FEATURE	FIGURE NUMBER	SAMPLES: San Diego Salt Pond	Rancho Delicias Lateritic Paleosol	Friars Formation FPA	Friars Formation FPB	Friars Formation FPE (Caliche)
Crystal Molds	1	--	--	--	R	R
Cleavage						
flat surface	2	R	--	C	C	C
deep straight fracture	3	C	--	R	R	C
flat plates	4	--	--	--	--	R
parallel steps	5	--	--	R	R	C
Conchoidal Fracture	6	R	R	C	A	C
Blistering	7	--	--	--	R	--
Chemical Features						
oriented pits	8,9a	C	A	--	R	R
corroded surface	9	C	A	C	R	A
irregular solution	10	C	--	C	A	C
precipitated silica	3,9b	C	--	C	R	A

A = abundant, C = common, R = rare, -- = not observed

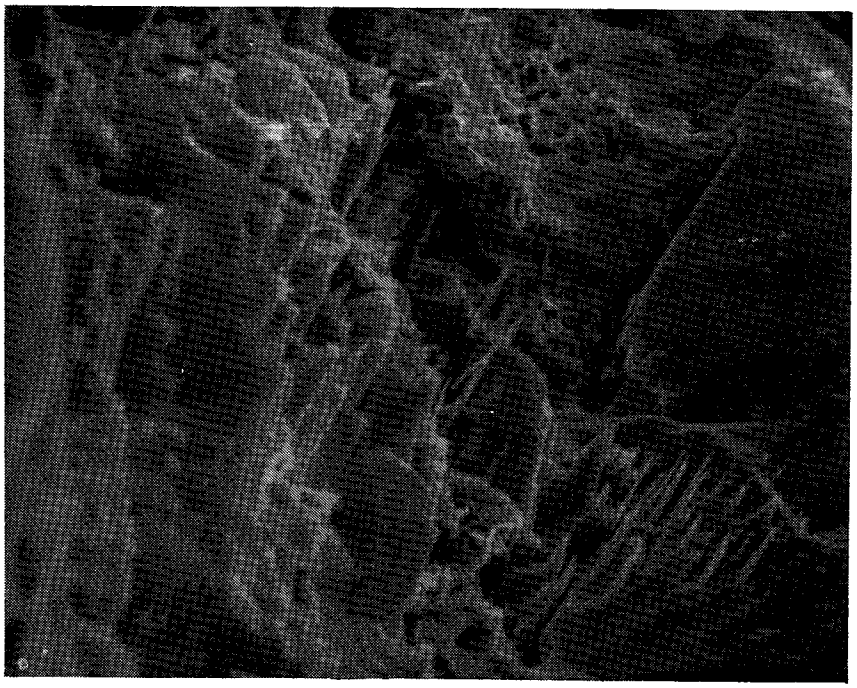

Figure 1. Scanning electron photomicrograph of crystal mold. This cross-hatched mold pattern may be of feldspar cleavage or polysynthetic twinning. Note enhancement by dissolution. Friars Fm. sample FPB. Magnification is 1,200x.

Figure 2. Scanning electron photomicrograph of flat cleavage surfaces. Note flat, relatively smooth upper surface and planar surfaces protruding from both sides of grain about half way down. Friars Fm. sample FPB. Magnification is 90x.

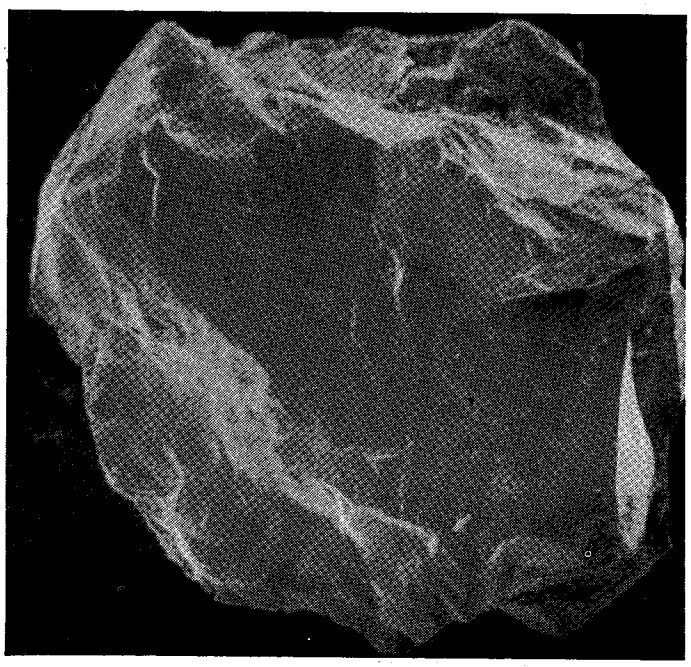

Figure 3. Scanning electron photomicrograph of deep straight fracture. Note depth and straightness of breakage pattern. Also present are small blocks of precipitated silica. Salt Pond sample. Magnification is 700x.

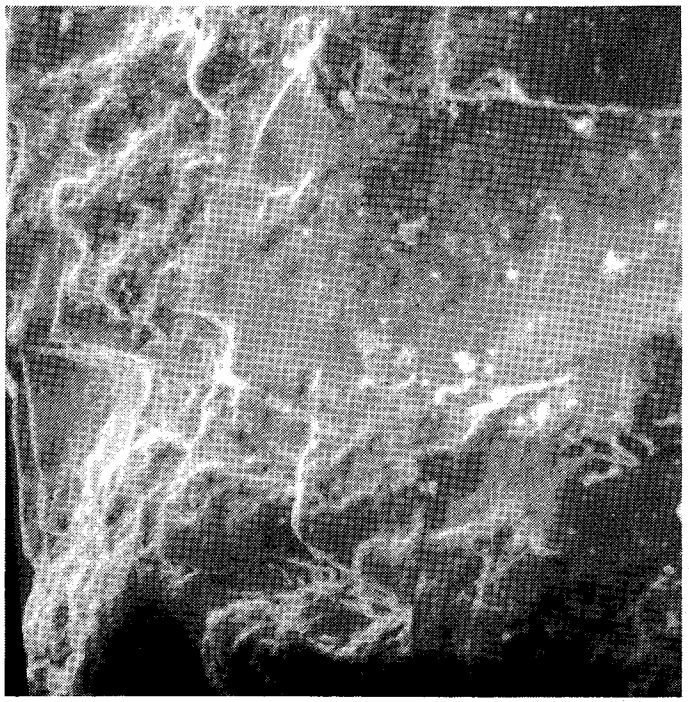

Figure 4. Scanning electron photomicrograph of flat cleavage plates. Friars Fm. sample FPE. Magnification is 2,000x.

Figure 5. Scanning electron photomicrograph of parallel steps. Friars Fm. sample FPB. Magnification is 1,000x.

have a similar origin, but in this case a cleavage plate also forms a grain face. Both could result from mechanical stresses imposed during transport. Deep fractures and flat surfaces may have been inherited from the source rock and/or created during transport as the grains preferentially broke along cleavage. Alternatively, cleavage may develop in evaporative depositional environments from growth of evaporite crystals in microfractures inherited from igneous cooling or metamorphic stress. Salt crystal cleaving is suggested by the mutual occurrence of flat surface and deep straight fracture micromorphologic surfaces in the San Diego salt pond and Friars Formation samples (Table 1).

CONCHOIDAL FRACTURE

Conchoidal fracture occurs in all samples although its size and abundance varies. The salt pond and Rancho Delicias paleosol samples rarely exhibit this feature, but where present, it generally does not exceed a few tens of microns in diameter (Figure 6c). By contrast, Friars Fm. samples have common to abundant conchoidal fracturing with large 100 to 200 micron size bowl-shaped features (Figure 6a,b).

Conchoidal breakage patterns in quartz are well known and have been observed on grains from many environments (Krinsley and Doornkamp, 1973; Margolis and Krinsley, 1974). Large, dish-shaped conchoidal fracture is produced by the application of uniform compressional stress, and is most typical of glacial, and high energy turbulent subaqueous and eolian environments. A high energy subaqueous or eolian environment seems more likely for San Diego grains. Figure 6b, however, shows a flake which is broken along a conchoidal fracture surface but is still delicately attached to the grain; certainly such a flake could not have survived high energy transport. Figure 6a shows a similar feature but not as advanced as in Figure 6b. Smaller-scale conchoidal fracture is more typical of primary source rocks and intense chemical weathering (Margolis, 1971).

BLISTERING

Blistering is a rare feature on the grains studied and was observed only in one Friars Fm. sample (Table 1). It appears as a lifting of a thin (0.05 micron) surface layer, perhaps a cleavage plate or precipitated silica coating, that is highest in the center and breaks off into three directions (Figure 7). Similar features have been attributed to salt-crystal growth just below the grain surface (Krinsley and Doornkamp, 1973).

CHEMICAL FEATURES

Four types of chemical features were found on the samples studied: oriented pits, corroded surface, irregular solution, and silica precipitation.

Oriented pits occur in all samples except one Friars Fm. sample (Table 1). However, the characteristics vary for each of the sample groups. Lateritic paleosol quartz grains have pits with sharp, well defined triangular shapes that range in size from 1 to 10 microns and are uniformly distributed on most grains (Figure 8a & 9a). By contrast, the pits that commonly occur on salt-pond grains are poorly defined, rounded triangular to rare rhombohedral shapes, and measure from 3 to 15 microns across (Figure 8b). The rare oriented pits on Friars Fm. grains are similar to those of the salt-pond grains except that these are smaller and shallower. The latter two

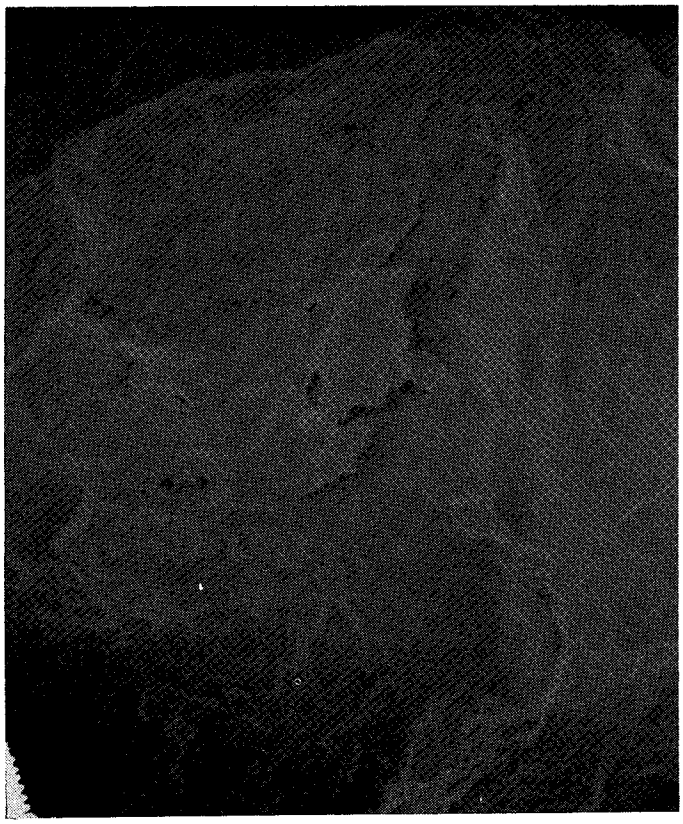

Figure 6. Scanning electron photomicrograph of conchoidal fracture. a) large bowl with interior blister. Friars Fm. sample FPB. Magnification is 200x. b) large bowl from Friars Fm. sample FPB. Magnification is 1,000x. c) small-scale from Salt Pond sample. Magnification is 700x.

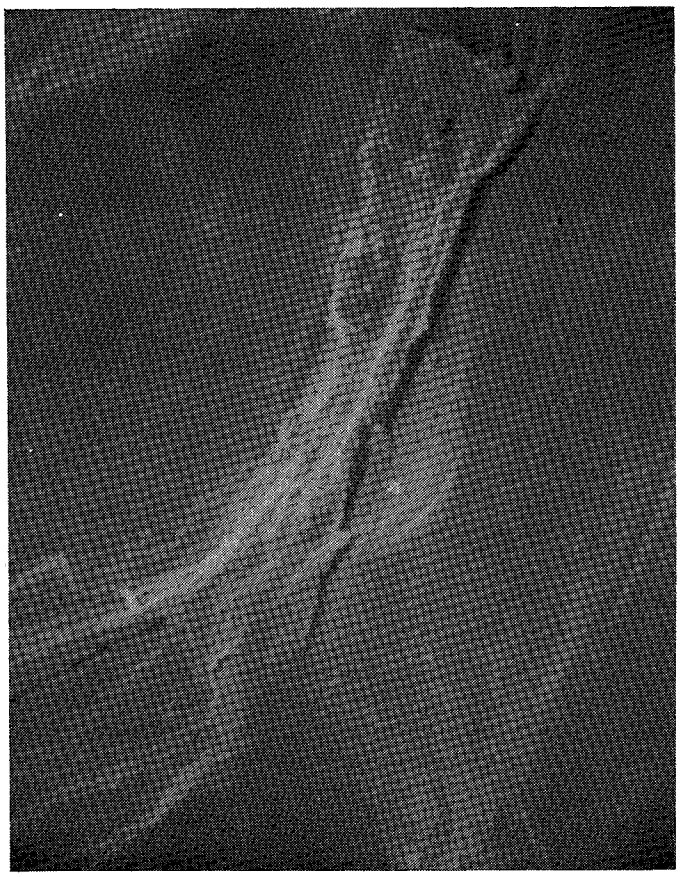

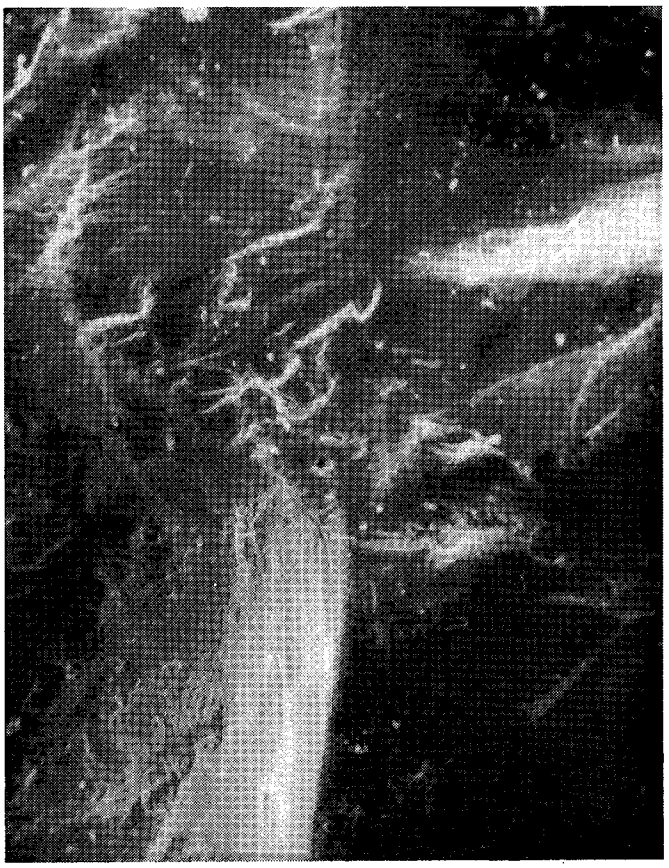

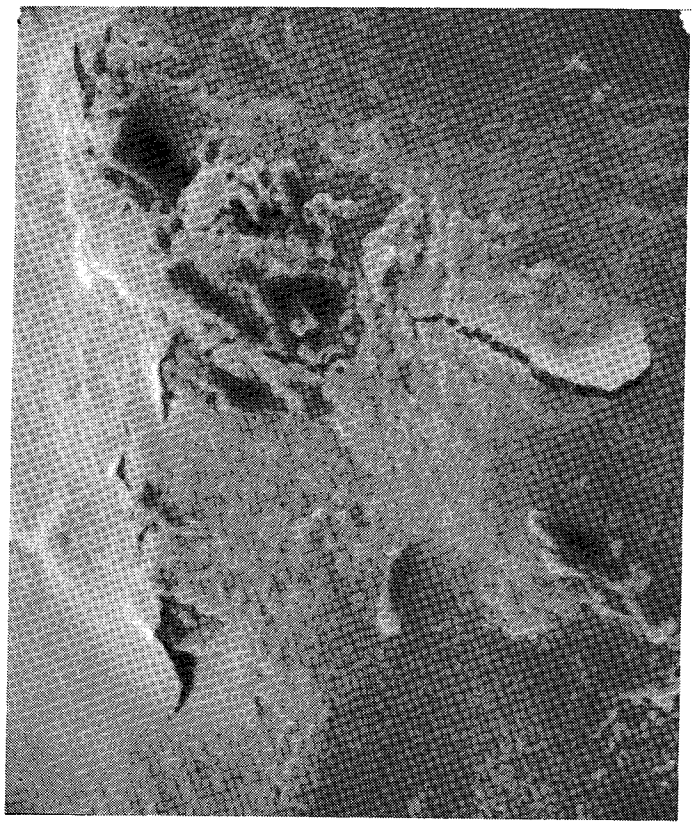

Figure 7. Scanning electron photomicrograph of blistering. Friars Fm. sample FPB. Magnification is 1,200x.

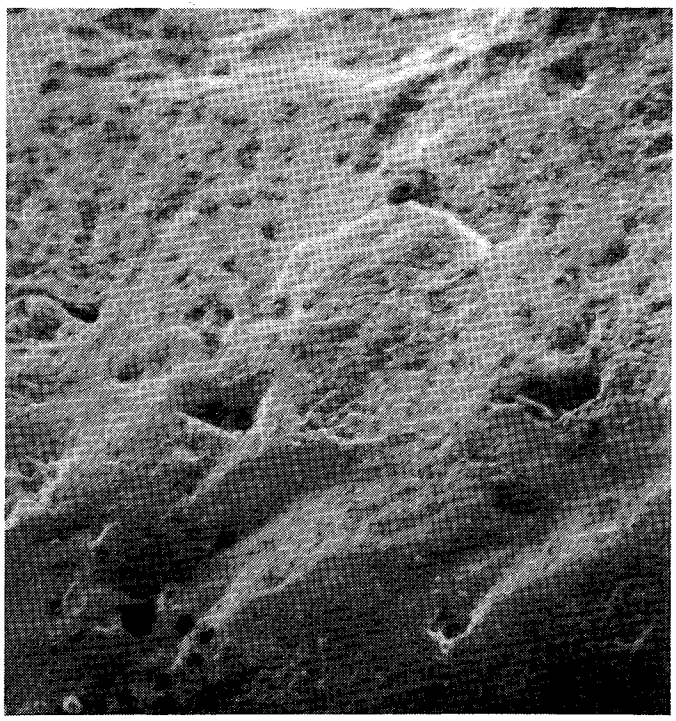

Figure 8. Scanning electron photomicrographs of oriented pits. a) from Rancho Delicias lateritic paleosol. Magnification is 1,000x. b) San Diego Salt pond. Magnification is 2,000x.

cases appear to be modifications by silica dissolution and reprecipitation in the pits found on the paleosol grains.

Corroded surface texture is common to abundant on all grains examined. It chiefly consists of very small (less than 1 micron), irregular pits that give a corroded appearance to the grain surface (Figure 9). On the paleosol grains, the corrosion indiscriminately affects the grain surface (Figure 9a). Whereas, on salt pond and Friars Fm. grains, this feature is most prevalent on thin, precipitated silica patinas (Figure 9b). Also included in this category is solution enlargement of cleavage planes, conchoidal fracture surfaces and crystal molds.

Irregular solution surface micromorphology is common to abundant on grains from San Diego salt pond and Friars Formation (Table 1). This feature resembles a series of anastomosing runnels, 1 to 5 microns deep (Figure 10). The areas standing in relief are 10 to 20 microns in diameter with most having an irregular outline, and few having a crudely triangular shape. Many of these areas are undermined by shallow fractures, which gives rise to a spalled appearance.

Precipitated silica features are common on salt pond grains and rare to abundant on Friars Fm. grains (Table 1). They occur in two modes. First, it occurs as small blocks or platelets adhering to grain surfaces, or as infilling of fractures and solution cavities (Figure 3). Only rarely do these blocks have triagonal or pseudohexagonal outlines. The second mode is 1/10 micron thick coating or patina which is typically corroded and in some areas partially detached from the grain surface (Figure 9b). This patina also locally covers or coats other observed microtextures.

All of the chemical microtextures described above are common to quartz grains of both tropical (Fitzpatrick and Summerson, 1971; Doornkamp and Krinsley, 1971) and arid (Margolis, 1971) regoliths, and usually occur together on individual grains. In general, quartz grains from tropical soils tend to show a higher degree of dissolution and disintegration. These features are also common to diagenetic environments. These textures are also known from eolian and subaqueous environments (Krinsley and Doornkamp, 1973).

Moreover, the chemical environment indicated by these features is directly related to the pH and silica saturation of interstitial waters in contact with the quartz grains. Krauskopf (1959) showed that silica is extremely soluble at a pH of 9.9 and higher, and is only slightly soluble in acid solutions. It is conceivable that given time, substantial dissolution of silica may occur under acidic conditions. In an open geochemical system where silica is removed (i.e. intense leaching), the interstitial fluids are undersaturated in silica, and with high enough pH's dissolution would progress. Conversely, if the system is closed or the silica saturation of the fluids fluctuates with time, silica dissolution might alternate with silica precipitation. Experimental work on naturally abraded quartz grains by Margolis (1968) showed that irregular solution patterns and corroded surfaces result from rapid dissolution in a very strong acid or strong base, and that oriented pits develop from slow dissolution in a weaker acid or base. Although the acidity of most natural waters lies between 4 to 9, pH's as low as 3.5 and as high as 10 have been recorded for humid soil waters, and arid soil waters and playa lakes, respectively (Krauskopf, 1967). In addition, high pH values would be expected in environments where sea water is evaporating.

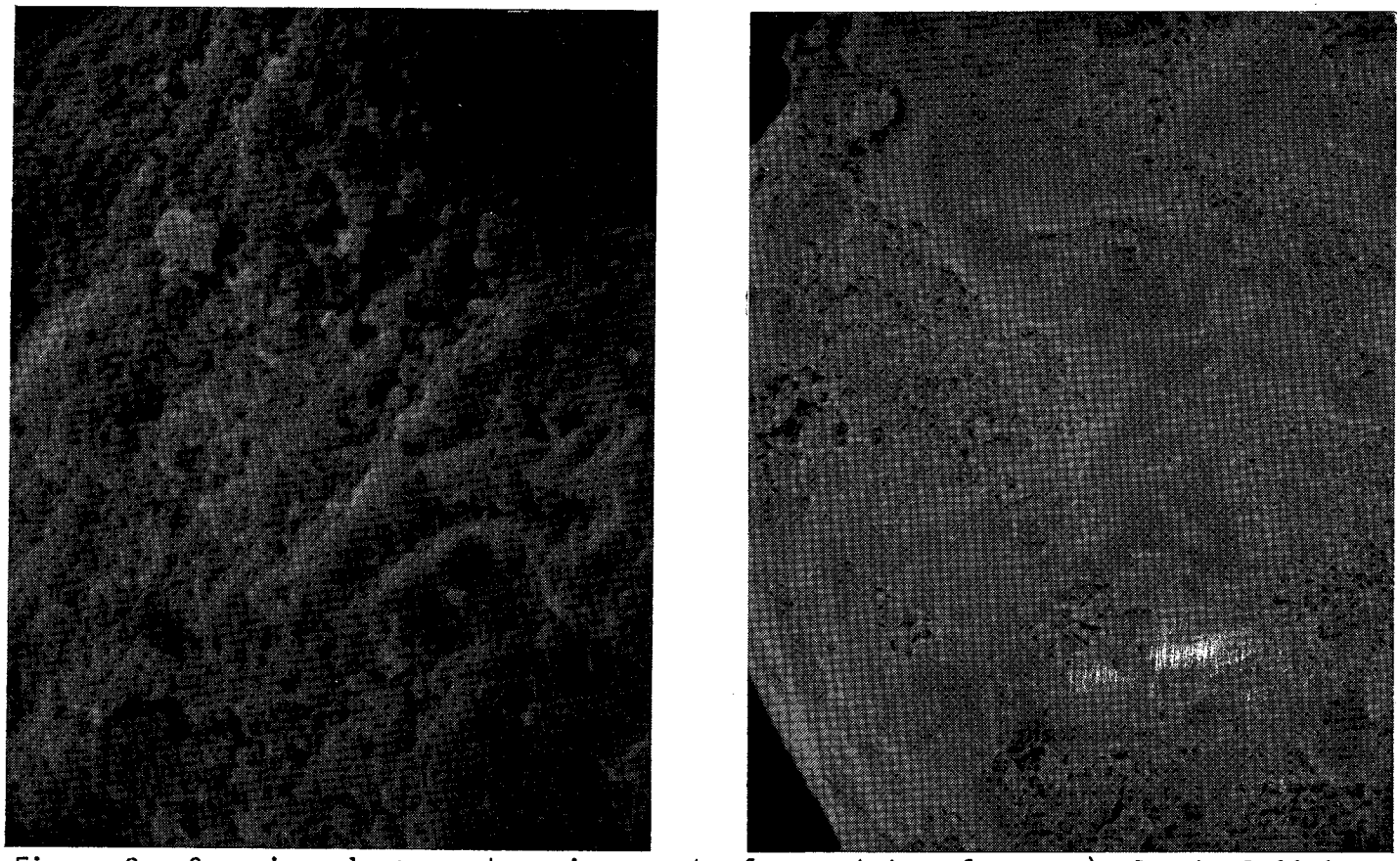

Figure 9. Scanning electron photomicrograph of corroded surface. a) Rancho Delicias paleosol - note oriented pits. Magnification is 5,000x. b) Friars Formation sample FPE - note preferential corrosion of silica patina. Magnification is 200x.

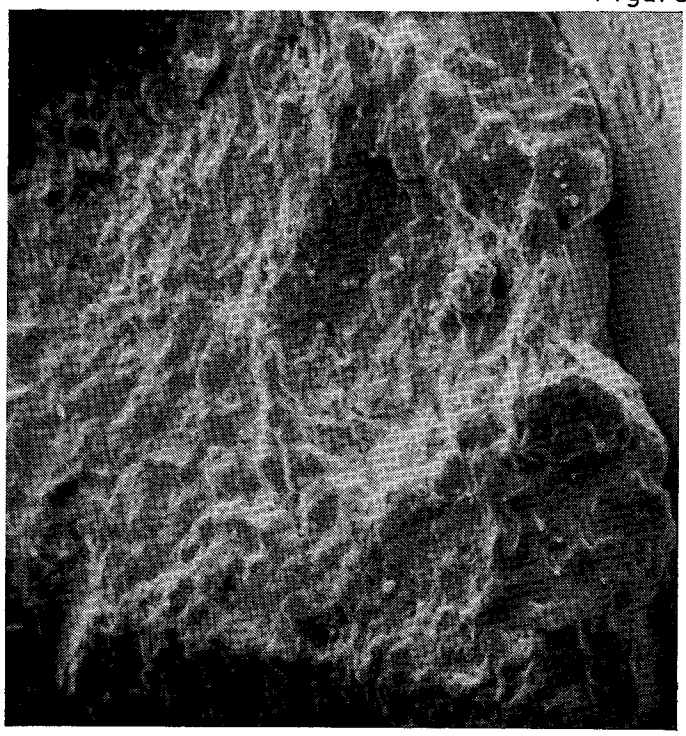

Figure 10. Scanning electron photomicrograph of irregular solution. Salt pond sample. Magnification is 400x.

DISCUSSION

It is clear that the Rancho Delicias lateritic paleosol is not a plausible analog for the fractured quartz grains in the Friars Fm. The oriented pits and corroded surfaces found on these quartz grains indicate an environment of silica leaching most likely under acid conditions of humid, tropical soil development as was suggested by Abbott et al. (1976).

The abundant expansive clay minerals were found wedged into fractures and cavities and required involved cleansing procedures to rid the quartz grains of them before SEM study began. The volume expansion of the immature clay minerals upon wetting creates another expansive force which may have contributed to the wedging and splitting apart of quartz grains.

On the other hand, the salt-evaporating pond in San Diego appears to be the best analog. Quartz grains from the salt pond, like those in the Friars Fm., are dominated by chemically produced, micromorphologic surface features which indicate fluctuating high pH's and intermittent saturation of interstitial waters with respect to silica. However, some differences are notable. Oriented pits are common on salt-pond grains and rare on Friars grains. Perhaps these salt-pond grains were derived from erosion of the once thick and widespread lateritic paleosol which would make the pits a relict feature. This interpretation is further supported by the modified appearance of these pits. Furthermore, this common versus rare occurrence might be simply a function of time of exposure, i.e. the salt ponds have been in operation for only about 75 years and, not surprisingly, the oriented pits on salt pond grains are less modified than those on Friars Fm. grains. In addition, the less common occurrence of mechanical breakage, cleavage and conchoidal fracture in the salt pond sample suggests that these grains had a lower energy transportational history than did the Friars Fm. grains. Despite these differences, the dominance of similar chemical features present in both suggests a similar environmental history within an evaporative basin.

In the Friars Fm., the micromorphologic feature that is directly attributed to salt crystal growth is blistering. Although cleavage and to a certain extent, conchoidal fracture are not in themselves environmentally definitive, the wedging, detachment and general enhancement of these features suggests that post-depositional mechanical modifications may have occurred. This is also implied by parallel fracture patterns seen in thin section. The wedging of, and subsequent infilling by, precipitated silica indicates that some breakage was closely associated in time with highly alkaline waters. The above points taken together certainly hint at the importance of the salt-weathering processes of crystal growth and differential thermal expansion within the dry coastal basin environment of the Friars Fm.

The effect of salt weathering on feldspars might be even more profound. Because they are cleaved more easily than quartz, feldspar sand grains should break into smaller pieces which in turn provides greater surface areas for alteration to clay minerals. This could account for the extreme alteration of feldspars seen in thin sections of the Friars Fm.

SEM results and petrologic textures suggest mechanical weathering processes may have played an important role in altering sediment deposited in the Middle to Late Eocene Friars "dry lagoon". Alternating flooding and desiccation resulted in the dissolution and reprecipitation of silica, the expansion and contraction of clay minerals, and the crystallization of

salts which, after penetrating cleavage planes, fracture surfaces and other cavities, exerted expansive forces which mechanically broke down sand grains.

REFERENCES

Abbott, P. L., Minch, J. A., and Peterson, G. L., 1976, Pre-Eocene paleosol south of Tijuana, Baja California, Mexico: Jour. Sed. Pet., v. 46, p. 355-361.

Doornkamp, J. C., and Krinsley, D. H., 1971, Electron microscopy applied to quartz grains from a tropical environment: Sedimentology, v. 17, p. 89-101.

Fitzpatrick, K. T., and Summerson, C. H., 1971, Some observations on electron micrographs of quartz sand grains: Ohio Jour. Sci., v. 71, p. 106-119.

Frondel, C., 1962, Silica minerals, Dana's system of mineralogy; v. 3, 7th edition: John Wiley and Sons Ltd., New York, 334 p.

Krauskopf, K. B., 1959, The geochemistry of silica in sedimentary environments: Soc. Econ. Paleontologist Mineralogist, Spec. Publ. 7.

Krauskopf, K. B., 1967, Introduction to geochemistry: McGraw-Hill, New York, 721 p.

Krinsley, D. H., and Doornkamp, J. C., 1973, Atlas of quartz sand surface textures: Cambridge University Press, 91 p.

Margolis, S. V., 1968, Electron microscopy of chemical solution and mechanical abrasion features on quartz grains: Sedimentary Geol., v. 2, p. 243-256.

Margolis, S. V., 1971, Surface microfeatures on quartz sand grains as paleoenvironmental indicators (Ph.D. dissertation): Univ. California, Riverside, 169 p.

Margolis, S. V., and Krinsley, D. H., 1974, Processes of formation and environmental occurrence of microtextures on detrital quartz grains: Am. Jour. Sci., v. 274, p. 449-464.

QUASI-SEDIMENTARY STRUCTURES IN THE GABBROIC COMPLEXES OF THE PENINSULAR RANGES BATHOLITH, SOUTHERN CALIFORNIA

by

Michael J. Walawender and Patrick L. Abbott
Department of Geological Sciences
San Diego State University
San Diego, CA 92182

ABSTRACT

The presence of layered rocks and quasi-sedimentary structures in gabbroic complexes around the world has led to considerable speculation on the role of crystal settling versus in-situ crystallization in the formation of such features. In the basic plutons of the Peninsular Ranges batholith, the earliest layers consist of alternating plagioclase- and olivine-rich horizons. They are steeply dipping and contain structures similar to those found in moderate-energy sedimentary regimes. These structures combined with mineral parageneses and estimates of the limiting properties of the parental melt indicate that the olivine-plagioclase layering is a result of the settling of both phases in the earliest stages of crystallization. Crudely planar layers of oikocrystic amphibole in more fractionated anorthositic bodies, however, lack any quasi-sedimentary structures despite their near-vertical inclination. These appear to develop in-situ parallel to the chamber walls as rates of plagioclase nucleation and growth vary.

INTRODUCTION

Basic and ultrabasic rocks around the world contain textures and structures that, on the surface, appear to have counterparts in the sedimentary regime. These include mineral layers, graded beds, cross bedding, and convolute bedding. Such comparisons have led some igneous petrologists to conclude that there are processes common to both environments. The single process most often called upon to explain these similarities is gravity-controlled sedimentation of individual grains or grain aggregates. In contrast to sedimentary environments, however, the fluid medium in magmatic systems has a density range that can overlap that of the crystallizing phases, and a viscosity that can impede or even eliminate any gravity-controlled movement of those phases. Thus, there has been and still is considerable discussion as to the effectiveness of crystal sedimentation in forming the quasi-sedimentary features found in many basic and ultrabasic bodies.

Wager and coworkers emphasized crystal settling as a means of producing the layered rocks and quasi-sedimentary structures in the Skaergaard complex of Greenland although allowing (Wager and Deer, 1939; Wager and Brown, 1968) that such a process could not explain all of the features in the complex. Jackson (1961) proposed that in-situ crystallization, as governed by physico-chemical rather than mechanical processes, was the dominant process in producing the layered rocks of the Stillwater complex of Montana. McBirney and Noyes (1979) considered in detail the theoretical properties of a Skaergaard-type magma and concluded that the layering was best explained by "a mechanism of oscillatory nucleation and diffusion-controlled crystallization next to the cooling surface." They also questioned the efficacy of bottom

sedimentation, confining it, to either "very hot ultramafic bodies or moving basaltic magmas in the earliest stages of crystallization."

The purpose of this article is to describe several structural and textural features in the basic plutons of the Peninsular Ranges batholith in terms of their similarities to sedimentary structures, and to argue that whereas in-situ crystallization is probably responsible for the layering in the intermediate and later stages of the development of these plutons, bottom sedimentation of olivine and plagioclase is a real factor in producing the layering and the compositional extremes of the earliest stage rocks.

GEOLOGIC SETTING

The basic plutons within the Peninsular Ranges batholith have been described elsewhere (Walawender and Smith, 1980) so only a brief summary will be presented here. The basic plutons are restricted to the western margin of the batholith and represent the earliest plutonic units. Their host rocks consist of the Late Jurassic volcanic-volcaniclastic Santiago Peak Formation and the metasedimentary quartzites and quartz-biotite schists known collectively as the Julian Schist Formation. The metavolcanic units are predominantly andesitic to dacitic in composition, and are concentrated on the extreme western margin of the batholith. The age of the Julian Schist is not well established but it may be as old as Triassic and appears to have formed in a stable-shelf environment.

The gabbros are everywhere older than the granitic plutons in their immediate area. The granitic plutons have generally intruded along the contacts between the gabbro and its host rocks. In the process, the peripheral areas of many gabbroic plutons have been wedged away from the parent body and exist as isolated blocks within the granitic plutons. Internally, the gabbros are multiple intrusive complexes such that early-formed rocks were disrupted by and may be inclusions in later pulses. Most of the magma chambers appear to have been small, narrow, and steep walled. In the Los Piños pluton (Walawender, 1976), for example, the anorthositic and peridotitic bodies formed in near-vertical fractures radiating from a central zone. Unlike their counterparts at divergent plate margine (e.g., Skaergaard and Duluth complexes), the gabbroic rocks in the Peninsular Ranges batholith contain abundant primary amphibole, suggesting that their parental melt was higher in dissolved volatile content and thus of lower viscosity.

Although the individual gabbroic plutons have their own emplacement histories (Walawender, 1976; Lillis et al, 1979), their crystallization histories combine to form a single composite sequence (Walawender and Smith, 1980). This, along with their consistent geochemical character, indicates that they were derived from a series of remarkably identical parental melts. The crystallization sequence began with the precipitation of plagioclase as calcic as An_{96} and of minor magnesian spinel. Plagioclase remained on the liquidus throughout the crystallization sequence but was joined at an early stage by magnesian olivine (Fo_{80}) and, at a more intermediate stage, by diopsidic clinopyroxene. Both ferromagnesian minerals had reaction relationships with the melt and in the intermediate and later stages of crystallization gave way to orthopyroxene and amphibole. Orthopyroxene is at or near the liquidus only in the intermediate stages of the crystallization sequence whereas amphibole, as subhedral grains, is limited to the very end stages of crystallization.

The layered rocks are best developed in the early stages of crystallization and consist of alternating plagioclase-rich and olivine-rich zones with small amounts of interstitial or oikocrystic amphibole. Boundaries between these zones are generally sharp. In the larger masses of anorthositic rocks, sparse layering may be present as crudely planar horizons rich in oikocrystic amphibole. Invariably, these layers are steeply dipping to vertical and are commonly subparallel to contacts with older rocks.

In the intermediate stages of crystallization, scarce, poorly defined mineralogical layering consists of narrow (1 cm) zones with variable plagioclase-pyroxene ratios in which the mineral phases are aligned subparallel to the layering. In the end stages of crystallization, comb layers (Moore and Lockwood, 1973) consisting of plagioclase and prismatic amphibole are not uncommon. The amphibole crystals are aligned subparallel and are perpendicular to a basal discontinuity which separates the individual layers. These layers range in thickness from a few centimeters to about one meter and are steeply dipping to vertical. They occur in sequences up to 200 m thick and are parallel to contacts between comagmatic units.

STRUCTURES

Several features found in the basic plutons of southern California are reminiscent of upper-lower flow-regime structures (Figures 1 and 2) and slump structures (Figure 3) found in clastic rocks. Counterparts to these structures are not uncommon in stratiform gabbroic complexes such as Skaergaard and Duluth. However, despite this similarity, the existence of such structures in a magmatic environment does not necessarily mean that the associated mineral layers formed strictly by crystal settling. Instead, additional evidence must be developed to argue for a sedimentological origin for these mineral layers as opposed to formation by an in-situ diffusion mechanism. The following outcrop features (Figures 4-9) are interpreted to support an origin via bottom sedimentation for the layered olivine-plagioclase rocks in the basic plutons of southern California.

Figures 4-6 illustrate that cognate inclusions with densities intermediate between plagioclase and olivine are capable of settling through the gabbroic magma with sufficient momentum to deform the mineral layers at the base of the magma chamber. This phenomenon has been observed in other basic intrusions (Thompson and Patrick, 1968; McBirney and Noyes, 1979) for inclusions up to several hundred meters in maximum dimension. The shape of the inclusion, however, appears to play a significant role in determining the impact velocity and, hence, the amount of deformation. Figure 4 shows a highly eccentric, elliptical inclusion (in outcrop view) whose long axis is parallel to the mineral layering. We interpret this to indicate that the drag on the inclusion was sufficient to impede its downward velocity so that a soft landing was achieved. In Figure 5, the shape of the lower inclusion is more streamlined, thus allowing sufficient impact velocity to slightly deform the underlying soft sediments. Figure 6 illustrates a more extreme situation wherein the orientation and shape of the projectile allowed for near maximum settling velocity and resulted in a high degree of penetration into the underlying crystal-rich mush.

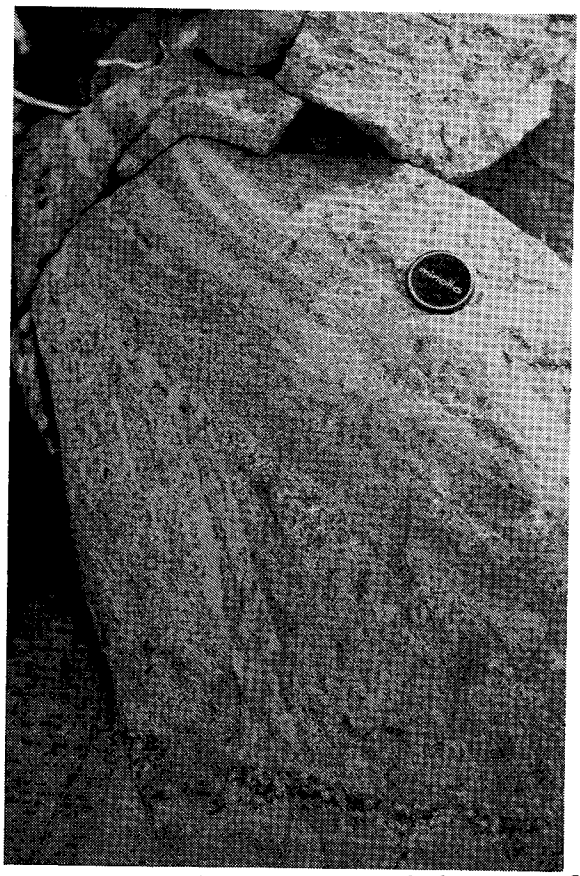

Figure 1. Structure reminiscent of an upper-lower flow-regime trough filled by foreset beds then capped by mineral layers that suffered some post-depositional, downslope sliding to produce minor drag folds. Alternately, all the structures in the photograph may have been produced by multiple episodes of scour, in-situ growth of layers parallel to the trough walls, and post-depositional sliding.

Figure 3. Note chevron folds with axes at low angles to the layering. Equivalent structures in San Diego County have formed by downslope sliding on Cretaceous submarine fans and on the flanks of a Miocene cinder cone. These structures suggest deposition of the crystal population on a steep slope followed by differential slip while still in a plastic state.

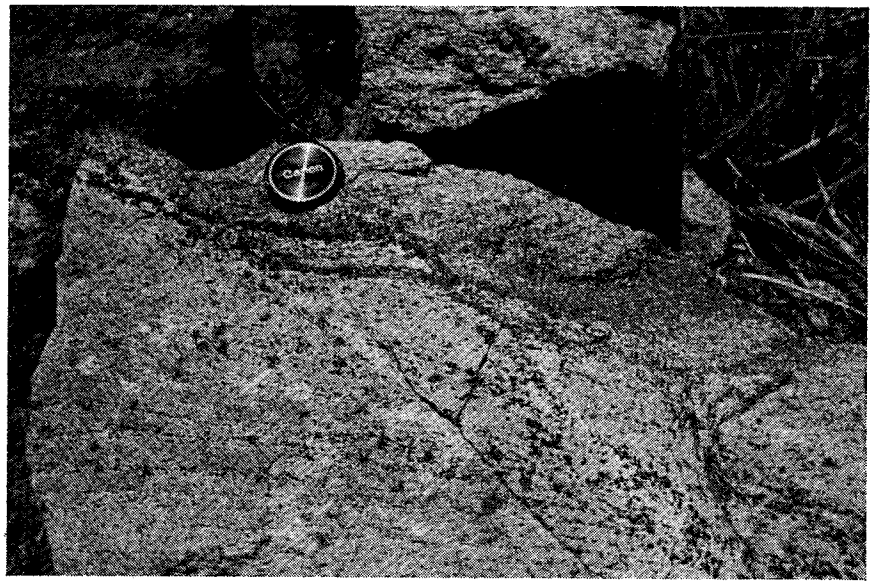

Figure 2. Nested complex of erosion channels. Note basal trough below lens cap, another to lower right of lens cap, and a larger, steeper-walled trough in the lower right-hand corner of the photograph. Note the truncation of mineral layers at the left margin of the lower-most channel. Occurrence of stacked troughs indicates repeated scour events by dense magmatic currents moving downslope with energy levels equivalent to the upper-lower flow regime in fluvial systems.

Figure 4. Rounded, highly elongate, boulder of gabbro with its long axis parallel to mineral layering which is inclined approximately 35° into the outcrop. The left side of the inclusion has been overridden by three layers, suggesting that there has been some down-dip movement of the inclusion and that some proportion of the present inclination is original dip.

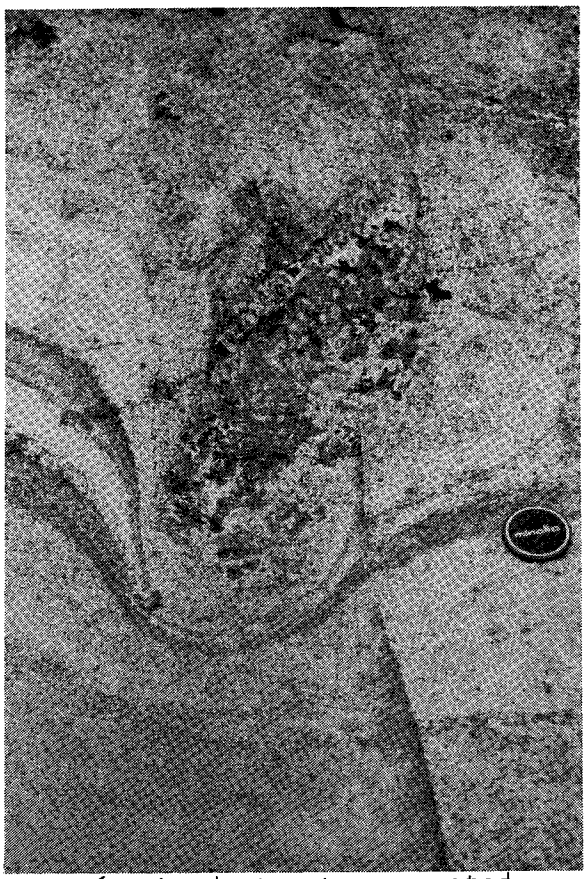

Figure 6. Load structure created by the nose-first impact of an elongate boulder. Downbowed layers were deformed to near vertical inclinations and suffered severe attenuation beneath the sinking boulder. As in Figure 5, a massive clinopyroxene-bearing troctolite overlies the inclusion.

Figure 5. Rounded elongate gabbroic cobble that settled into the crystal mush with downward displacement of the still soft layers to form load structures that are convex downward. Note the mild attenuation of the underlying layers. The upper, later deposited angular cobble is in a more massive clinopyroxene-bearing troctolitic horizon. Its angularity suggests fairly rapid settling whereas the lower, rounded cobble presumably stayed in suspension longer.

Figure 7 shows a series of small orbicules consisting of single crystals or sparse aggregates of olivine surrounded by uniformly thick plagioclase rims. These orbicules are touching but not penetrating one another and have an interorbicule cement of primary amphibole. This rock unit formed in a narrow, steep-walled chamber and has an overall graded character within its approximately 50 meters of vertical exposure. The orbicules are generally one centimeter or less in maximum dimension in the uppermost exposures but increase in size downwards to about three centimeters. Small inclusions of gabbroic rock found scattered throughout the exposed section are not only rimmed with calcic plagioclase but are also size graded. We interpret these orbicules to represent an olivine-rich zone that had accumulated from an initial magmatic pulse. This mush was then intruded by a new and relatively unfractionated batch of melt (± cognate inclusions) so as to scatter the olivine crystals throughout. Since plagioclase is, at all stages, the liquidus phase, the olivine crystals and crystal aggregates acted as nucleation centers. Plagioclase rims began to form on the olivine before the new melt could significantly resorb this now unstable phase. Settling then followed to produce the size-graded section with interstitial melt crystallization to accumulate plagioclase and/or poikilitic amphibole.

The settling of smaller crystals of olivine in the melt can be inferred from Figures 8 and 9. Figure 8 shows a series of layers each consisting of a narrow plagioclase-rich zone overlain by troctolitic zones approximately 15 cm in thickness. A closer view (Figure 9) of one of these layers reveals size-graded olivines ranging from less than 0.5 mm in the top of each layer to nearly 2.1 mm at the base. The plagioclase may exhibit a similar pattern but with larger crystal dimensions. The base of the layers may also have an increased olivine to plagioclase ratio which, along with the size variations, is consistent with an origin by crystal settling.

FORMATION OF THE LAYERING

The role of crystal settling in producing the layering and compositional extremes of gabbroic rocks is not fully agreed upon. Variations in chemical and thermal gradients could produce some of the compositional layering observed in many basic intrusions but it is difficult to visualize how that mechanism can form compositional extremes such as anorthosite and peridotite in significant amounts. We propose, instead, a qualitative model that involves both mechanisms with crystal settling dominant in the early stages, and diffusion mechanisms in control thereafter. Flow differentiation may also play a role but it is thought to be of limited extent and will not be considered further.

McBirney and Noyes (1979) calculated the densities of the major silicate minerals and of the gabbroic liquid for the Skaergaard complex as a function of the degree of crystallization of that liquid. Considering only density differential as a control on the possibility of crystal settling, the mafic minerals are clearly capable of sinking with density differences in excess of 0.5 gm/cc throughout the crystallization history of the melt. Plagioclase, however, is shown approximating the density of the melt only at the onset of crystallization and having lower densities thereafter -- a situation which could lead to crystal flotation rather than sinking. In the basic intrusions of this study, the plagioclase compositions are more calcic and thus of slightly higher density. In addition, we would anticipate that the density

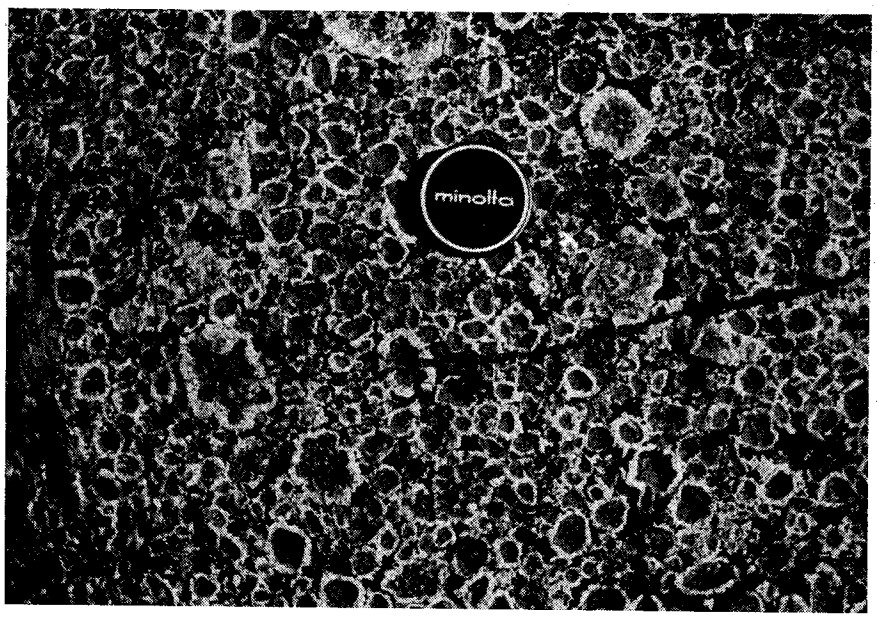

Figure 7. Orbicular gabbro consisting of single olivine crystals or crystal aggregates surrounded by plagioclase. Black interstitial material is amphibole.

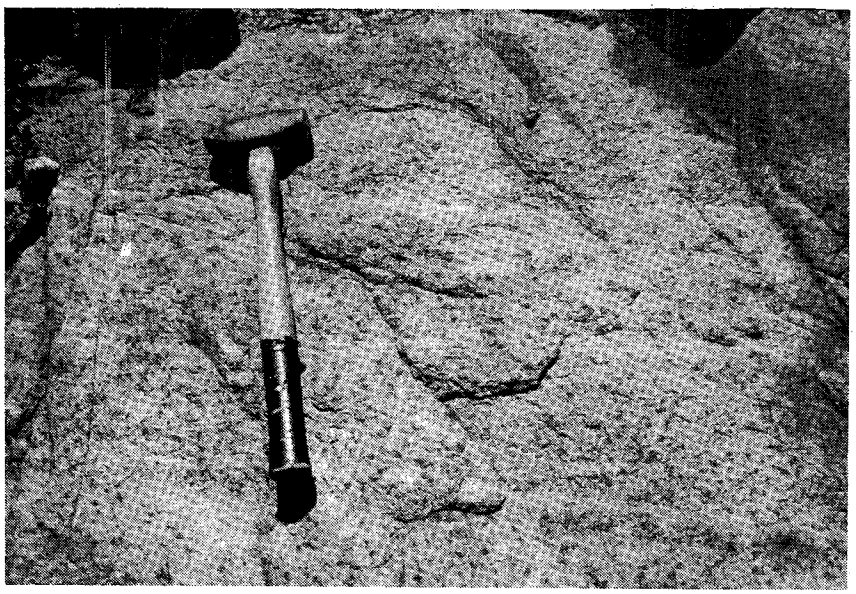

Figure 8. Thicker size-graded mineral layers consisting of troctolitic zones sandwiched between narrow anorthositic horizons. White grains are plagioclase, smaller grayish grains are olivine, and the larger, darker spots are oikocrystic amphibole. Figure 9 shows a closeup of one size-graded layer approximately one foot to the right of the hammer handle.

Figure 9. Close up of mineral layer. The larger dark patches are amphibole oikocrysts and the smaller dark spots are olivine. Note the size grading of the olivine from less than 0.5 mm at the top of the layer to nearly 2 mm at the bottom. The plagioclase grains (white) may also show a similar size gradation from 1 mm at the top to 3 mm at the bottom.

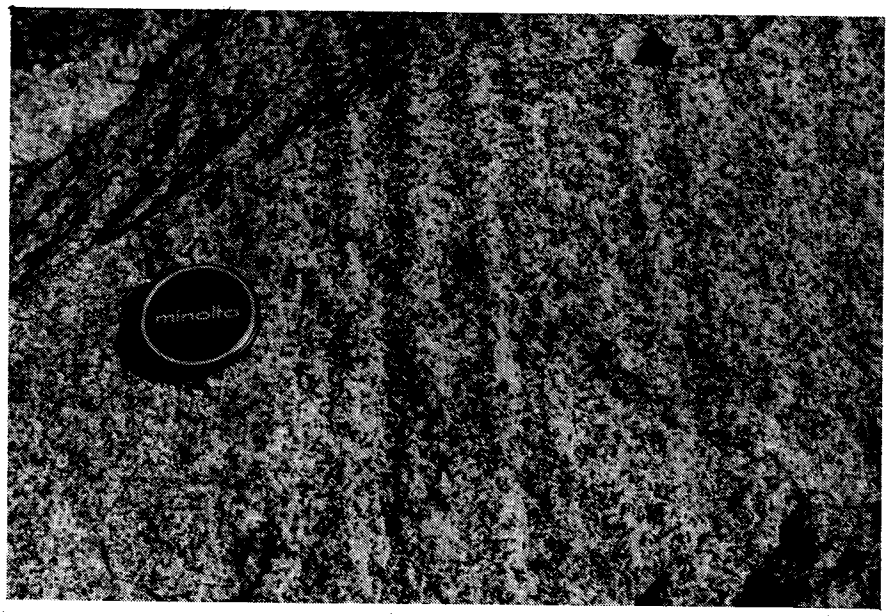

Figure 10. Vertical layering in a mafic-rich zone of an anorthositic body. Black material is interstitial amphibole and the white grains are plagioclase. Note lack of slump features in the layers.

of the parental melt was less than that calculated for the Skaergaard complex due to the relative abundance of water in the Peninsular Ranges basic plutons (See Bottinga and Weill, 1970, Table 8). The net effect of these changes could permit sinking, at a very early stage, of the plagioclase crystals that were sufficiently large to overcome the yield strength of the melt. This qualitative view is supported by the existence of coarse-grained basal anorthositic layers in several intrusions (Hoffman, 1975, unpublished MS thesis, San Diego State University; Walawender, 1976; Allinger, 1979, unpublished MS thesis, San Diego State University), the ubiquitous occurrence of anorthositic inclusions in the early stage rocks, and the presence of plagioclase on the liquidus of the parental melt. McBirney and Noyes (1979) also calculated that for a melt with a density of 2.7 gm/cc and a yield strength of 20 dynes/cm^2 (upper limits in our model), olivine grains must have a radius in excess of 1 mm to sink. Although these numbers are not strictly applicable to our situation, they are compatible with our observations in the olivine sized-graded layers.

The parental melt is inferred to have low yield strengths and a density less than 2.7 gms/cc. The earliest plagioclase from that melt under static conditions may then undergo accumulation via crystal settling, but with continued crystallization the yield strength of the magma would increase to some point that would effectively prohibit further gravitative accumulation. The remaining plagioclase would grow essentially in-situ. Olivine precipitation must have extended beyond the accumulation range of the plagioclase but its density was sufficient to overcome the higher yield strengths of the magma. These crystals would settle through the melt and nucleating plagioclase such that olivine accumulation would begin on the floor above the earliest pulse of plagioclase sedimentation. As the network of crystals (mainly plagioclase) is built up, less olivine would work its way through resulting in a proportional decrease in olivine upwards. Simultaneously, that portion of the melt contributing olivine may have become depleted in but not necessarily devoid of that phase. Diminished growth and settling rates could then produce potentially size-graded olivine layers. At this stage, clinopyroxene may have begun to nucleate but the yield strength of the magma would have increased to the point that neither mafic mineral could accumulate readily. Except for some downward movement of the opaques at this stage, the remaining crystals would form essentially in-situ. Convective overturn or influx of new melt could renew the process to begin the formation of additional layers at any point during the development of a single cycle.

The thickness of the individual layers and the layered zones depend on many factors which include the size of the magma chamber, the rate of convective overturn, and the rate of influx of fresh melt. For larger chambers, the earliest plagioclase may accumulate, mainly by settling, to the extent that the residual liquids were continuously displaced upward before other phases could crystallize in significant amounts. Rapid overturn of the remaining melt could have maintained the necessary conditions and kept plagioclase nucleating and accumulating until larger masses of anorthositic rocks formed. Interstitial liquids that eventually crystallized to amphibole and adcumulate plagioclase could have been trapped by pulses of plagioclase sedimentation to form the crude layering observed in these units. Alternately, these layers and the anorthositic bodies could form as a result of rapid displacement (by settling) of olivine towards the chamber floor to form peridotitic masses. At some stage, the viscosity and yield strength of the

magma may inhibit plagioclase settling so that a residue of more fractionated, finer grained plagioclase would remain along the chamber walls. Interstitial melt could then be trapped in crude layers subparallel to the walls (cooling front) as plagioclase growth rates vary due to fluctuations in thermal and chemical diffusion rates, and/or in the rate of convective overturn in the magma. We favor the latter mechanism for the formation of the larger anorthositic bodies mainly because their layering is consistently steep and commonly parallel to contacts with older rocks, and the plagioclase is less calcic and finer grained than in the basal anorthosites or layered zones. In contrast to the olivine-plagioclase layered rocks (Figures 1, 3, 4), this layering (Figure 10) is not deformed by downslope creep despite its steep inclination. This slope stability indicates that the grains were supported by the enclosing melt rather than by other grains and is consistent with an origin involving diffusion mechanisms rather than gravity-controlled sedimentation.

Moore and Lockwood (1973) described sequences of comb layers in the granitoid rocks of the Sierra Nevada. They concluded that the crystals grew normal to a melt-solid interface into a separate, upward-migrating aqueous phase of the melt. In their model, such conditions of concentrated volatile streaming would occur in overhangs or restricted channels along the melt-solid interface. Walawender (1976) came to similar conclusions for the comb layering developed in the late stages of crystallization of the basic plutons of the Peninsular Ranges batholith, and suggested that the layers were formed by periodic disruptions in the growth rates. These disruptions were effected by either the influx of new melt into the conduit zone or by degassing of the melt through eruption at the surface.

None of the anorthositic bodies examined thus far shows any sign of concentric zoning, as might be expected from in-situ crystallization. Cores of norite or gabbronorite that would develop in an idealized, inward crystallizing body are either missing or, if present, exist as inclusion trains. We anticipate that as crystallization proceeded to the intermediate stages, the ductility contrast between the partially molten interior and essentially solid exterior, and the concomitant volume changes with crystallization would result in the interior zone being forced upward through the roof carapace. The marginal anorthositic facies would then flow inward, destroying much of the original layering and possibly superimposing a flow fabric over it. Thus, small amounts of the interior magma could be left behind as inclusion trains or deformed dikes in the anorthositic rocks.

REFERENCES

Bottinga, U., and Weill, D.F., 1970, Densities of silicate liquid systems calculated from partial molar volumes of oxide components: American Jour. Sci., v. 269, p. 169-182.

Jackson, E.D., 1961, Primary textures and mineral associations in the ultramafic zone of the Stillwater complex, Montana: U.S. Geological Survey Professional Paper 358, 106 p.

Lillis, P.G., Walawender, M.J., Smith, T.E., and Wilson, J., 1979, Petrology and emplacement of the Corte Madera gabbro pluton, southern California, in Mesozoic Crystalline Rocks: Guidebook for the 92nd annual meeting of the Geological Society of America, Abbott, P.L., and Todd, V.R., eds., p. 143-150.

McBirney, A.R. and Noyes, R.M., 1979, Crystallization and layering of the Skaergaard intrusion: Journal of Petrology, v. 20, p. 487-554.

Moore, J.G., and Lockwood, J.P., 1973, Origin of comb layering and orbicular structure, Sierra Nevada batholith, California: Geological Society of America Bulletin, v. 84, p. 1-20.

Thompson, R.N. and Patrick, D.J., 1968, Folding and slumping in a layered gabbro: Geological Journal, v. 6, p. 139-146.

Wager, L.R. and Deer, W.A., 1939, Geological investigations in East Greenland, Part III. The petrology of the Skaergaard intrusion, Kangerdlugssuaq, East Greenland: Meddr. Grønland, v. 105, p. 1-352.

Wager, L.R., and Brown, G.M., 1968, Layered Igneous Rocks: Edinburgh, Oliver and Boyd.

Walawender, M.J., 1976, Petrology and emplacement of the Los Piños pluton, southern California: Canadian Journal of Earth Sciences, v. 13, p. 1288-1300.

Walawender, M.J. and Smith, T.E., 1980, Geochemical and petrologic evolution of the basic plutons of the Peninsular Ranges batholith, southern California: Journal of Geology, v. 88, p. 233-242.

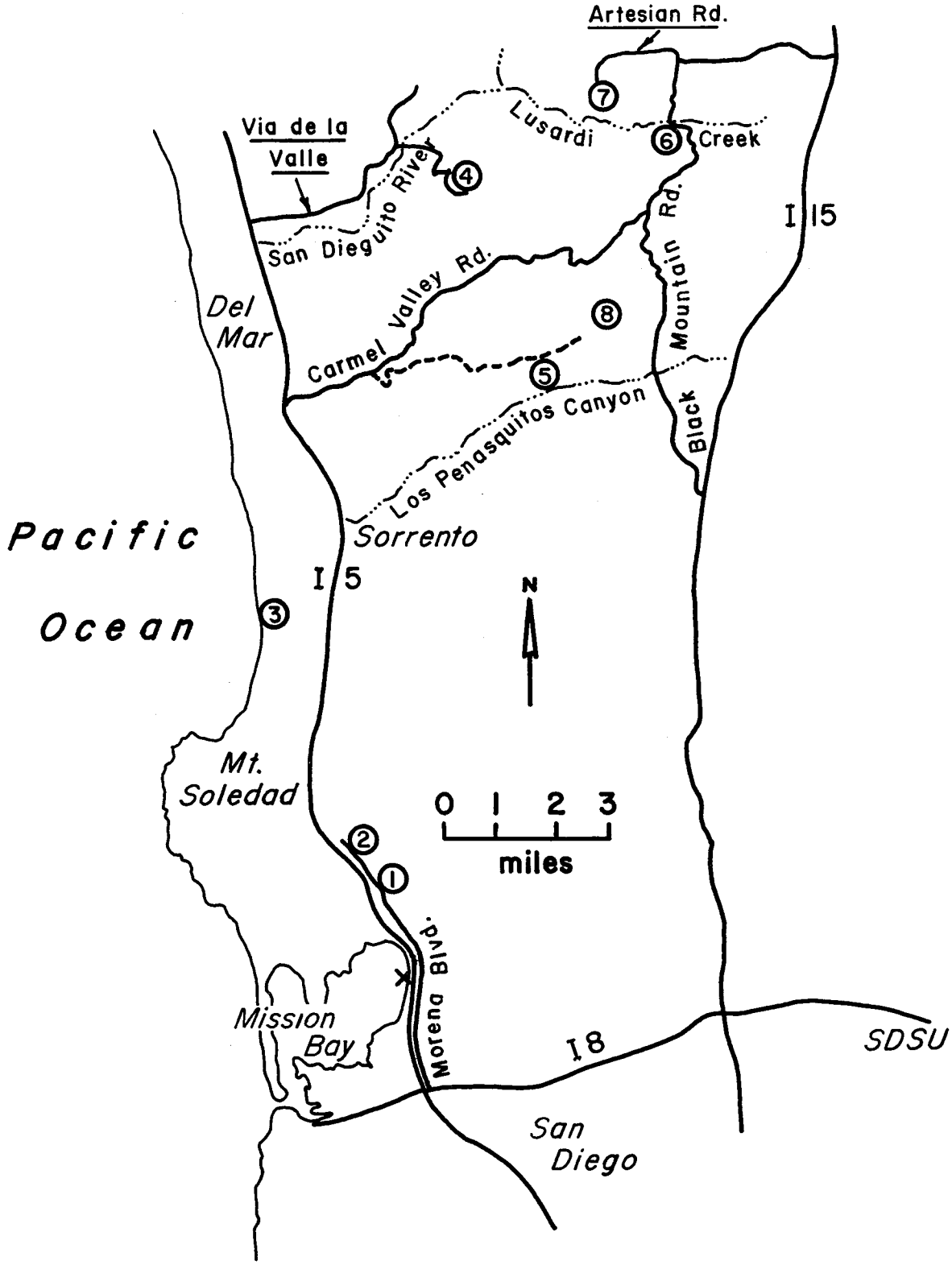
Artesian Rd.
Via de la Valle
Lusardi Creek
San Dieguito River
San Dieguito Rd.
I 15
Del Mar
Carmel Valley Rd.
Mountain
Black
Los Penasquitos Canyon
Pacific Ocean
Sorrento
I 5
N
Mt. Soledad
0 1 2 3
miles
Morena Blvd.
Mission Bay
I 8
SDSU
San Diego
1
2
3
4
5
6
7
8

FIELD TRIP STOPS

STOP 1. Faulted Mt. Soledad facies in roadcut across from 4140 Morena Blvd. Thomas Brothers Map coordinates 52 E5. Interpretation is in paper by Kies.

STOP 2. Rose Canyon fault exposure in cut-slope on north side of Jutland Dr. about 400 ft. east of Morena Blvd. Thomas Bros. 52 C1. See papers by Streiff and others (2) and Artim and Elder-Mills.

STOP 3. Black's Beach landslide viewed from top of beach cliffs west of Torrey Pines glider port. Thomas Bros. 38 A5. See paper by Vanderhurst and others.

STOP 4. Sedimentary facies of Jurassic Santiago Peak Volcanics (JSP). Turn right off Via de la Valle onto El Apajo, right on San Dieguito, left on Calle Bellota which changes into Circo Diegueno, go southerly then follow loop heading uphill to northeast, left on Adobe Villa (dirt road), then walk to outcrops at foot of slope. Thomas Bros. 31 A&B6. See papers by Balch and others, Jones and Miller, and Balch and Abbott.

STOP 5. Sedimentary facies of JSP in Los Penasquitos Canyon. Thomas Bros. 35 C5. See Balch papers (2) and Jones and Miller.

STOP 6. Volcanic facies of JSP along Black Mountain Road. Thomas Bros. 32 A4. See paper by Adams and Walawender.

STOP 7. Volcanic and sedimentary facies of JSP in northeastern Lusardi Canyon. Thomas Bros. 31 D3. See papers of Balch and others (2), Jones and Miller, and Adams and Walawender.

STOP 8. Vernal pools at Entreken and Sundance Avenues. Thomas Bros. 35 E3. See paper by Abbott.